

Special Issue Reprint

Processing Foods

Process Optimization and Quality Assessment

Edited by
Péter Sipos and Milivoj Radojčin

mdpi.com/journal/processes

Processing Foods: Process Optimization and Quality Assessment

Processing Foods: Process Optimization and Quality Assessment

Editors

Péter Sipos

Milivoj Radojčin

MDPI • Basel • Beijing • Wuhan • Barcelona • Belgrade • Manchester • Tokyo • Cluj • Tianjin



Editors

Péter Sipos
University of Debrecen
Debrecen
Hungary

Milivoj Radojčin
University of Novi Sad
Novi Sad
Serbia

Editorial Office

MDPI AG
Grosspeteranlage 5
4052 Basel, Switzerland

This is a reprint of articles from the Special Issue published online in the open access journal *Processes* (ISSN 2227-9717) (available at: https://www.mdpi.com/journal/processes/special_issues/Processing_Foods_Optimization).

For citation purposes, cite each article independently as indicated on the article page online and as indicated below:

Lastname, A.A.; Lastname, B.B. Article Title. <i>Journal Name</i> Year , Volume Number, Page Range.
--

ISBN 978-3-0365-7778-4 (Hbk)

ISBN 978-3-0365-7779-1 (PDF)

doi.org/10.3390/books978-3-0365-7779-1

© 2024 by the authors. Articles in this book are Open Access and distributed under the Creative Commons Attribution (CC BY) license. The book as a whole is distributed by MDPI under the terms and conditions of the Creative Commons Attribution-NonCommercial-NoDerivs (CC BY-NC-ND) license.

Contents

About the Editors	vii
Péter Sipos and Milivoj Radojčin Special Issue: Processing Foods: Process Optimization and Quality Assessment Reprinted from: <i>Processes</i> 2023 , <i>11</i> , 851, doi:10.3390/pr11030851	1
Charlène Leneuve-Jenvrin, Baptiste Quentin, Sophie Assemat and Fabienne Remize Maintaining Physicochemical, Microbiological, and Sensory Quality of Pineapple Juice (<i>Ananas comosus</i> , Var. 'Queen Victoria') through Mild Heat Treatment Reprinted from: <i>Processes</i> 2020 , <i>8</i> , 1186, doi:10.3390/pr8091186	4
Norazlin Abdullah and Nyuk Ling Chin Optimising Tropical Fruit Juice Quality Using Thermosonication-Assisted Extraction via Blocked Face-Centered Composite Design Reprinted from: <i>Processes</i> 2021 , <i>9</i> , 3, doi:10.3390/pr9010003	15
Krzysztof Kucharczyk, Krzysztof Żyła and Tadeusz Tuszyński Volatile Esters and Fusel Alcohol Concentrations in Beer Optimized by Modulation of Main Fermentation Parameters in an Industrial Plant Reprinted from: <i>Processes</i> 2020 , <i>8</i> , 769, doi:10.3390/pr8070769	30
Kexin Bi, Tong Qiu and Yizhen Huang A Deep Learning Method for Yogurt Preferences Prediction Using Sensory Attributes Reprinted from: <i>Processes</i> 2020 , <i>8</i> , 518, doi:10.3390/pr8050518	42
Eszter Benes, Marietta Fodor, Sándor Kovács and Attila Gere Application of Detrended Fluctuation Analysis and Yield Stability Index to Evaluate Near Infrared Spectra of Green and Roasted Coffee Samples Reprinted from: <i>Processes</i> 2020 , <i>8</i> , 913, doi:10.3390/pr8080913	55
Milivoj Radojčin, Ivan Pavkov, Danijela Bursać Kovačević, Predrag Putnik, Artur Wiktor, Zoran Stamenković, et al. Effect of Selected Drying Methods and Emerging Drying Intensification Technologies on the Quality of Dried Fruit: A Review Reprinted from: <i>Processes</i> 2021 , <i>9</i> , 132, doi:10.3390/pr9010132	69
Ivan Pavkov, Milivoj Radojčin, Zoran Stamenković, Krstan Kešelj, Urszula Tylewicz, Péter Sipos, et al. Effects of Osmotic Dehydration on the Hot Air Drying of Apricot Halves: Drying Kinetics, Mass Transfer, and Shrinkage Reprinted from: <i>Processes</i> 2021 , <i>9</i> , 202, doi:10.3390/pr9020202	90
Goran Šarić, Nada Vahčić, Danijela Bursać Kovačević and Predrag Putnik The Changes of Flavonoids in Honey during Storage Reprinted from: <i>Processes</i> 2020 , <i>8</i> , 943, doi:10.3390/pr8080943	112
Maja Repajić, Ena Čegledi, Valentina Kruk, Sandra Pedisić, Firat Çınar, Danijela Bursać Kovačević, et al. Accelerated Solvent Extraction as a Green Tool for the Recovery of Polyphenols and Pigments from Wild Nettle Leaves Reprinted from: <i>Processes</i> 2020 , <i>8</i> , 803, doi:10.3390/pr8070803	123

Arijit Nath, Burak Atilla Eren, Attila Csighy, Klára Pásztorné-Huszár, Gabriella Kiskó, László Abrankó, et al.	
Production of Liquid Milk Protein Concentrate with Antioxidant Capacity, Angiotensin Converting Enzyme Inhibitory Activity, Antibacterial Activity, and Hypoallergenic Property by Membrane Filtration and Enzymatic Modification of Proteins	
Reprinted from: <i>Processes</i> 2020 , <i>8</i> , 871, doi:10.3390/pr8070871	142
Róbert Nagy, Endre Máthé, János Csapó and Péter Sipos	
Modifying Effects of Physical Processes on Starch and Dietary Fiber Content of Foodstuffs	
Reprinted from: <i>Processes</i> 2021 , <i>9</i> , 17, doi:10.3390/pr9010017	167
Hubert Luzdemio Arteaga Miñano, Ana Carolina de Sousa Silva, Sergio Paulo Amaral Souto and Ernane José Xavier Costa	
Magnetic Fields in Food Processing Perspectives, Applications and Action Models	
Reprinted from: <i>Processes</i> 2020 , <i>8</i> , 814, doi:10.3390/pr8070814	183
Anna Rygala, Joanna Berłowska and Dorota Kregiel	
Heterotrophic Plate Count for Bottled Water Safety Management	
Reprinted from: <i>Processes</i> 2020 , <i>8</i> , 739, doi:10.3390/pr8060739	194

About the Editors

Péter Sipos

Péter Sipos, Ph.D., is a professor at the Faculty of Agricultural and Food Sciences and Environmental Sciences, University of Debrecen, and a member of the Hungarian Biophysical Society. With his technical and agronomic background, his research activities have focused mainly on the processing and qualification of cereals, other grain crops and horticultural products for more than 20 years. His research covers different fields of sustainable and cost-effective physical processing methods, with an emphasis on the nutritional aspects of bioactive compounds and the safety of foodstuffs. His current research interests include the development of high-biological-value sorghum-based bakery products, evaluation of extraction and utilisation of protein from legume seeds, and technological development of minimally processed fruits.

Milivoj Radojcin

Milivoj Radojcin, Ph.D., is an associate professor at the Faculty of Agriculture, Department of Agricultural Engineering, University of Novi Sad. His interests are directed towards thermal processes, drying, research of the physical properties of biomaterials, renewable energy sources and energy. The beginning of his career was dedicated to the research of drying processes and physical properties of biomaterial. In the last few years, his focus of interest has shifted towards biomass conversion processes, renewable energy sources and energy as an indispensable part of thermal processes.

Editorial

Special Issue: Processing Foods: Process Optimization and Quality Assessment

Péter Sipos ^{1,*} and Milivoj Radojčin ^{2,*}

¹ Institute of Nutrition, Faculty of Agricultural and Food Sciences and Environmental Management, University of Debrecen, Egyetem tér 1, H-4032 Debrecen, Hungary

² Faculty of Agriculture, University of Novi Sad, Trg Dositeja Obradovića 8, 21000 Novi Sad, Serbia

* Correspondence: siposp@agr.unideb.hu (P.S.); milivoj.radojcin@polj.uns.ac.rs (M.R.)

For a long time, the basic as well as the only function of foods is to provide the nutrients and energy needed for human physiological processes. Over the past century, since the conditions of food security have been reduced, the expectations placed on food have constantly changed and new demands have been emerging. It is expected that foods should not only be safe, but they also have to be tastier and attractive; have a long shelf-life; contain as much of the physiologically beneficial components of the raw materials as possible; and have a positive impact on consumers' health. Industrial food production needs to meet these diverse demands in a way that is economically viable and environmentally friendly, while being flexible to the ever-changing needs. Fortunately, there is a wealth of research to help the food industry, and there is an increase in the amount of information available on the physiological effects of the nutrients of our foods, their health protecting role, and how different processing operations change their quantitative and compositional values. At the same time, changing consumer needs are influencing the expectations and tasks related to offline and online quality analysis and quality assurance. This Special Issue, entitled "Processing Foods: Process Optimization and Quality Assessment", provides a snapshot of new advances in unit operations of food production for healthy nutrition.

Fruits show relatively rapid spoilage due to their high-water content; however, their sensory and nutritional properties are the best when they are fresh. Several methods are under evaluation to provide gentle nutrient-saving conservation that preserves the properties of natural goods. Leneveu-Jenvrin et al. [1] compared the storability and sensory and chemical properties of refrigerated and gently heat-treated pineapple juice. Their results showed that mild heat treatment is the easiest way for prolonging pineapple juice's shelf life; however, a 60 °C heat treatment can provide microbiological safety for a month, while a decrease in sensory values limits the storability to one week. Abdullah and Chin [2] investigated the efficiency of thermosonication-assisted juice extraction of different tropical fruits and compared this method to the water bath incubation method. The authors found that this novel method not only improves yield, but it also improves ascorbic acid and water-soluble dry matter content. Additionally, the response surface methodology was found to be useful in the optimization of the process parameters. Advanced statistical methods can be used for the improvement of the sensory properties of beer. Kucharczyk et al. [3] used a multiple-response optimization procedure on the parametrization of the fermentation process based on the changes in esters and higher alcohols caused by the modifications to the pitching rate, fermentation temperature, level of aeration, and time of tank filling. The authors proved that this method is suitable for quality prediction and process control of aroma- and taste-driven beer production. Apart from the fact that processing parameters can be optimized for ideal sensory properties, Bi et al. [4] created a deep learning method to help select product features that can be associated with consumer preferences, thereby resulting in an improvement in product development, storage, marketing, and overall commercial performance. In a pilot study, the key characteristics of yoghurt were identified

Citation: Sipos, P.; Radojčin, M. Special Issue: Processing Foods: Process Optimization and Quality Assessment. *Processes* **2023**, *11*, 851. <https://doi.org/10.3390/pr11030851>

Received: 25 February 2023

Accepted: 3 March 2023

Published: 13 March 2023



Copyright: © 2023 by the authors. Licensee MDPI, Basel, Switzerland. This article is an open access article distributed under the terms and conditions of the Creative Commons Attribution (CC BY) license (<https://creativecommons.org/licenses/by/4.0/>).

and used for hedonic contour mapping to associate these characteristics with Chinese consumers' acceptance. For evaluation, Benes et al. [5] applied the detrended fluctuation analysis on the results of a near-infrared spectral analysis of green and roasted coffee. This method successfully differentiated the samples based on the roasting levels, which was confirmed to be 100% accurate by the agglomerative hierarchical clustering. This method could be a useful tool for quality assurance of coffee production after an evaluation of its robustness.

To provide a longer shelf-life, drying is commonly used on fruits. However, the heat load results in nutritional and sensory damages. Radojčin et al. [6] made a comparison of traditional and recent, innovative methods and their possible combinations, helping in selection based not only on quality but also energy saving and environmental impacts. They underlined the efficiency of combining drying methods, hybrid drying, and advanced pre-treatments and emphasized the benefits of mathematical process modeling. Within this context, Pavkov et al. [7] investigated osmotic dehydration based on hot air drying of apricot and characterized the effects of the concentration and temperature of the osmotic solution on the increase in water loss, dry matter content, and shrinkage. The authors found the Peleg model to be effective in predicting these changes. During hot air drying, the osmotic dehydrating pre-treatment decreases the effective diffusivity of water and the shrinkage of the product.

Antioxidants, including polyphenols, flavonoids, and anthocyanins, have a significant role in healthy nutrition. Therefore, their evaluation is a trending research area. Šarić et al. [8] evaluated the composition of and changes in flavonoids in acacia and multifloral honey during a one-year-long storage period with different conditions and found that these foodstuffs are still a valuable source of antioxidants after a year of storage. The authors detected an increase in total flavonoid content in the first six months of storage, and further experiments are needed to clarify the background of this phenomenon. Nettle is another known source of polyphenols and pigments, and the study by Repajić et al. [9] increases our knowledge about their effective extraction. Accelerated ethanolic solvent extraction operated at different temperatures was evaluated, and the static times and cycle numbers were compared to ultrasound-assisted extraction. The authors found that the former method is better in terms of yield, resulting in 60% higher antioxidant recovery. Liquid milk concentrate can also be a source of antioxidants, as proven in the study by Nath et al. [10]. They applied cross-flow membrane filtration for concentration, and enzymatic modification of milk protein by trypsin was used in order to modify the biological activity. With this context, not only the antioxidant capacity, angiotensin-converting enzyme inhibitory activity, and antibacterial activity of the milk protein concentrate increase, but trypsin also reduces allergenic epitopes at more than 99.9%.

Several processes applied in the food industry are used to achieve specific results in the behavior as well as technological and/or nutritional properties of food components; for this reason, it is useful to summarize complex effects. In our Special Issue, Nagy et al. [11] reviewed the modifying effects of physical processing methods (such as size reduction, heat treatment, high pressure and its combination with heat treatment, extrusion, atmospheric and cold plasma, and radiation) on the starch and fiber content of foodstuffs. These methods are preferable in many situations because they are easy to apply, are toxicologically safer and more acceptable than chemical methods, are relatively inexpensive, and can be used to achieve a wide range of nutritional objectives. Miñano et al. [12] focused on different types of magnetic field applications and underlined their advantages: the use of a magnetic field is a non-invasive operation, which influences the properties of foods in different aspects, ranging from the physical-chemical to the microbiological level, and has shown promising preliminary results in material transformation and preservation.

There is increasing interest in food quality, especially the microbiological quality of bottled water due to the rapid increase in this market. Rygala et al. [13] revealed the critical points of water processing to help minimize the risk of food safety hazards. For monitoring, the plate count method and luminometry were used, and for identifying bacterial isolates,

polyphasic identification based on biochemical tests and molecular analysis using ribosomal RNA was applied. The most frequent microbial genera and the critical points of the system were identified, which could help improve the hygienic status of water processing lines.

A total of 13 papers are presented in this Special Issue. Initially, we focused on different areas of food processing, qualification, and quality assurance, and we had not expected to be able to present such interesting and forward-looking studies on such a wide range of research areas. The guest editors would like to thank the authors for their contribution.

Author Contributions: Conceptualization, P.S. and M.R.; writing—original draft preparation: P.S.; writing—review and editing: P.S. and M.R. All authors have read and agreed to the published version of the manuscript.

Conflicts of Interest: The authors declare no conflict of interest.

References

1. Leneveu-Jenvrin, C.; Quentin, B.; Assemat, S.; Remize, F. Maintaining Physicochemical, Microbiological, and Sensory Quality of Pineapple Juice (*Ananas comosus*, Var. 'Queen Victoria') through Mild Heat Treatment. *Processes* **2020**, *8*, 1186. [CrossRef]
2. Abdullah, N.; Chin, N.L. Optimising Tropical Fruit Juice Quality Using Thermosonication-Assisted Extraction via Blocked Face-Centered Composite Design. *Processes* **2021**, *9*, 3. [CrossRef]
3. Kucharczyk, K.; Żyła, K.; Tuszyński, T. Volatile Esters and Fusel Alcohol Concentrations in Beer Optimized by Modulation of Main Fermentation Parameters in an Industrial Plant. *Processes* **2020**, *8*, 769. [CrossRef]
4. Bi, K.; Qiu, T.; Huang, Y. A Deep Learning Method for Yogurt Preferences Prediction Using Sensory Attributes. *Processes* **2020**, *8*, 518. [CrossRef]
5. Benes, E.; Fodor, M.; Kovács, S.; Gere, A. Application of Detrended Fluctuation Analysis and Yield Stability Index to Evaluate Near Infrared Spectra of Green and Roasted Coffee Samples. *Processes* **2020**, *8*, 913. [CrossRef]
6. Radojčin, M.; Pavkov, I.; Bursać Kovačević, D.; Putnik, P.; Wiktor, A.; Stamenković, Z.; Kešelj, K.; Gere, A. Effect of Selected Drying Methods and Emerging Drying Intensification Technologies on the Quality of Dried Fruit: A Review. *Processes* **2021**, *9*, 132. [CrossRef]
7. Pavkov, I.; Radojčin, M.; Stamenković, Z.; Kešelj, K.; Tylewicz, U.; Sipos, P.; Ponjičan, O.; Sedlar, A. Effects of Osmotic Dehydration on the Hot Air Drying of Apricot Halves: Drying Kinetics, Mass Transfer, and Shrinkage. *Processes* **2021**, *9*, 202. [CrossRef]
8. Šarić, G.; Vahčić, N.; Bursać Kovačević, D.; Putnik, P. The Changes of Flavonoids in Honey during Storage. *Processes* **2020**, *8*, 943. [CrossRef]
9. Repajić, M.; Cegledi, E.; Kruk, V.; Pedisić, S.; Çınar, F.; Bursać Kovačević, D.; Žutić, I.; Dragović-Uzelac, V. Accelerated Solvent Extraction as a Green Tool for the Recovery of Polyphenols and Pigments from Wild Nettle Leaves. *Processes* **2020**, *8*, 803. [CrossRef]
10. Nath, A.; Eren, B.A.; Csighy, A.; Pászorné-Huszár, K.; Kiskó, G.; Abrankó, L.; Tóth, A.; Szerdahelyi, E.; Kovács, Z.; Koris, A.; et al. Production of Liquid Milk Protein Concentrate with Antioxidant Capacity, Angiotensin Converting Enzyme Inhibitory Activity, Antibacterial Activity, and Hypoallergenic Property by Membrane Filtration and Enzymatic Modification of Proteins. *Processes* **2020**, *8*, 871. [CrossRef]
11. Nagy, R.; Máthé, E.; Csapó, J.; Sipos, P. Modifying Effects of Physical Processes on Starch and Dietary Fiber Content of Foodstuffs. *Processes* **2021**, *9*, 17. [CrossRef]
12. Miñano, H.L.A.; Silva, A.C.d.S.; Souto, S.; Costa, E.J.X. Magnetic Fields in Food Processing Perspectives, Applications and Action Models. *Processes* **2020**, *8*, 814. [CrossRef]
13. Rygala, A.; Berłowska, J.; Kregiel, D. Heterotrophic Plate Count for Bottled Water Safety Management. *Processes* **2020**, *8*, 739. [CrossRef]

Disclaimer/Publisher's Note: The statements, opinions and data contained in all publications are solely those of the individual author(s) and contributor(s) and not of MDPI and/or the editor(s). MDPI and/or the editor(s) disclaim responsibility for any injury to people or property resulting from any ideas, methods, instructions or products referred to in the content.



Article

Maintaining Physicochemical, Microbiological, and Sensory Quality of Pineapple Juice (*Ananas comosus*, Var. 'Queen Victoria') through Mild Heat Treatment

Charlène Leneveu-Jenvrin ^{1,2,*}, Baptiste Quentin ^{1,2}, Sophie Assemat ^{2,3} and Fabienne Remize ^{1,2}

¹ QualiSud, University of La Réunion, CIRAD, Univ Montpellier, Institut Agro, Avignon University, 2 rue J. Wetzell, F-97490 Sainte Clotilde, France; b.quentin2605@gmail.com (B.Q.); fabienne.remize@univ-reunion.fr (F.R.)

² QualiSud, Univ Montpellier, Avignon University, CIRAD, Institut Agro, University of La Réunion, 97744 Montpellier, France; sophie.assemat@cirad.fr

³ CIRAD UMR QualiSud, F-97410 Saint Pierre, France

* Correspondence: charlene.leneveu@univ-reunion.fr

Received: 25 August 2020; Accepted: 15 September 2020; Published: 18 September 2020

Abstract: Shelf life of freshly prepared pineapple juice is short and requires refrigerated conditions of storage. Mild heat treatment remains the easiest way to prolong juice shelf life for small companies. This study was constructed to assess pineapple cv. Queen Victoria juice shelf life from a broad examination of its quality and to propose the most appropriate thermal treatment to increase shelf life without any perceptible decrease in quality. From 25 independent batches of pineapple, collected in different areas and seasons from Reunion Island, the variability of juice physicochemical and microbiological quality was determined. Juice pH values were the highest for fruit harvested in summer, but the juice acidity remained low enough to prevent pathogen spore-forming bacteria growth. During storage at 4 °C, color was modified, and yeasts and molds were the main microbial group exhibiting growth. Assessment of sensory quality resulted in the proposal of a shelf life comprising between three and seven days. Compared to higher temperatures, heat treatment at 60 °C was enough to ensure a good microbiological quality for 30 days, but sensory characteristics and color changes led to the proposal of a shelf life of seven days for pineapple juice treated at 60 °C.

Keywords: fruit; beverage; variability; seasonal variations

1. Introduction

Pineapple is a tropical fruit crop with several nutritional benefits. It is a good source of vitamin B1, B6, and vitamin C [1,2]. There are many cultivars of pineapple (*Ananas comosus*) in the world, but pineapple 'Queen Victoria' is particularly appreciated for its sweet flavor. Sweetness relies on the ratio between acidity and concentration of sugars [2], but depends also on climatic conditions and cultural practices [3]. Several studies show the impact of climatic conditions on physicochemical parameters of the fruit before harvest, especially in Reunion Island [3,4].

Pineapple is mainly consumed fresh and canned. The commercial 'Queen' cultivar class is not suitable for canning as it results in a large amount of waste due to its morphology. However, it can be processed into juice. Pineapple juice is the third most consumed fruit juice worldwide after orange and apple [5]. Quality and shelf life of untreated juice depend on the raw material and the applied processes [6]. Sensory defects during pineapple juice shelf life result from browning and carotenoid destruction. Similarly, a trained sensory panel described minimally processed pineapple as "sugared", "pineapple", and "fresh" when juice was tasted the day of preparation and "fermented", "alcoholic", and "chemical" after three to seven days of storage at 4 °C, together with being browner and shinier

and losing firmness [7]. Juice is highly susceptible to spoilage, and microbial metabolism leads to deterioration of organoleptic and physicochemical parameters, thereby causing rejection of the product by consumers and financial losses for producers. Browning of juice, resulting from the activity of fruit endogenous enzymes, is the other cause of consumers' rejection [8]. To increase fruit juice shelf life, physical treatments are mostly used as they inactivate both microorganisms and enzymes [9]. Several processing technologies have been applied to fruit juices, such as classical pasteurization, ohmic heating, microwave heating, thermosonication, pulsed electric fields (PEF), light treatment, supercritical carbon dioxide, and high hydrostatic pressure (HHP). For instance, PEF treatment improves shelf life of pineapple juice without compromising nutritional and antioxidant values [10]. These emerging technologies have the potential to preserve the freshness of pineapple juice. However, the equipment required to apply physical treatments still implies a high financial investment, which has to be balanced by innovative advantages of the technology [11]. For many small and medium enterprises, cost remains one of the most significant barriers to innovation meaning they will engage process innovation only if they can be sure it will provide significant financial gains [11,12]. Amongst all technologies, classical pasteurization or mild heat treatments are clearly affordable for small-scale processing units and the ability of these techniques to produce qualitative juices deserves to be more deeply investigated.

The impact of classical mild pasteurization treatment on pineapple juice quality has been only partly described [8,13,14]. In 2014, Hounhouigan et al. [8] concluded on a lack of knowledge of the impact of pasteurization on nutritional and sensory quality of pineapple juice. Pineapple juice pasteurization using hot-fill processing is usually performed at 92–105 °C for 15–30 s. Lower temperature treatments were described such as 75 °C for 3 min, 80 °C for 2 min, or 85 °C for 15 min and allowed storage at ambient temperature [13–15]. These treatments resulted in nonenzymatic browning due to Maillard reaction, pigment destruction, and possibly changes in the content of esters, lactones, furanoids, and carbonyl and sulfur compounds, but barely affected phenolic compounds. On the other side, microbiological quality of unpasteurized and pasteurized pineapple juice has been described more extensively [8,13].

The aim of the present study was to assess the quality of untreated pineapple juice, taking into account batch variability of its characteristics, and then to determine a mild pasteurization treatment so that both the physicochemical characteristics and the sensory quality were preserved through storage at 4 °C.

2. Materials and Methods

2.1. Sampling

In this study, 25 batches of “Queen Victoria” pineapple were compared. Pineapples were collected from different locations in Reunion Island over two years (2017–2019). For 22 sampling dates and origins, fruits with similar maturity level, corresponding to eyes turning yellow, were picked up (Table 1) [7]. Pineapples were transported in boxes at ambient temperature and stored at temperature 22–25 °C until processing. Three locations were distinguished according to their annual rainfall: west location was characterized by very low rainfall (500–1000 mm), south and north locations by moderate rainfall (1250–2000 mm), and east location by very high rainfall (2000–3000 mm). Whatever the location, average daily solar radiation was high (1700–2100 J/cm²). Two seasons, representative of Reunion Island climate, were observed: winter (colder and dry) from April to September, and summer (warmer and wet) from October to March [7]. In addition, three batches were collected from a local producer of minimally processed fruit, labeled as TP (Table 1) [7]. For the 22 other batches, interpolated meteorological data corresponding to one month before harvest were recovered from CIRAD/Météo-France [16].

Table 1. Pineapple batch numbers, sampling location, month of sampling (season), and juice processing. Batches labelled TP were collected from a local producer on minimally processed fruit.

Batch number	Location	Sampling Month	Juice Processing
1	East	October 2017 (summer)	Untreated
2	East	March 2018 (summer)	Untreated
3	East	May 2018 (winter)	Untreated
4	East	June 2018 (winter)	Untreated and Pasteurized
5	East	June 2018 (winter)	Untreated
6	East	July 2018 (winter)	Untreated
7	East	July 2018 (winter)	Untreated
8	East	July 2018 (winter)	Untreated
9	West	October 2017 (summer)	Untreated
10	West	October 2017 (summer)	Untreated
11	West	March 2018 (summer)	Untreated
12	West	April 2018 (winter)	Untreated and Pasteurized
13	West	April 2018 (winter)	Untreated
14	West	May 2018 (winter)	Untreated
15	West	May 2018 (winter)	Untreated
16	West	June 2018 (winter)	Untreated
17	North	December 2017 (summer)	Untreated and Pasteurized
18	South	March 2018 (summer)	Untreated
19	South	March 2018 (summer)	Untreated
20	South	March 2018 (summer)	Untreated
21	South	April 2018 (winter)	Untreated
22	South	May 2018 (winter)	Untreated
23 TP	Any	January 2019 (summer)	Untreated
24 TP	Any	February 2019 (summer)	Untreated and Pasteurized
25 TP	Any	May 2019 (winter)	Untreated and Pasteurized

2.2. Untreated Juice Processing and Sampling

Within 24 h after collection, at least three fruits with similar maturity level were manually peeled and cut, then prepared in juice (Extractor Wismer EW-01, CAPAVENIR, France) and shared into sterile bottles. Each bottle contained 75 mL of juice and was stored at 4 °C until analysis. One bottle was used for each date of analysis.

2.3. Pasteurized Juice Processing and Sampling

Within 24 h after collection, at least 17 fruits with similar maturity level were manually peeled and cut, then prepared in juice (Extractor Wismer EW-01, CAPAVENIR, France) so that at least 7 L of juice were obtained. For each batch, 1 L of untreated juice was directly stored at 4 °C (control). Pineapple juice was pasteurized in a Simaco (Bouzonville, France) tubular heat exchanger at 86, 80, 70, or 60 °C for 90 ± 5 s (average residential time) followed by hot fill in 1 L glass bottles previously sterilized. After the bottles were filled and closed with screw caps, they were cooled in a water bath (5 °C), labeled, and then stored under refrigeration (4 °C) until further analysis. One to four replicates were done for each pasteurization temperature. A total of five bottles (for each repetition) were collected for sensory attributes, physical, chemical, and microbiological analyses, before and after the pasteurization, and for each storage time point as indicated.

2.4. Microbiological Analyses

From juice samples stored at 4 °C, serial decimal dilutions were performed in SPW (saline peptone water, Condalab, Torrejón de Ardoz, Madrid, Spain). Enterobacteria were enumerated on VRBG agar (Biokar diagnostic, Solabia, Allonne, France) incubated for 48 h at 37 °C. Psychrotrophic bacteria were enumerated on nutrient agar (Merck, Darmstadt, Germany) incubated for three days at 10 °C. Yeasts and molds enumeration was performed on Sabouraud glucose agar with 100 mg/L chloramphenicol

(Biokar diagnostic, Solabia, Allonne, France) after incubation at 30 °C for 5 days. The detection level for these methods was 3 log CFU/mL.

2.5. Physicochemical Parameters

A pH meter (5231 Crison, and pH meter Model GLP22, Crison Instruments S.A. Barcelona, Spain) was used to determine pH values. Titration with 0.05 M NaOH (TitroLine easy, Schott, Mainz, Germany) was performed to determine titratable acidity (TA), which was expressed as citric acid equivalents in g/100 mL.

Pineapple juice total soluble solids (TSS), expressed as °Brix, were determined with a hand refractometer (Atago, Tokyo, Japan).

Three color determinations were performed for each sample (12 mL of juice). A spectrophotometer CM 3500d (Minolta®, Carrières-sur-Seine, France) was used to measure the color parameters L*, a*, and b*. Color difference, ΔE , was calculated from numerical values of L*, a*, and b* [7].

2.6. Sensory Quality Characteristics

Sensory quality of pineapple juice, placed at room temperature one hour before, was carried out by a panel of trained judges.

For each batch, descriptive profiles were determined from preliminary sessions, which enabled the generation of pineapple descriptive vocabulary [7]. An 11-point scale between 0 (no perception) and 10 (very strong perception) was used by the judges to rate the intensity of the different sensory descriptors. The ISO 11035 method was used [17].

Triangle test was used to determine if there was a detectable difference between two products: control sample and sample pasteurized, both the day of preparation or after seven days of storage according to the ISO 4120–2004 method [18]. Three samples were randomly served and arranged on the plate for evaluation. Each sample was coded differently, with a three-digit code. During this test, the panel was asked to point out their favorite sample.

2.7. Statistical Analysis

Statistical treatment of data was performed with the XLSTAT software (Addinsoft, Paris, France).

A *p*-value of 0.001 was used for one-way variance analysis (ANOVA). The REGWQ (Ryan–Einot–Gabriel–Welsh *F*) test was used for pair-wise comparisons.

Correlation tests were performed with Kendall's tau coefficient with a *p*-value of 0.05 (quantitative variables) or with the biserial correlation method, using the Monte Carlo simulation (correlation between one quantitative and one qualitative variable).

3. Results and Discussion

3.1. Freshly Prepared Juice Pineapple Characteristics

The 25 pineapple batches were independently transformed into juice. Physicochemical parameters (pH, TA, TSS, L*, a*, and b*, color parameters) and microbial counts were determined on the day of processing for each batch. Table 2 shows mean values and data dispersion between batches.

The juice pH was low, as previously observed for minimally processed pineapple from the same cultivar and location [7]. The maximal pH value was 4.25 and so the juice did not allow *Clostridium botulinum* growth.

TSS values were in a high range, compared to other studies [15,19,20]; for instance, °Brix from 13.1 to 14.4 were described by Sanya et al. [15]. Color parameters showed moderated variability, the widest range corresponding to b* value.

Table 2. Physicochemical and microbiological characteristics of untreated pineapple juice on the day of preparation.

Parameter	Mean	Variation Coefficient	Minimum Value	Maximum Value
pH	3.35	8%	3.08	4.25
TA (g/100 mL)	0.86	23%	0.66	1.35
TSS (°Brix)	15.2	9%	13.0	17.6
L*	69.1	9%	51.0	75.0
a*	2.0	70%	−0.5	5.6
b*	50.7	17%	23.6	60.1
Psychrotrophic bacteria (log CFU/mL)	3.3	21%	3.0 ¹	5.4
Enterobacteria (log CFU/mL)	3.9	26%	3.0 ¹	6.5
Yeasts and molds (log CFU/mL)	4.9	8%	4.0	5.5

¹: the indicated values correspond to the detection level. For psychrotrophic bacteria, one batch showed counts below this level. For enterobacteria, five batches showed counts below this level.

Microbiological counts were in the usual ranges for unpasteurized pineapple juice [8]. A large variability between batches, especially for psychrotrophic bacteria and enterobacteria, has to be underlined. The European Union regulation n°2073/2005 requires less than 3 log CFU/mL of *Escherichia coli* for unpasteurized fruit juices. In addition, the levels of yeasts and molds (Y&M) population were high, regarding the usual limit of 6 log (CFU/mL) for fruit juices at consumption level.

The impacts of location and season on batch characteristics were analyzed, taking into account meteorological data (Table 3) [16]. Neither color parameters nor microbiological counts varied according to crop location or harvest season. Meteorological factors (total solar radiation, temperatures, and potential evapotranspiration), juice pH, and TA of pineapple juice were significantly different between north-south, west, and east locations. Juice pH was the highest for fruit harvested in south-north locations, characterized by the highest solar radiation, temperatures, and evapotranspiration. Meteorological factors (total solar radiation, mean temperature, and potential evapotranspiration) and juice pH were significantly different between summer and winter. Biserial correlation showed a correlation between season and pH, with a *p*-value of 0.0001 and a coefficient of 0.70. Summer was characterized by higher solar radiation, temperatures, and evapotranspiration than winter and juice from fruit harvested in summer exhibited higher pH than the juice processed in winter.

Table 3. Meteorological data and influence of crop location and harvest season on pineapple juice physicochemical characteristics. For the same column, different letters indicate significant difference.

	Total Solar Radiation (J/cm ²)	Minimal Temperature (°C)	Mean Temperature (°C)	Maximal Temperature (°C)	Potential Evapotranspiration (mm)	pH	TA (%)
South-North	1728 b	20.0 b	23.1 b	28.1 b	3.69 b	3.7 b	0.86 a
West	1425 a	17.3 a	21.0 a	27.1 ab	2.79 a	3.4 a	1.08 b
East	1460 a	17.9 a	21.2 a	25.6 a	2.92 a	3.3 a	0.87 a
<i>p</i> -value (Location)	0.018	0.026	0.083	0.066	0.007	0.013	0.060
Summer	1695 b	19.4 b	22.8 b	28.0 b	3.56 b	3.7 b	0.86 a
Winter	1399 a	17.5 a	20.9 a	25.9 a	2.75 a	3.3 a	1.00 a
<i>p</i> -value (Season)	0.001	0.027	0.016	0.013	0.000	0.000	0.117

Pearson correlation tests showed positive correlations between pH and maximal (Pearson coefficient 0.735; *p*-value < 0.0001), minimal (Pearson coefficient 0.717; *p*-value = 0.0002), and mean (Pearson coefficient 0.734; *p*-value = 0.0001) temperatures, evapotranspiration (Pearson coefficient 0.630; *p*-value = 0.002), and to a lesser extent, solar radiation (Pearson coefficient 0.510; *p*-value 0.015). This observation is in agreement with previous literature [4], which shows a change in the physicochemical parameters (TSS) of a fruit in relation to the climate one month before harvest. However, no correlation between microbiological counts and physicochemical parameters was noticed.

3.2. Physicochemical Characteristics of Untreated Pineapple Juice over Refrigerated Shelf Life

Changes in physicochemical parameters were determined over the shelf life of pineapple juice (Table 4). From the 25 prepared independent batches, three were removed at day 7 and nine more at day 14 because of evident bad smell. During storage, pH, TA, and TSS did not significantly change. This indicates that fermentation did not modify juice properties. Contrarily, color modifications were noticed after three days. The a* green/red and the b* blue/yellow components gradually decreased. As a consequence, a color difference with the day 0 juice was detected after three days of storage and it increased after seven days. Hence, color appears as an indicator of untreated juice quality and a variation during storage could be used as spoilage indicator. Browning of untreated pineapple juice within 15 days was previously reported [21].

Table 4. Physicochemical parameters of untreated pineapple juice during storage at 4 °C. For the same line, different letters indicate significant difference.

Days of Storage	0	3	7	10	14
Number of Batches	25	25	22	22	13
	Mean (Minimum Value; Maximum Value)				
pH	3.45 (3.08; 4.25) a	3.40 (3.09; 4.00) a	3.39 (3.10; 3.96) a	3.38 (3.12; 3.88) a	3.24 (3.13; 3.25) a
TA (g/100 mL)	0.93 (0.66; 1.35) a	0.97 (0.74; 1.25) a	0.99 (0.67; 1.27) a	0.99 (0.68; 1.20) a	1.01 (0.72; 1.26) a
TSS (°Brix)	15.5 (13.0; 17.6) a	15.6 (12.4; 18.8) a	15.4 (12.4; 17.6) a	15.0 (8.2; 17.6) a	14.9 (12.3; 17.0) a
L*	66.5 (51.0; 75.0) a	68.5 (56.8; 74.0) a	69.9 (65.1; 74.6) a	69.2 (63.5; 74.2) a	69.9 (63.3; 75.2) a
a*	2.3 (−0.5; 5.7) c	1.4 (−1.2; 3.8) b	0.8 (−1.3; 2.6) ab	0.4 (−1.4; 2.2) a	0.3 (−0.2; 1.0) a
b*	48.1 (23.6; 60.1) b	45.9 (24.5; 57.7) ab	42.8 (27.7; 59.0) ab	41.2 (25.6; 56.2) ab	41.6 (28.6; 50.4) a
Color difference	¹ a	6.0 (0.7; 22.4) b	11.1 (1.9; 31.5) bc	13.2 (2.6; 36.1) c	11.5 (5.3; 27.8) bc

¹: control condition.

3.3. Increase of Microbiological Counts of Untreated Pineapple Juice over Refrigerated Shelf Life

The populations of psychrotrophic bacteria, enterobacteria, and Y&M were determined during pineapple juice storage at 4 °C. The average counts of psychrotrophic bacteria did not increase but a gradual increase in maximal population was noticed (Figure 1a). Enterobacteria population was significantly higher than the control (day 0) condition only after 14 days of storage (Figure 1b). Y&M population increase was significant after 10 days, but an increase in population range was noticed from three days of storage (Figure 1c). After three days of storage, one batch reached 6 log (CFU/mL) for Y&M. These observations strengthen the likely involvement of Y&M in untreated juice spoilage, as previously documented for minimally processed pineapple [7].

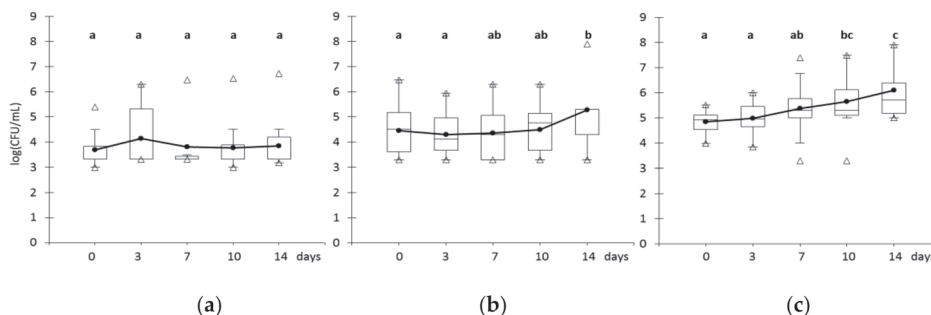


Figure 1. Microbial population (log CFU/g) modifications during refrigerated storage of untreated pineapple juice; (a) psychrotrophic bacteria, (b) enterobacteria, and (c) yeasts and molds. Black circles: mean; open triangle: extreme values; boxes: 1st and 3rd quartiles.

In pineapple juice and other pineapple products, the yeasts *Hanseniaspora uvarum* and *Pichia guilliermondii* were the most frequently detected species [22,23]. *Escherichia coli* cannot grow but can

survive several days in pineapple juice [24] and the presence of *Staphylococcus aureus* has been reported in untreated juice [8]. Both *Salmonella enterica* and *Listeria monocytogenes* exhibited population decline in pineapple juice within two days [25]. Considering pineapple juice pH and its variability, the main role of yeasts in spoilage is not surprising. The primary objective of thermal treatment was then to decrease Y&M population levels, together with inactivation of vegetative foodborne pathogens such as *E. coli*.

3.4. Sensory Quality of Untreated Pineapple Juice during Refrigerated Storage

A sensory analysis was performed to describe untreated pineapple juice freshly prepared or stored for 3, 7, 10, or 14 days at 4 °C. Olfactive, color, or aspect descriptors with the highest scores are presented in Table 5. For freshly extracted juice or juice stored for three or seven days, the first olfactive descriptors were “Pineapple” and “Sugared”, and sensory scores decreased when time of storage increased. For juices stored for 10 or 14 days, descriptors referred primarily to “Fermented” or “Acid”.

The overall sensory score of untreated juice the day of preparation and stored for three days at 4 °C was above average, 5.8 and 5.3 (in 10), respectively, followed by juice stored for seven days at 4 °C with an average score of 4.3. From all collected data, a shelf life of untreated juice of three to seven days can be assessed. This choice first results from sensory analysis, strengthened by microbiological data and color modifications.

Table 5. Main olfactive, color, or aspect descriptors of freshly prepared and stored untreated juice, in descending order of occurrence. Descriptors used by at least 1/3 of the panel are presented. Mean score values and standard mean errors are added in parentheses.

Days of Storage	0	3	7	10	14
Olfactive descriptors	Pineapple (7.1 ± 0.6)	Pineapple (6.9 ± 0.4)	Pineapple (4.8 ± 0.5)	Pineapple (3.6 ± 0.7)	Pineapple (4.1 ± 0.5)
	Sugared (5.8 ± 0.8)	Sugared (5.7 ± 0.7)	Sugared (5.5 ± 0.7)	Sugared (3.4 ± 0.7)	Sugared (4.1 ± 0.7)
	Fresh (4.8 ± 0.7)	Fresh (4.2 ± 0.7)		Fermented (4.2 ± 0.9)	Fermented (3.3 ± 0.8)
	Sweet (4.3 ± 0.9)	Sweet (3.8 ± 0.8)			
	Acid (3.8 ± 0.6)	Acid (4.3 ± 0.6)	Acid (3.8 ± 0.5)	Acid (3.3 ± 0.6)	Acid (4.6 ± 0.7)
Color descriptors	Yellow (5.4 ± 0.8)	Yellow (5.3 ± 0.8)	Yellow (5.1 ± 0.8)	Yellow (4.9 ± 0.8)	Yellow (5.6 ± 0.8)
	Opaque (4.7 ± 0.7)	Opaque (4.8 ± 0.7)	Opaque (4.8 ± 0.6)	Opaque (5.8 ± 0.6)	Opaque (5.3 ± 0.6)
	Dark (4.4 ± 0.5)	Dark (4.7 ± 0.5)	Dark (4.7 ± 0.6)	Dark (6.0 ± 0.3)	Dark (5.5 ± 0.3)
Aspect descriptors	Dense (3.6 ± 0.7)	Dense (3.5 ± 0.7)	Dense (3.9 ± 0.8)	Dense (4.5 ± 0.7)	Dense (4.1 ± 0.7)
			Lumpy (4.3 ± 0.7)		

3.5. Impact of Mild Heat Treatment on Pineapple Juice Quality

The examination of physicochemical parameters showed that pH, TA, and TSS were not affected significantly by the mild heat thermal processing, and neither by storage time (Supplementary Tables S1–S4). However, color parameters were modified (Figure 2a–c), and the color difference between untreated and pasteurized juice on day 0 was dependent on the pasteurization temperature (Figure 2d).

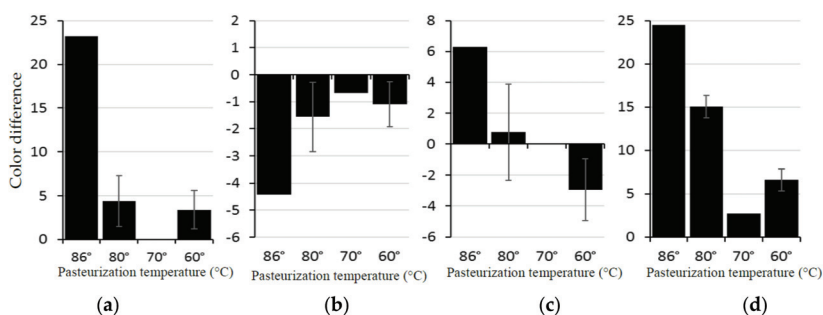


Figure 2. Variation of color parameters for different pasteurization temperatures. (a) L*, (b) a*, (c) b* and (d) color difference. Each bar represents the difference with the unpasteurized juice. For 86 °C, $n = 1$; for 80 °C, $n = 2$; for 70 °C, $n = 1$; and for 60 °C, $n = 4$.

Browning of pineapple juice caused by thermal treatment has been described [13]. Above 50 °C, nonenzymatic browning and degradation of pigments occur and result in decrease of L* and b* and increase of a*. However, a modification of color parameters of less than 5% was observed for temperatures up to 75 °C, though significant browning was reported after mild thermal treatment (65 °C, 15 min) [21].

During storage, color of the heat-treated juices moderately evolved (Table 6), suggesting that oxidases involved in browning were partly inactivated, even at 60 °C. This observation is not consistent with previous studies of polyphenol oxidase and peroxidase of pineapple showing a 10 to 40% inactivation of enzymes with a treatment of 5 min at 60 °C [26,27]. However, the hot filling process applied here probably resulted in keeping an elevated temperature of juice for an extended time.

Table 6. Microbiological counts for unpasteurized and pasteurized pineapple juice at different temperatures and at different refrigerated storage times.

Processing	Number of Batches	Psychrotrophic Bacteria			Enterobacteria			Yeasts and Molds			Color Difference		
		Day 0	Day 14	Day 30	Day 0	Day 14	Day 30	Day 0	Day 14	Day 30	Day 0	Day 14	Day 30
Control	1	3.3	3.3	− ²	<3.0	5.3	− ²	5	7.6	− ²	0	19.2	-
Heating 86 °C	1	<3.0	<3.0	<3.0	<3.0	<3.0	<3.0	<3.0	<3.0	<3.0	24.5	23.9	22.6
Control	2	3.3	3.3 ¹	− ²	<3.0	5.3 ¹	− ²	5	7.6 ¹	− ²	0	11.5	-
Heating 80 °C	2	<3.0	<3.0	<3.0	<3.0	<3.0	<3.0	<3.0	<3.0	<3.0	15.1	15.8	17.7
Control	1	5.4	6.7	− ²	4.8	7.4	− ²	5	5.6	− ²	0	11.8	-
Heating 70 °C	1	<3.0	<3.0	<3.0	<3.0	<3.0	<3.0	<3.0	<3.0	<3.0	2.7	2.4	5
Control	4	3.8	6.7 ¹	− ²	4.8	7.4 ¹	− ²	5	5.6 ¹	− ²	0	-	-
Heating 60 °C	4	<3.0	<3.0	<3.0	<3.0	<3.0	<3.0	<3.0	<3.0	<3.0	6.6	9	8.6

¹ for these values, n = 1 because of organoleptic spoilage after less than 14 days; ²: not determined.

As described above, the control conditions (unpasteurized juice) led to microbial population increase. Any temperature assayed resulted in the inactivation of psychrotrophic bacteria, enterobacteria, and Y&M to levels which allowed the absence of detection of these microbial groups after 30 days of storage (Table 6).

Considering the effect of heat treatment on color, which induces browning at 86 °C and at 80 °C (Figure 2), and the absence of detectable microbial growth after 30 days of storage whatever the pasteurization temperature (Table 6), the treatment at 60 °C appears to be the most interesting to preserve juice quality and to increase shelf life.

Heat resistance of yeasts corresponds to D 60 °C of less than 1 min, but *Saccharomyces cerevisiae* presents higher resistance with D 60 °C values ranging between 2.8 and 22 min [8,28]. Inactivation of *E. coli* in pineapple juice is in the range 2.9–5.3 log CFU/mL for a treatment of 5 min at 55 °C [29]. Hence, the treatment applied in this study at 60 °C was enough to decrease these microbial group populations below levels of concern. Other bacteria involved in juice spoilage are spore-forming acidophilic bacteria, such as *Alicyclobacillus acidoterrestris*. However, this bacterium is involved in spoilage of shelf-stable acid beverages. In this study, its growth can be controlled by the low temperature of storage [30,31].

A sensory analysis was performed to compare untreated pineapple juice and 60 °C pasteurized juices. Triangle tests revealed the absence of significant differences between freshly prepared and pasteurized juice (Figure 3a).

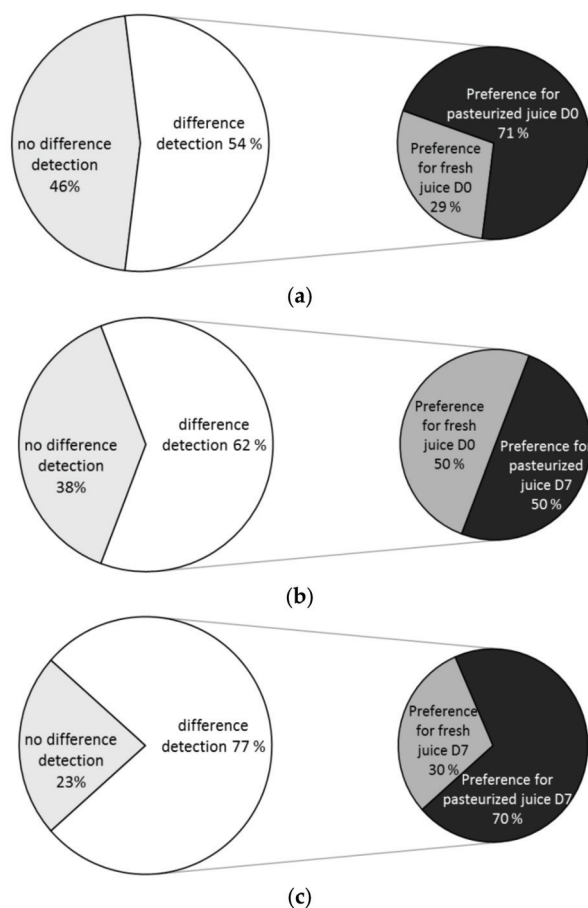


Figure 3. Proportion of panelist answers in triangle test comparison of (a) untreated juice at day 0 vs. pasteurized juice at day 0, (b) untreated juice at day 0 vs. pasteurized juice after 7 days of storage at 4 °C, (c) untreated juice after 7 days of storage at 4 °C vs. pasteurized juice after 7 days of storage at 4 °C.

Comparison between untreated juice stored for zero (Figure 3b) or seven (Figure 3c) days with pasteurized juice stored for seven days at 4 °C shows a significant difference at 95% and 99% levels, respectively. For the panelists which detected a difference, there was no preference between untreated juice the day of preparation and seven-day pasteurized juice, but this latter juice was preferred over the seven-day untreated juice.

Organoleptic quality of pineapple juice is rarely reported [8], and the effect of pasteurization on sensory characteristics has not been studied before. We show that a mild heat treatment can be imperceptible by a trained sensory panel, though it is satisfactory for microbiological quality.

4. Conclusions

A large variability of pH, TA, TSS, color, and microbial parameters was observed between pineapple juice batches which were sampled from different seasons and locations. Juice acidity was the lowest for fruit harvested in summer, which corresponded to higher mean temperatures, higher solar radiation, and higher potential evapotranspiration than winter. During storage, color parameters and microbial populations changed considerably and affected juice quality. Sensory analyses showed a decrease of quality between three and seven days of storage. A mild thermal treatment at 60 °C was the

best to maintain organoleptic properties close to an untreated pineapple juice. This treatment ensured a good microbiological quality after 30 days at 4 °C, whereas color difference with the untreated juice resulted mainly from the heat treatment but not from post-pasteurization storage change. Sensory assays revealed that the sensory quality of pasteurized pineapple juice was of the same level after seven days of storage as untreated juice.

Supplementary Materials: The following are available online at <http://www.mdpi.com/2227-9717/8/9/1186/s1>, Table S1: Mean values of quality parameters of pineapple juice before and after pasteurization at 60 °C, Table S2: Mean values of quality parameters of pineapple juice before and after pasteurization at 70 °C, Table S3: Mean values of quality parameters of pineapple juice before and after pasteurization at 80 °C, Table S4: Mean values of quality parameters of pineapple juice before and after pasteurization at 86 °C.

Author Contributions: Conceptualization and methodology, F.R., C.L.-J., and S.A.; experimental work, C.L.-J. and B.Q.; writing—original draft preparation, C.L.-J. and F.R.; writing—review and editing, F.R., C.L.-J., B.Q., and S.A.; funding acquisition, F.R. All authors have read and agreed to the published version of the manuscript.

Funding: This research was funded by European Union and Region Reunion (FEDER), grant number GURDTI-2017-0391-0002361. The APC was funded by the same.

Acknowledgments: The authors want to thank Colipays, France and SCA Les Avirons, Vivea, France for providing pineapples.

Conflicts of Interest: The authors declare no conflict of interest.

References

1. Septembre-Malaterre, A.; Remize, F.; Poucheret, P. Fruits and vegetables, as a source of nutritional compounds and phytochemicals: Changes in bioactive compounds during lactic fermentation. *Food Res. Int.* **2018**, *104*, 86–99. [CrossRef] [PubMed]
2. Sun, G.-M.; Zhang, X.-M.; Soler, A.; Marie-Alphonsine, P. Nutritional composition of pineapple (*Ananas comosus* (L.) Merr.). In *Nutritional Composition of Fruit Cultivars*; Simmonds, M., Preedy, V., Eds.; Elsevier: Amsterdam, The Netherlands, 2016; pp. 609–637. ISBN 978-0-12-408117-8.
3. Dorey, E.; Fournier, P.; Léchaudel, M.; Tixier, P. Modeling sugar content of pineapple under agro-climatic conditions on Reunion Island. *Eur. J. Agron.* **2015**, *73*, 64–72. [CrossRef]
4. Sanewski, G.M.; Bartholomew, D.P.; Paull, R.E. *The Pineapple, 2nd Edition: Botany, Production and Uses*; CABI: Wallingford, UK, 2018; ISBN 978-1-78639-330-2.
5. Upadhyay, A.; Lama, J.P.; Tawata, S. Utilization of pineapple waste: A Review. *J. Food Sci. Technol. Nepal* **2013**, *6*, 10–18. [CrossRef]
6. Montero-Calderón, M.; Martín-Belloso, O.; Soliva-Fortuny, R. Fresh-cut fruits: Pineapple. In *Controlled and Modified Atmospheres for Fresh and Fresh-Cut Produce*; Beaudry, R.M., Gil, M.I., Eds.; Elsevier: Amsterdam, The Netherlands, 2020; pp. 511–518. ISBN 978-0-12-804599-2.
7. Leneveu-Jenvrin, C.; Quentin, B.; Assemat, S.; Hoarau, M.; Meile, J.-C.; Remize, F. Changes of quality of minimally-processed pineapple (*Ananas comosus*, var. ‘Queen Victoria’) during cold storage: Fungi in the leading role. *Microorganisms* **2020**, *8*, 185. [CrossRef] [PubMed]
8. Hounhouigan, M.H.; Linnemann, A.R.; Soumanou, M.M.; Boekel, M.A.J.S.V. Effect of processing on the quality of pineapple juice. *Food Rev. Int.* **2014**, *30*, 112–133. [CrossRef]
9. Leneveu-Jenvrin, C.; Charles, F.; Barba, F.J.; Remize, F. Role of biological control agents and physical treatments in maintaining the quality of fresh and minimally-processed fruit and vegetables. *Crit. Rev. Food Sci. Nutr.* **2019**, 1–19. [CrossRef]
10. Abu, Y.; Md Anisur, R.; Rakib, M.U.; Md Mozammel, H.; Sayem, A.S.M.; Md Shahadat, H.; Md Shah, A.; Md Sazzad, A.; Mushaida, H. Pineapple juice preservation by pulsed electric field treatment. *Open J. Biol. Sci.* **2020**, *5*, 006–012. [CrossRef]
11. Fryer, P.J.; Versteeg, C. Processing technology innovation in the food industry: Innovation. *Innovation* **2008**, *10*, 74–90. [CrossRef]
12. Madrid-Guijarro, A.; Garcia, D.; Auken, H.V. Barriers to Innovation among Spanish Manufacturing SMEs. *J. Small Bus. Manag.* **2009**, *47*, 465–488. [CrossRef]
13. Rattanathanalerk, M.; Chiewchan, N.; Srichumpoung, W. Effect of thermal processing on the quality loss of pineapple juice. *J. Food Eng.* **2005**, *66*, 259–265. [CrossRef]

14. Saikia, S.; Manhot, N.K.; Mahanta, C.L. A comparative study on the effect of conventional thermal pasteurisation, microwave and ultrasound treatments on the antioxidant activity of five fruit juices. *Food Sci. Technol. Int.* **2016**, *22*, 288–301. [CrossRef] [PubMed]
15. Sanya, C.A.K.; Chadare, F.J.; Hounhouigan, M.H.; Fassinou Hotegni, N.V.; Gbaguidi, M.A.; Dekpemadoha, J.E.; Linnemann, A.R.; Hounhouigan, D.J. Effects of plant density and fertilizer formula on physicochemical and sensorial characteristics of pasteurized juice from Perolera sugarloaf pineapples grown in the long rainy season. *NJAS Wagening. J. Life Sci.* **2020**, *92*, 100320. [CrossRef]
16. METEOR. Available online: <https://smartis.re/METEOR> (accessed on 25 April 2020).
17. International Organization for Standardization ISO 11035:1994. Available online: <https://www.iso.org/cms/render/live/en/sites/isoorg/contents/data/standard/01/90/19015.html> (accessed on 7 September 2020).
18. International Organization for Standardization ISO 4120:2004. Available online: <https://www.iso.org/cms/render/live/en/sites/isoorg/contents/data/standard/03/34/33495.html> (accessed on 7 September 2020).
19. Laorko, A.; Tongchitpakdee, S.; Youravong, W. Storage quality of pineapple juice non-thermally pasteurized and clarified by microfiltration. *J. Food Eng.* **2013**, *116*, 554–561. [CrossRef]
20. Kaddumukasa, P.P.; Imathiu, S.M.; Mathara, J.M.; Nakavuma, J.L. Influence of physicochemical parameters on storage stability: Microbiological quality of fresh unpasteurized fruit juices. *Food Sci. Nutr.* **2017**, *5*, 1098–1105. [CrossRef] [PubMed]
21. Lagnika, C.; Adjovi, Y.C.S.; Lagnika, L.; Gogohounga, F.O.; Do-Sacramento, O.; Koulony, R.K.; Sanni, A. Effect of combining ultrasound and mild heat treatment on physicochemical, nutritional quality and microbiological properties of pineapple juice. *Food Nutr. Sci.* **2017**, *8*, 227–241. [CrossRef]
22. Chanprasartsuk, O.O.; Prakitchaiwattana, C.; Sanguandeeul, R.; Fleet, G.H. Autochthonous yeasts associated with mature pineapple fruits, freshly crushed juice and their ferments; and the chemical changes during natural fermentation. *Bioresour. Technol.* **2010**, *101*, 7500–7509. [CrossRef]
23. Di Cagno, R.; Cardinali, G.; Minervini, G.; Antonielli, L.; Rizzello, C.G.; Ricciuti, P.; Gobbetti, M. Taxonomic structure of the yeasts and lactic acid bacteria microbiota of pineapple (*Ananas comosus* L. Merr.) and use of autochthonous starters for minimally processing. *Food Microbiol.* **2010**, *27*, 381–389. [CrossRef]
24. Abadias, M.; Alegre, I.; Oliveira, M.; Altisent, R.; Viñas, I. Growth potential of *Escherichia coli* O157:H7 on fresh-cut fruits (melon and pineapple) and vegetables (carrot and escarole) stored under different conditions. *Food Control* **2012**, *27*, 37–44. [CrossRef]
25. Huang, J.; Luo, Y.; Zhou, B.; Zheng, J.; Nou, X. Growth and survival of *Salmonella enterica* and *Listeria monocytogenes* on fresh-cut produce and their juice extracts: Impacts and interactions of food matrices and temperature abuse conditions. *Food Control* **2019**, *100*, 300–304. [CrossRef]
26. Lee, T.H.; Chua, L.S.; Tan, E.T.T.; Yeong, C.; Lim, C.C.; Ooi, S.Y. Kinetics of thermal inactivation of peroxidases and polyphenol oxidase in pineapple (*Ananas comosus*). *Food Sci. Biotechnol.* **2009**, *18*, 661–666.
27. Chakraborty, S.; Rao, P.S.; Mishra, H.N. Kinetic modeling of polyphenoloxidase and peroxidase inactivation in pineapple (*Ananas comosus* L.) puree during high-pressure and thermal treatments. *Innov. Food Sci. Emerg. Technol.* **2015**, *27*, 57–68. [CrossRef]
28. Shearer, A.E.H.; Mazzotta, A.S.; Chuyate, R.; Gombas, D.E. Heat resistance of juice spoilage microorganisms. *J. Food Prot.* **2002**, *65*, 1271–1275. [CrossRef] [PubMed]
29. Tchuenchieu, A.; Sylvain, S.K.; Pop, C.; Jean-Justin, E.N.; Mudura, E.; Etoa, F.-X.; Rotar, A. Low thermal inactivation of *Escherichia coli* ATCC 25922 in pineapple, orange and watermelon juices: Effect of a prior acid-adaptation and of carvacrol supplementation. *J. Food Saf.* **2018**, *38*, e12415. [CrossRef]
30. Ciuffreda, E.; Bevilacqua, A.; Sinigaglia, M.; Corbo, M. *Alicyclobacillus* spp.: New insights on ecology and preserving food quality through new approaches. *Microorganisms* **2015**, *3*, 625–640. [CrossRef]
31. Bevilacqua, A.; Mischitelli, M.; Pietropaolo, V.; Ciuffreda, E.; Sinigaglia, M.; Corbo, M.R. Genotypic and phenotypic heterogeneity in *Alicyclobacillus acidoterrestris*: A contribution to species characterization. *PLoS ONE* **2015**, *10*, e0141228. [CrossRef]



Article

Optimising Tropical Fruit Juice Quality Using Thermosonication-Assisted Extraction via Blocked Face-Centered Composite Design

Norazlin Abdullah ^{1,2} and Nyuk Ling Chin ^{2,*}

¹ Department of Technology and Natural Resources, Faculty of Applied Sciences and Technology, Universiti Tun Hussein Onn Malaysia, UTHM Pagoh Campus, Pagoh Higher Education Hub, KM 1, Jalan Panchor, Muar 84600, Johor, Malaysia; norazlinh@uthm.edu.my

² Department of Process and Food Engineering, Faculty of Engineering, Universiti Putra Malaysia, UPM, Serdang 43400, Selangor, Malaysia

* Correspondence: chinnl@upm.edu.my; Tel.: +60-3-97696353

Abstract: Extraction of tropical fruit juice using simple, efficient, and environmentally friendly technologies is gaining importance to produce high quality juices. Juice from pink-fleshed guava, pink-fleshed pomelo, and soursop was extracted using direct and indirect thermosonication methods by varying intensity, time, and temperature, and compared to those extracted using water bath incubation. Improvised models of juice yield, ascorbic acid, and total soluble solids responses were generated by eliminating insignificant model terms of the factors in full quadratic model using backward eliminating procedure. Main effects, 3D, or 4D plots for each response were developed based on factors that influenced the response. Results showed that the best extraction method for guava and pomelo juices were within indirect thermosonication method of 1 kW, 55 °C and 30 min, and 2.5 kW, 54 °C and 23 min, respectively. Direct thermosonication method at 10% amplitude, 55 °C for 2 to 10 min was more suitable for soursop juice. Thermosonicated extraction of tropical fruit juice can improve its juice yield, ascorbic acid content, and total soluble solids content.

Keywords: response surface methodology; ultrasound; guava; pomelo; soursop

Citation: Abdullah N. and Chin N.L. Optimising Tropical Fruit Juice Quality Using Thermosonication-Assisted Extraction via Blocked Face-Centered Composite Design. *Processes* **2021**, *9*, 3. <https://dx.doi.org/10.3390/pr9010003>

Received: 26 October 2020

Accepted: 16 November 2020

Published: 22 December 2020

Publisher's Note: MDPI stays neutral with regard to jurisdictional claims in published maps and institutional affiliations.



Copyright: © 2020 by the authors. Licensee MDPI, Basel, Switzerland. This article is an open access article distributed under the terms and conditions of the Creative Commons Attribution (CC BY) license (<https://creativecommons.org/licenses/by/4.0/>).

1. Introduction

Preserving pink-fleshed guava, pink-fleshed pomelo, and soursop fruits in the form of juice concentrates is useful, as these three fruits are excellent in terms of fighting cancer and are claimed as cancer therapy fruits [1,2]. The pink-fleshed guava contains lycopene, which can prevent skin damage from ultraviolet rays and offers protection from prostate cancer. It is also rich in carotene, which can protect against lung and oral cavity cancers. The high vitamin C content of the pink-fleshed pomelo helps to strengthen and maintain elasticity of arteries. In addition to being good for the digestive system, pomelo can aid in weight loss process because the fat burning enzyme in pomelo can help to absorb and reduce starch and sugar in the body. The pink-fleshed pomelo is slightly sweeter and more nutritious than other pomelos because of its darker pigment. Soursop pulp is white and juicy and has a delightful sour-sweet aroma with a yogurt-like taste [3], in addition to containing annonaceous acetogenins, which are prostate cancer chemopreventive compounds [1]. The fruit is widely used in anticancer folk therapies in North, Central, and South America, and Southeast Asia [4].

In the ascending order of the amount of free-run juice from fresh fruit, the pink-fleshed guava ranks the lowest, followed by the soursop, and pink-fleshed pomelo. The pink-fleshed guava and soursop both contain high starch levels of 13% [5] and 27.3% [6], respectively. The high starch content and the thick, creamy, and fleshy, pink-fleshed guava and soursop pulps result in difficulty in cell wall disruption of the fruit tissue. Thus, only a small amount of juice can be pressed or squeezed out. A more advanced extraction process

is needed for production of these fruit juices. The pink-fleshed pomelo fruit, which is non-starchy [7] and has high watery properties, can serve as a control for extraction process comparisons.

Ultrasound is well known for its use in inactivating food spoilage, yeast, and pathogenic microorganisms [8–13]. In juice extraction, ultrasound can produce greater yields of juice [14], reduce time of juice extraction because of heat and mass transfer enhancement, and save extraction energy via facilitating extraction at medium temperature levels. The combination of low frequency ultrasound with mild heat can help in reducing processing temperature and time by 16 and 55%, respectively, minimising the negative effects on fruit juices quality and makes the processing more economically feasible [15]. The combination of ultrasound and mild heat treatment is also known as thermosonication. The thermosonication treatment is useful in acting against thermo-resistant enzymes where it is difficult to denature by thermal treatment alone. The use of extreme heat could lead to adverse changes in juice quality like cooked flavour and caramelisation [15–19]. Since enzymes are more thermo-resistant than microorganisms in citrus juices, the inactivation of enzymes promises achievement of required number of microbial destruction for spoilage prevention [20]. The thermosonication treatment can also penetrate fruit cell walls and release cell contents trapped inside fruit tissues. Although ultrasonically assisted extraction processes are able to release contents such as sugar, medicinal compounds, carotenoids, and protein from biological materials by disrupting cell walls [21,22], such techniques have not been used to extract juice from difficult-to-juice produce such as those having high starch content and creamy fruit pulp. Sin et al. [23] and Lee et al. [24] applied hot water extraction method to extract sapodilla and banana juice, respectively, while Cendres et al. [25] extracted juice from grapes, plums, and apricots using microwaves.

In extraction experiments that cannot be completed within a day, a blocking approach is used to obtain more precise and consistent results. The blocked face-centred central composite design, an experimental design in response surface methodology (RSM) is used to generate predictive equations to optimise thermosonic-assisted juice extraction process as opposed to the unblocked face-centred central composite design used in optimising hot water extraction for sapodilla juice [23] and banana juice [24]. The objective of this study was to determine the optimum extraction method and conditions for producing higher juice yield with maximum ascorbic acid and total soluble solids levels of pink-fleshed guava, pink-fleshed pomelo, and soursop fruit juices.

2. Materials and Methods

2.1. Fruit Pulp Preparation

Matured, pink-fleshed guava fruits at 75% ripeness with a pronounced typical aroma and yellow skin were purchased from Sime Darby Beverages Sdn. Bhd. The ripened fruits were washed under running tap water and any floral remnants at the apex were removed after the outer part dried. Then, the tip ends were cut with a sharp knife prior to dicing the fruit into small pieces.

Pink-fleshed pomelo fruits were purchased from Perniagaan Buah-buahan Ah Yew, Bidor, Perak. Pomelo with yellow rinds were chosen for peeling process. The very thick spongy rind was cut into four sections as close as possible to the flesh of the pomelo. Each section of peel was pulled away from the fruit prior to slicing the fruit and breaking it in half. The seeds and remaining pith, which are bitter, were completely removed.

Matured green soursop fruits were purchased from Federal Agricultural Marketing Authority (FAMA) of Malaysia. The fruits were allowed to ripen in an air-conditioned (18 ± 2 °C) room for 3 to 4 days prior to processing. They were considered ripened when they were soft to touch and the shiny green colour turned to lack-lustre green or yellowish-green. Approximately 5 kg of ripened fruits were processed while waiting for remaining fruits to ripen within 1 to 2 days. The fruits were washed and cut into half, cored, their skin hand-peeled, and seeds removed from the pulp manually.

For each fruit, 2.5 kg of pulp was crushed into a mash using a 1300 W commercial food blender (XB409, Ceado, Italy) with a pulse duration of 60 s at a high speed of 28,000 rpm, then 30 s off and 60 s at a low speed of 22,000 rpm for complete homogenisation of pulp mash.

2.2. Thermosonic-Assisted Extraction

The direct thermosonic-assisted extraction as shown in Figure 1 was performed using a 400 W digital ultrasonic processor (S-450D, Branson, MO, USA) with its probe tip immersed to a depth of 25 mm into a 150-mL beaker containing pulp mixture samples at ultrasonic amplitudes of 10, 55, or 100% for 2, 6, or 10 min. For indirect thermosonic-assisted extraction as illustrated in Figure 2, a glass bottle of the pulp sample mixture was partially immersed in an ultrasonic water bath [26], which contains distilled water as a medium to spread waves at a power of 1, 1.75, or 2.5 kW for 10, 20, or 30 min. The motion frequency, power, and amplitudes of ultrasonic energy dictate the intensity of treatment where high shear forces induced produce high-energy microbubbles that accelerated juice extraction process through release of energy by direct injection into fruit cell wall to obtain a high volume of extracted juice. Each extraction was conducted at three temperatures, i.e., 25, 40, and 55 °C, and the pulp mixture samples were mixtures of 50 g of blended pulp with distilled water at ratio of 1:1. The specified temperature was maintained manually by adding cold water into a water container that places the beaker for direct thermosonication or applying continuous flow of water in the bath for indirect thermosonication. The extraction by incubation in a water bath acted as a control with pulp mixture samples added in glass bottles, shaken for 30, 75, and 120 min at 20, 100, and 180 rpm in a shaking water bath (BS-21, Lab Companion, Korea) at incubation temperatures of 25, 40, and 55 °C.

The treated pulp was separated from the juice by centrifugation at 4000 rpm and 4 °C for 20 min using a refrigerated centrifuge (Mikro 22R, HettichZentrifugen, Germany). The supernatant was collected for determination of juice yield, ascorbic acid (AA) content, and total soluble solids (TSS) content.

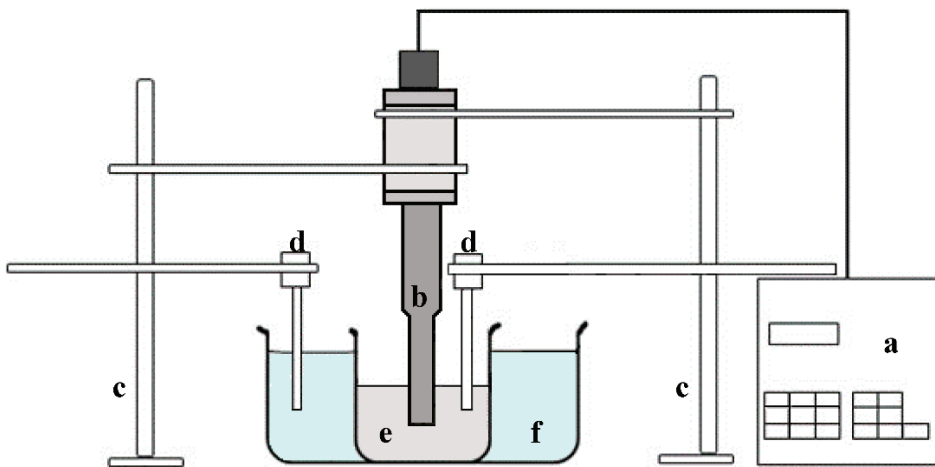


Figure 1. Experimental setup for direct thermosonic-assisted extraction. (a) Ultrasonic processor, (b) sonicator probe, (c) retort stand, (d) temperature probe, (e) fruit juice, and (f) water for controlling temperature.

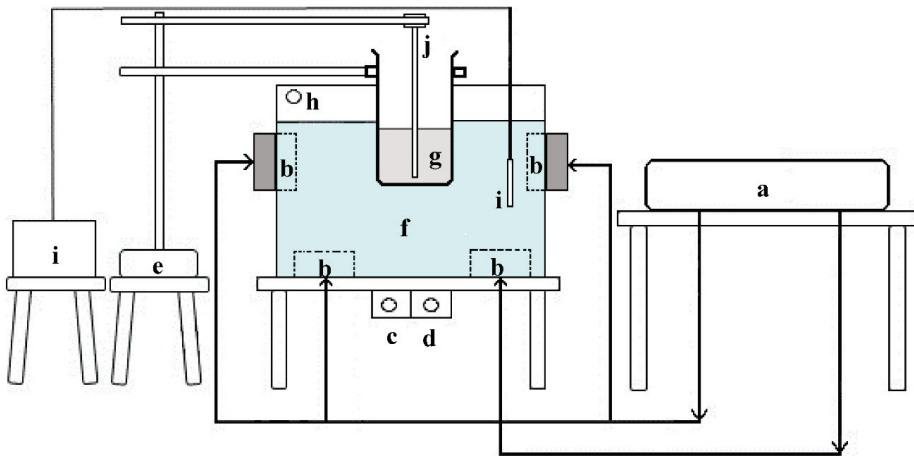


Figure 2. Experimental setup for indirect thermosonic-assisted extraction. (a) Ultrasonic generator, (b) transducer, (c) water inlet valve, (d) water drain valve, (e) retort stand, (f) ultrasonic tank, (g) fruit juice, (h) overflow outlet, (i) heater, and (j) temperature probe.

2.3. Blocked Face-Centred Central Composite Design

The blocked face-centred central composite design provides high-quality predictions over the entire design space and does not require using points outside the original factor range. Blocking was required to increase precision of experiments as variations of each batch of fruits could not be controlled, and all runs could not be completed within a day. Face-centred refers to alpha value of one and was chosen because the points were at operational limits, and equipment used could set the parameters to certain values only. The combination of factors for each run was generated and arranged using commercial software (MINITAB® Release 14, Minitab Inc., State College, PA, USA).

Table 1 shows experimental runs designed for one batch of fruits. There were 20 runs for each batch of fruits with three replications for each block and batch varying three factors, intensity, time, and temperature, at three levels, -1 , 0 , and 1 , which gave total runs of 60. Responses were measured as percentage change of juice yield, ascorbic acid (AA), and total soluble solids (TSS) content. Fitted regression models were obtained using MINITAB, whereas 4D surface plot was generated using ThreeDify Excel Grapher (v.3.3.8, ThreeDify Inc., Ottawa, ON, Canada) software. The plotted graph chosen depended on the significant factors involved in the improvised models.

The second-order model is widely used in RSM because of its flexibility in taking on a wide variety of functional forms and a good capability to estimate the true response surface [27]. As blocking was used in this study, the second-order model, Equations (1) and (2), were necessary to fit the data [28,29]. The best-fitted models were chosen, and values for the combined factors that satisfied all optimum responses simultaneously were generated.

$$Y = \beta_0 + \beta_{01} + \beta_{02} + \beta_{03} + \beta_{04} + \beta_{05} + \beta_{06} + \beta_{07} + \beta_{08} + \beta_{09} + \sum_{j=1}^k \beta_j x_j + \sum_{j=1}^k \beta_{jj} x_j^2 + \sum_{i < j=2}^k \beta_{ij} x_i x_j \quad (1)$$

$$\beta_{09} = -(\beta_{01} + \beta_{02} + \beta_{03} + \beta_{04} + \beta_{05} + \beta_{06} + \beta_{07} + \beta_{08}) \quad (2)$$

where Y is the response; β_0 is the constant for intercept; β_{01} to β_{09} are the constant for blocks; β_j is the linear coefficient; β_{jj} is the quadratic coefficient, and β_{ij} is the interaction coefficient. x_i and x_j are independent variables (i and j are in the range of 1 to k). k is the number of independent variables ($k = 3$).

Table 1. Design of experiments with coded variable levels.

Batch	Run	Block	Intensity ^a	Time (minutes)	Temperature (°C)	
1 ^b	1	1	−1	−1	−1	
	2	1	1	1	−1	
	3	1	1	−1	1	
	4	1	−1	1	1	
	5	1	0	0	0	
	6	1	0	0	0	
	7	2	1	−1	−1	−1
	8	2	−1	1	1	−1
	9	2	−1	−1	−1	1
	10	2	1	1	1	1
	11	2	0	0	0	0
	12	2	0	0	0	0
	13	3	−1	0	0	0
	14	3	1	0	0	0
	15	3	0	−1	0	0
	16	3	0	1	1	0
	17	3	0	0	0	−1
	18	3	0	0	0	1
	19	3	0	0	0	0
	20	3	0	0	0	0

Factors points represent by coded values: −1 = Low level; 0 = Centre point; +1 = High level. ^a Intensity represents motion frequency (rpm) for control, amplitude (%) for direct thermosonication and power (kW) for indirect thermosonication. ^b Each batch of fruits was replicated three times.

2.4. Response Analyses

The responses evaluated were the percentage change of juice yield, AA, and TSS content from the original fruit pulp-distilled water mixture before extraction process. The calculation of percentage change was performed using Equation (3) for each evaluated response.

$$\text{Percentage change (\%)} = \frac{\text{Treated sample} - \text{Original fruit pulp and distilled water mixture}}{\text{Original fruit pulp and distilled water mixture}} \times 100 \quad (3)$$

The percentage of juice yield (% *w/w*) was calculated following Equation (4) [23,24] based on weight of fruit pulp, distilled water and total centrifuged juice of each sample in duplicate.

$$\text{Juice yield (\%)} = \frac{\text{Weight of supernatant} - \text{Weight of distilled water}}{\text{Weight of fruit pulp}} \times 100 \quad (4)$$

AA content was measured using the 2,6-dichlorophenol-indophenol visual titration method [11]. A 10 mL juice sample was brought to a 100 mL volume with 3% metaphosphoric acid prior to titration with a 10 mL metaphosphoric acid extract of the sample with 2,6-dichlorophenol-indophenol to the pink end-point. AA content was calculated following Equation (5) and averaged from quadruplicate samples.

$$\text{Ascorbic acid content (mg/100mL)} = \frac{\text{Titre} \times \text{Dye factor} \times \text{Volume made up} \times 100}{\text{Aliquot of extract taken for estimation} \times \text{Weight of sample taken for estimation}} \quad (5)$$

TSS content was determined using a digital refractometer (PAL-Alpha, Atago, Bellevue, WA, USA) and reported as degree Brix (°Brix). The analysis for TSS was performed in triplicate.

3. Results and Discussion

3.1. Materials Characterisation

Table 2 shows the percentage of juice yield, AA, and TSS content of fresh pulp and fruit pulp mixture samples for guava, pomelo, and soursop. The AA and TSS content decreased by almost half from that of fresh fruit pulp after being mixed with distilled water in a ratio of one to one. The presented results are averages of all blocks.

Table 2. Properties ^a of fresh fruit pulps and control mixtures.

Response	Fresh Fruit Pulp			Pulp Mixture Sample		
	Guava	Pomelo	Soursop	Guava	Pomelo	Soursop
Juice yield (%)	ND	ND	ND	8.705 ±4.619	71.532 ±7.980	19.402 ±5.381
AA content (mg AA/100mL)	51.422 ±11.751	38.080 ±3.017	13.669 ±4.404	18.834 ±4.684	20.829 ±1.857	6.460 ±1.638
TSS content (°Brix)	8.024 ±1.594	10.648 ±0.466	15.026 ±0.868	3.231 ±0.601	5.156 ±0.211	6.109 ±0.501

^a Data are presented as the mean ± standard deviation. ND means not determined.

3.2. Response Surface Regression Analysis

Both the independent and dependent variables were fitted to full quadratic models, and the response surface regressions were generated to check the goodness of model fit. The standard deviation (S) is important for checking data distribution. The R^2 is important for measuring how much variation in the response is explained by the model. The adjusted regression (R^2_{adj}) is useful for comparing models with different numbers of predictors. The p -value of R^2 is useful for determining the relationship between dependent and independent variables, and the p -value of lack-of-fit indicates whether an adequate model has been chosen. A lower S value, p -value of R^2 less than 0.05 and higher R^2 , R^2_{adj} and p -value of lack of fit indicated a better data fit by the model. The R^2 can be small as long as the p -value of the regression coefficient is statistically significant ($p < 0.05$). The determination of S, R^2 , R^2_{adj} and p -value of lack of fit were, however, performed in the background when the model term reduction was performed.

Table 3 lists the final fitted models for all responses from direct and indirect thermosonication-assisted extraction procedure and the control after considering values of S, R^2 , R^2_{adj} , p -value of R^2 , and lack-of-fit. The best-fitted model was necessary to obtain true information on the effect of all three factors to each response. The models were improved by removing insignificant model terms using a backwards elimination procedure to make them easier to work with while maintaining the predictive efficiency [30]. The models' terms in Table 3 interprets the relationships among responses of juice yield, AA, and TSS content and input factors of intensity, time, and temperature for guava, pomelo, and soursop.

Table 3. Improved models for percentage change of juice yield, AA, and TSS contents.

Response	Model
Guava	
Control	$JY_{g,c} = -119.184 + 66.335\beta_{01} + 33.592\beta_{02} + 19.638\beta_{03} + 3.807\beta_{04} - 17.95\beta_{05} - 132.472\beta_{06} - 48.142\beta_{07} - 33.835\beta_{08} + \beta_{09} + 0.245t + 1.755T$ $AA_{g,c} = 28.994 - 11.878\beta_{01} - 12.248\beta_{02} - 11.257\beta_{03} - 2.836\beta_{04} + 1.024\beta_{05} + 24.340\beta_{06} + 22.026\beta_{07} - 6.916\beta_{08} + \beta_{09} + 0.265M - 0.194t - 0.182T - 0.003M^2 - 0.002MT + 0.005tT$ $TSS_{g,c} = 26.709 + 0.551\beta_{01} - 19.729\beta_{02} - 10.189\beta_{03} - 7.374\beta_{04} - 7.687\beta_{05} + 8.208\beta_{06} + 19.308\beta_{07} + 7.413\beta_{08} + \beta_{09} + 0.023M - 0.176t + 0.001T$

Table 3. Cont.

Response	Model
Direct thermo-sonication	$JY_{g,ds} = -358.544 + 29.421\beta_{01} + 42.911\beta_{02} + 33.138\beta_{03} + 75.117\beta_{04} + 19.311\beta_{05} - 80.813\beta_{06} - 53.193\beta_{07} - 30.769\beta_{08} + \beta_{09} - 4.454A + 20.147T + 0.032A^2 - 0.257T^2$
	$AA_{g,ds} = 1.967 - 4.092\beta_{01} - 4.647\beta_{02} + 2.543\beta_{03} - 9.729\beta_{04} - 5.947\beta_{05} + 12.754\beta_{06} + 19.029\beta_{07} - 9.351\beta_{08} + \beta_{09} + 0.192A + 1.125t$
	$TSS_{g,ds} = 1.849 + 9.301\beta_{01} - 12.067\beta_{02} - 3.032\beta_{03} - 5.049\beta_{04} - 2.751\beta_{05} + 1.509\beta_{06} + 4.093\beta_{07} + 2.321\beta_{08} + \beta_{09} + 0.382A + 0.529t - 0.002A^2$
Indirect thermo-sonication	$JY_{g,is} = -207.698 + 8.571\beta_{01} + 22.168\beta_{02} + 9.177\beta_{03} + 18.419\beta_{04} - 35.592\beta_{05} - 44.681\beta_{06} - 60.351\beta_{07} - 88.409\beta_{08} + \beta_{09} + 4.323T$
	$AA_{g,is} = 35.697 - 0.757\beta_{01} - 6.128\beta_{02} + 1.696\beta_{03} - 8.022\beta_{04} - 5.418\beta_{05} + 12.125\beta_{06} + 24.723\beta_{07} - 11.015\beta_{08} + \beta_{09} - 1.844t + 0.047t^2$
	$TSS_{g,is} = 59.548 + 2.596\beta_{01} - 15.611\beta_{02} - 8.043\beta_{03} - 6.927\beta_{04} - 3.599\beta_{05} + 9.601\beta_{06} + 11.603\beta_{07} + 2.356\beta_{08} + \beta_{09} - 23.038P - 1.082T + 6.491P^2 + 0.014T^2$
Pomelo	
Control	$JY_{p,c} = -14.473 + 1.021\beta_{01} - 11.193\beta_{02} - 8.285\beta_{03} - 7.267\beta_{04} - 10.846\beta_{05} + 13.429\beta_{06} - 4.978\beta_{07} + 4.132\beta_{08} + \beta_{09} + 0.368T$
	$AA_{p,c} = -6.706 + 1.924\beta_{01} - 2.790\beta_{02} + 5.741\beta_{03} - 3.565\beta_{04} - 8.983\beta_{05} + 4.753\beta_{06} + 0.193\beta_{07} - 0.752\beta_{08} + \beta_{09} + 0.0356t$
	$TSS_{p,c} = -4.672 - 0.739\beta_{01} + 0.410\beta_{02} - 1.101\beta_{03} - 0.531\beta_{04} + 3.331\beta_{05} + 1.204\beta_{06} - 0.425\beta_{07} - 0.328\beta_{08} + \beta_{09} + 0.005t + 0.221T - 0.002T^2$
Direct thermo-sonication	$JY_{p,ds} = 4.929 + 3.142\beta_{01} + 9.273\beta_{02} - 4.372\beta_{03} - 6.998\beta_{04} - 5.789\beta_{05} + 5.629\beta_{06} - 5.781\beta_{07} + 6.174\beta_{08} + \beta_{09} - 0.021A + 0.135t - 0.013At$
	$AA_{p,ds} = -23.401 + 3.475\beta_{01} + 1.600\beta_{02} + 5.993\beta_{03} - 4.219\beta_{04} - 9.351\beta_{05} + 0.359\beta_{06} - 0.648\beta_{07} - 0.691\beta_{08} + \beta_{09} + 0.067A + 0.016t + 0.929T - 0.009T^2 - 0.002AT$
	$TSS_{p,ds} = -0.730 - 0.184\beta_{01} - 0.070\beta_{02} - 1.784\beta_{03} - 0.796\beta_{04} + 3.026\beta_{05} + 1.182\beta_{06} + 0.682\beta_{07} + 0.524\beta_{08} + \beta_{09} + 0.008A + 0.034t + 0.029T + 0.003At$
Indirect thermo-sonication	$JY_{p,is} = -35.908 + 2.264\beta_{01} + 7.274\beta_{02} - 9.292\beta_{03} - 2.880\beta_{04} - 14.726\beta_{05} + 11.261\beta_{06} - 2.517\beta_{07} + 5.100\beta_{08} + \beta_{09} + 1.861T - 0.021T^2$
	$AA_{p,is} = 1.272 + 2.407\beta_{01} - 1.476\beta_{02} + 4.210\beta_{03} - 2.825\beta_{04} - 7.596\beta_{05} - 1.258\beta_{06} + 2.863\beta_{07} - 0.667\beta_{08} + \beta_{09} - 2.134P - 0.164T + 0.101PT$
	$TSS_{p,is} = -1.735 + 0.367\beta_{01} - 0.463\beta_{02} - 1.477\beta_{03} - 0.330\beta_{04} + 2.693\beta_{05} + 1.545\beta_{06} - 0.429\beta_{07} - 0.033\beta_{08} + \beta_{09} + 1.682P + 0.199t - 0.034T - 0.782P^2 - 0.004t^2 + 0.031PT$
Soursop	
Control	$JY_{s,c} = -98.879 - 9.461\beta_{01} - 40.967\beta_{02} - 28.190\beta_{03} + 39.719\beta_{04} - 20.356\beta_{05} + 0.347\beta_{06} + 2.809\beta_{07} + 10.248\beta_{08} + \beta_{09} + 0.272M + 0.197t + 1.456T$
	$AA_{s,c} = 6.471 + 14.336\beta_{01} - 22.515\beta_{02} + 8.432\beta_{03} + 24.046\beta_{04} - 12.567\beta_{05} + 1.852\beta_{06} - 5.9679\beta_{07} - 7.471\beta_{08} + \beta_{09} - 0.290T$
	$TSS_{s,c} = -6.729 - 2.236\beta_{01} + 7.774\beta_{02} - 9.679\beta_{03} + 21.366\beta_{04} - 6.394\beta_{05} - 6.120\beta_{06} - 8.946\beta_{07} + 7.293\beta_{08} + \beta_{09} + 0.001M + 0.414T + 0.001M^2 - 0.002MT$
Direct thermo-sonication	$JY_{s,ds} = -8.500 + 0.887\beta_{01} - 17.136\beta_{02} - 6.785\beta_{03} - 37.821\beta_{04} + 17.277\beta_{05} + 14.581\beta_{06} - 2.340\beta_{07} - 8.890\beta_{08} + \beta_{09} - 0.779A + 0.427T$
	$AA_{s,ds} = 17.871 + 5.324\beta_{01} - 23.631\beta_{02} + 18.792\beta_{03} + 14.569\beta_{04} - 13.571\beta_{05} + 21.751\beta_{06} - 13.381\beta_{07} - 3.718\beta_{08} + \beta_{09} - 0.576A + 0.005A^2$
	$TSS_{s,ds} = 9.100 - 3.037\beta_{01} + 6.608\beta_{02} - 9.097\beta_{03} + 13.090\beta_{04} - 6.514\beta_{05} - 6.467\beta_{06} - 6.879\beta_{07} + 10.683\beta_{08} + \beta_{09} - 0.152A + 0.002A^2$
Indirect thermo-sonication	$JY_{s,is} = -183.544 + 1.882\beta_{01} - 40.425\beta_{02} - 32.511\beta_{03} + 20.379\beta_{04} - 7.181\beta_{05} - 15.234\beta_{06} + 7.54\beta_{07} + 30.705\beta_{08} + \beta_{09} + 10.345t + 1.758T - 0.248t^2$
	$AA_{s,is} = 10.877 + 4.169\beta_{01} - 25.789\beta_{02} + 23.169\beta_{03} + 7.841\beta_{04} - 16.359\beta_{05} - 4.051\beta_{06} + 1.871\beta_{07} + 7.278\beta_{08} + \beta_{09} - 0.319T$
	$TSS_{s,is} = 1.909 - 1.125\beta_{01} + 7.76\beta_{02} - 10.196\beta_{03} + 13.617\beta_{04} - 7.685\beta_{05} - 4.491\beta_{06} - 7.662\beta_{07} + 10.642\beta_{08} + \beta_{09} - 7.420P + 0.362T + 4.191P^2 - 0.1400PT$

JY = juice yield; g = guava; p = pomelo; s = soursop; c = control; ds = direct thermo-sonication; is = indirect thermo-sonication; M = motion frequency; t = time; T = temperature; A = amplitude; P = power; β_{01} to β_{09} are the constant for blocks: at each block, one of them is equal to 1 for involved block, whereas the rest are equal to zero, except for β_{09} (Equation (2)).

3.3. Extraction Process Optimisation

For response optimisation, the combined goals of maximum increase in juice yield, AA, and TSS content for the studied range of all three input factors were satisfied by the conditions given in Table 4.

Table 4. Optimum values for extracting tropical fruit juices.

Factors	Guava	Pomelo	Soursop
Control			
Motion frequency (rpm)	20	NS	180
Time (minutes)	120	120	120
Temperature (°C)	55	55	55
Direct thermosonication			
Amplitude (%)	100	33	10
Time (minutes)	10	10	NS
Temperature (°C)	39	54	55
Indirect thermosonication			
Power (kW)	1	2.5	1
Time (minutes)	30	23	21
Temperature (°C)	55	54	55

NS means not significant.

Figure 3 shows the responses of the optimised method of guava juice extraction. The juice yield was affected by temperature linearly, where 47 °C was a point of change of the positive and negative juice yield percentage. It is believed that 47 °C is the cut-off temperature for water reactivity due to ultrasonic waves where trapped water molecules inside guava fruit tissue moved faster until they could break the cell walls for water release. Below 47 °C, the trapped water inside guava fruit tissue was not released and remained in the solid matter during centrifugation process. The AA content displayed a minimum increase after 20 min of extraction, whereas a minimum positive change of TSS content occurred in the middle range of the studied temperatures and power levels.

Figure 4 illustrates responses of optimised method of pomelo juice extraction, where temperatures above 28 °C were effective in increasing juice yield. Juice yield started to decrease drastically above 42 °C until the investigated temperature of 55 °C, where the temperature was high and water loss occurred due to evaporation. The AA content increased under a combination of high power and temperature, at 2.3 kW and a temperature of 45 °C. The change of TSS content was influenced by all three factors of power, time, and temperature. The combination of high power, time, and temperature provided minimal increase in TSS content. The highest range of TSS content increment of 2 to 2.5% occurred at high power as well as a short time and low temperature.

Figure 5 illustrates responses of optimised method of soursop juice extraction. Juice yield increased when the amplitude was low and temperature was high. Amplitude affected both the AA and TSS content, and they displayed positive changes for the studied amplitude range. The minimum increase in AA content occurred at an amplitude of 60%, whereas the minimum increase in TSS content occurred at 38% amplitude. The AA content was high when low amplitude was applied, whereas high TSS content occurred at high amplitude.

The sonication methods were able to increase AA content in all three fruit juices via removal of dissolved oxygen which favoured decomposition of AA during cavitation [31], whereas the negative change of AA content in pomelo juice was due to degrading of AA in acid solutions [32]. The content of TSS of all three fruit juices extracted using optimised method was greatly affected by heat and/or intensity of direct and indirect ultrasound systems. These factors were also found to be effective in the extraction of mayhaw fruit juice [33].

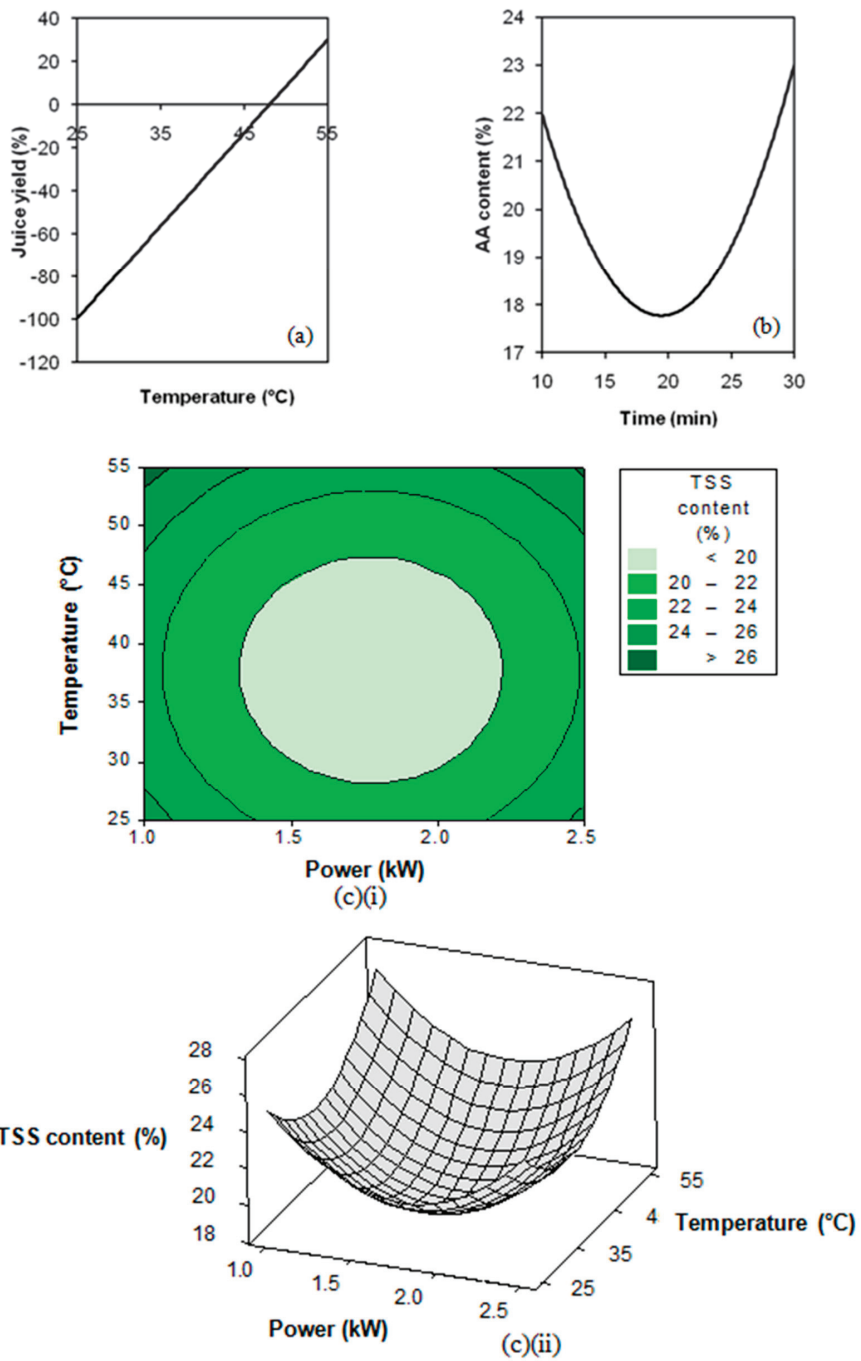


Figure 3. Plots of indirect thermosonication-assisted guava juice extraction responses. (a) Main effect plot of juice yield, (b) Main effect plot of AA content, (c) (i) 3D contour plot and (ii) 3D surface plot of TSS content.

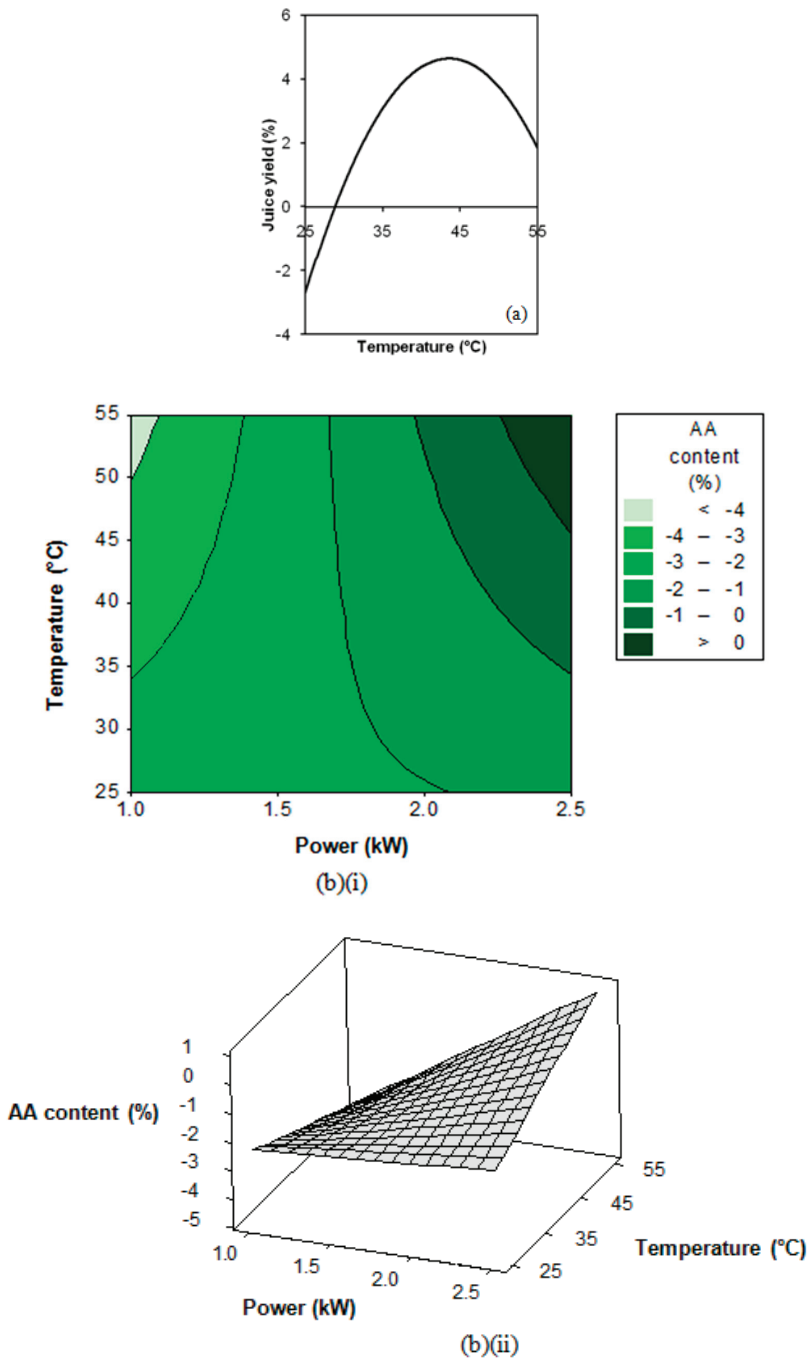


Figure 4. Cont.

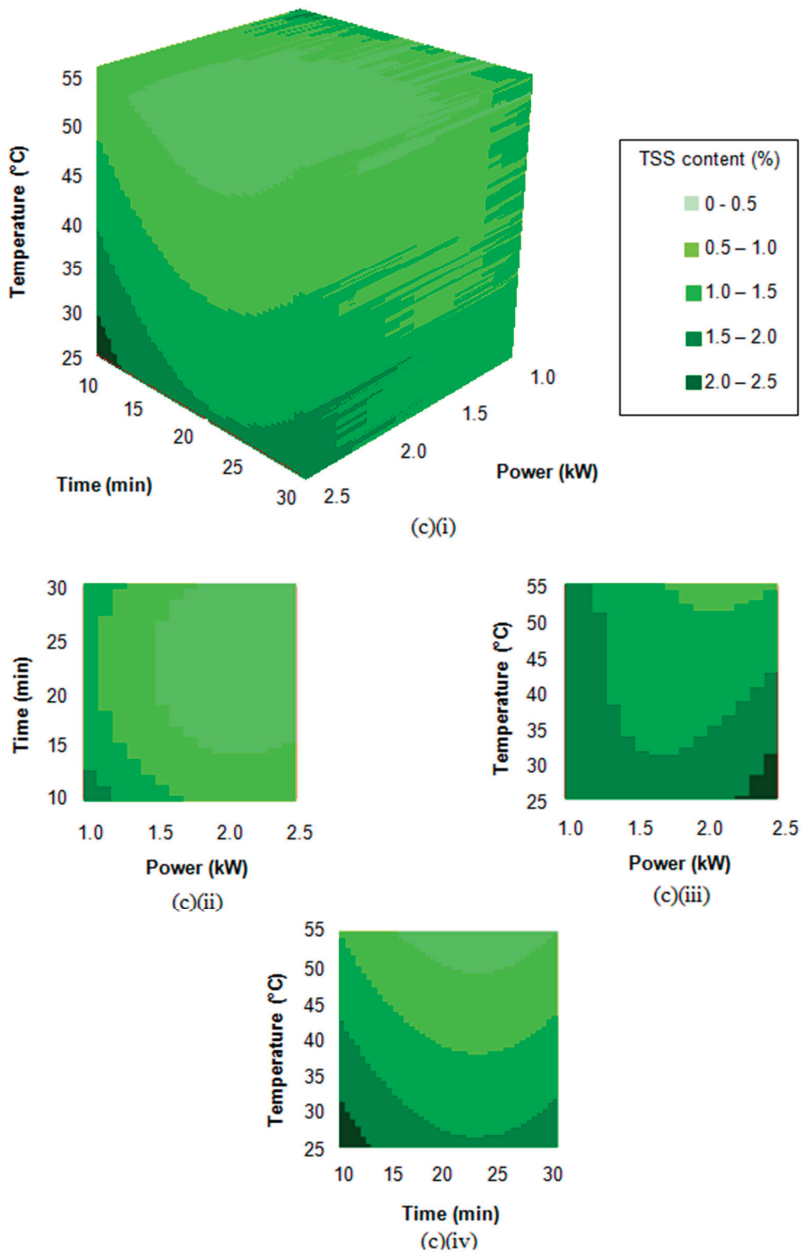


Figure 4. Plots of indirect thermosonication-assisted pomelo juice extraction responses. Plots of indirect thermosonication-assisted pomelo juice extraction responses. (a) Main effect plot of juice yield. (b) (i) 3D contour plot and (ii) 3D surface plot of AA content. (c) (i) 4D surface plot, (ii) 4D power-time contour plot, (iii) 4D power-temperature contour plot and (iv) 4D time-temperature contour plot of TSS content.

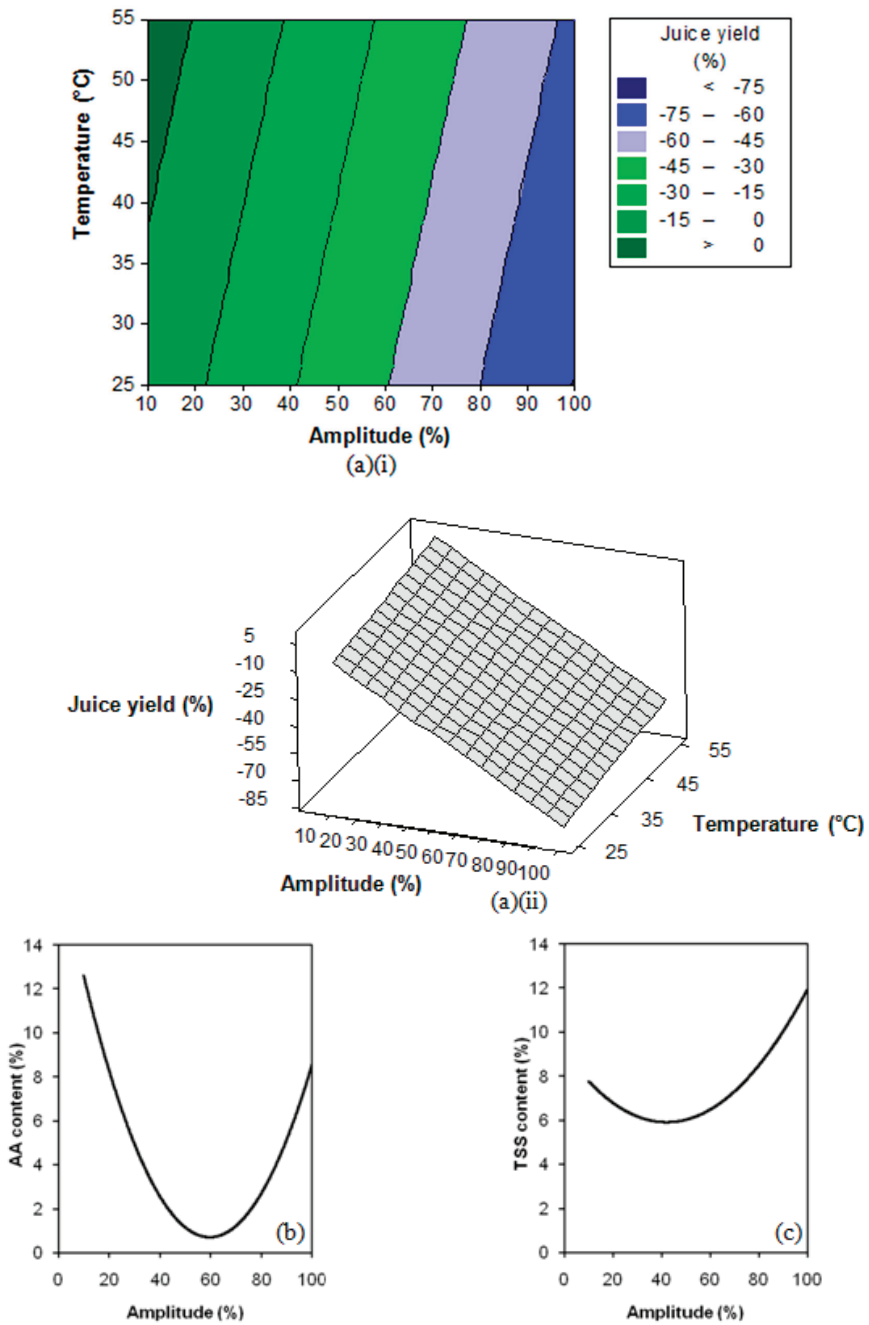


Figure 5. Plots of direct thermosonication-assisted soursop juice extraction responses. (a) (i) 3D contour plot and (ii) 3D surface plot of juice yield, (b) Main effect plot of AA content and (c) Main effect plot of TSS content.

3.4. Adequacy of Models and Verification

The adequacy of the models to predict optimum combined responses was validated experimentally using optimum conditions listed in Table 4. Table 5 shows that the trends and sequences were reasonably close between the predicted and experimental. The indirect thermosonication method was chosen for extracting guava juice because it achieved the highest increases in juice yield and TSS content. The indirect thermosonication method was also good for extracting pomelo juice as all response variables displayed positive trends as the other two methods presented decrease in AA content. The juice yield obtained via indirect thermosonication, however, had lower juice yield than the control. For extraction of soursop juice, the direct thermosonication method was suitable because it achieved a positive change of AA content as compared with the other two methods. A lower value of juice yield and TSS content increase was acceptable as long as AA content did not degrade, because it is the main nutrient that needs to be preserved in fruit juice production. AA also plays a role as an antioxidant, and it is an unstable compound that can degrade easily under inappropriate conditions [32].

Table 5. Predicted and experimental optimal responses of guava, pomelo, and soursop extraction.

Parameters Changes (%)	Control		Direct Thermosonication		Indirect Thermosonication	
	Predicted	Experiment	Predicted	Experiment	Predicted	Experiment
Guava						
Juice yield	6.7	7.6	−85.0	−79.3	30.1	28.1
AA content	22.9	25.1	32.4	32.5	23.0	27.1
TSS content	25.7	26.5	26.3	25.9	26.8	27.4
Pomelo						
Juice yield	5.8	8.7	1.3	0.6	2.4	3.7
AA content	−2.4	−3.5	−1.1	−2.5	0.7	1.2
TSS content	1.5	1.7	2.6	2.1	2.2	3.4
Soursop						
Juice yield	53.6	48.3	7.2	9.2	21.0	20.8
AA content	−9.5	−8.8	12.6	14.7	−6.7	−5.1
TSS content	22.1	25.2	7.8	7.7	10.9	11.5

Bold fonts indicate optimised extraction.

4. Conclusions

The blocked face-centred central composite design was suitable for tropical fruit juice extraction optimisation because blocking helps to control the variations of the fruits' properties. Based on advantages of extraction time reduction and prevention of AA content loss, ultrasound-assisted extraction methods were found to be helpful in the studies of three difficult-to-extract fruit juices. The best method for guava juice extraction was indirect thermosonication at 1 kW using distilled water incubated at 55 °C for 30 min. The indirect thermosonication was also good for extracting pomelo juice at 2.5 kW with water incubation temperature of 54 °C for 23 min. Extraction of soursop juice was suitable via direct thermosonication at 10% amplitude with distilled water at 55 °C for 2 to 10 min.

Author Contributions: N.A. designed the experiments, collected and analyzed the data, and wrote the manuscript. N.L.C. conceptualized the study, supervised the research, edited, and revised the manuscript. All authors have read and agreed to the published version of the manuscript.

Funding: The study was funded by the Malaysian Ministry of Higher Education's Fundamental Research Grant Scheme with project number 02-10-10-929FR.

Conflicts of Interest: The authors declare no conflict of interest.

References

- Atawodi, S. Nigerian foodstuffs with prostate cancer chemopreventive polyphenols. *Infect. Agents Cancer*. **2011**, *6* (Suppl. 2), S9. [CrossRef]
- Van Breemen, R.B.; Pajkovic, N. Multitargeted therapy of cancer by lycopene. *Cancer Lett.* **2008**, *269*, 339–351. [CrossRef] [PubMed]
- Worrell, D.B.; Carrington, C.M.S.; Huber, D.J. Growth, maturation and ripening of soursop (*Annona muricata* L.) fruit. *Sci. Horticult. Amsterdam*. **1994**, *57*, 7–15. [CrossRef]
- Ko, Y.-M.; Wu, T.-Y.; Wu, Y.-C.; Chang, F.-R.; Guh, J.-Y.; Chuang, L.-Y. Annonacin induces cell cycle-dependent growth arrest and apoptosis in estrogen receptor- α -related pathways in MCF-7 cells. *J. Ethnopharmacol.* **2011**, *137*, 1283–1290. [CrossRef] [PubMed]
- Chek Zaini, H.; Zaiton, H.; Zanariah, C.W.; Sakinah, N. High Fiber Cookies Made from Pink Guava (*Psidium guajava*) De-canter/Agro Waste. 2020. Available online: https://www.doc-developpement-durable.org/file/Arbres-Fruitiers/FICHES_ARBRES/goyavier_Psidium%20guajava/High%20fiber%20cookies%20made%20from%20pink%20guava.pdf (accessed on 18 November 2020).
- Nwokocha, L.M.; Williams, P.A. New starches: Physicochemical properties of sweetsop (*Annona squamosa*) and soursop (*Annona muricata*) starches. *Carbohydr Polym.* **2009**, *78*, 462–468. [CrossRef]
- Economos, C.; Clay, W.D. Food, Nutrition and Agriculture: Nutritional and Health Benefits of Citrus Fruits. 1999. Available online: <http://www.fao.org/docrep/x2650T/x2650t03.htm> (accessed on 18 November 2020).
- Tiwari, B.K.; Muthukumarappan, K.; O'Donnell, C.P.; Cullen, P.J. Colour degradation and quality parameters of sonicated orange juice using response surface methodology. *LWT Food Sci. Technol.* **2008**, *41*, 1876–1883. [CrossRef]
- Adekunte, A.; Tiwari, B.K.; Scannell, A.; Cullen, P.J.; O'Donnell, C. Modelling of yeast inactivation in sonicated tomato juice. *Int. J. Food Microbiol.* **2010**, *137*, 116–120. [CrossRef] [PubMed]
- Adekunte, A.O.; Tiwari, B.K.; Cullen, P.J.; Scannell, A.G.M.; O'Donnell, C.P. Effect of sonication on colour, ascorbic acid and yeast inactivation in tomato juice. *Food Chem.* **2010**, *122*, 500–507. [CrossRef]
- Bhat, R.; Kamaruddin, N.S.B.C.; Min-Tze, L.; Karim, A.A. Sonication improves kasturi lime (*Citrus microcarpa*) juice quality. *Ultrason Sonochem.* **2011**, *18*, 1295–1300. [CrossRef]
- Tiwari, B.K.; O'Donnell, C.P.; Muthukumarappan, K.; Cullen, P.J. Effect of sonication on orange juice quality parameters during storage. *Int. J. Food Sci. Technol.* **2009**, *44*, 586–595. [CrossRef]
- Valero, M.; Recrosio, N.; Saura, D.; Muñoz, N.; Martí, N.; Lizama, V. Effects of ultrasonic treatments in orange juice processing. *J. Food Eng.* **2007**, *80*, 509–516. [CrossRef]
- Chemat, F.; Zill, E.H.; Khan, M.K. Applications of ultrasound in food technology: Processing, preservation and extraction. *Ultrason Sonochem.* **2011**, *18*, 813–835. [CrossRef] [PubMed]
- Koshani, R.; Ziaee, E.; Niakousari, M.; Golmakani, M.T. Optimization of thermal and thermosonication treatments on pectin methyl esterase inactivation of sour orange juice (*Citrus aurantium*). *J. Food Process. Preserv.* **2014**, *39*, 567–573. [CrossRef]
- Tribess, T.B.; Tadini, C.C. Inactivation kinetics of pectin methylesterase in orange juice as a function of pH and temperature/time process conditions. *J. Sci. Food Agric.* **2006**, *86*, 1328–1335. [CrossRef]
- de Carvalho, J.M.; Maia, G.A.; da Fonseca, A.V.V.; de Sousa, P.H.M.; Rodrigues, S. Effect of processing on physicochemical composition, bioactive compounds and enzymatic activity of yellow mombin (*Spondias mombin* L.) tropical juice. *J. Food Sci. Technol.* **2013**, *52*, 1182–1187. [CrossRef]
- Wu, J.; Gamage, T.V.; Vilku, K.S.; Simons, L.K.; Mawson, R. Effect of thermosonication on quality improvement of tomato juice. *Innov. Food Sci. Emerg. Technol.* **2008**, *9*, 86–195. [CrossRef]
- Terefe, N.S.; Gamage, M.; Vilku, K.; Simons, L.; Mawson, R.; Versteeg, C. The kinetics of inactivation of pectin methylesterase and polygalacturonase in tomato juice by thermosonication. *Food Chem.* **2009**, *117*, 20–27. [CrossRef]
- Torres, E.F.; Bayarri, S.; Sampedro, F.; Martinez, A.; Carbonell, J.V. Improvement of the fresh taste intensity of processed clementine juice by separate pasteurization of its serum and pulp. *Food Sci. Technol. Int.* **2008**, *14*, 525–529. [CrossRef]
- Mason, T.J.; Paniwnyk, L.; Lorimer, J.P. The uses of ultrasound in food technology. *Ultrason Sonochem.* **1996**, *3*, S253–S260. [CrossRef]
- Ofori-Boateng, C.; Lee, K. Response surface optimization of ultrasonic-assisted extraction of carotenoids from oil palm (*Elaeis guineensis* Jacq.) fronds. *Food Sci. Nutr.* **2013**, *1*, 209–221. [CrossRef]
- Sin, H.N.; Yusof, S.; Abdul Hamid, N.S.; Rahman, R. Optimization of hot water extraction for sapodilla juice using response surface methodology. *J. Food Eng.* **2006**, *74*, 352–358. [CrossRef]
- Lee, W.C.; Yusof, S.; Hamid, N.S.A.; Baharin, B.S. Optimizing conditions for hot water extraction of banana juice using response surface methodology (RSM). *J. Food Eng.* **2006**, *75*, 473–479. [CrossRef]
- Cendres, A.; Chemat, F.; Maingonnat, J.F.; Renard, C.M.G.C. An innovative process for extraction of fruit juice using microwave heating. *LWT Food Sci. Technol.* **2011**, *44*, 1035–1041. [CrossRef]
- Chin, L.N.; Tan, C.M.; Pa, N.F.; Yusof, Y.A. Method and Apparatus for High Intensity Ultrasonic Treatment of Baking Materials. U.S. Patent 2013/01894.07 A1, 25 July 2013.
- Carley, K.M.; Kamneva, N.Y.; Reminga, J. *Response Surface Methodology*; Technical Report CMU-ISRI-04-136; CASOS: Pittsburgh, PA, USA, 2004.
- Khuri, A.I.; Mukhopadhyay, S. Response surface methodology. *Wires Comput. Stat.* **2010**, *2*, 128–149. [CrossRef]
- Lenth, R.V. Response-surface methods in R using RSM. *J. Stat. Softw.* **2009**, *32*, 1–17. [CrossRef]

30. Noordin, M.Y.; Venkatesh, V.C.; Sharif, S.; Elting, S.; Abdullah, A. Application of response surface methodology in describing the performance of coated carbide tools when turning AISI 1045 steel. *J. Mater. Process Technol.* **2004**, *145*, 46–58. [CrossRef]
31. Cheng, L.H.; Soh, C.Y.; Liew, S.C.; Teh, F.F. Effects of sonication and carbonation on guava juice quality. *Food Chem.* **2007**, *104*, 1396–1401. [CrossRef]
32. Burdurlu, H.S.; Koca, N.; Karadeniz, F. Degradation of vitamin C in citrus juice concentrates during storage. *J. Food Eng.* **2006**, *74*, 211–216. [CrossRef]
33. Trappey, A.F.; Johnson, C.E.; Wilson, P.W. Characterization of juice extraction methods utilizing fresh mayhaw (*Crataegus opaca* Hook.) fruit. *Int. J. Fruit Sci.* **2008**, *8*, 318–331. [CrossRef]

Article

Volatile Esters and Fusel Alcohol Concentrations in Beer Optimized by Modulation of Main Fermentation Parameters in an Industrial Plant

Krzysztof Kucharczyk ^{1,*}, Krzysztof Żyła ² and Tadeusz Tuszyński ¹

¹ Krakow School of Health Promotion, 31-158 Krakow, Poland; t.tuszynski@kwspz.pl

² Department of Food Biotechnology, Food Technology, University of Agriculture, 30-149 Krakow, Poland; k.zyła@ur.krakow.pl

* Correspondence: krzysztof.kucharczyk1@googlemail.com; Tel.: +48-885-156-451

Received: 9 June 2020; Accepted: 28 June 2020; Published: 30 June 2020

Abstract: Contents of selected volatile esters and fusel alcohols and their relation to the sensory quality of a bottom-fermented lager beer fermented under high-gravity conditions (15.5 °P) were analyzed using response surface methodology (RSM, Box–Behnken design). The influence of various pitching rates (6–10 mln cells/mL), aeration levels (8–12 mgO₂/mL), times (4.5–13.5 h) of filling CCTs (cylindroconical fermentation tanks; 3850 hL), and fermentation temperatures (8.5–11.5 °C) on the contents of selected esters, as well as on concentrations of amyl alcohols and on the sum of higher alcohols in beer, was determined in a commercial brewery fermentation plant. Beers produced throughout the experiments met or exceeded all criteria established for a commercial, marketed beer. Statistical analyses of the results revealed that within the studied ranges of process parameters, models with diversified significance described the concentrations of volatiles in beer. The multiple response optimization procedure analyses showed that the values of process parameters that minimized higher alcohols in beer (97.9 mg/L) and maximized its ethyl acetate (22.0 mg/L) and isoamyl acetate (2.09 mg/L) contents, as well as maximized the sensory quality of beer, (66.4 pts) were the following: Pitching rate 10 mln cells per mL; fermentation temperature 11.5 °C; aeration level 8.8 mg/L; and CCT filling time 4.5 h.

Keywords: beer brewing; volatile compounds; sensory quality; industrial plant; manufacturing scale; process optimization; response surface methodology

1. Introduction

Beer forms a complex chemical matrix of components that result from numerous metabolic pathways and chemical reactions. He et al. [1] underlined the importance of interaction among various biosynthetic pathways during the fermentation process in a living yeast cell. The acceptable sensory properties of beer depend greatly on the control of the formation of desired volatile compounds during fermentation that is also important for achieving a repeatable and balanced composition of the finished product [2].

Many compounds contribute to the flavor and aroma of beer. Due to the low taste thresholds for some of these substances, supposedly insignificant variations in their concentrations may produce an entirely different flavor of the final beer. Thus, for pilsner beer, at least twenty compounds are recognized as being important. These substances include several esters, fusel alcohols, vicinal diketones, and organic sulfur compounds [3]. The latter two, which are present in a fresh, ‘green’ beer, are significantly reduced during lagering. The following compounds are considered the most important: Isoamyl alcohol, ethyl acetate, isoamyl acetate, ethyl hexanoate, and ethyl octanoate. However, it would be an over-simplification to characterize the taste of beer just by the analytical determination

of these five compounds. In practice, the flavor of one compound may easily be suppressed by high concentrations of other substances [4].

High-gravity brewing (HGB) employs worts at higher than normal concentrations (15–20 °P original gravity), and, therefore, to obtain beer of sales-gravity, dilution with deaerated water is required at a later stage of processing. HGB increases production without significant expansion of brewing, fermenting, and storage facilities. Therefore, the principal advantage of HGB is the more efficient use of the existing processes. The disadvantages of HGB include decreased foam stability of beer, a variety of stress effects on yeast, and problems with desirable flavor. Finally, difficulties encountered in HGB include the inability of yeast to completely utilize maltotriose, which is the most abundant fermentable sugar in the wort. This is particularly the case during beer production by continuous fermentation of wort under HGB conditions [5].

A factor of great importance in determining the flavor of beer is the composition of the wort. Small differences in wort composition can exert significant effects on the flavor of the resulting beer. Amino acids are among the wort components that may significantly influence beer flavor [6]. Volatile esters introduce fruity flavor notes and are considered highly positive flavor attributes of a fresh beer. Isoamyl acetate, for example, is a source of a banana-like flavor. However, during storage, the concentration of this ester can decrease to the levels that are well below its threshold level [7,8]. Among the volatiles, acetate esters like ethyl acetate, hexyl acetate, isoamyl acetate, and 2-phenylethyl acetate are recognized as a special and characteristic group of important flavor compounds of a lager beer [9].

Aroma-active esters are synthesized by yeast during fermentation in the intracellular space. It has been demonstrated that the esters partition between cells and fermenting medium depends mainly on yeast species and on the fermentation temperature. A higher proportion of esters that remain inside the cells are characteristic for lager yeasts (*Saccharomyces pastorianus*, *Saccharomyces carlsbergensis*, *Saccharomyces uvarum*) [10]. Moonjai with co-workers [11] reported that by the enrichment of wort with lipids, and also by increasing the level of wort aeration, synthesis of volatile esters was drastically reduced. The authors investigated the influence of the addition of unsaturated fatty acid (mainly linoleic acid) to harvested yeast prior to pitching, on the fermentation yield and on the synthesis of volatile flavor compounds, and found that the supplemented pitching yeast showed growth, attenuation, and ethanol formation profiles similar to those obtained with unsupplemented yeast in pre-aerated medium, which simulated the normal brewing practice. Compared to fermentations with unsaturated fatty acids added to the medium, the supplemented cropped yeast did not induce a reduction in acetate ester synthesis. Results indicated that the supplementation of cropped yeast with unsaturated fatty acids could be an interesting alternative to wort oxygenation to restore the optimal membrane fluidity of the yeast. Renger et al. [4], in turn, showed the importance of carbon dioxide for the growth and metabolism of fermenting yeasts. The excess of carbon dioxide had an inhibiting effect on the production of aroma compounds.

Amyl alcohol is reported to be the most present and quantitatively significant flavor compound of the higher alcohols group. Amyl, and its active isomer isoamyl alcohols, are, most of the time, described as amyl alcohols. These compounds affect beer drinkability as beer flavor is described by sensory analysis as “heavier” when the content of amyl alcohol increases. Another higher alcohol that affects the sensory quality of beer is isobutyl alcohol [10]. It may be stressed, therefore, that for the proper sensory characteristics of beer, the process optimization must ensure the maximization of ester concentration and, particularly, ethyl acetate that, in the right amounts, gives beer the fruity aroma impression, and also isoamyl acetate, which, in turn, produces a banana scent. On the other hand, however, the well-chosen process parameters should minimize the content of higher alcohols that generate the undesirable fragrances like alcohol, sweet, or a solvent scent.

Trelea et al. [12] presented an intriguing possibility of reducing the fermentation time without changing the aroma profile of beer volatile components. A few groups of researchers successfully developed predictive experimental models that incorporated process parameters for modulating the

biosynthesis of flavor-active compounds in the fermenting yeast cells [3,13–15], but none of these endeavors were performed utilizing a commercial fermentation plant.

Currently, statistical process control (SPC) techniques are increasingly being used in brewing. They allow controlled process maintenance with a very high repeatability of the process and the desired quality of the final beer. The most optimal fermentation process parameters developed by response surface methodology (RSM) guarantee the obtaining of a high stability of processes calculated by SPC. The production of beer on an industrial scale often employs constant values of temperature and regular pressure profiles. For many reasons, determination of optimal process parameters for a particular production plant is crucial. The key fermentation parameters of bottom-fermented lager beers brewed on an industrial scale can be successfully predicted, modulated, and controlled by applying the RSM methodology so that appropriate flavor and aroma compounds are synthesized at optimal concentrations.

The purpose of the current study was to apply the RSM methodology by developing empirical models to modulate the values of the fermentation temperature, pitching rate, aeration levels, and different times of filling the cylindroconical fermentation tanks in the industrial brewery, to control and predict the concentrations of volatile esters and fusel alcohols in a lager beer. The variations in the key process parameters had been limited, however, to be acceptable and ready for the market, and lager beer was also produced under experimental regimes. Yet, another aim of the study was to optimize the flavor and aroma compound concentrations to levels that ensure the best sensory quality of the final beer.

2. Materials and Methods

2.1. Experimental Setup

The process of beer fermentation and maturation was investigated in industrial cylindroconical fermentation tanks (CCT—cylindroconical fermentation tanks; gross volume 3850 hL with diameter 5.15 m and height 20 m) with different times (4.5–13.5 h) of filling CCTs. The experiments were carried out in a big commercial brewery in Poland. Each fermentation tank was filled with three brews (wort volume in every CCT—3090 hL). HGB worts (high gravity 15.5 °P) were prepared from the same batch of malt under identical technological conditions. A pilsener-type malt from two malt houses was used throughout the experiments. The process of infusion mashing-in took place within the standard scale of 60–76 °C. Sample collection started after filling the CCT and was continued during the following 18 days of the production cycle. Sampling from a tank was performed using a sampling device equipped with an installed small pump working in a closed loop system, which let us take samples of fermenting wort and of matured beer. Samples of beer were taken from CCTs at a point located above the conical part, 5 m from the bottom of the tank. *Saccharomyces pastorianus* brewers W34/70 yeast strain from Weihenstephan TUM was used for the fermentation. Total fermentation time lasted between 7 and 9 days depending on the selected fermentation parameters. The process of maturation was divided into two phases: Warm maturation and lagering. Yeast for experiments was cropped from CCTs during the 5th day of maturation (at temperature 13 °C). The warm maturation lasted 5 days at a temperature of 13 °C. After cropping, the yeast in the YST (yeast stored tank) was stored for a maximum of 4 days at temperatures of 1.3–1.8 °C with an overpressure of 0.05 bar. After cropping, the beer was cooled down to −0.7 °C (to phase of lagering). Yeast was pitched for first brews, using the fully automatic high-precision ABER system for rate control. Worts were aerated by compressed, sterile air during transfer to each CCT, with an identical intensity of 10 mg O₂/L wort. The processes of fermentation and maturation were carried out in the same technological conditions. The yeast growth ranged from volume factor 2.60 to 4.0 in relation to the initial pitching rate, and the Free Amino Acids (FAN) consumption varied from 112 to 144 mg/L.

2.2. Analytical Procedures

Extract marking was performed using an automatic wort and beer analyzer (Beer Analyzer DMA 4500+ Anton Paar, Graz, Austria), at 20 °C, and the specific weight was measured using an oscillating densitometer. The Tabarié formula was the basis for 'Alcolyzer' beer calculations [16].

Qualitative and quantitative analysis of volatile components (the identification was done on the basis of retention time) was performed using gas chromatograph GC 8000 (Fisons Instruments, Ipswich, UK) fitted with a flame ionization detector GC-FID and detector GC-ECD for detection of diacetyl, 2,3-pentanedione. The column temperature was kept at 45 °C for 10 min, increased to 120 °C at 5 °C/min, and then held at that temperature for 8 min, eventually being lowered to 45 °C at 15 °C/min. The temperature of the injection zone was fixed at 140 °C. The carrier gas was helium at a pressure of 65 kPa, with a flow of 4–6 mL/min. Injection of samples (0.75 mL) was performed with an HS-800 autosampler. The sample annealing temperature was 40 °C for 40 min. The temperature of the autosampler syringe was 60 °C. Concentrations were calculated using a quantitative computer program based on the calculated peak area. Selected components of beer were determined using surfaces under the curves produced relative to internal standards. The internal standard method involved introducing an internal standard to a test sample and determining the relationship between the peak area ratio of the test substance and the internal standard and the mass ratio of the test substance and the internal standard. The standards had to be well separated from other peaks in the sample and have a similar concentration as the substance to be determined. The sample of beer, with a volume of 2.5 mL, was placed in a vial and conditioned at 40 °C for 40 min to equilibrate the liquid and gas phase (head space method). The capillary column DB-WAX (dimensions: 60 m long, 0.53 mm internal diameter, and 1 µm thick) packed with polar polyethylene glycol was used for the separation. A mixture of 3-panthenol and n-butanol was used as an internal standard for the determination of esters, amyl alcohols, and the sum of higher alcohols. The chromatograph was calibrated once a month. Before and after each series of measurements, a comparative analysis was carried out with a beer sample used as a control (reference) batch.

2.3. Sensory Analysis

Sensory evaluation of bottling beer used a comparison test, with the test sample compared to the reference beer profile. The beer was tested in black glasses. Profile tests involved the evaluation of attributes of the beer, including fruity aroma esters, hops, bitterness, sulfur compounds, sweetness, acidity, fullness, balance, and flavor. The sensory analysis panel consisted of nine employees from the production, analysis, and technology departments whose standard job was to routinely assess the sensory quality of beer. The sample coding procedures used ensured objective evaluations. The sensory quality beer was evaluated using a gradation scale from 50 to 75 points where 70–75 points meant a very good or perfect example of beer; 65–69 points represented good, clean, and fresh beer; 60–64 points were allocated to neither good nor bad beer with low levels of undesirable flavors and aromas, 55–59 points - beer with one or more intense undesirable flavors and aromas, and 50–54 points represented a very bad - unfit for consumption, wrong product.

2.4. Statistical Analyses

Processing factors were tested using the Experimental Design Module of the Statgraphics Centurion XVII ver. 17.1.12 (Professional Edition statistical software, Statpoint Technologies, Inc., Warrenton, Virginia).

2.4.1. Optimization of The Volatiles and Sensory Quality of Beer

The influences of process parameters on the volatile concentrations and on the sensory quality of beer were studied using a fully randomized Box–Behnken design with four factors at three levels each and two blocks, including 3 centerpoints per block, which yielded 54 experimental runs and

38 degrees of freedom. There were two blocks with repetitions (all experiments were performed twice) serving as a block. The central composite design could not be used in this work, because it would generate experimental values of process parameters, resulting in the production of abnormal beer, not acceptable on the market. Table 1 illustrates the coded and actual values of the input variables (fermentation process parameters). Experimental worts were fermented using various pitching rates (6–10 mln cells/mL), aeration levels (8–12 mg/mL), times (4.5–13.5 h) of filling CCTs (cylindroconical fermentation tanks; 3850 hL), and fermentation temperatures (8.5–11.5 °C). The manufactured beer was then subjected to the volatile concentration and sensory quality analyses (measured responses). The relationship between the measured exposures and fermentation process parameters was expressed using second-order polynomial equations:

$$y = \beta_0 + \beta_1x_1 + \beta_2x_2 + \beta_3x_3 + \beta_4x_4 + \beta_{11}x_1^2 + \beta_{22}x_2^2 + \beta_{33}x_3^2 + \beta_{44}x_4^2 + \beta_{12}x_1x_2 + \beta_{13}x_1x_3 + \beta_{23}x_2x_3 + \beta_{14}x_1x_4 + \beta_{24}x_2x_4 + \beta_{34}x_3x_4 + \gamma$$

where y is a volatile concentration or sensory quality; x_1 is the pitching rate (mln yeast cells/mL of wort); x_2 is the fermentation temperature (°C); x_3 is the aeration level (mg O₂/L); x_4 is the total time used for CCT filling (h); β_0 is the intercept coefficient; β_{1-4} are the linear coefficients; β_{11} , β_{22} , β_{33} , and β_{44} are the quadratic coefficients; and β_{12} , β_{13} , β_{23} , β_{14} , β_{24} , and β_{34} are the interaction coefficients, whereas γ is the block effect.

Table 1. Coded and actual values of the variables for the Box–Behenken design.

Independent Variables	Units	Symbol	Coded Levels		
Pitching rate	Mln cells/mL	x_1	−1	0	+1
Fermentation temperature	°C	x_2	8.5	10	11.5
Aeration level	mg/L	x_3	8	10	12
Total time of CCT filling	h	x_4	4.5	9	13.5

The established models were subjected to ANOVA and Pareto chart (data not shown) analyses, and the non-significant ($p > 0.05$) components were removed from the models. To evaluate the statistical significance of the second-order polynomial model, the coefficient of determination (R^2) and the probability of the lack-of-fit values were calculated.

2.4.2. Multiple Response Optimization Procedures

The module Multiple Response Analysis of the Statgraphics Centurion XVII ver. 17.1.12 (Professional Edition statistical software, Statpoint Technologies, Inc., Warrenton, Virginia) was used to establish the values of technological parameters that simultaneously optimized the content of a few measured responses.

3. Results and Discussion

3.1. Model Fitting

A significant influence of the process parameters with the coefficient of determination exceeding 0.70 on the ethyl acetate, isoamyl acetate, higher alcohols, amyl alcohols, and isobutanol concentrations was observed, but in the case of methanol, 1-propanol, ethyl formate, ethyl capronate, and ethyl propionate, lower values of R^2 were calculated within the studied ranges of the pitching rate, fermentation temperature, aeration level, and times of CCT filling (Table 2). The volatiles with a determination coefficient lower than 0.60 were excluded from further optimization.

Table 2. Analysis of variance of volatile esters and fusel alcohols: Significance of model components and assessment of adequacy of the models.

Dependent Parameter	Analysis of Variance						Significant Components of the Model	
	R ²	Lack-of-Fit	x ₁	x ₂	x ₃	x ₄		
	Probability							
Higher alcohols	0.91	0.932	0.022	0.0193	Ns	0.0003	0.0473	x ₃ x ₄
Amyl alcohols	0.91	0.808	0.027	0.025	Ns	0.0001	0.0473	x ₃ x ₄
Methanol	0.53	0.578	0.0307	ns	Ns	0.0400	0.0327	blocks
Isobutanol	0.68	0.358	0.0039	0.0461	Ns	0.035	0.0061	x ₁ ²
1-propanol	0.30	0.000	0.0001	0.027	Ns	0.0001	0.0001	x ₁ ²
Ethyl acetate	0.89	0.967	0.0032	0.0019	Ns	ns	-	-
Isoamyl acetate	0.69	0.953	0.0298	0.0054	Ns	ns	-	-
Ethyl formiate	0.62	0.813	0.0356	ns	Ns	ns	0.0488	x ₁ x ₄
Ethyl capronate	0.56	0.0967	ns	ns	Ns	0.0247	-	-
Ethyl propionate	0.39	0.450	0.0179	0.0131	Ns	ns	-	-
		0.0951	0.0213	0.0012	0.0089	0.0272	0.0021	x ₁ ²
							0.0474	x ₁ x ₂
							0.0299	x ₁ x ₄
Sensory analysis	0.71						0.0040	x ₂ ²
							0.0021	x ₂ x ₃
							0.0102	x ₃ ²
							0.0384	x ₄ ²

3.2. Polynomial Equations for the Measured Responses

Ethyl acetate

Table 3 shows the analysis of variance for ethyl acetate content in matured beer after removing insignificant components from the model. The relationship between the only two significant factors and the predicted responses of ethyl acetate concentrations was modeled as follows:

$$y_1 = -1.295 + 0.850 x_1 + 1.293 x_2 \quad (1)$$

where y_1 denotes ethyl acetate concentration.

Table 3. Analysis of variance: the empirical model for predicting ethyl acetate.

Source	Sum of Squares	Df	Mean Square	F-Ratio	p-Value
x ₁	69.2920	1	69.2920	54.14	0.0000
x ₂	90.2682	1	90.2682	70.53	0.0000
blocks	0.0308	1	0.0308	0.02	0.8776
Lack-of-fit	24.1341	14	1.7239	1.35	0.2295
Pure error	46.0771	36	1.2799		
Total (correlation)	229.8020	53			

As shown in Table 3, small p values (<0.05) were observed for the constant, a linear term x_1 , and linear term x_2 , indicating that only pitching rate and fermentation temperature were the crucial process parameters affecting amounts of ethyl acetate in beer. The subsequent application of the established model to predict the process parameters optimal for ethyl acetate biosynthesis using the Optimize Response module revealed that over the studied range of process parameters, to achieve maximized ethyl acetate concentrations, the values of process parameters should be set to $x_1 = 10$, $x_2 = 11.5$, $x_3 = 10$, and $x_4 = 9$. Under these conditions, 22.07 mg/L of ethyl acetate was predicted to be synthesized, a value that can be perceived as an acceptable level of this volatile in beer. Verstrepen with co-workers [17], who reviewed the literature on wort specific gravity and wort sugar profiles, reported the problem of overproduction of acetate esters in the HGB.

There seems to be a general consensus in the literature, however, that with growing fermentation temperature, the biosynthesis of acetate esters is enhanced [12,15,17]. In the work of Lee and Davis [18], a 10-fold increase in pitching rate caused a two-fold increase in the concentration of ethyl acetate in beer that seems to be in line with the results of our studies. The data presented by other researchers, however, did not confirm these observations. Verbelen et al. [19] did not show changes in the content of ethyl acetate with increasing amounts of inoculum from 10 to 120 mln cells/mL. Similar findings were provided by Erten [20] who reported that, as a result of increasing yeast pitching rate from 1×10^7 to 1×10^8 cells/mL, the concentration of that volatile remained within the range of 13–14 mg/L and was not statistically significant. These discrepancies might mainly be attributed to differences in working volumes of the experimental fermentors used and, consequently, to differences in hydrostatic pressure that affected the metabolism of yeast.

Isoamyl acetate

Similarly to ethyl acetate, the analysis of variance for isoamyl acetate concentrations in beer revealed that yeast pitching rate and fermentation temperature significantly affected the biosynthesis of this ester (Table 4).

Table 4. Analysis of variance: the empirical model for predicting isoamyl acetate.

Source	Sum of Squares	Df	Mean Square	F-Ratio	p-Value
x_1	0.7245	1	0.7245	22.50	0.0000
x_2	1.9982	1	1.9982	62.05	0.0000
Blocks	0.0011	1	0.0011	0.03	0.8566
Lack-of-fit	0.5608	14	0.0400	1.24	0.2885
Pure error	1.1592	36	0.0322		
Total (correlation)	4.4437	53			

Linear in nature, a simple equation that links amounts of isoamyl acetate with process parameters was the following:

$$y_2 = -0.857 + 0.0869 x_1 + 0.192 x_2 \quad (2)$$

where y_2 denotes isoamyl acetate concentration in mg/L.

Maximizing the predicted isoamyl acetate concentrations by means of the Optimize Response module allowed us to achieve 2.22 mg of that volatile per liter of beer. The values of process parameters set at $x_1 = 10$, $x_2 = 11.5$, $x_3 = 10$, and $x_4 = 9$ were calculated as optimal for the highest ethyl acetate concentrations. Nakatani with co-workers [21] reported double the rate of isoamyl acetate synthesis, which resulted from rising fermentation temperature from 10 to 15 °C. Lima et al. [15] and Brown and Hammond [13] observed similar tendencies. In yet another study, Saerens et al. [22] demonstrated that increasing the fermentation temperature by 3 °C resulted in a 50% increase in the concentration of isoamyl acetate. Our studies also suggest that the initial rate of yeast addition to wort was positively related to concentrations of this volatile in beer. Verbelen with co-workers [19] provided evidence of the significance of such a correlation within the range of yeast concentrations from 10 to 40 mln cells/mL.

Amyl alcohols and the sum of higher alcohols

The analysis of variance for amyl alcohol concentrations in beer is given in Table 5, whereas similar analysis for the sum of higher alcohols is shown in Table 6.

Table 5. Analysis of variance: the empirical model for predicting amyl alcohols.

Source	Sum of Squares	Df	Mean Square	F-Ratio	p-Value
x ₁	209.5690	1	209.5690	43.40	0.0027
x ₂	218.6480	1	218.6480	45.28	0.0025
x ₃	0.4817	1	0.4817	0.10	0.7679
x ₄	968.5020	1	68.5020	200.56	0.0001
x ₃ x ₄	38.6760	1	38.6760	8.01	0.0473
Blocks	7.7521	1	7.7521	1.61	0.2739
Lack-of-fit	129.9700	43	3.0226	0.63	0.8077
Pure error	19.3162	4	4.8291		
Total (correlation)	1592.9100	53			

Table 6. Analysis of variance: the empirical model for predicting the sum of higher alcohols.

Source	Sum of Squares	Df	Mean Square	F-Ratio	p-Value
x ₁	496.4050	1	496.4050	49.00	0.0022
x ₂	145.2880	1	145.2880	14.34	0.0193
x ₃	2420	1	4.2420	0.42	0.5528
x ₄	1515.1100	1	1515.1100	149.55	0.0003
x ₃ x ₄	81.1538	1	81.1538	8.01	0.0473
Blocks	30.1953	1	30.1953	2.98	0.1594
Lack-of-fit	250.8160	43	5.8329	0.58	0.8406
Pure error	40.5250	4	10.1312		
Total (correlation)	2563.7400	53			

The striking similarity of significant components in models predicting concentrations of amyl alcohols and the sum of higher alcohols suggested the important role of the volatile amyl alcohols in these beer flavor components. With the exception of aeration rate, all other process parameters of beer fermentation significantly modulated the concentrations of volatile alcohols in beer. As shown in Tables 5 and 6, among process parameters, *p* values < 0.05 were observed for linear terms of x₁, x₂, and x₄, as well as for interaction term x₃ x₄.

The polynomial functions for amyl alcohols:

$$y_3 = 9.498 + 1.478x_1 + 2.012x_2 + 2.270x_3 + 3.854x_4 - 0.244x_3x_4 \quad (3)$$

and for the sum of higher alcohols:

$$y_4 = 18.116 + 2.274x_1 + 1.640x_2 + 3.395x_3 + 5.305x_4 - 0.354x_3x_4 \quad (4)$$

allowed us to recognize the time of CTT filling as the most significant factor. The established models were subsequently applied to predict the optimal process parameters for minimizing higher alcohol concentrations in beer. The value of each of the process parameters when kept at the lowest levels guaranteed values as low as 62.30 mg/L of amyl alcohols, and 85.6 mg/L of higher alcohols in beer.

There have been multiple experiments undertaken to assess the impact of process parameters on the higher alcohol concentration in fermenting wort. Jones with co-workers [23] showed that the content of fusel alcohols like isobutanol, isoamyl alcohol, and 1-propanol was only slightly higher when additional amounts of oxygen were applied 12 h post-inoculation. Erten et al. [20] reported that a higher pitching rate led to an increase in the concentration of isobutanol but also to a decrease in the content of active amyl alcohols, like 2-methyl-1-butanol. Jones with co-workers [23], however, reported that the concentrations of 1-propanol increased with higher yeast pitching rates. The experiments conducted by Lima et al. [15] also confirmed that increased pitching rate from 15 to 22 mln cells/mL caused a rise in the concentration of 1-propanol. There seems to be a general agreement in the literature

that biosynthesis of fusel alcohols is positively related to the temperature of fermentation [3,13,24,25]. All these reports seem to be in good agreement with the observations of this study.

Sensory quality

The proper and unchanging sensory quality of beer is one of the most important problems in brewing, particularly in the HGB method. The flavor stability and repeatability of good sensory properties of beer were maintained throughout the current study (65.7 to 66.7 points).

Table 7 lists significant components of the model that relates the sensory quality of beer to the values of process parameters applied during fermentation. A few two-factor interaction terms were found insignificant in the original model, and each of the process parameters had a significant quadratic term. Fermentation temperature appeared to be the key factor influencing the sensory characteristic of lager beer. Both a linear and quadratic component of the temperature, as well as a significant interaction of the temperature with aeration level, were among the main determinants of the sensory quality. There was also a significant negative effect of the pitching rate and a positive effect of its quadratic component. The complete polynomial equation that related the sensory quality of beer to the values of process parameters was the following:

$$y_5 = 61.255 - 0.691 x_1 + 1.693 x_2 - 0.148 x_3 + 0.0370 x_4 + 0.0828 x_1^2 - 0.0542 x_1 x_2 - 0.0167 x_1 x_4 - 0.115 x_2^2 + 0.121 x_2 x_4 - 0.057 x_3^2 + 0.0083 x_4^2 \quad (5)$$

where y_6 denotes the sensory quality of beer (in points).

Table 7. Analysis of variance: the empirical model predicting the sensory quality of beer.

Source	Sum of Squares	Df	Mean Square	F-Ratio	p-Value
x_1	0.3267	1	0.3267	17.40	0.0145
x_2	1.4259	1	1.4259	74.40	0.0010
x_3	0.6176	1	0.6176	32.22	0.0048
x_4	0.2017	1	0.2017	10.52	0.0316
x_1^2	1.1704	1	1.1704	61.07	0.0014
$x_1 x_2$	0.2113	1	0.2113	11.02	0.0294
$x_1 x_4$	0.1800	1	0.1800	9.39	0.0375
x_2^2	0.7177	1	0.7177	37.44	0.0036
$x_2 x_3$	1.0513	1	1.0513	54.85	0.0018
x_3^2	0.5551	1	0.5551	28.96	0.0058
x_4^2	0.3038	1	0.3038	15.85	0.0164
Blocks	0.0007	1	0.0007	0.03	0.8648
Lack-of-fit	3.2974	37	0.0891	4.65	0.0716
Pure error	0.09	4	0.0225		
Total (correlation)	11.457	53			

It appears that due to the significant interaction term ($x_2 x_3$), the level of wort aeration determined the character of changes in the sensory quality of beer, which resulted from different fermentation temperatures. At high aeration level, the raising temperature enhanced the sensory quality of beer almost linearly, but at a low aeration rate, there was a plateau and then a decline in beer quality. When Equation (5) was applied for maximizing sensory quality, a lager with excellent sensory quality (67 points) was predicted when the pitching rate was set at the low level and all the other parameters were maintained at their respective high values. In one-factor experiments, a direct, positive relationship between fermentation temperature and the sensory quality of beer was reported by Brown and Hammond [13]. The direct connection of a correct wort oxygenation and the sensory quality of beer that was observed in this study had also been reported earlier [19].

3.3. Multiple Response Optimization Procedures

Effects of process parameters on the multiple measured exposures were assessed by the Multiple Response Optimization procedure of the Statgraphics software.

At first, combined maximization of volatile esters (ethyl acetate and isoamyl acetate) concentrations was undertaken. The next optimization that involved all volatile components comprised the maximization of ester concentrations and simultaneous minimization of volatile alcohols, i.e., isobutanol and the sum of higher alcohols. The final optimization (“optimize all”) also included the maximization of beer sensory quality. A comparison of results from the single response optimizations described earlier to those originating from the multiple response optimization procedure, as well as the predicted values for each of the measured beer volatile and the sensory quality of beer, is presented in the Table 8.

Table 8. Values of process parameters that optimized ethyl acetate, isoamyl acetate, isobutanol concentration, and the sensory quality of beer with corresponding predicted values, and the multiple response optimization: Esters = ethyl acetate + isoamyl acetate; alcohols = butanol + higher alcohols, volatiles = esters + alcohols, and all = esters + alcohols + sensory quality.

Technological Parameters	Levels		Optimum/Goal									
			EtAcet	IsAc	Esters	Isobutanol	HA	Alcohols	Sensory	Volatiles	All	
	−1	+1	Maximize			Minimize			Maximize	Optimize	Optimize	
Pitching rate (mln cells/mL)	6.0	10.0	10.0	10.0	10.0	6.0	6.1	6.0	6.0	10.0	10.0	
Temperature of fermentation (°C)	8.5	11.5	11.5	11.5	11.5	11.3	8.8	9.6	11.5	11.5	11.5	
Wort aeration level (mg/L)	8.0	12.0	10.0	9.6	10.0	8.0	8.0	8.0	11.1	8.1	8.8	
Total filling time CCTs (h)	4.5	13.5	9.0	13.5	13.5	4.5	4.5	4.6	13.5	4.7	4.5	
Volatiles/Sensory	Predicted Values											
Ethyl acetate (EtAcet; mg/L)			22.1	22.1					22.1	22.0		
Isoamyl acetate (IsAc; mg/L)			2.34	2.34					2.1	2.09		
Isobutanol (mg/L)					11.8	12.6				12.6	12.9	
Higher alcohols (HA; mg/L)							83.5	85.2			97.4	97.9
Sensory quality (pts)									67			66.4

As evidenced in Table 8, the fermentation temperature set at the high level (11.5 °C; +1) optimized the concentrations of volatile esters, the sum of volatile substances, and the sensory quality of beer and was also required for the overall optimization. The low pitching rate (−1) guaranteed the highest sensory quality, but the high pitching rate (+1) was necessary for both optimal volatile concentrations, and for the general optimization. The time of CTT filling was calculated to be set at 13.5 h (+1) for optimal volatile ester concentration and for good sensory quality of beer; however, for the overall optimization, which, in addition to sensory quality, comprised both volatile esters and volatile alcohols, the short time of CTT filling (4.5 h; −1) was simulated. With the exception of fermentation temperature, the levels of process parameters that were simulated to guarantee optimal concentrations of volatile compounds in beer differed from those that were calculated as optimal for the sensory quality of beer. This finding clearly suggests that volatiles other than esters and fusel alcohols play a predominant role in determining the sensory quality of beer. In our previous study [26], the process parameters that optimized acetaldehyde and DMS concentrations were the same as those that maximized the sensory quality of beer. Volatile compounds in fermented beverages have been found to strongly influence the sensory characteristics of the product, and, therefore, their identification and optimization are of utmost importance for understanding the relationships among different process parameters and chemical composition, as well as for maintaining and for further enhancements in the product quality [27].

There have been attempts to optimize process parameters in high-gravity brewing fermentations performed in a laboratory or in a pilot plant by varying values of the most important process parameters

in statistically designed experiments [23]. None of these endeavors, however, have aimed to provide a direct relationship between results of such optimization and the sensory quality of beer produced on an industrial scale.

4. Conclusions

The multiple response optimization procedure of the Statgraphics software allowed us to find levels of the process parameters that optimized concentrations of esters, higher alcohols, and the sensory quality of a lager beer. The values of process parameters that maximized the concentrations of volatile esters differed from those that minimized the concentrations of higher alcohols. The simultaneous optimization of volatile compounds and the sensory quality of beer yielded overall values of process parameters: Pitching rate—10 mln cells per mL; fermentation temperature—11.5 °C; aeration level—8.8 mgO₂/L, and time of filling CCTs—4.5 h. These levels may be perceived as a result of a compromise between optimal volatile esters and higher alcohol concentrations. It is suggested that volatiles other than esters and fusel alcohols must have played a predominant role in determining the sensory quality of beer. We suggest that the RSM modeling can be successfully used for prediction and control of important process parameters of fermentation performed in an industrial plant to have desirable taste and aroma of bottom-fermented lager beers.

Author Contributions: Conceptualization, K.Ž.; K.K. and T.T.; methodology, K.K. and K.Ž.; software, K.Ž.; formal analysis, K.Ž.; investigation, K.Ž.; resources, K.K.; data curation, K.K.; writing—original draft preparation, K.Ž., K.K. and T.T.; writing—review and editing, T.T.; visualization, K.Ž.; supervision, K.K.; project administration, K.K. All authors have read and agreed to the published version of the manuscript.

Funding: This research received no external funding.

Conflicts of Interest: The authors declare no conflict of interest.

References

1. He, Y.; Dong, J.; Yin, H.; Zhao, Y.; Chen, R.; Wan, X.; Chen, P.; Hou, X.; Liu, J.; Chen, L. Wort composition and its impact on the flavour-active higher alcohol and ester formation of beer—A review. *J. Inst. Brew.* **2014**, *120*, 157–163. [CrossRef]
2. Titica, M.; Landaud, S.; Trelea, I.; Latrille, E.; Corrieu, G.; Cheruy, A. Modeling of the kinetics of higher alcohols and ester production on CO₂ emission with a view to control of beer flavor by temperature and top pressure. *J. Am. Soc. Brew. Chem.* **2000**, *58*, 167–174. [CrossRef]
3. Pires, E.; Teixeira, J.; Branyik, T.; Vicente, A. Yeast: The soul of beer’s aroma—a review of flavour-active esters and higher alcohols produced by the brewing yeast. *Appl. Microbiol. Biotechnol.* **2014**, *98*, 1937–1949. [CrossRef]
4. Renger, S.; Van Hateren, S.; Luyben, K. The formation of esters and higher alcohols during brewery fermentation; the effect of carbon dioxide pressure. *J. Inst. Brew.* **1992**, *98*, 509–513. [CrossRef]
5. Stewart, G. High gravity brewing and distilling—Past experiences and future prospects. *J. Am. Soc. Brew. Chem.* **2010**, *68*, 1–9. [CrossRef]
6. Ferreira, I.; Guido, L. Impact of wort amino acids on beer flavour: A review. *Fermentation* **2019**, *4*, 23. [CrossRef]
7. Vanderhaegen, B.; Necen, H.; Verachtert, H.; Derdelinckx, G. The chemistry of beer aging—a critical review. *Food Chem.* **2007**, *95*, 357–381. [CrossRef]
8. Holt, S.; Miks, M.; Carvalho, B.; Moreno, M.; Thevelein, J. The molecular biology of fruity and floral aromas in beer and other alcoholic beverages. *FEMS Microbiol. Rev.* **2019**, *43*, 193–222. [CrossRef] [PubMed]
9. Yilmaztekin, M.; Cabaroglu, T.; Erten, H. Effects of fermentation temperature and aeration on production of natural isoamyl acetate by *Williopsis saturnus* var. *saturnus*. *BioMed Res. Int.* **2013**, *2013*, 1–6. [CrossRef]
10. Humia, B.; Santos, K.; Barbosa, A.; Sawata, M.; Mendoca, M.; Padilha, F. Beer molecules and its sensory and biological properties: A review. *Molecules* **2019**, *24*, 1568. [CrossRef]

11. Moonjai, N.; Verstrepn, K.; Delvaux, F.; Derdelinckx, G.; Verachtert, H. The effects of linoleic acid supplementation of cropped yeast on its subsequent fermentation performance and acetate ester synthesis. *J. Inst. Brew.* **2002**, *108*, 227–235. [CrossRef]
12. Trelea, I.; Titica, M.; Corrieu, G. Dynamic optimisation of the aroma production in brewing fermentation. *J. Process Control* **2004**, *14*, 1–16. [CrossRef]
13. Brown, A.; Hammond, J. Flavour control in small-scale beer fermentations. *Inst. Chem. E* **2003**, *81*, 40–49. [CrossRef]
14. Dragone, G.; Silva, D.; Almeida e Silva, J. Factors influencing ethanol production rates at high-gravity brewing. *Lebensm. Wiss. Technol.* **2004**, *37*, 797–802. [CrossRef]
15. Lima, L.; Brandão, T.; Lima, N.; Teixeira, J. Comparing the impact of environmental factors during very high gravity brewing fermentation. *J. Inst. Brew.* **2011**, *3*, 359–367. [CrossRef]
16. Miedaner, H. *Brautechnische Analysenmethoden, Band II, Methodensammlung der Mitteleuropäischen Brautechnischen Analysenkommission*, MEBAK 4th ed.; Selbstverlag der MEBAK: Munich, Germany, 2002.
17. Verstrepn, K.; Derdelinckx, G.; Dufour, J.; Winderickx, J.; Thevelein, J.; Pretorius, I.; Delvaux, F. Flavour-active esters: Adding fruitiness to beer. *J. Biosci. Bioeng.* **2003**, *2*, 110–118. [CrossRef]
18. Lee, M.; Davis, D. Fermentation intensification—Part III: The effect of increasing yeast biomass concentration on fermentation performance. *BRI Q.* **2000**, *3*, 1–4.
19. Verbelen, P.; Dekoninck, T.; Saerens, S.; Van Mulders, S.; Thevelein, M.; Delvaux, F. Impact of pitching rate on yeast fermentation performance and beer flavour. *Appl. Microbiol. Cell Physiol.* **2009**, *82*, 155–167. [CrossRef]
20. Erten, H.; Tanguler, H.; Cakiroz, H. The effect of pitching rate on fermentation and flavour compounds in high gravity brewing. *J. Inst. Brew.* **2007**, *113*, 75–79. [CrossRef]
21. Nakatani, K.; Fukui, N.; Nagami, K.; Nishigaki, M. Kinetic analysis of ester formation during beer fermentation. *J. Am. Soc. Brew. Chem.* **1991**, *4*, 152–157. [CrossRef]
22. Saerens, S.; Verbelen, P.; Vanbeneden, N. Monitoring the influence of high-gravity brewing and fermentation temperature on flavour formation by analysis of gene expression levels in brewing yeast. *Appl. Microbiol. Biotechnol.* **2008**, *80*, 1039–1051. [CrossRef]
23. Jones, H.L.; Margaritis, A.; Stewart, R. The combined effect of oxygen supply strategy, inoculum size and temperature profile on Very-High-Gravity beer fermentations by *Saccharomyces cerevisiae*. *J. Inst. Brew.* **2007**, *113*, 168–184. [CrossRef]
24. Landaud, S.; Latrille, E.; Corrieu, G. Top pressure and temperature control the fusel alcohol/ester ratio through yeast growth in beer fermentation. *J. Inst. Brew.* **2001**, *2*, 107–117. [CrossRef]
25. Olaniran, A.O.; Hiralal, L.; Mokoena, M.P.; Pillay, B. Flavour-active volatile compounds in beer: Production, regulation and control. *J. Inst. Brew.* **2017**, *123*, 13–23. [CrossRef]
26. Kucharczyk, K.; Żyła, K.; Tuszyński, T. Optimization of wort aeration, wort-filling time, pitching rate, and temperature levels for high-gravity brewing fermentation in an industrial brewery on volatile carbonyls, sulphur compounds and quality of a lager beer. *Czech J. Food Sci.* **2020**, in consideration.
27. Coelho, E.; Lemos, M.; Genisheva, Z.; Domingues, L.; Vilanova, M.; Oliveira, J.M. Validation of a LLME/GC-MS methodology for quantification of volatile compounds in fermented beverages. *Molecules* **2020**, *25*, 621. [CrossRef]



© 2020 by the authors. Licensee MDPI, Basel, Switzerland. This article is an open access article distributed under the terms and conditions of the Creative Commons Attribution (CC BY) license (<http://creativecommons.org/licenses/by/4.0/>).

Article

A Deep Learning Method for Yogurt Preferences Prediction Using Sensory Attributes

Kexin Bi ^{1,2}, Tong Qiu ^{1,2,*} and Yizhen Huang ^{3,4,*}

¹ Department of Chemical Engineering, Tsinghua University, Beijing 100084, China; bkx16@mails.tsinghua.edu.cn

² Beijing Key Laboratory of Industrial Big Data System and Application, Beijing 100084, China

³ COFCO Nutrition Health Research Institute, Beijing 102209, China

⁴ School of Food Science and Technology, Dalian Polytechnic University, Dalian 116034, China

* Correspondence: qitutong@tsinghua.edu.cn (T.Q.); huangyizhen929@163.com (Y.H.)

Received: 9 March 2020; Accepted: 14 April 2020; Published: 27 April 2020

Abstract: During the development of innovative products, consumer preferences are the essential factors for yogurt producers to improve their market share. A high-performance prediction method will be beneficial to understand the intrinsic relevance between preferences and sensory attributes. In this study, a novel deep learning method is proposed that uses an autoencoder to extract product features from the sensory attributes scored by experts, and the sensory features acquired are regressed on consumer preferences with support vector machine analysis. Model performance analysis, hedonic contour mapping, and feature clustering were implemented to validate the overall learning process. The results showed that the deep learning model can vouch an acceptable level of accuracy, and the hedonic mapping reflected could supply a great help for producers' product design or modification. Finally, hierarchical clustering analysis revealed that for all three brands of yogurts, low temperature (4 °C) storage for no more than 4 weeks can promise the highest consumer preferences.

Keywords: yogurt; sensory attributes; consumer preference; autoencoder; support vector machine

1. Introduction

As human living standards continue to rise, yogurt is getting popular among people from all walks of life. Taking the Chinese market as an example, market research by the National Bureau of Statistics of China [1] showed that the yogurt sales of China were increased from 33 billion yuan in 2010 to 101 billion yuan in 2016, while milk sales were increased from 67 billion yuan to 110 billion yuan over the same period. Further, yogurt sales reached 122 billion yuan in 2017, surpassing pure milk sales for the first time. It is estimated that by 2020, yogurt sales in China will reach 190 billion yuan [2].

For consumers of dairy products, the smooth texture and refreshing taste of yogurt are appealing, and the probiotics in yogurt, which may have positive effects on immune, cardiovascular, and metabolic health, can also enhance consumers' partiality [3]. The rapidly expanding yogurt market has delivered huge profits to yogurt producers, and catering to consumers' tastes is one of the most important factors for yogurt producers to enlarge their market shares [4]. Thus, the accurate prediction of consumer preferences is crucial for yogurt producers aiming to attract new consumers as well as to maintain their brand loyalty [5].

Knowledge about consumers' preference for yogurt sensory qualities can help producers' processing. However, it is not economic to undertake large-scale sensory evaluations and market surveys [6]. Thus, market demand is usually estimated via consumer preference predictions using sensory attributes as an input. Some previous studies have focused on exploring the correlation between sensory attributes and consumer preferences for dairy products. Ares et al. [7] compared different preference mapping techniques and recommended that the external preference mapping used

by the dairy industry to modify the texture of dulce de leche is a method better meeting consumer requirement. Zhi et al. [8] established a relationship between product characteristics and overall preferences using partial least squares regression (PLSR) to identify the preferences of consumers from different regions in relation to flavored milk. Castada et al. [9] used the principal component analysis (PCA) method and found a positive correlation between five sensory attributes and consumer preferences in relation to Swiss cheese.

These studies applied a range of conventional statistical correlation methods in an attempt to predict consumer preferences based on sensory attributes. However, when applied to large volumes of high-dimensional data, these conventional methods may not provide enough accuracy, extendibility, and generalization [10]. In addition, errors of the prediction results may be incurred by potential issues, such as the individual difference of evaluators or bad data quality in sensory experiments [11]. To overcome these deficiencies, we propose a high-performance computer-aided model for more efficient algorithms of regression. The core aim of this model is to extract the unique features that reflect the intrinsic characteristics of a yogurt product from sensory evaluation data using a deep learning method. These features can not only be used to regress consumer preferences, but they can also help yogurt producers for product classification, design, processing, and the adjustment of storage conditions.

Deep learning algorithms are used for dimensionality reduction and feature extraction [12]. The autoencoder (AE) approach is proved to be accurate and efficient in feature extraction and noise decreasing of original data [13]. Among these autoencoders, a general autoencoder framework using fully connected layers (FCAE) is the most widely used [14]. With the development of machine learning technology, another deep convolutional autoencoder (DCAE) proposed by Cheng et al. [15] is becoming highly recognized and increasingly prevalent. The structure of DCAE combines a convolutional neural network (CNN) [16] with a simple autoencoder. The convolution and pooling operations in the structure of the DCAE enable the model to comprehensively consider the latent features of all the evaluators' scoring habits and reveal the relationships among the coupled sensory attributes elements during preference regression [17].

After identifying the key features, a support vector machine (SVM) algorithm [18] can be applied to predict preferences [10]. A previous study [19] showed that SVM was the most practical method in relation to high-dimensional regression problems with small sample sizes. The complete set of SVM regression models has been packaged as an Industrial Internet plug-in. Using this plug-in, the hedonic contour mapping [20,21] of key sensory properties is feasible. Similar to external preference mapping [7], hedonic contour mapping, which is generated by orthogonal experiments [22] implemented by computer programs, can determine an area composed of consumers' favorable sensory attributes. In addition, it has been reported that the sensory qualities of yogurt are closely associated with storage duration and temperature [23]. Therefore, hierarchical clustering [24] of the extracted features is applied to classify consumers' preference levels for the yogurts of different brands stored under various conditions, and thus the optimal storage conditions could be identified.

In this study, the overall process of consumer preference prediction based on sensory evaluation data is introduced, including sensory and consumer analysis, feature extraction by deep learning, and overall preference regression using SVM, hedonic contour mapping, and hierarchical clustering based on sensory features. Yogurt samples are used to provide the dataset for the model and test the feasibility of the overall process.

2. Materials and Methods

2.1. Sample Preparation

Three newly developed yogurt products of different brands were provided by the yogurt producers in China. Every product was stored at 12 kinds of conditions composed of various storage periods and storage temperatures: 2L, 3L, 4L, 5L, 1R, 2R, 3R, 4R, 5R, 2H, 3H, and 4H, in which Arabic numerals

denote the storage weeks, while L, R, and H express low temperature (4 °C), room temperature (25 °C), and high temperature (38 °C), respectively.

2.2. Panelists

Ten expert panelists and 100 consumer respondents were recruited for the sensory study and hedonic test, respectively. The expert panelists, including 5 males and 5 females aging from 22 to 46, were enrolled externally and constantly trained by COFCO Nutrition Health Research Institute (NHRI), the research and development (R&D) center of China National Cereals, Oils and Foodstuffs Corporation (COFCO) in Beijing. The volunteer employees from the non-R&D and non-marketing departments of COFCO were adopted as the consumer respondents for the hedonic test. These volunteers, aging from 22 to 46 with a male to female ratio of 2.125:1, generally have the habit of purchasing yogurt products. In advance, all participants assured of no allergy or resistance to dairy products.

The selection and training of sensory experts were processed according to ISO 8586:2012 [25]. The people who had no less than 4 years of experiences in sensory evaluation were considered, and the ones who could restate the sample attributes and whose assessment intensities could be calibrated into similar scales were invited for the sensory descriptive analysis of yogurts. Before the formal test, they were requested to join a training program consisting of 1–2 sessions per week over a four-week period. The training was performed mainly with triangle, ranking, and matching tests to ensure panelists' abilities of descriptive vocabulary, matching, and discrimination. During the training, panelists' performance levels were also monitored with three identical yogurt samples marked by different three-digital numbers.

2.3. Implement of Evaluations

2.3.1. Sensory Descriptive Test

The 36 yogurt samples were randomly divided into 3 groups, each of which contained 12 samples. In each sensory evaluation, which was conducted once a day, the expert panelists were asked to evaluate one group of samples based on 22 preselected descriptive attributes. The assessment of all samples was completed within 3 consecutive working days. The sensory descriptors were predetermined by panel leaders, and the intensity of each attribute was scored on a line scale of 10 cm anchored by verbal endpoints at both ends [26]. All the yogurt samples were kept overnight in a refrigerator set at 4 ± 2 °C and incubated for 20 min at 26 ± 2 °C before serving. In the environment of 26 ± 2 °C, approximate 30 mL of yogurt samples in 60 mL plastic cups were marked by 3 digital numbers and presented to the panelists in stochastic orders. Between the samples, a 3-minute break was taken, and mineral water and unsalted steamed buns were served to clean assessor' palates. Samples S1, S2, and S3, stirred yogurt respectively stored at room temperature, 4 °C, and 38 °C for 2 weeks were applied as blind reference samples in the evaluation procedure. Sense Whisper (test.sensewhisper.com) and PanelCheck (programming by Oliver Tomic and Henning Risvik) were used to collect and calculate the evaluation data [27]. More information related to the 22 yogurt sensory attributes and the experts' performance is appended to the supplementary file, in Figures S1–S5.

2.3.2. Hedonic test

The 36 yogurt samples were sent to the 100 consumer respondents in various offices of COFCO. After tasting each sample, the respondents were asked to provide a rating on a 9-point hedonic scale in which scores 1 and 9 are explained as extremely unpleasant and extremely pleasant, respectively [26].

The high degree of randomness and human error in the consumer ratings make it infeasible to precisely predict the entire distribution of consumer preferences. Thus, the scores were divided into three categories for the further analysis: preferred (scores between 7 and 9), neutral (scores between 4 and 6), and disliked (scores between 1 and 3). The percentages of consumers' preferences for the 36 samples are shown in Table 1.

Table 1. Percentages of consumers favoring and disliking each yogurt sample.

Sample No.	1	2	3	4	5	6	7	8	9
Preferred	23%	30%	22%	24%	18%	21%	18%	20%	27%
Disliked	16%	11%	13%	20%	20%	15%	24%	12%	12%
Sample No.	10	11	12	13	14	15	16	17	18
Preferred	28%	13%	48%	17%	12%	30%	36%	21%	24%
Disliked	14%	23%	8%	27%	28%	8%	4%	17%	20%
Sample No.	19	20	21	22	23	24	25	26	27
Preferred	25%	19%	18%	38%	34%	18%	22%	19%	12%
Disliked	17%	25%	8%	4%	19%	21%	14%	20%	18%
Sample No.	28	29	30	31	32	33	34	35	36
Preferred	23%	48%	34%	14%	21%	24%	20%	26%	29%
Disliked	16%	8%	19%	13%	18%	27%	14%	10%	14%

2.4. Feature Extraction Based on Deep Learning

For each yogurt sample, 22 attributes were assessed by 10 experts, generating a two-dimensional matrix with a size of 10×22 . As the matrix elements, the attribute values of 36 samples were collected from line scales of 10 cm and linear normalized to the range of 0 to 1. Through Python 3.6, the normalized data corresponding to various experts could be expressed by heatmaps [28]. The detailed dataset can be found in Figures S1–S5 of the supplement file.

For comprehensive evaluation of the experts' sensory scores, the conventional statistical correlation methods may not completely satisfy the regression due to the large dimension. The usage of conventional methods, such as PCA or PLSR, could also result in the loss of key sensory information during dimensionality reduction and feature extraction [29]. Thus, we tried to apply deep learning methods to extract the product features from their sensory attribute scores. Among the various deep learning methods, autoencoder (AE) may be an efficient algorithm for dimensionality reduction and ignoring noises. AE firstly learned a representation for a set of data by dimensionality reduction, which was the encoding operation, and then created the closest possible reconstruction of the original data from the extracted representation, which was the decoding operation. The representation was of the features extracted from the original data by converting the 10 experts' attribute scores with the low-dimension vector. To better extract the features, both FCAE and DCAE methods were simultaneously attempted for the same dataset, and their graphical structures are shown in Figure 1. The operations in Figure 1 were executed with eight Intel core i7-7700HQ CPUs @3.8GHz and one GTX Force 1050Ti GPU @CUDA 9.0, running Python 3.6 using a Keras frame on a TensorFlow back end [30].

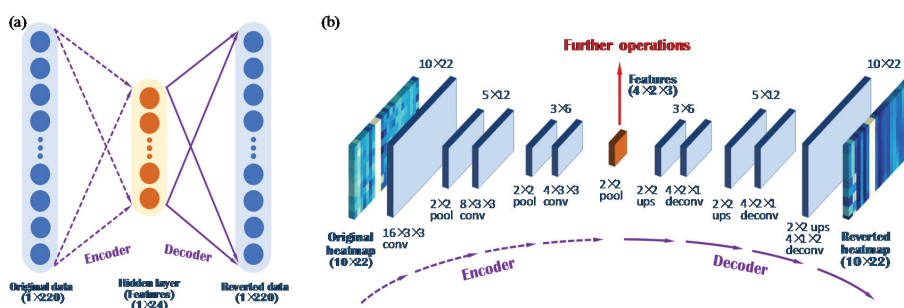


Figure 1. Graphical structures of the (a) fully connected autoencoder (FCAE), (b) deep convolutional autoencoder (DCAE).

As shown in Figure 1a, the structure of FCAE is composed of original data (220 nodes), hidden layer (24 nodes), and reverted data (220 nodes). The normalized original data is obtained by a heatmap

flattened into one dimension. All the layers are fully connected, and then FCAE is trained to minimize the deviation between input data and output data. The hidden layer, which can be reverted to a similar vector as the input, is considered as the features of sensory attributes in a specific yogurt sample.

As shown in Figure 1b, the encoding operations, including convolutions and poolings, were used to extract features from the original data for further regression. The subsequent deconvolution network reverted the features into the original heatmap through a decoding operation (upsampling and deconvolution) for network parameter optimization and feature correctness verification. Four original heatmaps were randomly selected from the testing sets, and a comparison between the original heatmaps and their reverted heatmaps is shown in Figure 2. In the original heatmaps, the x -axis represents 22 various sensory attributes, while the y -axis represents 10 different experts.

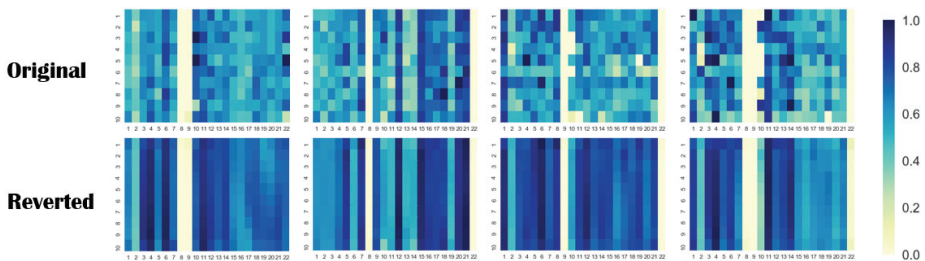


Figure 2. The effect of DCAE treatment on the yogurt sensory heatmap.

Compared to conventional PCA and PLSR methods, the deep learning treatment of original sensory evaluation data gave a comprehensive consideration of all evaluators' scoring habits and the mutual couplings among sensory attributes. In FCAE, the features could be easily extracted and explicit significances could be expressed, which were stored in the hidden layer for further uses. In DCAE, the reverted heatmaps were reconstructed by extracting features from the distribution information of the sensory attribute dimension in each column and reducing the distribution fluctuation among sensory evaluators in each row, which effectively helps data denoising and feature robustness.

After determination of the FCAE and DCAE structures and parameters, all features (with 24 dimensions) were input for further analyses using AE and SVM as the main algorithms. The entire deep learning process in relation to consumer preference prediction, hedonic contour mapping, and classification of brand/storage conditions was performed, as shown in Figure 3. To explore the effectiveness and robustness of feature extraction, the averages of sensory attributes are also used as a type of extracted features for comparison.

2.5. Intelligent SVM Regression for Preference Prediction

The features were structured into 24-dimensional vectors for input, which provided output in the form of the percentages of the consumer preference groups. A conversion between the high-dimensional features and the two-dimensional percentages (preferred and disliked) was needed. Thus, the ϵ -support vector regression (ϵ -SVR) algorithm, which is suitable for the problems of high-dimensional data versus small sample size, was selected for the conversion processing. The branch algorithm of SVM based on VC dimension theory and the minimum structural risk principle was consistently outperformed in terms of generalization ability and global optimization [31]. In addition, the solution obtained from ϵ -SVR was understandable and expressed as below [32]:

$$\bar{y}(x) = \sum_{x_i \in SV} (\alpha_i - \alpha_i^*) K(x_i, x_j) + b$$

$$b = \left\{ \sum_{0 < \alpha_i < C} [y_i - \sum_{x_j \in SV} (\alpha_j - \alpha_j^*) K(x_j, x_i) - \epsilon] + \sum_{0 < \alpha_i^* < C} [y_i - \sum_{x_j \in SV} (\alpha_j - \alpha_j^*) K(x_j, x_i) + \epsilon] \right\} / N_{NSV}$$

$$K(x_i, x_j) = \exp(-\gamma \|x_i - x_j\|^2)$$

where \bar{y} represents the preference prediction output, x represents the extracted features, α_i and α_i^* are Lagrange multipliers, b is the intercept of linear regression, SV is the support vector, N_{NSV} represents the amount of standard support vectors, and K represents the kernel function. C , ε , and γ are the penalty coefficient, tolerance boundary, and distribution width in the kernel function, respectively, which are the parameters to be optimized in the model. The optimization process based on the swarm intelligence algorithm [19] is included as an Industrial Internet plug-in with the ε -SVR algorithm, and the entire process can be executed automatically. To evaluate different methods, the optimization process of these three parameters are set in a same parameter space as $\{(C, \varepsilon, \gamma) | C \in (16, 64), \varepsilon \in (0.06, 0.12), \text{ and } \gamma \in (0.05, 0.09)\}$.

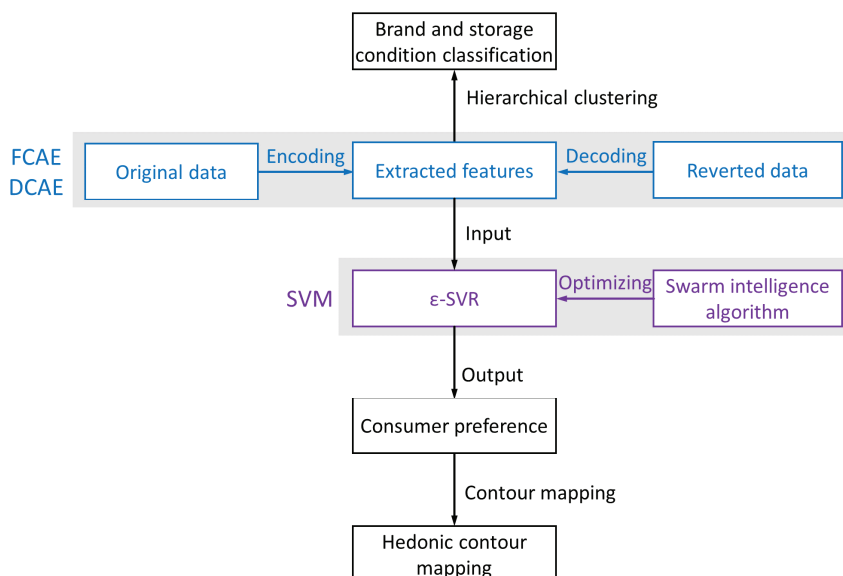


Figure 3. The overall deep learning process for yogurt sensory and preference analysis.

2.6. Evaluation of Consumer Preferences Using Hedonic Contour Mapping

Product sensory properties can vary over a wide range, so it is impossible to collect the actual consumer preferences on all data points. However, using the deep learning process outlined above, consumer preferences can be predicted if the specific sensory attributes were provided. The hedonic contour mapping method can generally identify preferences based on some key sensory dimensions using the process shown in Figure 3. To help the yogurt producers to improve their product quality, the hedonic contour mapping is obtained using specific sensory dimensions instead of principle components or other explanatory variables [33]. After collecting the preference predictions, a contour map can be generated whereby the points on the map indicate preference percentages.

Compared to the previous mapping methods, the hedonic contour mapping method can clearly display the consumer preference characteristics for specific attributes and the future improvement direction for a specific product.

2.7. Classification of Brands and Storage Conditions

The features extracted by AEs can also be used to classify the yogurt samples in relation to aspects such as brands and storage conditions. Hierarchical clustering analysis is frequently used to identify similarities among various variables. In this study, hierarchical clustering analysis with Euclidean distance and Ward's criteria [34] was used to classify the 36 yogurt samples of various brands and storage conditions, as shown in Figure 3.

3. Results

3.1. Overall Performance of Preference Predictions

The 36 yogurt samples were randomly divided into two groups, 25 (70%) for training of AEs and 11 (30%) for testing by the trained AEs. After the AE system was trained to optimize its ϵ -SVR, the original heatmap of each sample, which contains the full information regarding the scores of sensory attributes, was transformed into consumer preference percentages using the deep learning process shown in Figure 3. The averages of sensory attribute scores were also set as an input of ϵ -SVR. Five tests were repeated for each approach. For comparison, the percentages of consumer preference were also calculated using the PLSR algorithm that had been previously applied to this dataset [35]. The root mean square error (RMSE) was used as an evaluation index. The results generated from different methods are listed in Table 2.

Table 2. Root mean square error (RMSE) of preference predictions based on deep learning and partial least squares regression (PLSR). SVM: support vector machine.

Group	Method	Dataset	RMSE				
Preferred	PLSR	Training			5.49%		
		Testing			9.12%		
	Averages	Training	3.05%	3.43%	2.72%	2.66%	3.03%
		Testing	5.75%	5.36%	5.65%	5.91%	5.60%
	FCAE-SVM	Training	2.72%	3.50%	2.56%	3.32%	2.80%
		Testing	6.01%	6.14%	4.28%	4.16%	5.23%
	DCAE-SVM	Training	3.19%	3.26%	2.90%	3.69%	3.07%
		Testing	3.41%	4.14%	3.56%	4.73%	3.46%
Disliked	PLSR	Training			4.12%		
		Testing			7.21%		
	Averages	Training	3.35%	2.99%	3.23%	2.83%	2.84%
		Testing	3.89%	4.03%	4.00%	3.88%	3.82%
	FCAE-SVM	Training	2.72%	2.87%	1.92%	2.37%	2.00%
		Testing	3.39%	3.34%	2.67%	3.57%	2.55%
	DCAE-SVM	Training	2.55%	2.57%	2.85%	2.08%	2.27%
		Testing	2.76%	2.71%	3.30%	2.48%	2.57%

The RMSE results in Table 2 indicated that compared to the PLSR method, the possible deviations of preference predictions could be largely decreased by using the ϵ -SVR based models. Among the ϵ -SVR based models, the deviations resulted from either FCAE or DCAE are also lower than those from the model using averages as features in most of the cases. In the preferred group, a better accuracy could be obtained by DCAE. Nevertheless, DCAE and FCAE showed a similar performance in the disliked group.

The performance of FCAE and DCAE was further evaluated on algorithm stability during feature extraction. The loss function of the two methods, which represents the difference between reverted data and original data, was recorded and plotted in Figure 4. The training process of DCAE maintained a stable convergence after around 60 iterations with a total time consumption of 32.4 s. However, intermittent vibration kept appearing during the training process of FCAE, which seemed not to be convergent after 1000 iterations with a total time consumption of 67.2 s.

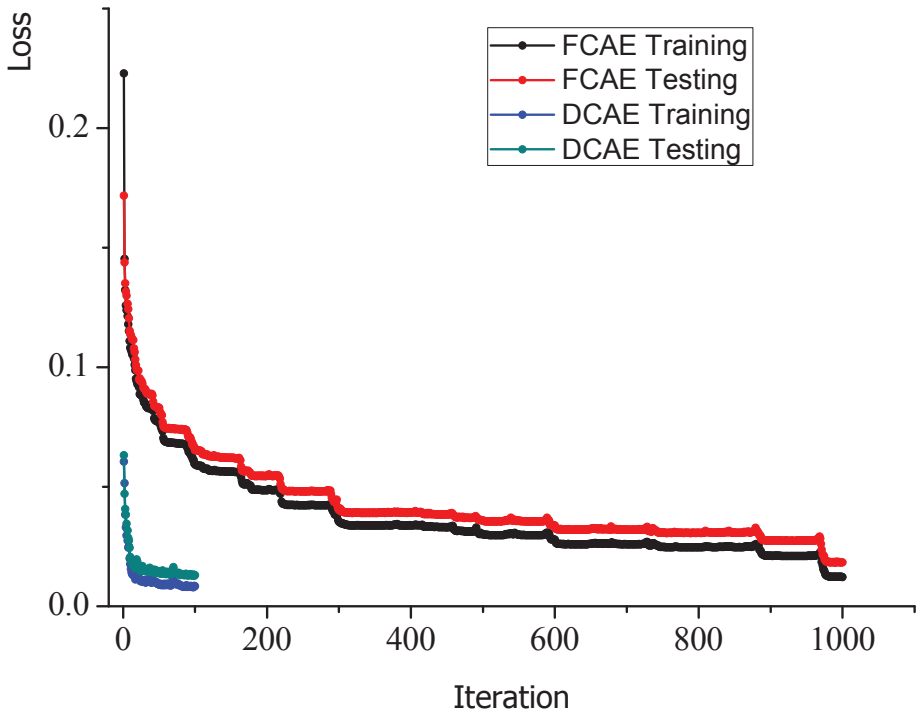


Figure 4. Loss function of the FCAE and DCAE on the dataset.

In addition, smaller gaps between the training and testing sets demonstrated that the DCAE-SVM model could avoid overfitting to a certain degree compared to the other methods. Considering the overall performance, further analysis was implemented using this model. The prediction results based on the selected DCAE-SVM models for the 11 testing samples are shown in Figure 5.

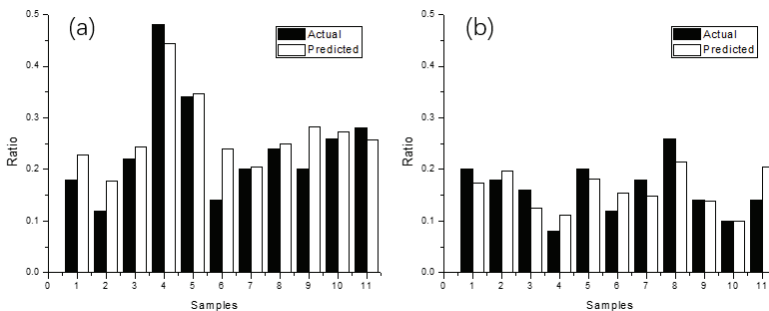


Figure 5. The prediction results of the 11 testing samples resulting from the DCAE-SVM models selected from the (a) preferred group and (b) disliked group.

3.2. Hedonic Contour Mapping Based on the Prediction Model

After the deep learning process was packed, the consumer preferences for product design could be obtained by entering the sensory attributes into the program. Several hedonic mappings elicited from the key sensory attributes of dairy products are shown in Figure 6. According to our previous researches [35], there are eight key sensory attributes playing an important role in determining consumers' preference for yogurt products. These eight key sensory property dimensions, including acidity, smoothness, sweetness, milkiness, adhesiveness (effort to draw through a straw), oxidization,

graininess, and whiteness of yogurt were used as the independent variables, while the percentage of consumers' preferred group for each sample was set as the dependent variable.

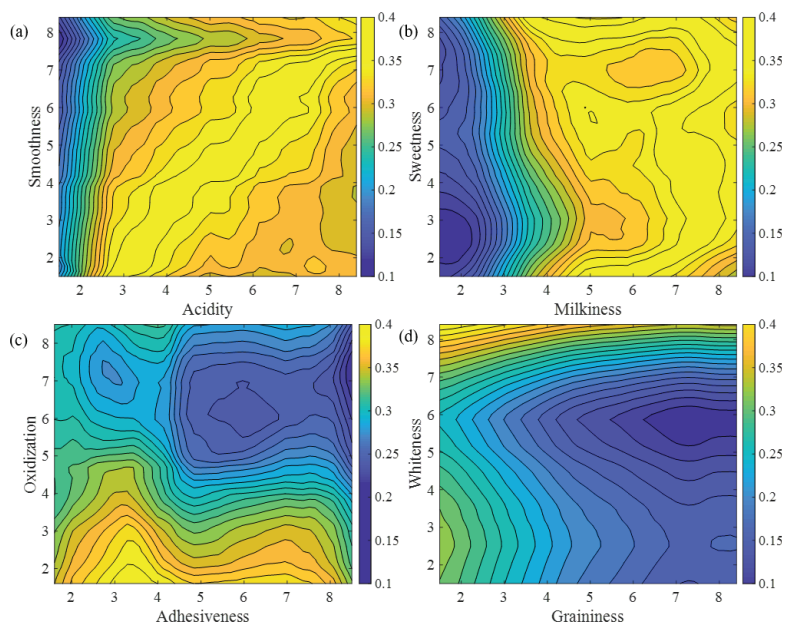


Figure 6. Hedonic contour mapping of a specific type of yogurt for the attributes combination of (a) acidity and smoothness, (b) milkiness and sweetness, (c) adhesiveness and oxidization, (d) graininess and whiteness.

The subplots in Figure 6 were generated with Matlab R2018a (MathWorks Inc.), and the color bars displayed the color scale of the preferred ratio of yogurt samples. The brightest (yellow) area represents the sensory qualities most favored by consumers. Using the hedonic contour maps in Figure 6, conclusions for consumer preference characteristics and product improvement schemes could be drawn on within the experimental measurement range of a specific product. As revealed by Figure 6a, consumer preference was the highest when the acidity value was around 5.8 and the smoothness value was around 5.9, and the positive slope of the yellow area indicates the product design principle for this kind of yogurt. For example, if the yogurt is very high in smoothness, it should also have a more acidic taste to balance the overall texture. On the contrary, if the yogurt lacks smoothness, its taste should be less acidic. This area also indicated the boundaries of the optimal yogurt design parameters. The acidity value for this kind of yogurt should not be less than 2.4, and the smoothness value should not be more than 7.6. Figure 6b shows that milky taste is important to consumers, and it should have a value of no less than 4.8. The preferred range for sweetness is between 4.0 and 5.0, and the corresponding milkiness is between 6.5 and 8.0. Figure 6c shows that oxidized flavor was not welcome by consumers, and its value should be as low as possible. When the oxidized flavor value is lower than 2.0, the adhesiveness value should also not be too high: preferably between 3.0 and 4.0. Figure 6d expresses the hedonic mapping for whiteness and graininess. It can be seen that the most favorable area is on the upper left corner, which means that the whiteness value should be as high as possible, while the graininess value should be as low as possible.

3.3. Hierarchical Clustering of Yogurt Samples with the Extracted Features

Through the deep learning process, 24-dimensional vectors were extracted as the key variables. To strengthen the interpretability of these features extracted, a hierarchical clustering analysis was

implemented using these features as inputs to classify the yogurt brands (Brands 1, 2, and 3) and storage conditions. The results are shown in Figure 7.

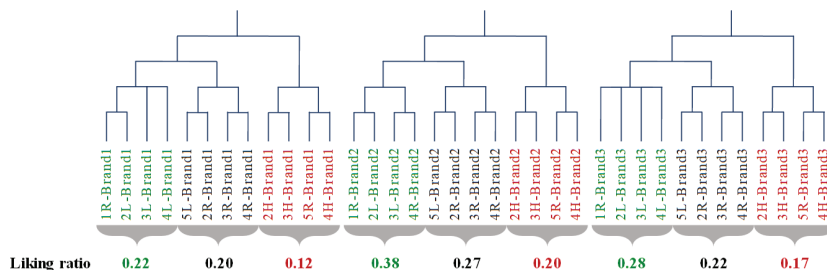


Figure 7. The hierarchical clustering results of 36 yogurt samples.

In Figure 7, hierarchical clustering can clearly divide these three brands of yogurts with the extracted features as variables. The microclusters showed the sensory divergence under different storage conditions. The green labels represent the suitable conditions for yogurt storage, which result in high favored percentages. It indicates that yogurt should be stored at around 4 °C for less than four weeks or at around 25 °C for less than one week. The red labels represent the improper conditions that lower the sensory quality of yogurt and result in low consumer preferences. It reveals that yogurt should not be stored at around 38 °C for more than two weeks or at around 25 °C for more than five weeks.

4. Discussion

Although at present, deep learning methods are rarely applied to food research, they have been widely used in the field of process engineering, such as process fault diagnosis [36], and have been demonstrated more effective than the traditional methods for nonlinear dynamic processes with high uncertainty [37]. Similarly, correlation between food sensory evaluation and consumer preference is also a dynamic, nonlinear, and highly uncertain modeling process. Thus, a novel deep learning approach combining several ideas from previous papers is proposed and compared with one of the representative traditional correlation models, PLSR. Our numerical experiments illustrated that SVR using the features extracted by AEs as input has advantages over the conventional method.

The two AEs proposed in the present work, FCAE and DCAE, both have their strength and weakness. For FCAE, its excellent learning ability could be demonstrated by the low training RMSE. The concise structure and high interpretability of FCAE make it more efficient and feasible for the application of sensory laboratories. However, when the size of the dataset is small, FCAE may face some instability and overfitting problems. For DCAE, the overfitting is reduced, and the stability is strengthened by the sparsity of convolution. With convolution and pooling operations, DCAE can consider the original heatmap more comprehensively in view of the scale of the coupling relationship among the sensory attributes. The deviations among the expert evaluators are considered as unnecessary features or noises for a yogurt sample, so they were denoised by convolution and average pooling. However, the preprocess of the dataset for DCAE is a bit time-consuming, and the size of its compiled file model is a bit large. In addition, compared to FCAE, the complexity of DCAE is higher, and its interpretability is worse. The further application of DCAE may be hindered by these factors. Even though at present, DCAE could be a good choice to treat the problem of high-dimensional regression with a small sample size, similar to our yogurt preference prediction, we expect that the excellent learning ability of FCAE may make it a more powerful model once its problem in dataset expansion is improved in the future.

Application of the deep learning approach to preference prediction provides plenty of opportunities for the future processing of food product design. The proposed hedonic contour mapping can reduce the workload of consumer investigation compared to the traditional methods, such as a series

of just-about-right (JAR) questions. To explore another group of consumers' preferences for the similar food product background, only the hedonic scores need to be acquired instead of long JAR questionnaires, because the essential food product features have been extracted and recorded in the deep learning process. In addition, the hedonic contour mapping method is effective for coupling the relationship between any two variables, which will help food enterprises explicitly improve the recipe and sensory qualities of their products. As a result of the limited dataset, the mapping results still cannot be completely correct. The market analysis using these preference data is not within the scope of this manuscript. Our role here as data scientists is to provide data, not the market analysis indicator makers. However, the results of this research can provide food enterprises and sensory researchers with more choices for the future work.

In addition, some of the data resulting from the deep learning approach can benefit the further analyses of samples, as shown by our hierarchical clustering of yogurt samples with the extracted features. Compared to the clustering results obtained from the PLSR key components in our previous study [35], hierarchical clustering of the features extracted with AE provides better results in terms of storage condition classification, demonstrating the effectiveness of the deep learning process.

5. Conclusions

In this study, a complete AE-SVM deep learning framework is proposed for consumer preferences prediction, and the dataset of yogurt sensory attributes and corresponding consumer preferences demonstrate the feasibility, accuracy, and stability of this model. The process of feature extraction with AE is highly interpretable, and the results obtained can be also extended to the other applications. Further analyses based on the extracted features can contribute to yogurt the improvement of product processing, storage, marketing, etc. By combining hedonic contour mapping with this deep learning approach, it is interpreted that Chinese consumers prefer the yogurts of minimum oxidization/graininess, maximum whiteness, and certain levels of acidity, smoothness, sweetness, milkiness, and adhesiveness. Since the optimal values of various quality attributes revealed by hedonic contour mapping can provide helpful information to the food enterprises, it is recommended that fixed sensory assessors should be trained and prepared to perform sensory evaluation regularly. By the way, application of the proposed AE-SVM deep learning method is proven feasible and effective for quality control of food products. In addition, the feature extraction process mentioned above may provide more useful information if the other techniques for big data collection are followed.

Supplementary Materials: The following are available online at <http://www.mdpi.com/2227-9717/8/5/518/s1>, Figure S1: Detailed sensory evaluation results of 36 yogurt samples assessed by 10 experts on 22 sensory attributes after normalization, Figure S2: P*MSE plot of the experts as a blind reference in three ratings, Figure S3: F plot of the experts as a blind reference in three ratings, Figure S4: Tucker-1 plot for 22 attributes (a) of blind references (b) of 36 samples, Figure S5: 2-way ANOVA analysis of 36 samples

Author Contributions: Conception and design: K.B., T.Q., Y.H.; Experiment Section: Y.H.; Data collection: K.B., Y.H.; Process modeling and optimization: K.B., T.Q.; Establishment of AE structure: K.B., T.Q.; Analysis and interpretation: K.B., T.Q.; Writing the article: K.B., T.Q., Y.H. All authors have read and agreed to the published version of the manuscript.

Funding: This research was funded by National Natural Science Foundation of China, Grant No. U1462206, 21991100, 21991104.

Conflicts of Interest: The authors declare no conflict of interest.

References

1. National Data of China. Available online: <http://data.stats.gov.cn/easyquery.htm?cn=B01&zb=A030105&sj=2019B> (accessed on 27 August 2019).
2. Wang, Q.; Parsons, R.; Zhang, G. China's dairy markets: Trends, disparities, and implications for trade. *China Agr. Econ. Rev.* **2010**, *2*, 356–371. [CrossRef]
3. Rijkers, G.T.; de Vos, W.M.; Brummer, R.-J.; Morelli, L.; Corthier, G.; Marteau, P. Health benefits and health claims of probiotics: Bridging science and marketing. *Br. J. Nutr.* **2011**, *106*, 1291–1296. [CrossRef] [PubMed]

4. Horvat, A.; Granato, G.; Fogliano, V.; Luning, P.A. Understanding consumer data use in new product development and the product life cycle in European food firms—An empirical study. *Food Qual. Prefer.* **2019**, *76*, 20–32. [CrossRef]
5. Yan, G.; He, Y.; Wang, Y. Study on price fluctuation and countermeasures of dairy products in China. *China Dairy Ind.* **2018**, *46*, 38–42.
6. Ramírez-Rivera, E.d.J.; Díaz-Rivera, P.; Guadalupe Ramón-Canul, L.; Juárez-Barrimentos, J.M.; Rodríguez-Miranda, J.; Herman-Lara, E.; Prinyawiwatkul, W.; Herrera-Corredor, J.A. Comparison of performance and quantitative descriptive analysis sensory profiling and its relationship to consumer liking between the artisanal cheese producers panel and the descriptive trained panel. *J. Dairy Sci.* **2018**, *101*, 5851–5864. [CrossRef] [PubMed]
7. Ares, G.; Giménez, A.; Gámbaro, A. Preference mapping of texture of dulce de leche. *J. Sens. Stud.* **2006**, *21*, 553–571. [CrossRef]
8. Zhi, R.; Zhao, L.; Shi, J. Improving the sensory quality of flavored liquid milk by engaging sensory analysis and consumer preference. *J. Dairy Sci.* **2016**, *99*, 5305–5317. [CrossRef]
9. Castada, H.; Hanas, K.; Barringer, S. Swiss Cheese Flavor Variability Based on Correlations of Volatile Flavor Compounds, Descriptive Sensory Attributes, and Consumer Preference. *Foods* **2019**, *8*, 78. [CrossRef]
10. Jiménez-Carvelo, A.M.; González-Casado, A.; Bagur-González, M.G.; Cuadros-Rodríguez, L. Alternative data mining/machine learning methods for the analytical evaluation of food quality and authenticity—A review. *Food Res. Int.* **2019**, *122*, 25–39. [CrossRef]
11. Ross, C.F. Sensory science at the human–machine interface. *Trends Food Sci. Technol.* **2009**, *20*, 63–72. [CrossRef]
12. Yuan, X.; Huang, B.; Wang, Y.; Yang, C.; Gui, W. Deep Learning-Based Feature Representation and Its Application for Soft Sensor Modeling with Variable-Wise Weighted SAE. *IEEE Trans. Ind. Inform.* **2018**, *14*, 3235–3243. [CrossRef]
13. Wu, T.; Zhong, N.; Yang, L. Application of VIS/NIR Spectroscopy and SDAE-NN Algorithm for Predicting the Cold Storage Time of Salmon. *J. Spectrosc.* **2018**, *2018*, 1–9. [CrossRef]
14. Baldi, P. Autoencoders, unsupervised learning, and deep architectures. *Proc. ICML Workshop Unsuperv. Transf. Learn.* **2012**, *27*, 37–49.
15. Cheng, Z.; Sun, H.; Takeuchi, M.; Katto, J. Deep convolutional autoencoder-based lossy image compression. In Proceedings of the Picture Coding Symposium (PCS), San Francisco, CA, USA, 24–27 June 2018; pp. 253–257.
16. Mežgec, S.; Koroušič Seljak, B. NutriNet: A Deep Learning Food and Drink Image Recognition System for Dietary Assessment. *Nutrients* **2017**, *9*, 657. [CrossRef] [PubMed]
17. Liu, Q.; Yu, F.; Wu, S.; Wang, L. A convolutional click prediction model. In Proceedings of the 24th ACM International Conference on Information and Knowledge Management, Melbourne, Australia, 19–23 October 2015; pp. 1743–1746.
18. Du, C.-J.; Sun, D.-W. Learning techniques used in computer vision for food quality evaluation: A review. *J. Food Eng.* **2006**, *72*, 39–55. [CrossRef]
19. Bi, K.; Qiu, T. An intelligent SVM modeling process for crude oil properties prediction based on a hybrid GA-PSO method. *Chin. J. Chem. Eng.* **2019**, *27*, 1888–1894. [CrossRef]
20. Faber, N.K.M.; Mojet, J.; Poelman, A.A.M. Simple improvement of consumer fit in external preference mapping. *Food Qual. Prefer.* **2003**, *14*, 455–461. [CrossRef]
21. Gonzalez, N.J.; Adhikari, K.; Sancho-Madriz, M.F. Sensory characteristics of peach-flavored yogurt drinks containing prebiotics and synbiotics. *LWT Food Sci. Technol.* **2011**, *44*, 158–163. [CrossRef]
22. Gabrielsen, G. Paired comparisons and designed experiments. *Food Qual. Prefer.* **2000**, *11*, 55–61. [CrossRef]
23. Routray, W.; Mishra, H.N. Scientific and Technical Aspects of Yogurt Aroma and Taste: A Review. *Compr. Rev. Food Sci. Food Saf.* **2011**, *10*, 208–220. [CrossRef]
24. Saint-Eve, A.; Granda, P.; Legay, G.; Cuvelier, G.; Delarue, J. Consumer acceptance and sensory drivers of liking for high plant protein snacks. *J. Sci. Food Agric.* **2019**, *99*, 3983–3991. [CrossRef] [PubMed]
25. The International Organization for Standardization. *ISO 8586-2. Sensory Analysis-General Guidance for the Selection, Training and Monitoring of Assessors-Part 2: Expert Sensory Assessors*; The International Organization for Standardization: Geneva, Switzerland, 2008.
26. Pohjanheimo, T.; Sandell, M. Explaining the liking for drinking yoghurt: The role of sensory quality, food choice motives, health concern and product information. *Int. Dairy J.* **2009**, *19*, 459–466. [CrossRef]

27. Tomic, O.; Nilsen, A.; Martens, M.; Næs, T. Visualization of sensory profiling data for performance monitoring. *LWT Food Sci. Technol.* **2007**, *40*, 262–269. [CrossRef]
28. Fahad, S.A.; Yahya, A.E. Big Data Visualization: Allotting by R and Python with GUI Tools. In Proceedings of the International Conference on Smart Computing and Electronic Enterprise (ICSCEE), Shah Alam, Malaysia, 11–12 July 2018; pp. 1–8.
29. Wu, L.; Pu, H.; Sun, D.-W. Novel techniques for evaluating freshness quality attributes of fish: A review of recent developments. *Trends Food Sci. Technol.* **2019**, *83*, 259–273. [CrossRef]
30. Vidnerová, P.; Neruda, R. Evolving KERAS Architectures for Sensor Data Analysis. In Proceedings of the Federated Conference on Computer Science and Information Systems (FedCSIS), Prague, Czech Republic, 3–6 September 2017; pp. 109–112.
31. Shawe-Taylor, J.; Bartlett, P.L.; Williamson, R.C.; Anthony, M. Structural risk minimization over data-dependent hierarchies. *IEEE Trans. Inf. Theory* **1998**, *44*, 1926–1940. [CrossRef]
32. Yang, Y.; Full, R.; Huiyov, C. SVR mathematical model and methods for sale prediction. *J. Syst. Eng. Electron.* **2007**, *18*, 18–769.
33. Yenket, R.; Chambers, E., IV; Adhikari, K. A comparison of seven preference mapping techniques using four software programs. *J. Sens. Stud.* **2011**, *26*, 135–150. [CrossRef]
34. Murtagh, F.; Legendre, P. Ward’s Hierarchical Agglomerative Clustering Method: Which Algorithms Implement Ward’s Criterion? *J. Classif.* **2014**, *31*, 274–295. [CrossRef]
35. Bi, K.; Zhang, D.; Song, Z.; Qiu, T.; Huang, Y. A PLSR Model for Consumer Preference Prediction of Yoghurt from Sensory Attributes Profiles. In *Computer Aided Chemical Engineering*; Elsevier: Amsterdam, The Netherlands, 2019; Volume 46, pp. 1477–1482.
36. Wu, H.; Zhao, J. Deep convolutional neural network model based chemical process fault diagnosis. *Comput. Chem. Eng.* **2018**, *115*, 185–197. [CrossRef]
37. Cheng, F.; He, Q.P.; Zhao, J. A novel process monitoring approach based on variational recurrent autoencoder. *Comput. Chem. Eng.* **2019**, *129*, 106515. [CrossRef]



© 2020 by the authors. Licensee MDPI, Basel, Switzerland. This article is an open access article distributed under the terms and conditions of the Creative Commons Attribution (CC BY) license (<http://creativecommons.org/licenses/by/4.0/>).

Article

Application of Detrended Fluctuation Analysis and Yield Stability Index to Evaluate Near Infrared Spectra of Green and Roasted Coffee Samples

Eszter Benes^{1,2}, Marietta Fodor¹, Sándor Kovács^{3,*} and Attila Gere²

¹ Institute of Food Quality, Safety and Nutrition, Szent István University, Villányi Str. 29-31, H-1118 Budapest, Hungary; eszter.benes@gmail.com (E.B.); Fodor.Marietta@etk.szie.hu (M.F.)

² Institute of Food Technology, Szent István University, Villányi Str. 29-31, H-1118 Budapest, Hungary; gereattilaphd@gmail.com

³ Department of Economical and Financial Mathematics, University of Debrecen, Böszörményi út 138, H-4032 Debrecen, Hungary

* Correspondence: kovacs.sandor@econ.unideb.hu

Received: 25 June 2020; Accepted: 21 July 2020; Published: 1 August 2020

Abstract: Coffee quality, and therefore its price, is determined by coffee species and varieties, geographic location, the method used to process green coffee beans, and particularly the care taken during coffee production. Determination of coffee quality is often done by the nondestructive and fast near infrared spectroscopy (NIRS), which provides a huge amount of data about the samples. NIRS data require sophisticated, multivariate data analysis methods, such as principal component analysis, or linear discriminant analysis. Since the obtained data are a set of spectra, they can also be analyzed by signal processing methods. In the present study, the applications of two novel methods, detrended fluctuation analysis (DFA) and yield stability index (YSI), is introduced on NIR spectra of different roasting levels of coffee samples. Fourteen green coffee samples from all over the world have been roasted on three different levels and their NIR spectra were analyzed. DFA successfully differentiated the green samples from the roasted ones, however, the joint analysis of all samples was not able to differentiate the roasting levels. On the other hand, DFA successfully differentiated the roasting levels on samples level, which was strengthened by a 100% accurate agglomerative hierarchical clustering. YSI was first used in NIR signal processing and was able to detect that a light roast is the most stable among all roasting levels. Future research should focus on the application of DFA in terms of the analysis of the effects of other transformation methods of the spectra.

Keywords: *Coffea arabica*; grouping; different roasting levels; yield stability index; detrended fluctuation analysis

1. Introduction

Coffee is one of the most marketed products worldwide. On a large scale, the quality of the beverage depends on the physical properties and chemical composition of raw coffee beans, respectively, on the roasting process. The quality of the coffee beverage is manifested differently depending on its geographic origin, and there are notable variations in sensory profile according to country of origin, microregions, and even different planting locations in the same farm [1].

Currently, over 100 species within the genus *Coffea* are catalogued. Despite this diversity, only two species are actually of great importance in the world market, *C. arabica* L. and *C. canephora* Pierre [1]. These two species have distinct characteristics, especially regarding the quality of the beverage. However, within the species *C. arabica*, there are also differences in the peculiarity of the varieties [2]. Coffee quality, and therefore price, is determined by coffee species and varieties,

geographic location, the method used to process green coffee beans, and particularly the care taken during coffee production [3,4]. To make difference between commodity and specialty coffee, different grading systems are used. Increasing awareness of quality, taste and health among consumers is increasing demand for high-quality and specialty coffees [5].

Chemical constituents of the roasted beans determine the quality of coffee as a beverage. Raw coffee beans contain a wide range of different chemical compounds, which react and interact amongst themselves at all stages of coffee roasting, resulting in greatly diverse final products [6]. Hence, certain coffees due to their chemical composition are better roasted to certain colors. In case of specialty coffees, lighter roasts have come to predominate. The roaster's responsibility is now phrased as revealing the character of the beans. While lighter roasts are trendy in specialty coffee, roasting too light, under-roasting, produces a thin, grassy flavor. Coffee assessment is usually undertaken when the bean is just past this stage but still fairly light. The beans are properly roasted and all the potential details of the coffee are apparent [6].

Near infrared spectroscopy (NIRS) is a nondestructive and noninvasive analytical technique, with minimal or no sample preparation. It is fast, low cost, robust, and can be used in different environments such as laboratories and industrial plants [3]. It is widely used in different fields of food industry for qualitative and quantitative analysis of products from raw material to finished products [7–9].

Several scientific studies have been published about the use of NIRS to investigate various properties of raw and roasted coffee beans, such as caffeine and chlorogenic acid content [10,11], color and defectiveness of beans [12]. Besides, NIRS can be used to analyze roasting conditions [13]; determine the roasting degree [14] and Arabica/Robusta ratio [15,16] in ground coffee; the place of origin of coffee beans [17,18]; chemical composition of coffee grounds [19] and the sensory properties of beverages [20–23]. However, in order to extract the most information from NIRS measurements, different data analyses methods are needed. In the aforementioned scientific papers, different pre-processing techniques (MSC, SNV, first and second derivatives, normalization, OSC) and multivariate statistical tools such as PCA, PLSR, linear discriminant analysis (LDA) and PLS-DA were used to analyze various properties of coffee.

The first step in NIR data analysis is the visual representation of the recorded signal responses on the recording wavelengths. The characteristics of the created curves might be able to explain differences among samples and highly different samples can be differentiated visually. The obtained NIR spectra, however, need to be further analyzed using multivariate statistical methods in order to extract more information to be able to define small differences among samples. Several different statistical methods have been introduced such as partial least squares discriminant analysis (PLS-DA) [17], soft independent modelling of class analogy (SIMCA) [24], principal component analysis (PCA), and locally weighted regression (LWR) [25], multivariate curve resolution-alternating least squares (MCR-ALS) method [26], and k-nearest neighbors and support vector machine (SVM) [27]. The majority of these methods treat NIR spectra as an observations–variables table, where the samples are considered as observations and the given wavelengths are used as variables. However, NIR spectra can also be considered as time series since the responses are recorded at equally distanced wavelengths.

One promising technique, detrended fluctuation analysis (DFA) has been introduced for the analysis of chromatograms [28]. DFA is a widely used time series data analysis tool and was successfully applied in the past few years for the evolution of high-viscosity gas–liquid flows [29], water contaminant classification [30], for EEG patterns associated with real and imaginary arm movements [31], air traffic flow analysis [32], and even for the analysis of NBA results [33], for instance. As the above list of completely different fields of application of DFA suggests, the method is highly flexible and can easily be integrated into different systems.

Another promising approach in NIRS data analysis would be the application of yield stability index (YSI) [34]. Agricultural production might provide high fluctuations due to environmental factors. However, there is always a clear yield range a farmer can handle. In most years, the yield fluctuates

within this range; however, there are years when extremely high or low yields might cause serious economic losses. YSI has been developed to measure these extremities in a time series by quantifying the level of stability for a yield series by measuring the proportion of annual yields being reasonably close to the expected trend value within a time period [35]. In NIRS data analysis, YSI is expected to provide information about the stability of the signals of the different roasting levels, e.g., which spectra shows the highest fluctuation.

In this study, the applications of detrended fluctuation analysis and yield stability index is introduced on NIR spectra of different roasting levels of coffee samples. The aims of the study are as follows:

- Introduce new tools for the analysis of near infrared spectra;
- Differentiate coffee samples based on their roasting levels using detrended fluctuation analysis.

2. Materials and Methods

2.1. Samples

Fourteen green *Coffea arabica* samples from different geographical origin and one *Coffea canephora* sample from India were purchased from Semiramis Kft. (Budapest, Hungary). Detailed information about the samples are shown in Table 1. These samples were divided in three part after recording their near infrared spectra to perform the roasting experiment.

Table 1. Description of coffee samples.

Sample Number	Geographical Origin
1	Brazil, South America
2	India, Asia
3	Uganda, Africa
4	Colombia, South America
5	Uganda, Africa
6	Colombia, South America
7	Sumatra, Asia
8	Papua New Guinea, Asia
9	Guatemala, Central America
10	Kenya, Africa
11	Ethiopia, Africa
12	Panama, Central America
13	Mexico, Central America
14	India, Asia
15	Uganda, Africa

2.2. Roasting Experiment

The samples were small scale roasted using a pre-determined roasting method. Three roasting levels were set up considering the first crack of samples: light, medium and dark roast. In the case of light roasted coffees, the samples were removed from the roaster 40 s after the first crack. To obtain the other two levels, the roasting time was raised to 60 s and 90 s after the first crack. The initial temperature of roasting was around 150 °C and the final temperature around 190 °C. From each raw sample, about 300 g were roasted to each level using a Probat roaster (Sample Coffee Roaster, Leogap, Curitiba, PR, Brazil).

2.3. Near-Infrared Spectroscopy (NIRS)

The near-infrared spectra of the green and roasted coffee beans were collected using a Bruker MPA™-Multipurpose FT-NIR analyzer (Bruker, Ettlingen, Germany). For the measurement, the whole amount of the raw and roasted samples was used, of which 40–60 g were measured using a rotating

cuvette (Ø85 mm) in six replicates. The spectral data were collected in diffuse reflection measurements mode within the range of 12,500–3800 cm^{-1} (resolution 16 cm^{-1} ; scanning speed 10 kHz), using the OPUS 7.2 (Bruker, Ettlingen, Germany) software. Each spectrum was calculated as the average of 32 subsequent scans. Background scans were recorded with a gold-coated integrating sphere.

2.4. Principal Component Analysis (PCA)

In NIR spectroscopy, there is a need for data-reduction methods because of the high number of spectral variables. PCA is used to decompose the matrix of the interest into several independent and orthogonal principal components [36]. An important application of PCA is classification and pattern recognition. The fundamental idea behind this approach is that data vectors representing objects in a high-dimensional space can be efficiently projected into a low-dimensional space by PCA and viewed graphically as scatter plots of PC scores. Objects that are similar to each other will tend to cluster in the score plots, whereas objects that are dissimilar will tend to be far apart. By “efficient,” we mean the PCA model must capture a large fraction of the variance in the data set, say 70% or more, in the first few principal components [37]. Multiplicative Scatter Correction (MSC), a widely used pre-processing technique for NIRS was used to reduce the impact of light scattering. The concept behind MSC is that artifacts or imperfections (e.g., undesirable scatter effect) will be removed from the data matrix prior to data modeling. MSC is comprised of the following two steps:

1. Estimation of the correction coefficients (additive and multiplicative contributions),

$$x_{org} = b_0 + b_{ref,1} \cdot x_{ref} + e;$$

2. Correcting the recorded spectrum,

$$x_{corr} = \frac{x_{org} - b_0}{b_{ref,1}} = x_{ref} + \frac{e}{b_{ref,1}},$$

where x_{org} is one original sample spectra measured by the NIR instrument, x_{ref} is a reference spectrum used for pre-processing of the entire dataset, e is the un-modeled part of x_{org} , x_{corr} is the corrected spectra, and b_0 and $b_{ref,1}$ are scalar parameters, which differ for each sample. In most applications, the average spectrum of the calibration set is used as the reference spectrum [38]. PCA and MSC were performed using Unscrambler X 10.4 (ver. 10.4, CAMO Software AS, Oslo, Viken, Norway, 2016) software.

2.5. Agglomerative Hierarchical Clustering (AHC)

Agglomerative Hierarchical Clustering (AHC), an unsupervised classification method, was used to group the coffee samples based on the obtained DFA coefficients (see Section 2.7). Ward method was used to compute the distance matrix and while the grouping was done using single linkage. Silhouette index was computed to obtain the optimal number of clusters. AHC and Silhouette index was computed using R-project (R version 4.0.0 (Arbor Day), R Core Team, Vienna, Austria, 2019) [39].

2.6. Multiple Correspondence Analysis (MCA)

Multiple Correspondence Analysis (MCA) is a multivariate method that provides a graphical representation of cross tabulations. Cross tabulations arise whenever it is possible to place events into two or more different sets of categories. CA is conceptually similar to principal component analysis but applies to categorical rather than continuous data. In a similar manner to principal component analysis, it provides a means of displaying or summarizing a set of data in two-dimensional graphical form [40]. MCA was carried out using XL-Stat software (ver. 2019.4.2, Addisonsoft, Paris, IDF, France, 2019).

2.7. Detrended Fluctuation Analysis (DFA)

Generally, DFA is used to analyze long-range correlations in time series. In case of NIRS, there is no time-related information; however, absorbance data as a function of wavenumber can be analyzed using DFA because of the large number of variables in the spectral data. The absorbance data are collected at regular interval depending on the resolution of the measurement. Detrended fluctuation analysis is a scaling analysis method providing a simple quantitative parameter—the scaling exponent α —to represent the correlation properties of a signal [41]. The basic principle of DFA is to divide the time series into equal ranges and determine the fluctuation of the individual ranges by computing the scaling exponent. In order to create overlapping ranges, sliding window DFA approach was developed, which has been successfully used for pattern recognition and grouping. The presented paper uses the algorithm introduced by Radványi and co-workers [28]. Physisonet [42] was used to perform DFA and additional computations were carried out using R-project (R version 4.0.0 (Arbor Day), R Core Team, Vienna, Austria, 2019) [39].

2.8. Yield Stability Index

Yield stability index (YSI) was developed by Vízvári and Bacsí [34] and is able to capture the level of stability for a time series (or a signal) by fitting a trend line and quantifying the proportion of difference from the trend compared to a normal distribution as follows (Figure 1):

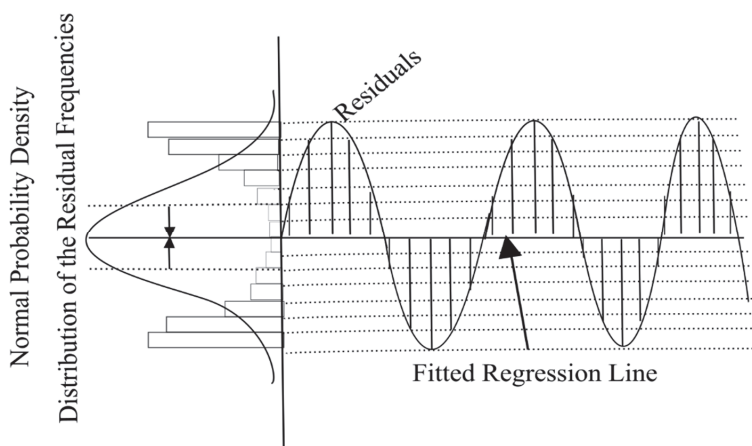


Figure 1. Visual representation of the underlying concept of yield stability index. Source: Papp and co-workers [43].

According to Vízvári and Bacsí [34], the signal should be normalized by dividing the whole signal by its mean and after that a trend line is fitted to the normalized signal (a polynomial of a degree of 1, 2 or 3) and the residuals are determined by subtracting the trend from the normalized signal. This process must be performed for all the investigated signals of a kind creating a single residual distribution function. We then fit a normal distribution and a histogram to the residual distribution. The favorable residual frequency (FRF) is the fraction of residuals falling into the middle four segments of the histogram and the favorable normal frequency (FNF) is the fraction of the middle 4 segments from the fitted normal distribution. YSI is calculated as the difference of the FRF and the FNF as follows:

$$YSI = 2 \times (FRF - FNF)$$

The YSI index values should fall between -2 and 2 , because both FRF and FNF can take values between 0 and 1 . Negative values indicate that the distribution of the residuals significantly deviates

from normal implying larger oscillations around the trend line. In case the signal is stable, residuals should be located in the middle four segments around zero; therefore, the YSI should be zero or greater suggesting the lack of large oscillations.

We adapted and extended the methodology of Vizvari and Bacsı [34]. Our development compared to the above presented methodology is that we bin the values into $\lceil \log_2(n) \rceil + 1$ equal segments according to the Sturges' formula and further divided the middle four segments to 20 parts and we calculated the YSI value by gradually narrowing the border (dashed lines in Figure 1) of the middle four segments on both sides closer to 0 in 10 steps resulting 10 different YSI values. In the next step, we calculated how many times the YSI values were greater than 0 or a predefined cut value. In this way, we obtained a final index (between 0 and 10) that can be used to compare signal oscillation and stability—0 means higher oscillations and less stability and the signals were under the cut value most of the time, the higher values indicate stronger stability and less oscillations. Calculation of YSI were done using R-project (R version 4.0.0 (Arbor Day), R Core Team, Vienna, Austria, 2019) [39]. The signals were pre-processed by taking their logarithm to smooth the signals for the trend fit as much as possible.

3. Results

3.1. Spectral Characteristics

Before the statistical evaluation, it is practical to analyze the original spectra of the samples and first or second derivative of the spectra. First derivatives remove additive baseline shift so this is very useful in NIR spectroscopy. However, first derivatives produce peaks where the original spectrum had maximum slope and crosses zero where the original had a peak and are thus rather difficult to interpret. NIR spectra also tend to have linear baseline increases and these are removed by second derivatives which have negative peaks where the original had a peak and are thus more readily comprehensible. For these reasons second derivatives are often preferred [44]. Figure 2a shows that the spectral characteristics of raw and roasted coffee samples are similar in the main absorption bands, but the absorbance intensity of raw coffee is higher from 8500 to 3800 cm^{-1} . The differences evolve with the roasting process causing changes in chemical composition. The broad absorption bands (5210–5155 and 6945–6805 cm^{-1}) are assigned to water; however, water present in the sample affects the absorption of all other components.

The absorbance values of the sample spectra decreased in the spectral range 7500–3800 cm^{-1} , as roasting time increased (water content decreased), which are in accordance with earlier studies [14,21]. This characteristic was reversed in the spectral region nearest to visible range (12,500–8000 cm^{-1}). This phenomenon can be the result of the darker color of samples.

The second derivative spectra of coffee samples (see Figure 2b) are more detailed, because the overlapping peaks are resolved using the Savitzky–Golay transformation. The spectral characteristics of raw coffee samples can be discriminated visually from the roasted coffee spectra. During roasting, a large number of chemical transformations take place simultaneously (i.e., Maillard and Strecker reactions, degradation of proteins, polysaccharides, trigonelline and chlorogenic acids), leading to the formation of thousands of molecules that give the peculiar aroma of coffee [16]. The molecular overtone and combination bands seen in the NIR range are typically very broad, leading to complex spectra, thus, making it difficult to assign particular features to specific chemical components [6]. According to the scientific literature [14,17,21,23], a great amount of absorption bands are assigned to different chemical components which are perceptible on the second derivative spectra of coffee samples.

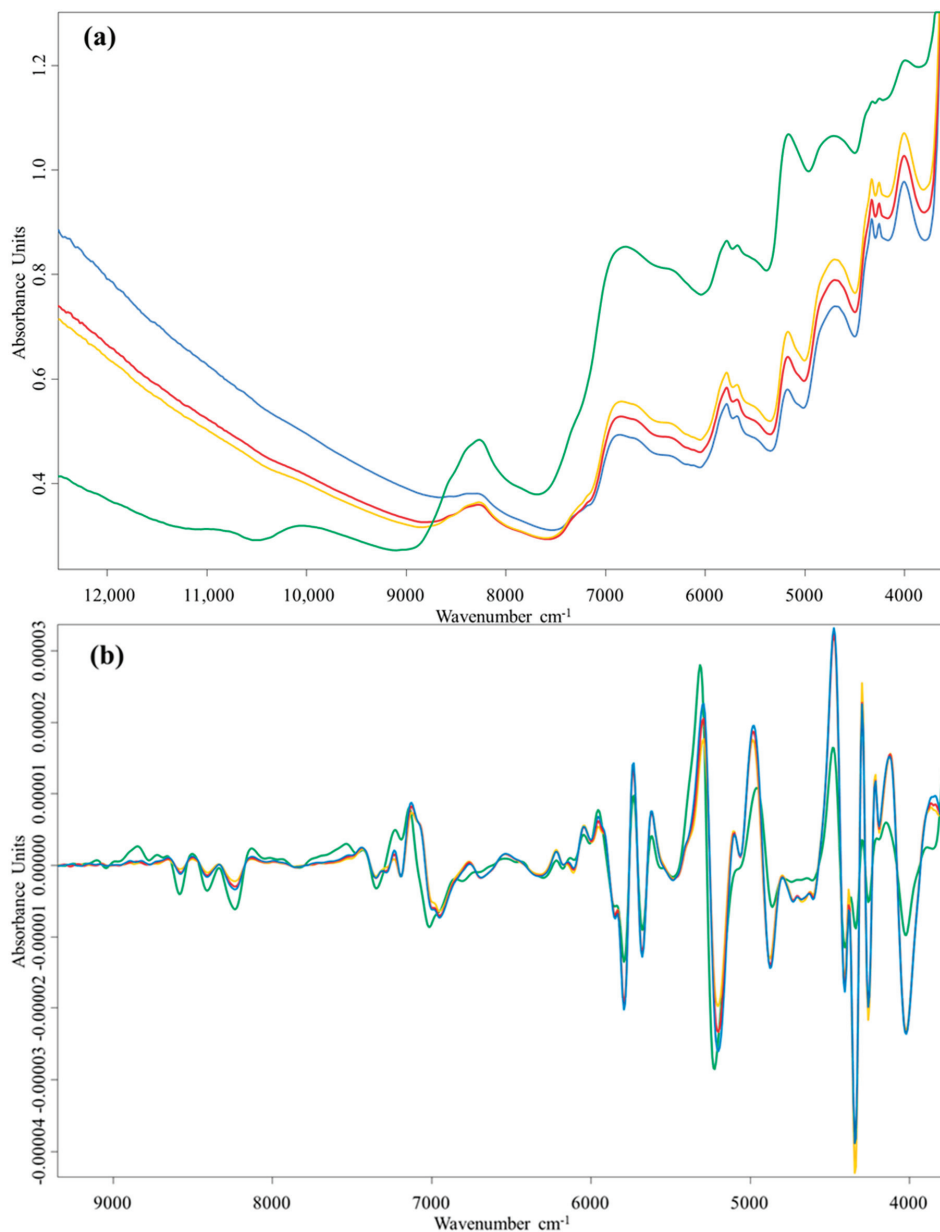


Figure 2. (a) The original average spectra of sample 1: raw (●), light roasted (●), medium roasted (●), dark roasted (●). (b) The second derivative spectra of sample 1: green (●), light roasted (●), medium roasted (●), dark roasted (●).

3.2. Principal Component Analysis (PCA)

PCA was performed on the original and transformed (MSC) data in the 12,500–3800 cm^{-1} spectral range. In case of the original data, the first principal component had a smaller impact on the separation of the samples. There is a tendency among the samples, namely the dark roasted samples are

characterized by negative scores along PC1, while medium and light roasted samples are located to the right of the plot (plot not shown). MSC transformation was performed on the spectra of each roasting stage separately.

Figure 3a shows the scores plot of the first two principal components (PCs), which capture 98% of the variance. The main direction is described by PC1 (93%). According to the loading plot, the variables between 12,500–7500 cm^{-1} have a negative effect on the sample distribution along PC1, therefore all dark roasted samples can be found on the left side of scores plot. These features have a high impact on differentiating roasting stages. Both PC1 and PC2 values play a role in the separation of the roasting levels. It has to be noted that the loading plot values of PC3 (1%) describes important absorption bands (of the 6800–3800 cm^{-1} region; see in Section 3.3.).

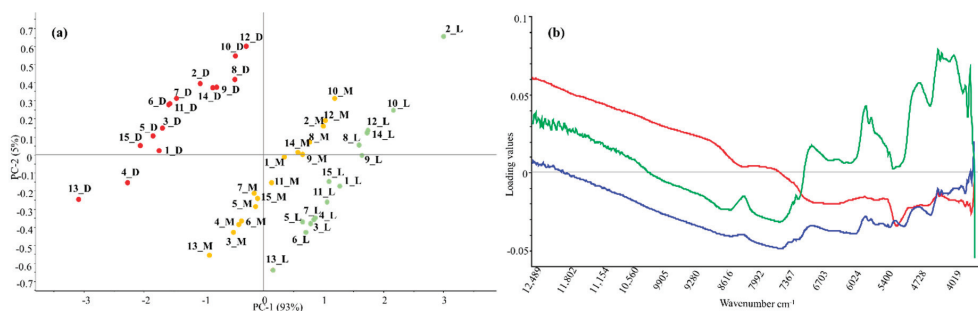


Figure 3. (a) Scores plot (PC1 vs PC2) of roasted coffee samples labelled with sample number and roasting level (L—light; M—medium; D—dark roasted). (b) Loading plots of the first three PC: PC1 (●), PC2 (●), PC3 (●).

3.3. Detrended Fluctuation Analysis

Detrended fluctuation analysis (DFA) was run on the average FT-NIR spectra of six parallel measurements of the same sample. The obtained α_1 and α_2 coefficients were used to plot the samples and to compute their distances. DFA differentiated green samples from the roasted samples clearly. As Figure 4 shows, samples having an $\alpha_1 = 1.95$ and $\alpha_2 = 1.65$ coefficients can be classified as green samples. Differentiation among green samples is done by the distinct chemical composition, which are also affected by diverse cultivation and post-harvest processes. The size, shape and color of the beans, as well as the silver skin and parchment left on their surface, also have an effect on the spectra.

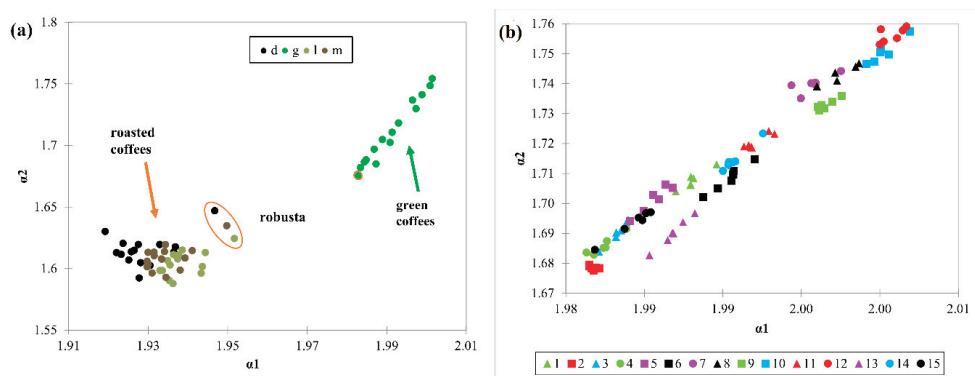


Figure 4. α_1 and α_2 coefficients obtained from detrended fluctuation analysis. (a) averaged spectra of the green (g), light (l), medium (m) and dark roast (d) samples. Different colors denote different roasting levels (b) the six replicates of the green samples. Different colors and symbols denote different countries.

According to the second derivative spectra of the green samples, smaller but noticeable differences can be observed. These are manifested in band shifts and higher or smaller absorption for the given band location, which are assigned for example to water (5210 cm^{-1}), fatty acids (around $5600\text{--}4000\text{ cm}^{-1}$, $8300\text{--}8100\text{ cm}^{-1}$), fibers (around 7450 cm^{-1} , $5800\text{--}4700\text{ cm}^{-1}$), caffeine (around 8665 , 8250 , $5300\text{--}5100$ and 4700 cm^{-1}) and proteins (5700 , $4800\text{--}4600\text{ cm}^{-1}$).

The three roasting levels show a distinct pattern, where the dark roasted samples usually show lower α_1 and higher α_2 coefficient values. Light roasted samples are grouped on the bottom right corner of the plot, having the highest α_1 and lowest α_2 coefficient values. Based on these, a straight line can be drawn which shows the roasting level of the individual samples (Figure 5).

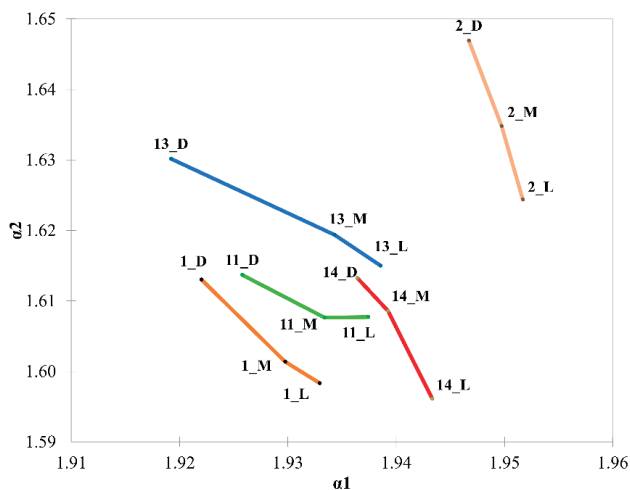


Figure 5. α_1 and α_2 coefficients obtained from detrended fluctuation analysis. Averaged spectra of the green, light, medium and dark roast samples. Different colors denote different coffee origins.

When the DFA coefficients are evaluated within one sample, the differentiation among the roasting levels are clear. Figure 6 introduces the α_1 and α_2 coefficients of the six parallel measurements of the Colombian sample (all roasting levels). Although it is visually clear that the samples do not overlap, we used Agglomerative Hierarchical Clustering to justify the grouping of the samples. On the right of Figure 6, we can see the results of AHC. Clear clusters are formed, no misclassification was done. It can also be seen that medium and light roasted samples are located closer to each other than the dark roasted samples.

There is some differentiation among the cultivars, the only robusta sample is placed further from the other arabica samples. It is caused by the distinct spectral features of the robusta sample, since robusta coffees contain diverse levels of caffeine, chlorogenic acids, lipids and sucrose compared to arabica coffees [5]. It has to be noted, however, that we analyzed only one robusta sample, hence further generalization cannot be drawn. The three roasting levels cannot be differentiated clearly when all samples are analyzed together, however, within one sample the roasting levels were differentiated.

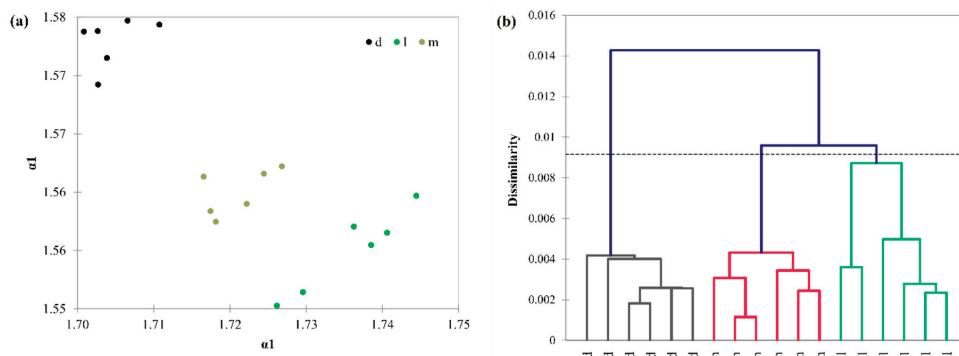


Figure 6. Detrended fluctuation analysis of the parallel measurements of the Columbian coffee samples. (a) α_1 and α_2 coefficients obtained from detrended fluctuation analysis. Spectra of the light (l), medium (m) and dark (d) roast samples are coded by different colors. (b) Agglomerative hierarchical cluster analysis of the α_1 and α_2 coefficients using Euclidean distance and complete linkage.

3.4. Yield Stability Index

Yield stability index gives an additional information about the analyzed spectra. As YSI attempts to filter extremities among the set of the analyzed spectra, the obtained result of the YSI analysis is a contingency table, where the sample sets (in our case the roasting levels such as green, light, medium and dark) are presented, while in the rows the number of times the YSI index was over the cut value. Table 2 presents the numerical results obtained after running the YSI on the original NIR data set. A chi-square test indicated that the rows and columns of the table shows significant associations ($\chi^2(24, N = 36) = 49.31, p = 0.0017$). In order to visualize the observed associations, correspondence analysis was run on the contingency table presented by Table 2. Correspondence analysis visualized the similarities among the green and light roasted samples (Figure 7). These samples show similar distribution of residuals, close to the mean but from the cut values we can see that light roast is more stable as its signal had higher YSI values. As the roasting time increases, the difference from the mean trend also increases, meaning that dark roasted samples show extreme fluctuations.

Table 2. Distribution of YSI indices by roasting level *.

YSI <i>n</i>	Green	Light Roast	Medium Roast	Dark Roast
0	0	0	0	0
1	0	0	0	0
2	0	2	0	1
3	1	1	4	0
4	1	4	3	3
5	5	5	3	0
6	2	2	1	0
7	1	1	4	0
8	1	0	0	0
9	2	0	0	6
10	2	0	0	5
N	15	15	15	15
Cut value for YSI	0	0.2	0.1	0

* quadratic polynomial was used in case of all signals except green roast where a linear polynomial fitted the best.

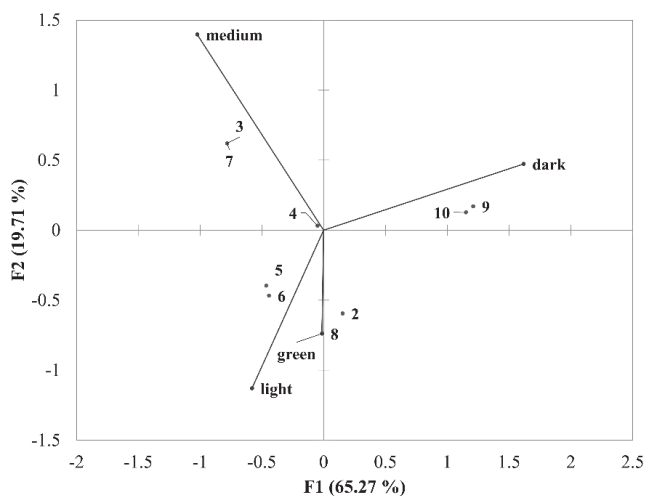


Figure 7. Correspondence analysis run on the data presented by Table 2. Numbers denote the number of times YSI was over the cut value.

Table 2 presents the results of yield stability index (YSI) analysis. The number of spectra over the YSI cut value is presented in each row. Grey background indicates the highest numbers of occurrences. N denotes sample number. YSI_n : Number of times YSI was over the cut value.

4. Conclusions

Differentiation of the roasting levels was successfully completed using principal component analysis (PCA), however, only after applying multiple scatter correction (MSC). MSC had no effect on the differentiations when detrended fluctuation analysis (DFA) was applied. It has to be noted that PCA was able to differentiate the different roasting levels when all samples were analyzed together. The three roasting levels cannot be differentiated clearly by DFA as only the green samples were differentiated clearly and the three roasting levels showed only tendencies. On the other hand, DFA successfully differentiated the roasting levels sample-wise, meaning that it captured the within-sample differences well. It is an important aspect here since usually the question of producers is how to tell if a green coffee is roasted well (e.g., on a level that highlights the proper quality of the given coffee). A simple cluster analysis applied on the coefficients of the DFA showed clear groupings, making the results robust and creating the opportunity to perform classifications as well. Another advantage of DFA here comes from the nature of the method. DFA analyses one spectrum at a time, therefore it is not influenced by the others. When performing PCA, the whole data set (e.g., all samples) are analyzed at the same time. Naturally, the more samples we have the better results we can get in terms of validity and generalization. However, it is a disadvantage when we have a set of new samples since the scores obtained from PCA will change. Using DFA, global thresholds can be set for each sample, e.g., if the α_1 and α_2 coefficients are within the given ranges, the sample can be classified as green, light, medium or dark roasted. Therefore, DFA might be a valuable tool in coffee quality control. It is also an advantage, when the number of samples (or spectra) is too low to perform multivariate data analyses. Yield Stability Index was first used in signal processing. The methodology was able to detect that light roast is the most stable among all roasting levels.

Future research should focus on the application of DFA in terms of the analysis of the effects of other transformation methods of the spectra. Additionally, different samples should also be analyzed to evaluate the robustness of the method, e.g., if there are any effects of the samples being analyzed on the performance of DFA.

Author Contributions: E.B.: Data curation, Formal analysis, Investigation, Validation, Visualization, Writing—original draft, Writing—review & editing; M.F.: Data curation, Validation, Supervision, Project administration, Resources, Writing—original draft, Writing—review & editing; S.K.: Formal analysis, Methodology, Software, Resources, Supervision, Visualization, Writing—original draft, Writing—review & editing; A.G.: Formal analysis, Funding acquisition, Methodology, Project administration, Supervision, Writing—original draft, Writing—review & editing. All authors have read and agreed to the published version of the manuscript.

Funding: The Project was funded by the European Union and co-financed by the European Social Fund (grant agreement no. EFOP-3.6.3-VEKOP-16-2017-00005). The APC was funded by the European Union and co-financed by the European Social Fund (grant agreement no. EFOP-3.6.3-VEKOP-16-2017-00005).

Acknowledgments: A.G. thanks the support of the Premium Postdoctoral Researcher Program of the Hungarian Academy of Sciences. This project was supported by the János Bolyai Research Scholarship of the Hungarian Academy of Sciences. The Project is also supported by the Doctoral School of Food Science SZIU.

Conflicts of Interest: The authors declare no conflict of interest.

References

1. Farah, A. *Coffee: Production, Quality and Chemistry*; Farah, A., Ed.; Royal Society of Chemistry: London, UK, 2019; ISBN 9781782620044.
2. Malta, M.R.; de Fassiio, L.O.; Liska, G.R.; Carvalho, G.R.; Pereira, A.A.; Botelho, C.E.; Ferraz, V.P.; Silva, A.D.; Pedrosa, A.W.; Alvaro, L.N.; et al. Discrimination of genotypes coffee by chemical composition of the beans: Potential markers in natural coffees. *Food Res. Int.* **2020**, *134*, 109219. [CrossRef]
3. Preedy, V.R. *Coffee in Health and Disease Prevention*; Academic Press: London, UK, 2014; ISBN 9780124167162.
4. International Coffee Organization. *ICO Indicator Prices—May 2020*; International Coffee Organization: London, UK, 2020; p. 1. Available online: <http://www.ico.org/prices/p1-May2020.pdf> (accessed on 24 June 2020).
5. Cheng, B.; Furtado, A.; Smyth, H.E.; Henry, R.J. Influence of genotype and environment on coffee quality. *Trends Food Sci. Technol.* **2016**, *57*, 20–30. [CrossRef]
6. Barbin, D.F.; Felicio, A.L.; Sun, D.W.; Nixdorf, S.L.; Hirooka, E.Y. Application of infrared spectral techniques on quality and compositional attributes of coffee: An overview. *Food Res. Int.* **2014**, *61*, 23–32. [CrossRef]
7. Benes, E.; Gere, A.; Fodor, M. Predicting macronutrients and energy content of snack products using FT-NIR analysis and chemometric techniques. *J. Food Eng.* **2020**, *280*, 109954. [CrossRef]
8. Fodor, M.; Woller, A.; Turza, S.; Szegedi, T. Development of a rapid, non-destructive method for egg content determination in dry pasta using FT-NIR technique. *J. Food Eng.* **2011**, *107*, 195–199. [CrossRef]
9. Mikola, E.; Geösel, A.; Stefanovits-Bányai, É.; Fodor, M. Quantitative determination of macro components and classification of some cultivated mushrooms using near-infrared spectroscopy. *J. Food Process. Preserv.* **2020**, *44*, e14540. [CrossRef]
10. Shan, J.; Suzuki, T.; Suhandy, D.; Ogawa, Y.; Kondo, N. Chlorogenic acid (CGA) determination in roasted coffee beans by Near Infrared (NIR) spectroscopy. *Eng. Agric. Environ. Food* **2014**, *7*, 139–142. [CrossRef]
11. Magalhães, L.M.; Machado, S.; Segundo, M.A.; Lopes, J.A.; Páscoa, R.N.M.J. Rapid assessment of bioactive phenolics and methylxanthines in spent coffee grounds by FT-NIR spectroscopy. *Talanta* **2016**, *147*, 460–467. [CrossRef] [PubMed]
12. Craig, A.P.; Botelho, B.G.; Oliveira, L.S.; Franca, A.S. Mid infrared spectroscopy and chemometrics as tools for the classification of roasted coffees by cup quality. *Food Chem.* **2018**, *245*, 1052–1061. [CrossRef] [PubMed]
13. De Luca, S.; De Filippis, M.; Bucci, R.; Magri, A.D.; Magri, A.L.; Marini, F. Characterization of the effects of different roasting conditions on coffee samples of different geographical origins by HPLC-DAD, NIR and chemometrics. *Microchem. J.* **2016**, *129*, 348–361. [CrossRef]
14. Alessandrini, L.; Romani, S.; Pinnavaia, G.; Rosa, M.D. Near infrared spectroscopy: An analytical tool to predict coffee roasting degree. *Anal. Chim. Acta* **2008**, *625*, 95–102. [CrossRef] [PubMed]
15. Esteban-Díez, I.; González-Sáiz, J.M.; Pizarro, C. An evaluation of orthogonal signal correction methods for the characterisation of arabica and robusta coffee varieties by NIRS. *Anal. Chim. Acta* **2004**, *514*, 57–67. [CrossRef]
16. Bertone, E.; Venturolo, A.; Giraud, A.; Pellegrino, G.; Geobaldo, F. Simultaneous determination by NIR spectroscopy of the roasting degree and Arabica/Robusta ratio in roasted and ground coffee. *Food Control* **2016**, *59*, 683–689. [CrossRef]

17. Giraud, A.; Grassi, S.; Savorani, F.; Gavoci, G.; Casiraghi, E.; Geobaldo, F. Determination of the geographical origin of green coffee beans using NIR spectroscopy and multivariate data analysis. *Food Control* **2019**, *99*, 137–145. [CrossRef]
18. Jesztl, B.; Benes, E.; Fodor, M. FT-NIR origin identification of coffee samples. *J. Food Investig.* **2019**, *65*, 2360–2377.
19. Kárpáti, Z.; Benes, E.; Fodor, M. Nutritional analysis of coffee dregs for utilization purposes using classical, ICP-OES and FT-NIR techniques. *J. Food Investig.* **2018**, *64*, 2178–2183.
20. Tolessa, K.; Rademaker, M.; De Baets, B.; Boeckx, P. Prediction of specialty coffee cup quality based on near infrared spectra of green coffee beans. *Talanta* **2016**, *150*, 367–374. [CrossRef]
21. Esteban-Díez, I.; González-Sáiz, J.M.; Pizarro, C. Prediction of sensory properties of espresso from roasted coffee samples by near-infrared spectroscopy. *Anal. Chim. Acta* **2004**, *525*, 171–182. [CrossRef]
22. Barbosa, M.D.; dos Santos Scholz, M.B.; Kitzberger, C.S.; de Toledo Benassi, M. Correlation between the composition of green Arabica coffee beans and the sensory quality of coffee brews. *Food Chem.* **2019**, *292*, 275–280. [CrossRef]
23. Ribeiro, J.S.; Ferreira, M.M.C.; Salva, T.J.G. Chemometric models for the quantitative descriptive sensory analysis of Arabica coffee beverages using near infrared spectroscopy. *Talanta* **2011**, *83*, 1352–1358. [CrossRef]
24. Márquez, C.; López, M.I.; Ruisánchez, I.; Callao, M.P. FT-Raman and NIR spectroscopy data fusion strategy for multivariate qualitative analysis of food fraud. *Talanta* **2016**, *161*, 80–86. [CrossRef]
25. Grassi, S.; Amigo, J.M.; Lyndgaard, C.B.; Foschino, R.; Casiraghi, E. Beer fermentation: Monitoring of process parameters by FT-NIR and multivariate data analysis. *Food Chem.* **2014**, *155*, 279–286. [CrossRef] [PubMed]
26. del Río, V.; Callao, M.P.; Larrechi, M.S.; de Espinosa, L.M.; Ronda, J.C.; Cádiz, V. Chemometric resolution of NIR spectra data of a model aza-Michael reaction with a combination of local rank exploratory analysis and multivariate curve resolution-alternating least squares (MCR-ALS) method. *Anal. Chim. Acta* **2009**, *642*, 148–154. [CrossRef] [PubMed]
27. Jin, G.; Wang, Y.; Li, L.; Shen, S.; Deng, W.-W.; Zhang, Z.; Ning, J. Intelligent evaluation of black tea fermentation degree by FT-NIR and computer vision based on data fusion strategy. *LWT* **2020**, *125*, 109216. [CrossRef]
28. Radványi, D.; Gere, A.; Sipos, L.; Kovács, S.; Jókai, Z.; Fodor, P. Discrimination of mushroom disease-related mould species based solely on unprocessed chromatograms. *J. Chemom.* **2016**, *30*, 197–202. [CrossRef]
29. Hernández, J.; Galaviz, D.F.; Torres, L.; Palacio-Pérez, A.; Rodríguez-Valdés, A.; Guzmán, J.E.V. Evolution of high-viscosity gas-liquid flows as viewed through a detrended fluctuation characterization. *Processes* **2019**, *7*, 822. [CrossRef]
30. Zhu, Y.; Wang, K.; Lin, Y.; Yin, H.; Hou, D.; Yu, J.; Huang, P.; Zhang, G. An Online Contaminant Classification Method Based on MF-DCCA Using Conventional Water Quality Indicators. *Processes* **2020**, *8*, 178. [CrossRef]
31. Pavlov, A.N.; Runnova, A.E.; Maksimenko, V.A.; Pavlova, O.N.; Grishina, D.S.; Hramov, A.E. Detrended fluctuation analysis of EEG patterns associated with real and imaginary arm movements. *Phys. A Stat. Mech. Its Appl.* **2018**, *509*, 777–782. [CrossRef]
32. Zhang, X.; Liu, H.; Zhao, Y.; Zhang, X. Multifractal detrended fluctuation analysis on air traffic flow time series: A single airport case. *Phys. A Stat. Mech. Its Appl.* **2019**, *531*, 121790. [CrossRef]
33. Ferreira, P. What detrended fluctuation analysis can tell us about NBA results. *Phys. A Stat. Mech. Its Appl.* **2018**, *500*, 92–96. [CrossRef]
34. Vizvári, B.; Bacsí, Z. Technological development and the stability of technology in crop production. *J. Cent. Eur. Agric.* **2002**, *3*, 63–72.
35. Bacsí, Z.; Hollósy, Z. A yield stability index and its application for crop production. *Analecta Tech. Szeged.* **2019**, *13*, 11–20. [CrossRef]
36. Chau, F.-T.; Liang, Y.-Z.; Gao, J.; Shao, X.-G. *Chemometrics: From Basics to Wavelet Transform*; Winefordner, J.D., Ed.; John Wiley & Sons, Inc.: Hoboken, NJ, USA, 2004; ISBN 978-0-471-45473-1.
37. Gemperline, P. *Practical Guide to Chemometrics*, 2nd ed.; CRC Press: Boca Raton, FL, USA, 2006; ISBN 1574447831.
38. Rinnan, Å.; van den Berg, F.; Engelsen, S.B. Review of the most common pre-processing techniques for near-infrared spectra. *TrAC Trends Anal. Chem.* **2009**, *28*, 1201–1222. [CrossRef]
39. R Core Team. *R: A Language and Environment for Statistical Computing*; R Foundation for Statistical Computing: Vienna, Austria, 2019.

40. Greenacre, M.; Blasius, J. *Multiple Correspondence Analysis and Related Methods*, 1st ed.; Chapman and Hall/CRC: New York, NY, USA, 2006; ISBN 9780429141966.
41. Lan, T.H.; Gao, Z.Y.; Abdalla, A.N.; Cheng, B.; Wang, S. Detrended fluctuation analysis as a statistical method to study ion single channel signal. *Cell Biol. Int.* **2008**, *32*, 247–252. [CrossRef] [PubMed]
42. Goldberger, A.L.; Amaral, L.A.; Glass, L.; Hausdorff, J.M.; Ivanov, P.C.; Mark, R.G.; Mietus, J.E.; Moody, G.B.; Peng, C.K.; Stanley, H.E. PhysioBank, PhysioToolkit, and PhysioNet: Components of a new research resource for complex physiologic signals. *Circulation* **2000**, *101*, E215–E220. [CrossRef] [PubMed]
43. Papp, F.; Hajdu, P.; Tajti, G.; Toth, A.; Nagy, E.; Fazekas, Z.; Kovacs, S.; Vámosi, G.; Varga, Z.; Panyi, G. Periodic membrane potential and Ca²⁺ oscillations in t cells forming an immune synapse. *Int. J. Mol. Sci.* **2020**, *21*, 1568. [CrossRef] [PubMed]
44. Davis, A.M.; Fearn, T. Back to basics: Spectral pre-treatments—Derivatives. *Spectrosc. Eur.* **2007**, *19*, 32–33.



© 2020 by the authors. Licensee MDPI, Basel, Switzerland. This article is an open access article distributed under the terms and conditions of the Creative Commons Attribution (CC BY) license (<http://creativecommons.org/licenses/by/4.0/>).

Review

Effect of Selected Drying Methods and Emerging Drying Intensification Technologies on the Quality of Dried Fruit: A Review

Milivoj Radojčin ^{1,*}, Ivan Pavkov ¹, Danijela Bursać Kovačević ², Predrag Putnik ³, Artur Wiktor ⁴, Zoran Stamenković ¹, Krstan Kešelj ¹ and Attila Gere ⁵

- ¹ Faculty of Agriculture, University of Novi Sad, Trg Dositeja Obradovića 8, 21000 Novi Sad, Serbia; ivan.pavkov@polj.uns.ac.rs (I.P.); zoran.stamenkovic@polj.uns.ac.rs (Z.S.); krstan.keselj@polj.uns.ac.rs (K.K.)
 - ² Faculty of Food Technology and Biotechnology, University of Zagreb, Pierottijeva 6, 10000 Zagreb, Croatia; dbursac@pbf.hr
 - ³ Department of Food Technology, University North, Trg dr. Žarka Dolinara 1, 48000 Koprivnica, Croatia; pputnik@alumni.uconn.edu
 - ⁴ Department of Food Engineering and Process Management, Faculty of Food Sciences, Warsaw University of Life Sciences, Nowoursynowska 159c, 02-776 Warsaw, Poland; artur_wiktor@sggw.edu.pl
 - ⁵ Institute of Food Technology, Szent István University, Villányi Str. 29-31, H-1118 Budapest, Hungary; gereattilaphd@gmail.com
- * Correspondence: milivoj.radojcin@polj.uns.ac.rs

Abstract: Drying is one of the oldest methods for food preservation that removes the water from fruit and makes it available for consumption throughout the year. Dried fruits can be produced by small- and large-scale processors, which makes them a very popular food among consumers and food manufacturers. The most frequent uses of drying technology include osmotic dehydration, vacuum drying, freeze-drying and different combinations of other drying technologies. However, drying may provoke undesirable changes with respect to physicochemical, sensory, nutritional and microbiological quality. Drying process energy efficiency and the quality of dried fruits are crucial factors in fruit drying. Recently, innovative technologies such as ultrasound, pulsed electric field and high pressure may be used as a pretreatment or in combination with traditional drying technologies for process intensification. This could result in quality improvements of dried fruits and enhanced efficiency and capacity of the production process, with a positive impact on environmental and economic benefits.

Keywords: processing; drying; fruits; pretreatments; quality; emerging technologies

Citation: Radojčin, M.; Pavkov, I.; Bursać Kovačević, D.; Putnik, P.; Wiktor, A.; Stamenković, Z.; Kešelj, K.; Gere, A. Effect of Selected Drying Methods and Emerging Drying Intensification Technologies on the Quality of Dried Fruit: A Review. *Processes* **2021**, *9*, 132. <https://doi.org/10.3390/pr9010132>

Received: 17 December 2020

Accepted: 6 January 2021

Published: 9 January 2021

Publisher's Note: MDPI stays neutral with regard to jurisdictional claims in published maps and institutional affiliations.



Copyright: © 2021 by the authors. Licensee MDPI, Basel, Switzerland. This article is an open access article distributed under the terms and conditions of the Creative Commons Attribution (CC BY) license (<https://creativecommons.org/licenses/by/4.0/>).

1. Introduction

The term drying usually refers to the operation by which the moisture present in a material evaporates because of heat and matter exchange between the product and the working medium. Fresh fruits have high moisture contents as they are classified as highly perishable commodities; therefore, storage at refrigerated temperatures and controlled humid conditions is required [1]. Fruits are rich sources of nutrients, including vitamins, minerals, dietary fibers, phenolics, carotenoids, etc., that are useful for human health. Drying is an alternative method for the preservation of the nutritional value of fruits, which increases their relative concentration, extends their shelf life, and minimizes packaging, handling and transportation costs [2]. In addition, drying is an alternative to expensive postharvest management and selling surpluses of fruits on the market. The drying of fruits by conventional methods, such as sun drying or open-air drying, can degrade quality and food safety. Numerous disadvantages of these technologies led to the development of new technologies, such as oven drying, microwaving, vacuuming, as well as infrared, freeze and different hybrid drying, which are being used successfully for different kinds of

fruits [3–5]. Each drying technique depends on various factors, such as the required type of product, size, level of ripeness, structure, color, aroma, chemical composition, nutritional composition, together with expected final quality, availability of a dryer and costs.

Sette et al. [6] investigated the application of wet and dry infusion as a pretreatment to air and freeze-drying on the physical properties of raspberries. Freeze-dried pretreated samples exhibited higher firmness and lower deformability as compared to air-dried ones. Moreover, the highest volume reduction was developed after air-drying, while freeze-dried samples showed 11% shrinkage.

Color is a very sensitive parameter in terms of the influence of drying methods. Krokida et al. [7] stated that color parameters L^* , a^* and b^* of dried banana, apple, potato and carrot were significantly affected by convective, vacuum and microwave drying techniques. On the other hand, the same samples preserved their original color after freeze and osmotic drying.

Fruits are commonly subjected to various chemical and/or physical pretreatments prior to thermal drying to shorten the drying time, reduce the energy consumption and preserve the quality of products. By modifying the properties of fruit tissue, pretreatments could increase the drying rate, inhibit the bio-enzymes, and minimize possible deterioration reactions during drying and subsequent storage [8]. Therefore, each product needs to be dried by using appropriate pre- and post-processing steps, such as osmotic dehydration, blanching, soaking, or by the use of innovative approaches, e.g., ultrasound (US), pulsed electric field (PEF), high hydrostatic pressure (HHP), cold plasma (CP) or other treatments to add satisfactory value after drying [9,10]. This review presents the effects of different drying technologies and following treatments and/or pretreatments on dried fruits by providing the most important quality aspects.

2. Drying of Fruits

There are various studies on the topic of fruit drying where researchers have discussed the drying of fruit under different methods. The most commonly reported method is convective drying [11]. The other methods used for fruit drying are osmotic and osmo-convective [12–15], vacuum [16,17], solar drying [18,19], microwave [20,21] and freeze-drying [22–24].

2.1. Convective Hot Air Drying

Dehydration/drying is still the most commonly used method due to economic benefits. Widely used equipment components are chambers, belts or tunnel dryers. Having a closed atmosphere with regulated airflow and temperature makes this method more advantageous than solar drying. In addition, convective drying is a quite effective and simple method; nevertheless, it is energetically inefficient. Kalra and Bhardwaj [25] found that convective drying in comparison to solar drying is faster and more efficient for mangos, papayas and apricots. On the contrary, the disadvantages of the convective drying method and heating can cause progressive physical, mechanical, chemical and nutritional changes in products. In particular, Stamenkovic et al. [26] revealed losses of 32–40% for total phenols, 3–25% for flavonoids and 44–60% for anthocyanins in dried raspberries as compared to controls (fresh samples). Moreover, in comparison to fresh samples, L-ascorbic acid content was significantly reduced during convective drying (0.94–97.93%), whereas the losses observed by freeze-drying were around 2.36%. The main drawbacks also include the length of the drying during the last stage and the slow heating of the material. Cavusoglu [27] studied the effects of high air temperatures on the drying kinetics and quality of tomato. It was reported that the treatment of raw tomatoes with air temperatures 150 °C, 130 °C and 100 °C within short intervals could reduce drying time without degradation of product quality. To remediate this, hot air drying can be assisted with other methods (e.g., microwave, osmotic or infrared) or different pretreatments (e.g., US, PEF or CP), which can yield better quality of product.

2.2. Osmotic Drying

Osmotic drying is used to partially remove water from biological tissues by immersion in a highly concentrated osmotic solution. The driving force for the transport of moisture from the tissues into the solution is provided by the higher osmotic pressure of the highly concentrated solution. Moisture diffusion is accompanied by simultaneous diffusion of the dissolved substance from the osmotic solution into the tissue. Since the cell membrane responsible for the transport of matter is not absolutely selective, other solutions that are present in the cells can also reach the osmotic solution [28].

Osmotic drying is most often applied as a pretreatment to another process to reduce the moisture content of a product, improve its quality during storage, and reduce the total amount of energy for other subsequent processes to osmotic drying. Due to the non-selective nature of a cell membrane, components such as sugar, acids, minerals, and vitamins can be diffused in minuscule quantities from the plant material to the surrounding solution while still affecting the sensory, nutritional and functional characteristics of the final product [15]. To ensure greater stability and longer shelf life of osmotically dried products, they must be subjected to additional preservation methods, including freezing, sublimation drying [29], vacuum drying [30], convective drying, and microwave drying [31,32]. One of the benefits of osmotic drying as a pretreatment for convective drying is energy savings due to moisture transport without phase change [33]. Osmotic pretreatment also increases the sugar–acid ratios, which can be important for fruits with high acid contents. In this way, the taste of the final product is better preserved [34]. This also improves the texture, volume reduction in the material and the stability of the pigmentation during drying and storage [34–36]. The osmotic drying process could be enhanced by using different pretreatments, including: pulsed electric field [37,38], sonication [39,40], blanching [41,42], and microwaving [43].

2.3. Microwave Drying

Microwaves (MWs) are electromagnetic (EM) waves that are synchronized perpendicular oscillations of electric and magnetic fields in a frequency between 300 MHz and 300 GHz, with wavelengths from 1 m to 1 mm. The mechanisms of microwave heating are based on the oscillation of ions and molecules when a material is exposed to the EM waves, which causes the internal friction and conversion of kinetic energy into heat [44]. The MWs provide volumetric and rapid heating of fruits with low energy consumption [45], while the literature usually reports MW drying with applied constant power.

There are different opinions in the literature regarding the homogeneity and control of heating with MWs. While some researchers confirm a homogenous heating rate of material [17], others state it as a drawback of this type of drying [44,45]. The reasons for uneven heating with MWs are due to several factors: (i) large product size; (ii) resonance phenomena; (iii) heterogeneous material composition; and (iv) shape of product.

Dried tomato and onion with and without MW power control are shown in Figure 1 [44]. Successful application of MW drying was found with potato chips, pasta, and snacks [46]. Because of the supply of drying energy directly to the volume of a product, its internal pressure will increase, which will drive water to the plant surface, resulting in an increase in drying rates [47,48]. However, depending on the type of material, MWs in some cases cannot fully complete drying and are usually combined with hot air drying or vacuuming. So even though both MW heating and hot air drying separately have disadvantages, combining these two methods could prove very beneficial. In that sense, the application of MW to the finalized drying of banana slices ($T = 60\text{ }^{\circ}\text{C}$) reduced hot air drying by about 64%.

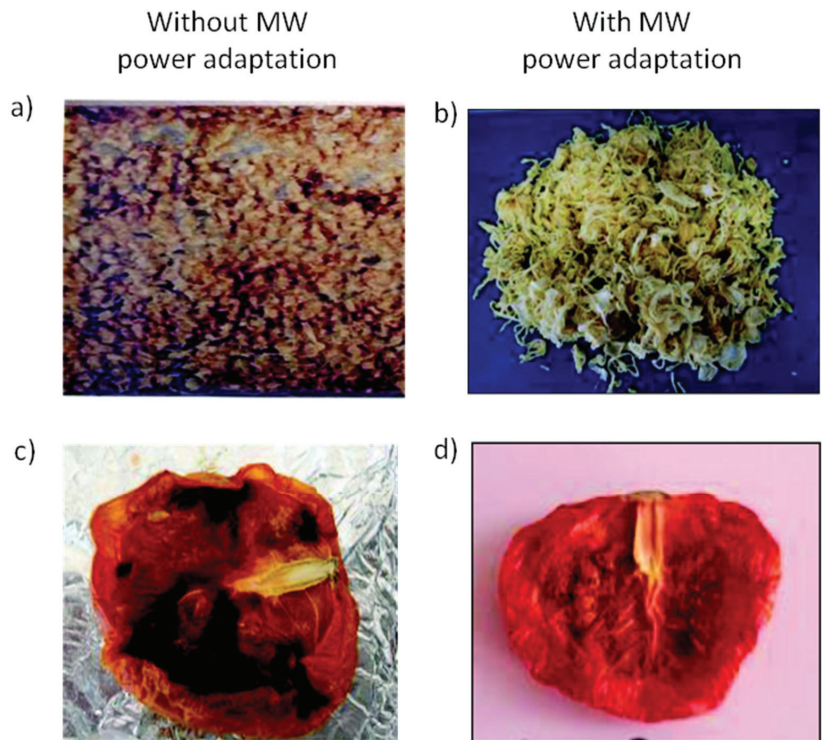


Figure 1. Effect of controlled microwave (MW) power on dried product [44]: (a) onion treated with MW without power adaptation; (b) onion with power adaptation; (c) tomato treated with MW without power adaptation; (d) tomato with power adaptation.

2.4. Freeze-Drying

Freeze-drying is a technique, first used for the preservation of thermally sensitive biological material, that employs the principle of sublimation of frozen water. The process takes place at a low temperature, where biologically active compounds remain preserved in large quantities. Over the last decade, freeze-dried food has gained popularity, especially for fruits such as berries [49]. Hammami and Rene [50] reported that optimal freeze-drying parameters for strawberry are 30 Pa and 50 °C of a drying plate, and that under these conditions, neither off-flavors nor the off-tastes were formed. Since the key difference in the freeze-drying is actually the time it takes while using different settings; therefore, several examples of freeze-dried fruits with operational parameters are given in Table 1.

The advantages of freeze-drying, in terms of chemical and nutritional quality, over other drying methods have been reported by numerous authors. However, in comparison to other drying technologies, freeze-drying has a high energy consumption and prolonged processing time [6,26,50,51]. However, this can be reduced by using PEF treatment. For instance, Lammerskitten et al. [52] reported that PEF pretreatment of apple slices intensifies freeze-drying kinetics and thus reduces processing time by 57% in comparison to untreated samples. Despite many advantages linked with freeze-drying, high initial costs are still a limiting factor for many producers.

Table 1. Examples of freeze-dried fruits with various operational parameters.

Dried Material	Shape and Form	Freezing Temperature	Pressure of the Chamber	Drying Time	Monitored Properties	Ref.
Raspberry	Whole	−20 °C	1 Pa	48 h	Bioactive compounds, shrinkage, color change	[26]
Strawberries	Pieces—3.5 cm high layer	−20 °C and −80 °C	15–200 Pa	60–65 h	Moisture, rehydration ratio, appearance, shape, color, texture	[50]
Saskatoon berry	Whole	n/a	n/a	24 h	Moisture, water activity, color, polyphenolic compounds	[51]
Raspberry	Whole	Frozen with liquid nitrogen	4 Pa	48 h	Water sorption, glass transition temperature (T _g), molecular mobility, texture and rehydration properties	[6]
Apple	Slices of a thickness of 6 ± 0.5mm, average diameter 72 ± 3 mm	Samples were not frozen	100 Pa	Needed to achieve MR = 0.004 840 ± 21 and 368 ± 10min, for the untreated and the pulsed electric field (PEF) treated	Moisture, rehydration, hygroscopic properties, water activity	[52]
Strawberries	5 and 10 mm slices and wholes	−40 °C	50 Pa	12 and 24 for slices 48 for whole fruit	Moisture, color, volume,	[53]
Carrot	Cylinders with a diameter of 20 mm and 8 mm height	−35 °C for 48 h, 1 h in liquid N ₂	3–300 Pa	24 h	Volume, bulk density, glass transition temperature, porosity	[54]
Kiwi	Whole fruit (without peel)	−40 °C	12, 20, 42, 85, and 103 Pa	n/a	Color, texture, rehydration, total phenolic content, antioxidant properties and sensory analysis	[55]
Banana	Cylinders with a diameter of 20 mm, height 8 mm	−35 °C for 48 h, 1 h in liquid N ₂	3–300 Pa	24 h	Volume, bulk density, glass transition temperature, porosity	[54]
Blackberries	Juice with carrier agents	n/a	0.0004 Pa	48 h	Moisture, thermal property, density, morphology, antiradical activity	[56]
Blueberries	Whole fruit	−35 °C	13 Pa	n/a	Mass transfer, drying time, berry-busting, skin perforation	[57]

n/a, not available.

3. Quality of Dried Fruits

The intensity of changes in quality parameters during drying depends on the nature of material, pretreatment, used process and their parameters. The majority of these changes include color, shape, volume, density, texture, flavor, nutrients, water activity, microbiology, rehydration ability, etc. [58]. These changes and influencing factors are reviewed below.

3.1. Physical Quality

The physical properties of food products are responsible for perceived quality. Shape, appearance and color are characteristics in sight of customers and liable for product acceptability. Currently, the color of food is measured directly and non-destructively by using apparatus like colorimeters. They use several color spaces for the expression of color values. The usually used color space is CIELAB (CIE L*a*b*, color system), and this method was useful for the monitoring of color changes during the drying of quince [34], kiwifruit [59], persimmon [60,61], etc. Commonly, the most color deterioration is associated with air heat drying, while enzymatic browning can be responsible for both color changes and off flavor. To this extent, this problem can be controlled by the thermal control of drying and the addition of a sulfur dioxide, acids and osmotic pretreatments. Rodrigues et al. [61] stated that the color of osmotically treated papaya is very similar to the color of

fresh fruit. The layer of sugar that forms on the surface of the fruits during osmotic drying presented a barrier to air during convective drying that prevented browning [30].

Although freeze-drying was mentioned as a gentle dehydration process, it still led to higher color changes of raspberries compared to the hot air drying [6,26,62]. Sette et al. [6] reported that increased color change was due to the decomposition of pigments; therefore, it was recommended to consider internal structure when observing color changes during drying.

Texture properties that include structural and mechanical characteristics greatly influence the quality of dried products. Freeze-dried products have superior quality, better-preserved color, flavor and appearance, a higher rehydration ratio, and are crispier in comparison to the products dried with traditional drying technologies. Conventionally dried fruits tend to be chewy and tough to bite, but with an optimal moisture content that is pleasant for consumption. Hot air drying usually has destructive influences on the structure of fruits, as drying provokes structural collapse in fruit tissues due to moisture removal [63]. However, by the selection of optimal drying parameters, excessive changes in volume in fruits can be avoided, as is the case with raspberry fruit. Hot air drying at a temperature of 70 °C and a velocity of 1 ms⁻¹ provokes volume shrinkage by 23.17%. Convective drying by an air temperature of 50 °C will lead to a total collapse, while samples dried with an air temperature of 80 °C reached a volume shrinkage of 43.13% [64]. Here, lower temperatures totally collapsed samples, while higher temperatures led to the creation of a porous outer rigid crust or shell that fixed the volume [65]. Radojčin et al. [41] reported that the shrinkage of osmotically pretreated quince cubes was proportional to the moisture losses. This was also observed by Krokida and Maroulis [66] and Lozano et al. [67] for carrot drying during the entire process. In other studies for squid flesh [68,69] as well as potato and sweet potato [67,70], it was found that the volume of removed water during the final stages of drying was higher than the reduction in sample volume. One theory proposed for the explanation of this shrinkage was the process of glass transition. However, this concept may not be useful for the freeze-drying of all biomaterials, as it was shown with the latest experimental results [17]. For some cases, the incorporation of other factors, such as mechanisms of moisture transport, structure, surrounding pressure and surface tension, was also required [71,72]. More so, puffing effect under a vacuum had significant influences on the shrinkage, structure and porosity of dried materials [73,74].

Pretreatments can enhance drying with respect to energy savings and improved quality of dried product. Namely, PEF, US or HHP are able to induce cell damages, with increased permeability and mass transfer. For example, PEF treatment with assisted hot air drying at atmospheric pressure reduced the drying time of apple up to 12% and carrots up to 8% when 10 kV cm⁻¹, 50 pulses, air temperature 70 °C, and 5 kV cm⁻¹, 10 pulses, air temperature 70 °C were applied, respectively. The specific energy of pulsed electric field treatment was 80 and 8 kJ kg⁻¹ [75,76]. Other authors also reported reductions by 5–28% for parsnips and carrots at 60 °C. The specific energy of pulsed electric field delivered was about 65 kJ kg⁻¹ for carrots and parsnips. PEF (400 V cm⁻¹) assisted the freeze-drying of potatoes expedite freezing, reduced drying by 18% (0 °C and 0.04 mbar pressure), lowered residual moisture content, decreased shrinkage, and improved the appearance of samples [77].

3.2. Chemical Quality

Applied higher temperatures and prolonged exposure to oxygen could ultimately decrease vitamin content during the drying of fruits [78]. Nevertheless, one study concluded that applied solar drying even at lower temperatures (24.5–40.3 °C) could significantly ($p < 0.05$) reduce the vitamin content in the fruits [79]. Due to dehydration of the pieces to a moisture level of 10% or even lower, the relative increases in the concentrations of the mineral content, total acidity, carbohydrates and total sugars were significantly higher in the dried fruits as compared to the fresh samples. These findings broadly supported the work of Suna et al. [80], who established a clear positive correlation between the dry

matter and mineral elements in different fruit varieties during and subsequent to drying. An increased temperature had negative effects on certain chemical profiles. For instance, comparisons of hot air drying (AD), freeze-drying (FD), and refractance window drying (RWD) exhibited significant changes in the content of vitamins B and C in blueberries, cherries, cranberries and strawberries [81]. FD samples, except blueberries, showed higher levels of thermolabile vitamin C in comparison to AD and RWD. Moreover, in AD samples the lowest content of vitamin C was observed. Vitamins B2, B6 and total vitamin B contents were thermally unstable during the drying of berries, and their lowest content was determined in the AD samples. The stability of the B vitamins in the FD and RWD samples was heavily dependent on the berry type. In particular, blueberries and cherries showed significantly higher total vitamin B during FD processing than the RWD, whereas for cranberry and strawberry, the RWD displayed a significantly greater total vitamin B retention than the FD samples [81]. The operating conditions of convective infrared drying could significantly affect fluctuations in nutrient elements in fruits such as strawberries [82]. A higher drying air temperature increased the concentrations of chemical elements such as N, P, K, and Mn, while the contents of Zn and Ca were reduced. By applying the various infrared power, it was found that concentrations of N, P, and K increased, while the contents of Ca, Mg, Fe, Mn and Zn were lowered. Further, different drying air velocities increased concentrations of N, P and K and decreased contents of Ca, Mg, Fe and Zn, hence it is important to optimize the drying process to ensure the best chemical compositions of a dried product.

3.3. Nutritional Quality

A recent study aimed to explore the optimal conditions for the convective infrared drying of strawberries with the aim to achieve a high nutritive product [82]. Drying experiments were conducted under: (i) constant drying air temperature (80 °C) and velocity (2.0 m s⁻¹) at various infrared powers (100, 200, 300 W); (ii) constant infrared power (200 W) and drying air velocity (2.0 m s⁻¹) at various air temperatures (60, 80 and 100 °C); and (iii) constant infrared power (200 W) and drying air temperature (80 °C) under various air velocities (1.0, 1.5 and 2.0 m s⁻¹). The authors reported a decrease in total phenols, total anthocyanins and antioxidant activity as a result of higher temperature, while 60 °C was found to be the optimal value with respect to the nutritive quality. Higher levels of total phenolics and anthocyanins were determined at 1.0 m s⁻¹, whereas increasing the velocity from 1.0 m s⁻¹ to 2.0 m s⁻¹ promoted higher values of antioxidant activity. Moreover, increasing the infrared power from 100 W to 300 W increased antioxidant activity, total anthocyanin and phenolic contents. Consequently, the authors concluded that the range of 200 W–300 W is a preferable setting for the processing [82].

Associating different drying technologies with the nutritional quality of fruits is a very common approach in the literature. For instance, freeze-dried, microwave-vacuum dried and osmo-microwave-vacuum dried cranberries were compared with respect to the changes in the bioactive compounds during drying [83]. Higher retention of polyphenols and antioxidant capacity was achieved by microwave-vacuum drying and osmo-microwave-vacuum drying as compared to the freeze-drying, although no significant differences were observed in polyphenolic contents among microwave-vacuum dried and osmo-microwave-vacuum cranberries. Another study aimed to evaluate the influences of three drying treatments, namely hot (AD), FD, and RWD on the stability of polyphenols and antioxidant capacity in four berry samples [81]. In comparison to AD and RWD, FD samples retained a higher total phenolic content. However, the authors did not find any statistically significant differences between the FD and RWD cranberry samples. The authors explained an observed trend with a lower temperature applied during freeze-drying as compared to the one applied during the RWD, which might stabilize flavonoids to a greater extent in the FD samples. A recent study highlighted the drying process by intermittent ohmic heating (IOH), which requires lower energy consumption while offering products with advanced quality as compared to intermittent air drying (IAD) and

air drying [84]. Approximately 70–80% of polyphenolic compounds were retained in IAD dried litchi fruit (*Litchi Chinensis* Sonn.), while for AD samples the retention was only 60%. The potential explanation could be attributed to the reduced oxygen exposure in IAD and consequent phenolic preservation [84]. The pretreatments of fruits prior to drying may also influence the quality of the final dried product. To that end, Stamenković et al. [26] researched the impact of convective drying of fresh and frozen raspberries at operating conditions: air temperature (60, 70, and 80 °C) and air velocity (0.5 and 1.5 m s⁻¹). Freeze-drying was used as a control procedure to compare the obtained results. The exposure time to higher oxygen levels during the convective drying induced a greater reduction in vitamin C than elevated temperatures. It seems that the degradation of vitamin C in berry fruits does not depend on temperature for ranges between 80–90 °C. Therefore, it was concluded that the presence of oxygen plays a crucial role in vitamin C deterioration [85]. Although convective drying reduced the total anthocyanin in a range of 44–60%, the authors still concluded that red pigments were better preserved in dried raspberries than in the initial fresh state. In general, freeze-drying resulted in better preservation of nutritional quality, whereas the optimal conditions for the convective drying of raspberries were set at an air temperature of 60 °C and an air velocity of 1.5 m s⁻¹. This was calculated with regard to the equivalent of a freeze-drying procedure. Nguyen et al. tested the convective microwave-assisted drying of fruits abundant with thermally sensitive bioactive compounds at lower temperatures (of up to 30 °C) [86]. The authors dried bitter melon (*Momordica charantia* L.) at various microwave power densities (1.5, 3.0, 4.5 W g⁻¹), drying temperatures (20, 25, 30 °C), and air velocities (1.0, 1.2 and 1.4 m s⁻¹), while monitoring the impact on phenolic compounds and corresponding antioxidant activity. As the drying process involved coupled influences of heat and mass transfer, the obtained results revealed that the higher air velocity along with extended drying time initiated higher losses in total phenols and antioxidant capacity. Total phenols and antioxidant activity reached maximum at a microwave power density of 3.0 W g⁻¹. A further increase to 4.5 W g⁻¹ led to significant losses, as polar bonds in phenolic structures become increasingly weak due to the effect of microwave irradiation with possible residual enzymatic reaction. Currently, novel research on food drying processes is mostly oriented towards advanced technologies that provide energy-savings and are able to produce high quality products. Here, focus is mainly given to solar-assisted drying with the perspective to endorse sustainability in the food industry [78]. For example, five different solar drying methods were investigated for drying mangoes and pineapples, namely open sun drying (OSD), black-cloth shade (BCS), white-cloth shade (WCS), a conventional solar dryer (CSD), and an improved solar dryer (ISD). The drying processes were conducted outdoors, with a mean daily temperature and relative humidity of 26.8 °C and 26.7%, respectively. The fruits that were dried under the OSD, WCS and BCS methods revealed a significantly higher decrease in total phenols than the CSD and ISD methods [79]. The authors explained this trend with increased temperatures and prolonged drying times during the OSD, WCS and BCS methods. These findings were consistent with previously published results that attributed additional losses of phenols during drying to the direct exposure to ultraviolet solar radiation [87].

Another study documented the effects of solar convective drying over 12 months of storage on the bioactive compounds in sweet cherry samples. The operating conditions were 60, 70 and 80 °C during 8, 6 and 4 h, respectively [88]. A reduced drying time positively affected preservation of the total phenols, total flavonoids and total anthocyanins, while the drying temperatures showed no significant differences on this outcome. After the drying process, total flavonoid content decreased by 24% and slowly continued to decrease during the storage, with a final loss of 30% after the 12 months of storage. Moreover, dried samples exhibited 2-fold higher antioxidant activity from the initial values (18.32% vs. 37.64%). It is possible that these results were influenced by the shorter time of drying and the formation of a novel constituent(s) with antioxidant activity (e.g., Maillard reaction products) that could be continuously formed and released during an extended storage time.

3.4. Sensory Quality

Sensory evaluation is a method to assess the perceivable qualities of a food product using untrained (consumer) or trained panelists. Consumer panelists are recruited when the focus of the studies is on the acceptance (or liking) of certain sensory attributes. Trained panels receive thorough sensory training according to the relevant ISO standards [89–91]. Additionally, their performance is continuously monitored in order to ensure data validity and quality [92].

One of the key elements of fruit drying is the effect of the different drying methods on the sensory aspects of the fruits. Drying is performed by removing the water content of the fruits, which directly affects sensory and chemical properties. Traditional drying techniques, e.g., convective drying (CD), use high temperatures and a high content of oxygen in the drying agent, which deteriorate color, aroma and texture properties [93]. Several authors reported that convective drying preserves flavors well in quince [94] and jujube fruits [95]; however, the presence of a measurable off-flavor intensity (burnt flavor) has also been reported. Additionally, CD provided darker color compared to other drying methods. Papers have also reported that lower drying temperatures produce better accepted products [96]. Freeze-drying (FD) has been identified as one of the best drying methods when it comes to preserving the sensory and nutritional quality of fruits [17]. On the contrary, FD is identified as one of the most expensive methods; therefore, there is a continuous search among researchers to find affordable methods which provide the same (or as close as possible) quality as FD. Vacuum-microwave drying (VMD) was shown to cause intermediate color changes, positive effects on texture and low intensities of off-flavors [97]. VMD has been used to dry several fruits, e.g., quince [94], jujube fruits [95], cranberry [97], etc. However, it must be noted that since microwave drying methods replace thermal energy with electric energy, textural attributes change significantly. Crisp texture results from puffing due to expansion when water evaporates within the product, and it is also related to porosity [98]. Heat-pump drying (HPD) also shows promising results on the nutrient content and sensory aspects of fruits. HPD has been shown to consume 22 to 40% less power compared to electrically heated dryers [17]. When HPD and modified atmosphere heat-pump drying (MAHPD) were compared to vacuum drying and freeze drying, it turned out that MAHPD led to better physical properties, such as reduced shrinkage, decreased firmness and more porous structure of the materials, which resulted in quicker rehydration. When using inert gas, the color of the heat pump dried food proved to be similar to vacuum or freeze-drying [99].

3.5. Comparison of Drying Methods

As it has been introduced, there are several techniques available for drying. Additionally, different settings of the given drying methods also have a significant effect on the final quality of the fruits. When it comes to comparison, novel statistical techniques provide substantial help to compare different methods. The key problem here is that the comparison of drying methods is not always clear, and sometimes there are contradictory results. For example, freeze-drying is considered to be one of the best drying methods for biological samples when dealing with nutritional and sensory quality variables. However, when technological parameters such as energetic demands and maintenance costs are considered, freeze-drying is far from the best alternative. In such cases, when different variables assess the performance of the methods differently, multicriteria decision making (MCDM) methods can provide valuable help. MCDM methods have been developed to compare multiple methods/products based on multiple aspects [100]. When it comes to comparing methods, models and products, the sum of ranking differences (SRD) method is one of the most widely applied in food science [101]. It has been successfully applied to compare horticultural products [102], sensory attributes affecting overall liking [103], energy drinks [104], the nutritional value of insect species [105] and raspberry drying [106], just to name a few.

A typical SRD input matrix consists of the comparable methods in the columns and the measured variables in the rows. The comparison of the methods is completed based on the rows. The last column of the input matrix serves as the reference (or benchmark) column. The reference can be set as minimum, maximum, average and user defined (e.g., golden standard). This is really important, as the data values in each column are ranked in increasing magnitude and these rankings are compared to the ranks of the reference column. Finally, the absolute differences between the rank-variables and the rank-reference columns in each case are calculated and summed. These values (SRD values) give the ordering of the variables. The smaller the SRD value, the better (or the more consistent) the variable. The procedure above is explained in detail in one of the recent works. The visual representation of the method is provided by Figure 2 [107].

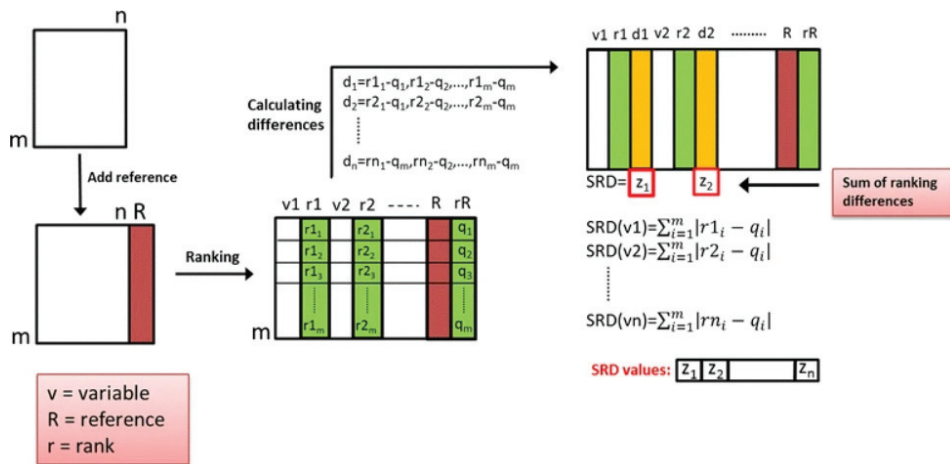


Figure 2. Scheme to calculate sum of ranking differences. The input matrix contains the methods to be compared ($n = 8$) in the columns and the measured variables ($m = 99$) in the rows. A reference column (golden standard, here: average of the measured variables) is added in the data fusion step (red). Then, all columns are doubled (green) and the molecules in each column are ranked by increasing magnitude (columns r_1, r_2, \dots, r_n). The differences (yellow columns) are calculated for each similarity measure and each molecule (i.e., each cell) between its rank (r_{11}, r_{12} to r_{m1}) and the rank assigned by the known reference method ($rR = q_1, q_2, \dots, q_m$). In the last step, the absolute values of the differences are summed up for each measure to give the final sum of ranking differences (SRD) values, which are to be compared. Smaller SRD mean proximity to the reference—the smaller the better. Adapted from [107].

A recent example of using the SRD method for the comparison of drying methods based on several measured parameters was published by Stamenković and co-workers in 2020 [107]. A comparative experiment was conducted in order to identify the most suitable process parameters for convective drying that may be considered as alternatives to freeze-drying, which is a widely used preservation method for raspberries even though it is a costly and energy-consuming method. Twelve convective drying regimens were applied with a combination of three influencing factors: air temperature (60°C , 70°C , and 80°C), air rate (0.5 and 1.5 ms^{-1}), and stage of raspberry (fresh and frozen). The final product, a dried raspberry, was assessed for chemical, physical, and mechanical properties and rehydration capacity. SRD showed that the convective drying of fresh raspberries proved to be more similar to freeze-dried raspberries than the convective drying of frozen ones. Fresh samples dried at 60°C air temperature and 1.5 ms^{-1} air flow proved to be the most similar to the reference freeze-drying method. Such analyses can help practitioners to develop cheaper and simpler drying methods that could replace costly and energy-consuming methods but keep the same quality of the dried products.

4. Unconventional/Emerging Drying Intensification Technologies

Many different strategies can be applied in order to enhance the drying process and/or to improve dried food properties. These strategies usually consider the modification of drying parameters or material properties. The approach that is based on changing the parameters of drying, such as temperature, flow rate and humidity, is usually sufficient to enhance the first period of drying, which is governed by external mass transfer resistance. In turn, intensification of the second stage of drying can usually be achieved by the introduction of a pretreatment step that will change the material properties, for example, its dimensions or integrity of cellular structure. A reduction in dimensions, which can intensify drying kinetics to a great extent, is not always possible. The rupture of cellular structure can be thermally achieved, e.g., blanching [108,109]. Additionally, this can be done by non-thermal methods such as high hydrostatic pressure (HHP), cold plasma (CP), ultrasound or pulsed electric field (PEF) treatment [110]. Non-thermal treatments, in principle, allow better preservation of thermo-sensitive compounds and are linked with lower energy consumption in comparison to thermal based technologies. Currently, existing publications show that, among non-thermal pretreatment technologies, US and PEF are the most promising for dehydration intensification. It has to be emphasized that the utilization of non-thermal methods as a pretreatment before drying does not have to result in better outcomes than the implementation of unconventional drying techniques. The decision about the potential implementation of a pretreatment method before drying should be preceded by deep studies in relation to the desired technological aim. Such analysis, in addition to a literature review, should also include optimization and economical studies.

4.1. Ultrasound

Ultrasound can be described as a cyclic sound pressure with a frequency that is inaudible to humans (>20 kHz). In food processing, ultrasound can be used for the enactment of traditional technologies or to replace them. Ultrasound can be utilized either as low-frequency but high-energy or as high-frequency but low-energy assays. The first one is usually associated with the facilitation of different unit operations such as extraction, freezing and thawing, emulsification and homogenization or drying, while the second one is mainly associated with control, analytical and diagnostic procedures [111]. The application of low-frequency but high intensity ultrasound causes different phenomena depending on the type of the medium where they propagate. The application of ultrasound in the fluid systems results in cavitation and microstreaming, which intensifies mass and heat transfer but can also lead to the formation of free radicals and reactive oxygen species. Cavitation bubbles that are collapsing may also erode and degrade the surface or structure of the materials that they contact [112,113]. When ultrasound propagates through solid-like material, for instance food matrix, cyclic compression and expansion of material can occur—such behavior is called sponge effect and it can lead to the formation of micro-channels, which facilitate mass transfer between the treated material and its surroundings [114,115]. Ultrasound can be applied using direct and contact methods or indirectly using ultrasound baths [105]. In the case of drying, ultrasound can be used not only prior to drying, but also during the process [116].

The literature about the effect of US on drying kinetics is ambiguous and the effects of pretreatment depend strongly on food matrix (Figure 3). There are reports that indicate that sonication can reduce the drying time of apples by 11–40% in comparison to untreated material [117,118], and there are articles which demonstrate that US pretreatment has no effect on process course or that it can even extend drying, as it was reported for carrots [119].

Moreover, drying kinetics seem to depend not only on the type of raw material but also on the parameters of US. The influence of sonication time is one of the most studied issues. It was found that the relation between the time of sonication and drying reduction is not linear. For instance, the sonication of 20 min of apple tissue reduced air drying better than the treatment of 30 min [118]. Similar findings were reported for other raw materials, such as pineapples or parsley leaves [120,121].

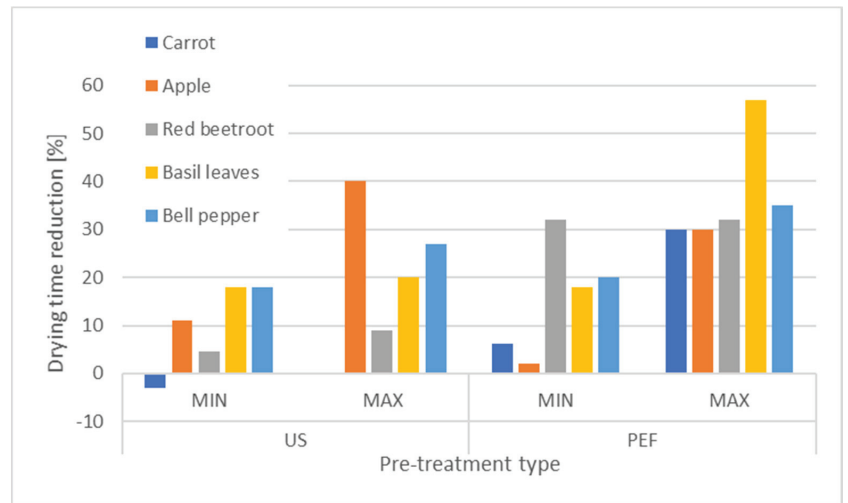


Figure 3. Minimum (MIN) and maximum (MAX) air drying time reductions for different food matrices as reported in the scientific literature for pulsed electric field (PEF) and ultrasound (US) pre-treatment.

The possibility of process intensification by sonication was also exemplified by other drying methods, such as microwave assisted air drying or vacuum drying. It has been demonstrated that microwave and ultrasound assisted air drying reduced processing time by 79% in comparison to traditional, convection processes. In addition, samples produced with the assistance of US exhibited higher porosity and better reconstitution properties than untreated material [122].

The vacuum drying of nectarine with sonication was 50% shorter than the control process, plus US treated samples demonstrated higher retention of phenols and smaller changes in color. The authors of this study stated that there is a synergistic effect of vacuum drying and ultrasound treatment [123]. The positive addition of ultrasound during drying on rehydration and color retention was also demonstrated for purple-fleshed potatoes [124].

4.2. Pulsed Electric Fields

PEF is an electro-based technology since it involves electric fields for its application. PEF treatment of food depends on the exposition of material into short-lasting pulses characterized by high electric field intensity that varies from 0.1 to 50 kVcm⁻¹, depending on the desired technological effect [125,126]. PEF treatment results in a rupture of cell membrane continuity due to a phenomenon and a process of electroporation [127]. The electroporation can be irreversible or reversible depending on the induced transmembrane potential of the cell that it treated, which in turn depends on many different factors. Among them are the cell diameter and external electric field, which are the most important [128]. Figure 4 presents the SEM images of apple tissue treated by PEF at different parameters with indicated ruptures in cellular structure.

The majority of PEF applications in food processing involves irreversible electroporation. Such PEF treatment can be used to enhance extraction, juice pressing, freezing, osmotic dehydration or drying [129]. However, there are some data which demonstrated that reversible electroporation could also be applied for the improvement of drying [130]. It is worth noting that the effectiveness of PEF treatment has been proved on an industrial scale for winemaking, juice preservation or in potato processing [131–133].

As a contrast to ultrasound, the vast majority of scientific publications show that PEF pretreatment facilitates mass transfer during drying. Drying reduction by PEF prior to water removal varies from 2% to 57% in comparison to untreated material, as it was

reported for apples and basil leaves, respectively (Figure 3). The effect of PEF on drying depends on many different factors which are related to the material properties and processing parameters: electric field intensity, energy input, number of pulses, pulse width and geometry or drying methods [134].

For instance, the intensification of drying depends on the cell disintegration index (CDI) of the material (which varies from 0 to 1, for untreated and hypothetical totally disintegrated samples). Here, the effective water diffusion coefficient of apples subjected to air drying was equal to 1.044, 1.090 and 1.252 $\text{m}^2 \text{s}^{-1}$, for untreated samples, samples with CDI = 0.33 and with CDI = 0.88, respectively [76].

A higher water diffusion coefficient of PEF pretreated samples was also reported by Ostermeier et al. [135] for the two-step convective drying of onion tissue. Further, PEF treatment was also characterized by 14.5% higher pyruvic acid content and a 47% higher rehydration coefficient.

The exposition of the material to PEF treatment was also demonstrated as an efficient method for freeze-drying improvements. Wu et al. [136] reported that the application of 30 pulses at an electric field intensity of 1 kV cm^{-1} reduced freeze-drying time by 22.5% in comparison to untreated apples. The higher reduction in freeze-drying time of 31.5%, as compared to intact material, was reported for potatoes treated by 45 pulses at 1.5 kV cm^{-1} . A very interesting approach for the utilization of PEF in the freeze-drying process was demonstrated by Lammerskitten et al. [52]. In this case, the authors did not freeze the apple slices before freeze-drying using a freezer, rather the freezing occurred inside the freeze-drying chamber as a result of a pressure drop during the initial phases of freeze-drying. Such treated material kept its original shape (low drying shrinkage) and it was characterized by high crunchiness index, high porosity, and had similar chemical properties to the untreated material [137]. Similar findings were also reported by Fauster et al. [138] for freeze-dried strawberries and bell peppers. Some of the research papers indicated that PEF can also improve vacuum drying, similar to how it improves air and freeze-drying. As it has been reported by Liu et al. [139], PEF pretreatment of carrots reduced vacuum drying time by 33–55% and improved the retention of carotenoids.

Although the number of publications in the field of PEF and drying is growing, the research should also focus on the combination of PEF with other unconventional drying methods, such as infrared drying or microwave vacuum drying. Although some of the drying techniques in combination with PEF are well tested, optimization studies, using advanced experimental planning methods, are needed. Such an approach could address the questions related to the potential modification of drying parameters, such as temperature, in order to get the best possible quality and economic outcomes. Moreover, there is a gap in knowledge about the effectiveness of PEF pretreatment before drying for pilot and industrial scale processes enhancement and the sustainability aspects of its utilization.

4.3. High Hydrostatic Pressure

High hydrostatic pressure (high pressure processing, HHP, HPP) is one of the oldest and most popular non-thermal food processing methods. However, it is used mainly for preservation purposes since it inactivates microorganisms but keeps low molecular weight substances (like vitamins) intact. HHP is also used in industrial scale. It has been reported that in 2015, more than 300 units of HHP were operating all over the world [140]. The utilization of HHP, like PEF or US, can also modify the cell membrane permeability and thus it can enhance water transfer during dehydration processes [141]. HHP pretreatment has been demonstrated to reduce the drying time of vegetables such as carrots, green beans and potatoes [142] or fruits such as apples [143,144] and pineapples [145]. This method has also been demonstrated as effective in the intensification of drying of ginger—processes preceded by HHP treatment (10 min, 100–400 MPa) were characterized by much higher moisture diffusivity ($2.84\text{--}6.09 \times 10^{-9} \text{m}^2 \text{s}^{-1}$) than the reference operation ($2.03\text{--}4.87 \times 10^{-9} \text{m}^2 \text{s}^{-1}$). Moreover, HHP pretreatment also increased the extractability of oleoresin and 6-gingerol from dried material [146]. HHP pretreatment has also been reported to

increase the antioxidant activity of osmodehydrated strawberries [147]. However, the effect of HHP treatment applied prior to drying depends on the quality changes of dried material and depends strongly on matrix type. It has been reported that HHP may result in undesirable color changes like the darkening of tissue, as it has been reported in the case of garlic [148]. One of the main drawbacks of HHP treatment is cost of the processing and batch (or quasi-continuous) operating mode. Some studies report the costs of HHP to be three times higher than the costs of PEF treatment [149].

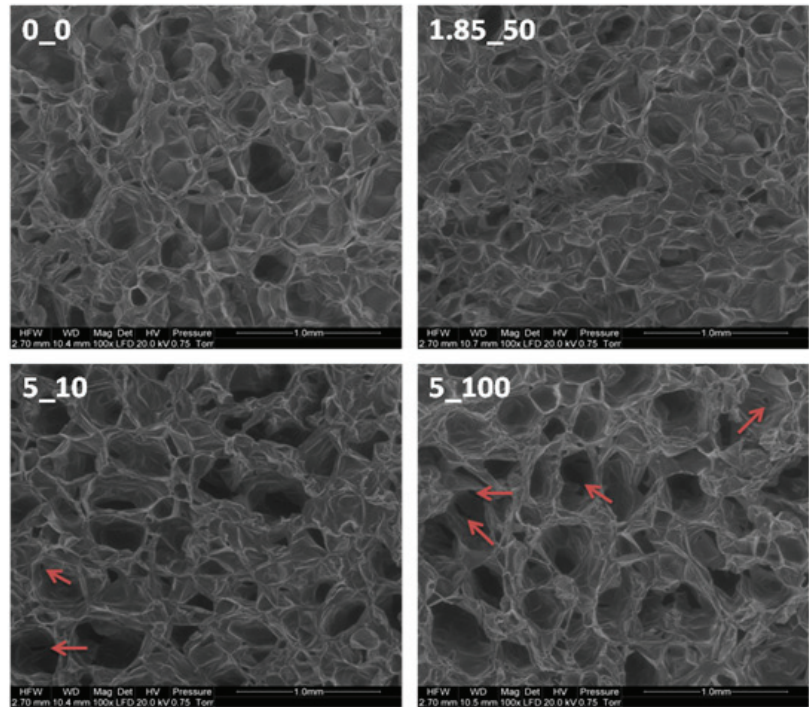


Figure 4. SEM images of untreated (0_0) and PEF treated (1.85_50—E = 1.85 kV cm⁻¹, n = 50 pulses; 5_10—E = 5 kV cm⁻¹, n = 10 pulses; 5_100—E = 5 kV cm⁻¹, n = 100 pulses) fresh apple tissue. Red arrows indicate the damages and ruptures in cell structure. Magnification of × 100. E—electric field intensity of applied PEF [kV cm⁻¹]; n—number of pulses. Source: own elaboration, unpublished data.

4.4. Cold Plasma

Plasma is considered as a fourth, quasi-neutral, like gas, state of matter. It is, in fact, an ionized gas which is a mixture of anions and cations, electrons, free radicals, molecules in an excited state and non-ionized molecules [150]. The presence of very active chemical molecules, such as free radicals or reactive oxygen species, makes plasma a potential tool for the decontamination of food and food contact surfaces. Indeed, most of the literature data about possible plasma utilization in food processing deal with preservation and microbial quality [151]. However, plasma application can also modify the surface properties of materials subjected for treatment, like some of the polymers [152]. The modification of the surface by cold plasma treatment was also reported for food products, such as black pepper seeds [153]. Recently, cold plasma has been reported as a pretreatment method for drying enhancement. Such an approach is related to the aforementioned possibility of modification of the surface and structure by plasma application by the physical and chemical processes—plasma can etch large cavities into the structure of material, which facilitates subsequent moisture removal during drying [154]. The time of wolfberry drying was reduced by 50%

when processes were preceded by cold plasma treatment. Moreover, the plasma treated dried material exhibited better reconstitution properties and higher retention of phenolics in comparison to the untreated material. The authors of this study stated that in addition to the alteration of the surface, the cellular structure was disintegrated as well due to cold plasma treatment [155]. The acceleration of drying by cold plasma treatment has also been reported for shitake mushroom [156] or corn kernel [157] drying. Nevertheless, the data about the impact of plasma radiation of food before drying are limited, but the method seems to be very promising, especially for the facilitation of drying of peel containing raw materials such as chili pepper [158]. Moreover, since plasma consists of very reactive chemical molecules, research should also focus on the chemical property changes and safety aspects of such treated food. Another important issue related to the utilization of this method is the possibility of its scale-up ability.

5. Conclusions

Drying provides extended shelf life, reduced transportation costs and minimized losses for various foods, and it is an indispensable part in the food processing industry around the world. Recent literature is focused on applying advanced technologies for drying intensification to improve conventional drying performances with respect to product quality and energy savings. Combinations of drying methods/hybrid drying and advanced pretreatments are useful for optimal results for both product quality and environmental impacts. Therefore, the right selection of drying methods and mathematical optimizations (modeling) of the process can reduce energy consumption, operational costs and provide superior quality products. Thermal drying techniques, such as hot air, have significant adverse effects on shrinkage, color, and textural properties, but they are economic. Furthermore, microwaves due to volumetric effect increase drying rate and reduce drying time and energy consumption, with the final quality close to hot air drying. Introducing vacuuming during drying will cause the avoidance of thermal and oxidative stress, with positive repercussions on product quality. In conclusion, combinations of advanced and conventional techniques have the potential to overcome inherited disadvantages of single technologies, while improving the economic outlook of food manufacturing.

Author Contributions: All coauthors have made important contributions to the manuscript realization by their participation in the following areas: Conceptualization, M.R.; Methodology, M.R.; Contributions to sample and analysis experiments, M.R., I.P., D.B.K., P.P., A.W., A.G., Z.S., K.K.; Writing—original draft preparation, M.R., I.P., D.B.K., P.P., A.W. and A.G.; writing—review and editing, M.R., I.P., D.B.K., P.P., A.W. and A.G.; supervision, P.P., and D.B.K. All authors have read and agreed to the published version of the manuscript.

Funding: This manuscript is a result of the research within the national project number 451-03-68/2020-14/200125, 2011–2020, supported by the Ministry of Education, Science and Technology, Republic of Serbia.

Institutional Review Board Statement: “Not applicable” for studies not involving humans.

Informed Consent Statement: “Not applicable” for studies not involving humans.

Acknowledgments: Attila Gere thanks the support of the Premium Postdoctoral Research Program of the Hungarian Academy of Sciences and the support of National Research, Development and Innovation Office of Hungary (OTKA, contracts No. K134260).

Conflicts of Interest: The authors declare no conflict of interest.

References

1. Orsat, V.; Changrue, V.; Raghavan, G.S.V. Microwave drying of fruits and vegetables. *Stewart Postharvest Rev.* **2006**, *2*, 1–7. [CrossRef]
2. Ratti, C. Advances in Food Dehydration. In *Dehydration of Foods*; Araya-Farias, M., Ratti, C., Eds.; CRC Press: Boca Raton, FL, USA, 2009.
3. Mercer, D.G. *An Introduction to the Dehydration and Drying of Fruits and Vegetables*; University of Guelph: Guelph, ON, Canada, 2014; p. 166.

4. Chua, K.J.; Chou, S.K. Low-cost drying methods for developing countries. *Trends Food Sci. Tech.* **2003**, *14*, 519–528. [CrossRef]
5. Çoklar, H.; Akbulut, M. Effect of sun, oven and freeze-drying on anthocyanins, phenolic compounds and antioxidant activity of black grape (Eksişikara) (*Vitis vinifera* L.). *S. Afr. J. Enol. Vitic.* **2017**, *38*, 264–272. [CrossRef]
6. Sette, P.; Salvatori, D.; Schebor, C. Physical and mechanical properties of raspberries subjected to osmotic dehydration and further dehydration by air- and freeze-drying. *Food Bioprod. Process.* **2016**, *100*, 156–171. [CrossRef]
7. Krokida, M.K.; Maroulis, Z.B.; Saravacos, G.D. The effect of the method of drying on the colour of dehydrated products. *Int. J. Food Sci. Tech.* **2001**, *36*, 53–59. [CrossRef]
8. Deng, L.-Z.; Mujumdar, A.S.; Zhang, Q.; Yang, X.-H.; Wang, J.; Zheng, Z.-A.; Gao, Z.-J.; Xiao, H.-W. Chemical and physical pretreatments of fruits and vegetables: Effects on drying characteristics and quality attributes—a comprehensive review. *Crit. Rev. Food Sci.* **2017**, *59*, 1408–1432. [CrossRef] [PubMed]
9. Mujumdar, A.S.; Devahastin, S. Fundamental principles of drying. In *Guide to Industrial Drying*; Mujumdar, A.S., Ed.; Universiti Kebangsaan Malaysia: Hyderabad, India, 2008.
10. Chen, X.D.; Mujumdar, A.S. *Food Processing*; Blackwell Publishing: West Sussex, UK, 2008.
11. Nijhuis, H.H.; Toringa, H.M.; Muresan, S.; Yuksel, D.; Leguijt, C.; Kloek, W. Approaches to improving the quality of dried fruit and vegetables. *Trends Food Sci. Tech.* **1998**, *9*, 13–20. [CrossRef]
12. Le Maguer, M. *Osmotic Dehydration: Review and Future Directions*; CERIA: Bruxelles, Belgium, 1998; pp. 283–309.
13. Pavkov, I.; Stamenković, Z.; Radojčin, M.; Krstan, K.; Bursić, V.; Bikić, S.; Mitrevski, V. Osmotic and convective drying of strawberries: Effects of experimental parameters on the drying kinetics, color and rehydration. *PTEP J. Proces. Energy Agric.* **2018**, *22*, 58–64. [CrossRef]
14. Lazarides, H.N.; Katsanidis, E.; Nickolaidis, A. Mass transfer kinetics during osmotic pre-concentration aiming at minimal solid uptake. *J. Food Eng.* **1995**, *25*, 151–166. [CrossRef]
15. Mayor, L.; Moreira, R.; Chenlo, F.; Sereno, A.M. Kinetics of osmotic dehydration of pumpkin with sodium chloride solutions. *J. Food Eng.* **2006**, *74*, 253–262. [CrossRef]
16. Rastogi, N.K.; Raghavarao, K.S.M.S. Kinetics of osmotic dehydration under vacuum. *LWT Food Sci. Technol.* **1996**, *29*, 669–672. [CrossRef]
17. Sagar, V.R.; Kumar, P.S. Recent advances in drying and dehydration of fruits and vegetables: A review. *J. Food Sci. Technol.* **2010**, *47*, 15–26. [CrossRef] [PubMed]
18. Lahsasni, S.; Kouhila, M.; Mahrouz, M.; Jaouhari, J.T. Drying kinetics of prickly pear fruit (*Opuntia ficus indica*). *J. Food Eng.* **2004**, *61*, 173–179. [CrossRef]
19. Toğrul, İ.T.; Pehlivan, D. Mathematical modelling of solar drying of apricots in thin layers. *J. Food Eng.* **2002**, *55*, 209–216. [CrossRef]
20. Garcia, R.; Leal, F.; Rolz, C. Drying of bananas using microwave and air ovens. *Int. J. Food Sci. Technol.* **2007**, *23*, 73–80. [CrossRef]
21. Li, Z.; Raghavan, G.S.V.; Orsat, V. Optimal power control strategies in microwave drying. *J. Food Eng.* **2010**, *99*, 263–268. [CrossRef]
22. Ezhilarasi, P.N.; Indrani, D.; Jena, B.S.; Anandharamakrishnan, C. Freeze drying technique for microencapsulation of Garcinia fruit extract and its effect on bread quality. *J. Food Eng.* **2013**, *117*, 513–520. [CrossRef]
23. Ceballos, A.M.; Giraldo, G.I.; Orrego, C.E. Effect of freezing rate on quality parameters of freeze dried soursop fruit pulp. *J. Food Eng.* **2012**, *111*, 360–365. [CrossRef]
24. Topić, R.M.; Topić, G.R.; Aćimović, D. Justifying using of sublimation drying with aspect of characteristics and energy demand value. *PTEP J. Proces. Energy Agric.* **2010**, *5*, 81–84.
25. Kalra, S.K.; Bhardway, K.C. Use of simple solar dehydrator for drying fruits and vegetable products. *J. Food Sci. Technol.* **1981**, *8*, 23–26.
26. Stamenković, Z.; Pavkov, I.; Radojčin, M.; Tepić Horecki, A.; Kešel, K.; Kovačević, D.B.; Putnik, P. Convective drying of fresh and frozen raspberries and change of their physical and nutritive properties. *Foods* **2019**, *8*, 251. [CrossRef] [PubMed]
27. Cavusoglu, C. *Investigations into the High-Temperature Air Drying of Tomato Pieces*; Universität Bonn, Rheinische Friedrich-Wilhelms-Universität: Bonn, Germany, 2008.
28. Giangiacomo, R.; Torreggiani, D.; Abbo, E. Osmotic dehydration of fruit: Part 1. Sugars exchange between fruit and extracting syrups. *J. Food Process. Preserv.* **1987**, *11*, 183–195. [CrossRef]
29. Tregunno, N.B.; Goff, H.D. Osmodehydrofreezing of apples: Structural and textural effects. *Food Res. Int.* **1996**, *29*, 471–479. [CrossRef]
30. Rahman, S.M.A.; Mujumdar, A.S. Effect of osmotic treatment with concentrated sugar and salt solutions on kinetics and color in vacuum contact drying. *J. Food Process. Preserv.* **2007**, *31*, 671–687. [CrossRef]
31. Islam, M.N.; Flink, J.N. Dehydration of potato. *Int. J. Food Sci. Technol.* **2007**, *17*, 387–403. [CrossRef]
32. Kowalska, H.; Belka, M.; Lenart, A. Influence of microwave heating on mass transfer during osmotic dehydration of apples. *Pol. J. Food Nutr. Sci.* **2007**, *57*, 317–323.
33. Bolin, H.R.; Huxsoll, C.C.; Jackson, R.; Ng, K.C. Effect of osmotic agents and concentration on fruit quality. *J. Food Sci.* **1983**, *48*, 202–205. [CrossRef]
34. Radojčin, M.; Babić, M.; Babić, L.; Pavkov, I.; Bukurov, M.; Bikić, S.; Mitrevski, V. Effects of osmotic pretreatment on quality and physical properties of dried quinces (*Cydonia oblonga*). *J. Food Nutr. Res.* **2015**, *54*, 142–154.

35. Babić, M.; Babić, L.; Pavkov, I.; Radojčin, M. Changes in physical properties through osmotic drying of quince (*Cydonia oblonga* mill.). *PTEP J. Proces. Energy Agric.* **2008**, *12*, 101–107.
36. Raoult-Wack, A.L. Recent advances in the osmotic dehydration of foods. *Trends Food Sci. Tech.* **1994**, *5*, 255–260. [CrossRef]
37. Taiwo, K.A.; Angersbach, A.; Ade-Omowaye, B.I.O.; Knorr, D. Effects of pretreatments on the diffusion kinetics and some quality parameters of osmotically dehydrated apple slices. *J. Agric. Food Chem.* **2001**, *49*, 2804–2811. [CrossRef] [PubMed]
38. Ade-Omowaye, B.I.O.; Rastogi, N.K.; Angersbach, A.; Knorr, D. Effects of high hydrostatic pressure or high intensity electrical field pulse pre-treatment on dehydration characteristics of red paprika. *Innov. Food Sci. Emerg.* **2001**, *2*, 1–7. [CrossRef]
39. Cárcel, J.A.; Benedito, J.; Rosselló, C.; Mulet, A. Influence of ultrasound intensity on mass transfer in apple immersed in a sucrose solution. *J. Food Eng.* **2007**, *78*, 472–479. [CrossRef]
40. Duan, X.; Zhang, M.; Li, X.; Mujumdar, A.S. Ultrasonically enhanced osmotic pretreatment of sea cucumber prior to microwave freeze drying. *Dry. Technol.* **2008**, *26*, 420–426. [CrossRef]
41. Radojčin, M.; Babić, M.; Babić, L.; Pavkov, I.; Stamenković, Z. Influence of different pretreatments on the colour of dried pears. *PTEP J. Proces. Energy Agric.* **2013**, *17*, 176–179.
42. Rahman, M.S.; Perera, C. Drying and food preservation. In *Hand-Book of Food Preservation*; Rahman, M.S., Ed.; Marcel Dekker: New York, NY, USA, 1999; pp. 173–216.
43. Azarpazhooh, E.; Ramaswamy, H.S. Microwave-osmotic dehydration of apples under continuous flow medium spray conditions: Comparison with other methods. *Dry. Technol.* **2009**, *28*, 49–56. [CrossRef]
44. Laguerre, J.-C.; Hamoud-Agha, M.M. Microwave heating for food preservation. In *Food Preservation and Waste Exploitation*; Socaci, S.A., Fărcaș, A.C., Aussenac, T., Laguerre, J.C., Eds.; IntechOpen: London, UK, 2020. [CrossRef]
45. Cohen, J.S.; Yang, T.C.S. Progress in food dehydration. *Trends Food Sci. Tech.* **1995**, *6*, 20–25. [CrossRef]
46. Schiffmann, R.F. Microwave processes for the food industry. In *Handbook of Microwave Technology for Food Applications*; Datta, A.K., Anantheswaran, R.C., Eds.; Marcel Dekker: New York, NY, USA, 2001; pp. 229–338.
47. Onwude, D.I.; Hashim, N.; Chen, G. Recent advances of novel thermal combined hot air drying of agricultural crops. *Trends Food Sci. Tech.* **2016**, *57*, 132–145. [CrossRef]
48. Morais, R.M.S.C.; Morais, A.M.M.B.; Dammak, I.; Bonilla, J.; Sobral, P.J.A.; Laguerre, J.C.; Afonso, M.J.; Ramalhosa, E.C.D. Functional dehydrated foods for health preservation. *J. Food Qual.* **2018**, *2018*, 1–29. [CrossRef]
49. Nowak, D.; Jakubczyk, E. The freeze-drying of foods-The characteristic of the process course and the effect of its parameters on the physical properties of food materials. *Foods* **2020**, *9*, 1488. [CrossRef]
50. Hammami, C.; René, F. Determination of freeze-drying process variables for strawberries. *J. Food Eng.* **1997**, *32*, 133–154. [CrossRef]
51. Lachowicz, S.; Michalska, A.; Lech, K.; Majerska, J.; Oszmiański, J.; Figiel, A. Comparison of the effect of four drying methods on polyphenols in saskatoon berry. *LWT Food Sci. Technol.* **2019**, *111*, 727–736. [CrossRef]
52. Lammerskitten, A.; Mykhailiyk, V.; Wiktor, A.; Toepfl, S.; Nowacka, M.; Bialik, M.; Czyżewski, J.; Witrowa-Rajchert, D.; Parniakov, O. Impact of pulsed electric fields on physical properties of freeze-dried apple tissue. *Innov. Food Sci. Emerg.* **2019**, *57*, 57. [CrossRef]
53. Shishegarha, F.; Makhlouf, J.; Ratti, C. Freeze-drying characteristics of strawberries. *Dry. Technol.* **2002**, *20*, 131–145. [CrossRef]
54. Krokida, M.K.; Karathanos, V.T.; Maroulis, Z.B. Effect of freeze-drying conditions on shrinkage and porosity of dehydrated agricultural products. *J. Food Eng.* **1998**, *35*, 369–380. [CrossRef]
55. Domin, M.; Džiki, D.; Kłapsia, S.; Blicharz-Kania, A.; Biernacka, B.; Krzykowski, A. Influence of the freeze-drying conditions on the physicochemical properties and grinding characteristics of kiwi. *Int. J. Food Eng.* **2020**, *16*(1–2), 20180315. [CrossRef]
56. Franceschinis, L.; Salvatori, D.M.; Sosa, N.; Schebor, C. Physical and functional properties of blackberry freeze- and spray-dried powders. *Dry. Technol.* **2013**, *32*, 197–207. [CrossRef]
57. Munzenmayer, P.; Ulloa, J.; Pinto, M.; Ramirez, C.; Valencia, P.; Simpson, R.; Almonacid, S. Freeze-drying of blueberries: Effects of carbon dioxide (CO₂) laser perforation as skin pretreatment to improve mass transfer, primary drying time, and quality. *Foods* **2020**, *9*, 211. [CrossRef]
58. Ong, S.P.; Law, C.L. Hygrothermal properties of various foods, vegetables and fruits. In *Drying of Foods, Vegetables and Fruits-Vol. 1*; Jangam, S.V., Law, C.L., Mujumdar, A.S., Eds.; University of Singapore: Singapore, 2012; pp. 31–58.
59. Maskan, M. Kinetics of colour change of kiwifruits during hot air and microwave drying. *J. Food Eng.* **2001**, *48*, 169–175. [CrossRef]
60. Cárcel, J.A.; García-Pérez, J.V.; Sanjuán, N.; Mulet, A. Influence of pre-treatment and storage temperature on the evolution of the colour of dried persimmon. *LWT Food Sci. Technol.* **2010**, *43*, 1191–1196. [CrossRef]
61. Rodrigues, A.C.C.; Cunha, R.L.; Hubinger, M.D. Rheological properties and colour evaluation of papaya during osmotic dehydration processing. *J. Food Eng.* **2003**, *59*, 129–135. [CrossRef]
62. Bustos, M.C.; Rocha-Parra, D.; Sampietro, I.; de Pascual-Teresa, S.; León, A.E. The influence of different air-drying conditions on bioactive compounds and antioxidant activity of berries. *J. Agric. Food Chem.* **2018**, *66*, 2714–2723. [CrossRef] [PubMed]
63. Omolola, A.O.; Jideani, A.I.O.; Kapila, P.F. Quality properties of fruits as affected by drying operation. *Crit. Rev. Food Sci.* **2015**, *57*, 95–108. [CrossRef] [PubMed]
64. Pavkov, I.; Stamenković, Z.; Radojčin, M.; Babić, M.; Bikić, S.; Mitrevski, V.; Lutovska, M. Convective and freeze drying of raspberry: Effect of experimental parameters on drying kinetics, physical properties and rehydration capacity. In Proceedings of the INOPTEP 5th International Conference Sustainable Postharvest and Food Technologies, Vršac, Serbia, 23–28 April 2017; pp. 261–266.

65. Mayor, L.; Sereno, A.M. Modelling shrinkage during convective drying of food materials: A review. *J. Food Eng.* **2004**, *61*, 373–386. [CrossRef]
66. Krokida, M.K.; Maroulis, Z.B. Effect of drying method on shrinkage and porosity. *Dry. Technol.* **1997**, *15*, 2441–2458. [CrossRef]
67. Lozano, J.E.; Rotstein, E.; Urbicain, M.J. Shrinkage, porosity and bulk density of foodstuffs at changing moisture contents. *J. Food Sci.* **1983**, *48*, 1497–1502. [CrossRef]
68. Rahman, M.S.; Potluri, P.L. Shrinkage and density of squid flesh during air drying. *J. Food Eng.* **1990**, *12*, 133–143. [CrossRef]
69. Rahman, M.S.; Perera, C.O.; Chen, X.D.; Driscoll, R.H.; Potluri, P.L. Density, shrinkage and porosity of calamari mantle meat during air drying in a cabinet dryer as a function of water content. *J. Food Eng.* **1996**, *30*, 135–145. [CrossRef]
70. Wang, N.; Brennan, J.G. Changes in structure, density and porosity of potato during dehydration. *J. Food Eng.* **1995**, *24*, 61–76. [CrossRef]
71. Sablani, S.S.; Rahman, M.S. Pore formation in selected foods as a function of shelf temperature during freeze drying. *Dry. Technol.* **2007**, *20*, 1379–1391. [CrossRef]
72. Meda, L.; Ratti, C. Rehydration of freeze-dried strawberries at varying temperatures. *J. Food Process. Eng.* **2005**, *28*, 233–246. [CrossRef]
73. Kowalska, H.; Marzec, A.; Kowalska, J.; Ciużyńska, A.; Samborska, K.; Bialik, M.; Lenart, A. Rehydration properties of hybrid method dried fruit enriched by natural components. *Int. Agrophys.* **2018**, *32*, 175–182. [CrossRef]
74. Zhang, L.; Qiao, Y.; Wang, C.; Liao, L.; Liu, L.; Shi, D.; An, K.; Hu, J.; Xu, Q. Effects of freeze vacuum drying combined with hot air drying on the sensory quality, active components, moisture mobility, odors, and microstructure of kiwifruits. *J. Food Qual.* **2019**, *2019*, 1–11. [CrossRef]
75. Wiktor, A.; Iwaniuk, M.; Ślędz, M.; Nowacka, M.; Chudoba, T.; Witrowa-Rajchert, D. Drying kinetics of apple tissue treated by pulsed electric field. *Dry. Technol.* **2013**, *31*, 112–119. [CrossRef]
76. Wiktor, A.; Nowacka, M.; Dadan, M.; Rybak, K.; Lojkowski, W.; Chudoba, T.; Witrowa-Rajchert, D. The effect of pulsed electric field on drying kinetics, color, and microstructure of carrot. *Dry. Technol.* **2015**, *34*, 1286–1296. [CrossRef]
77. Ammar, J.B.; Lanouisellé, J.-L.; Lebovka, N.I.; Van Hecke, E.; Vorobiev, E. Effect of a pulsed electric field and osmotic treatment on freezing of potato tissue. *Food Biophys.* **2010**, *5*, 247–254. [CrossRef]
78. Kamiloglu, S.; Toydemir, G.; Boyacioglu, D.; Beekwilder, J.; Hall, R.D.; Capanoglu, E. A review on the effect of drying on antioxidant potential of fruits and vegetables. *Crit. Rev. Food Sci.* **2015**, *56*, S110–S129. [CrossRef]
79. Mohammed, S.; Edna, M.; Siraj, K. The effect of traditional and improved solar drying methods on the sensory quality and nutritional composition of fruits: A case of mangoes and pineapples. *Heliyon* **2020**, *6*, e04163. [CrossRef]
80. Suna, S.; Tamer, C.E.; Inceday, B.; Sinir, G.Ö.; Çopur, Ö.U. Impact of drying methods on physicochemical and sensory properties of apricot pestil. *Indian J. Tradit. Knowl.* **2014**, *13*, 47–55.
81. Nemzer, B.; Vargas, L.; Xia, X.; Sintara, M.; Feng, H. Phytochemical and physical properties of blueberries, tart cherries, strawberries, and cranberries as affected by different drying methods. *Food Chem.* **2018**, *262*, 242–250. [CrossRef]
82. Adak, N.; Heybeli, N.; Ertekin, C. Infrared drying of strawberry. *Food Chem.* **2017**, *219*, 109–116. [CrossRef] [PubMed]
83. Zielinska, M.; Zielinska, D.; Markowski, M. The effect of microwave-vacuum pretreatment on the drying kinetics, color and the content of bioactive compounds in osmo-microwave-vacuum dried cranberries (*Vaccinium macrocarpon*). *Food Bioprocess. Tech.* **2017**, *11*, 585–602. [CrossRef]
84. Cao, X.; Islam, M.N.; Xu, W.; Chen, J.; Chitrakar, B.; Jia, X.; Liu, X.; Zhong, S. Energy consumption, colour, texture, antioxidants, odours, and taste qualities of litchi fruit dried by intermittent ohmic heating. *Foods* **2020**, *9*, 425. [CrossRef] [PubMed]
85. Verbeyst, L.; Bogaerts, R.; Van der Plancken, I.; Hendrickx, M.; Van Loey, A. Modelling of vitamin C degradation during thermal and high-pressure treatments of red fruit. *Food Bioprocess. Tech.* **2012**, *6*, 1015–1023. [CrossRef]
86. Nguyen, T.V.L.; Nguyen, Q.D.; Nguyen, P.B.D.; Tran, B.L.; Huynh, P.T. Effects of drying conditions in low-temperature microwave-assisted drying on bioactive compounds and antioxidant activity of dehydrated bitter melon (*Momordica charantia* L.). *Food Sci. Nutr.* **2020**, *8*, 3826–3834. [CrossRef]
87. Bennett, L.E.; Jegasothy, H.; Konczak, I.; Frank, D.; Sudharamarajan, S.; Clingeleffer, P.R. Total polyphenolics and anti-oxidant properties of selected dried fruits and relationships to drying conditions. *J. Funct. Foods* **2011**, *3*, 115–124. [CrossRef]
88. Ouabou, R.; Nabil, B.; Ouhammou, M.; Idlimam, A.; Lamharrar, A.; Ennahli, S.; Hanine, H.; Mahrouz, M. Impact of solar drying process on drying kinetics, and on bioactive profile of Moroccan sweet cherry. *Renew. Energy* **2020**, *151*, 908–918. [CrossRef]
89. ISO. Sensory analysis - Identification and selection of descriptors for establishing a sensory profile by a multidimensional approach. In *ISO 11035*; ISO: Switzerland, 1994; Volume 67, pp. 1–26.
90. ISO. Sensory analysis-Methodology, General guidance for establishing a sensory profile. In *ISO 13299*; ISO: Switzerland, 2003; Volume 67, pp. 1–24.
91. ISO. Sensory analysis -General guidelines for the selection, training and monitoring of selected assessors. In *ISO 8586:2012*; ISO: Switzerland, 2012; Volume 67, pp. 1–28.
92. Naes, T.; Brockhoff, P.B.; Tomic, O. *Statistics for Sensory and Consumer Science*; John Wiley & Sons, Ltd: Hoboken, NJ, USA, 2010. [CrossRef]
93. Kowalski, S.J.; Pawłowski, A.; Szadzińska, J.; Lechtańska, J.; Stasiak, M. High power airborne ultrasound assist in combined drying of raspberries. *Innov. Food Sci. Emerg.* **2016**, *34*, 225–233. [CrossRef]

94. Szychowski, P.J.; Lech, K.; Sendra-Nadal, E.; Hernández, F.; Figiel, A.; Wojdyło, A.; Carbonell-Barrachina, Á.A. Kinetics, biocompounds, antioxidant activity, and sensory attributes of quinces as affected by drying method. *Food Chem.* **2018**, *255*, 157–164. [CrossRef]
95. Wojdyło, A.; Figiel, A.; Legua, P.; Lech, K.; Carbonell-Barrachina, Á.A.; Hernández, F. Chemical composition, antioxidant capacity, and sensory quality of dried jujube fruits as affected by cultivar and drying method. *Food Chem.* **2016**, *207*, 170–179. [CrossRef]
96. Leite, J.B.; Mancini, M.C.; Borges, S.V. Effect of drying temperature on the quality of dried bananas cv. prata and d'água. *LWT Food Sci. Technol.* **2007**, *40*, 319–323. [CrossRef]
97. Sunjka, P.S.; Rennie, T.J.; Beaudry, C.; Raghavan, G.S.V. Microwave-convective and microwave-vacuum drying of cranberries: A comparative study. *Dry. Technol.* **2004**, *22*, 1217–1231. [CrossRef]
98. Krulis, M.; Kühnert, S.; Leiker, M.; Rohm, H. Influence of energy input and initial moisture on physical properties of microwave-vacuum dried strawberries. *Eur. Food Res. Technol.* **2005**, *221*, 803–808. [CrossRef]
99. Hawlader, M.N.A.; Perera, C.O.; Tian, M. Properties of modified atmosphere heat pump dried foods. *J. Food Eng.* **2006**, *74*, 392–401. [CrossRef]
100. Hendriks, M.M.W.B.; de Boer, J.H.; Smilde, A.K.; Doornbos, D.A. Multicriteria decision making. *Chemom. Intell. Lab. Syst.* **1992**, *16*, 175–191. [CrossRef]
101. Héberger, K. Sum of ranking differences compares methods or models fairly. *TRAC Trend Anal. Chem.* **2010**, *29*, 101–109. [CrossRef]
102. Sipos, L.; Bernhardt, B.; Gere, A.; Komáromi, B.; Orbán, C.; Bernáth, J.; Szabó, K. Multicriteria optimization to evaluate the performance of *Ocimum basilicum* L. varieties. *Ind. Crop. Prod.* **2016**, *94*, 514–519. [CrossRef]
103. Gere, A.; Sipos, L.; Kovács, S.; Kókai, Z.; Héberger, K. Which just-about-right feature should be changed if evaluations deviate? A case study using sum of ranking differences. *Chemom. Intell. Lab. Syst.* **2017**, *161*, 130–135. [CrossRef]
104. Rácz, A.; Bajusz, D.; Fodor, M.; Héberger, K. Comparison of classification methods with “n-class” receiver operating characteristic curves: A case study of energy drinks. *Chemom. Intell. Lab. Syst.* **2016**, *151*, 34–43. [CrossRef]
105. Gere, A.; Radványi, D.; Héberger, K. Which insect species can best be proposed for human consumption? *Innov. Food Sci. Emerg.* **2019**, *52*, 358–367. [CrossRef]
106. Stamenković, Z.; Radojčin, M.; Pavkov, I.; Bikić, S.; Ponjičan, O.; Bugarin, R.; Kovács, S.; Gere, A. Ranking and multicriteria decision making in optimization of raspberry convective drying processes. *J. Chemom.* **2020**, *34*, e3224. [CrossRef]
107. Bajusz, D.; Rácz, A.; Héberger, K. Why is Tanimoto index an appropriate choice for fingerprint-based similarity calculations? *J. Cheminform.* **2015**, *7*, 1–13. [CrossRef] [PubMed]
108. Sobukola, O.P.; Dairo, O.U.; Odunewu, A.V. Convective hot air drying of blanched yam slices. *Int. J. Food Sci. Technol.* **2008**, *43*, 1233–1238. [CrossRef]
109. Doymaz, İ. Influence of blanching and slice thickness on drying characteristics of leek slices. *Chem. Eng. Process.* **2008**, *47*, 41–47. [CrossRef]
110. Witrowa-Rajchert, D.; Wiktor, A.; Sledz, M.; Nowacka, M. Selected emerging technologies to enhance the drying process: A review. *Dry. Technol.* **2014**, *32*, 1386–1396. [CrossRef]
111. Tao, Y.; Sun, D.-W. Enhancement of food processes by ultrasound: A review. *Crit. Rev. Food Sci.* **2014**, *55*, 570–594. [CrossRef]
112. Ashokkumar, M. Applications of ultrasound in food and bioprocessing. *Ultrason. Sonochem.* **2015**, *25*, 17–23. [CrossRef]
113. Wu, J.; Nyborg, W.L. Ultrasound, cavitation bubbles and their interaction with cells. *Adv. Drug Deliv. Rev.* **2008**, *60*, 1103–1116. [CrossRef]
114. de la Fuente-Blanco, S.; de Sarabia, E.R.-F.; Acosta-Aparicio, V.M.; Blanco-Blanco, A.; Gallego-Juárez, J.A. Food drying process by power ultrasound. *Ultrasonics* **2006**, *44*, e523–e527. [CrossRef]
115. Miano, A.C.; Ibarz, A.; Augusto, P.E.D. Mechanisms for improving mass transfer in food with ultrasound technology: Describing the phenomena in two model cases. *Ultrason. Sonochem.* **2016**, *29*, 413–419. [CrossRef]
116. Musielak, G.; Mierzwa, D.; Kroehnke, J. Food drying enhancement by ultrasound—A review. *Trends Food Sci. Tech.* **2016**, *56*, 126–141. [CrossRef]
117. Magalhães, M.L.; Cartaxo, S.J.M.; Gallão, M.I.; García-Pérez, J.V.; Cárcel, J.A.; Rodrigues, S.; Fernandes, F.A.N. Drying intensification combining ultrasound pre-treatment and ultrasound-assisted air drying. *J. Food Eng.* **2017**, *215*, 72–77. [CrossRef]
118. Nowacka, M.; Wiktor, A.; Śledź, M.; Jurek, N.; Witrowa-Rajchert, D. Drying of ultrasound pretreated apple and its selected physical properties. *J. Food Eng.* **2012**, *113*, 427–433. [CrossRef]
119. Nowacka, M.; Wedzik, M. Effect of ultrasound treatment on microstructure, colour and carotenoid content in fresh and dried carrot tissue. *Appl. Acoust.* **2016**, *103*, 163–171. [CrossRef]
120. Fernandes, F.A.N.; Linhares, F.E.; Rodrigues, S. Ultrasound as pre-treatment for drying of pineapple. *Ultrason. Sonochem.* **2008**, *15*, 1049–1054. [CrossRef]
121. Śledź, M.; Nowak, P.; Witrowa-Rajchert, D. Drying of parsley leaves pre-treated by ultrasound. *ZPPNR* **2014**, *579*, 91–99.
122. Szadzińska, J.; Lechtańska, J.; Pashminehazar, R.; Kharaghani, A.; Tsotsas, E. Microwave- and ultrasound-assisted convective drying of raspberries: Drying kinetics and microstructural changes. *Dry. Technol.* **2018**, *37*, 1–12. [CrossRef]
123. da Silva, E.S.; Brandão, S.C.R.; da Silva, A.L.; da Silva, J.H.F.; Coêlho, A.C.D.; Azoubel, P.M. Ultrasound-assisted vacuum drying of nectarine. *J. Food Eng.* **2019**, *246*, 119–124. [CrossRef]
124. Liu, Y.; Sun, Y.; Yu, H.; Yin, Y.; Li, X.; Duan, X. Hot air drying of purple-fleshed sweet potato with contact ultrasound assistance. *Dry. Technol.* **2016**, *35*, 564–576. [CrossRef]

125. Timmermans, R.A.H.; Mastwijk, H.C.; Berendsen, L.B.J.M.; Nederhoff, A.L.; Matser, A.M.; Van Boekel, M.A.J.S.; Groot, M.N. Moderate intensity Pulsed Electric Fields (PEF) as alternative mild preservation technology for fruit juice. *Int. J. Food Microbiol.* **2019**, *298*, 63–73. [CrossRef]
126. Kayalvizhi, V.; Pushpa, A.J.S.; Sangeetha, G.; Antony, U. Effect of pulsed electric field (PEF) treatment on sugarcane juice. *J. Food Sci. Technol.* **2016**, *53*, 1371–1379. [CrossRef] [PubMed]
127. Weaver, J.C.; Chizmadzhev, Y.A. Theory of electroporation: A review. *Bioelectrochem. Bioenerg.* **1996**, *41*, 135–160. [CrossRef]
128. Kotnik, T.; Frey, W.; Sack, M.; Meglič, S.H.; Peterka, M.; Miklavčič, D. Electroporation-based applications in biotechnology. *Trends Biotechnol.* **2015**, *33*, 480–488. [CrossRef]
129. Barba, F.J.; Parniakov, O.; Pereira, S.A.; Wiktor, A.; Grimi, N.; Boussetta, N.; Saraiva, J.A.; Raso, J.; Martin-Belloso, O.; Witrowa-Rajchert, D.; et al. Current applications and new opportunities for the use of pulsed electric fields in food science and industry. *Food Res. Int.* **2015**, *77*, 773–798. [CrossRef]
130. Thamkaew, G.; Galindo, F.G. Influence of pulsed and moderate electric field protocols on the reversible permeabilization and drying of Thai basil leaves. *Innov. Food Sci. Emerg.* **2020**, *64*, 102430. [CrossRef]
131. Maza, M.; Álvarez, I.; Raso, J. Thermal and Non-Thermal Physical Methods for Improving Polyphenol Extraction in Red Winemaking. *Beverages* **2019**, *5*, 47. [CrossRef]
132. Min, S.; Jin, Z.T.; Zhang, Q.H. Commercial scale pulsed electric field processing of tomato juice. *J. Agric. Food Chem.* **2003**, *51*, 3338–3344. [CrossRef]
133. Fauster, T.; Schlossnikl, D.; Rath, F.; Ostermeier, R.; Teufel, F.; Toepfl, S.; Jaeger, H. Impact of pulsed electric field (PEF) pretreatment on process performance of industrial French fries production. *J. Food Eng.* **2018**, *235*, 16–22. [CrossRef]
134. Wiktor, A.; Singh, A.P.; Parniakov, O.; Mykhailyk, V.; Mandal, R.; Witrowa-Rajchert, D. PEF as an alternative tool to prevent thermolabile compound degradation during dehydration processes. In *Pulsed Electric Fields to Obtain Healthier and Sustainable Food for Tomorrow*; Barba, F., Parniakov, O., Wiktor, A., Eds.; Academic Press: London, UK, 2020; pp. 155–202.
135. Ostermeier, R.; Parniakov, O.; Töpfl, S.; Jäger, H. Applicability of pulsed electric field (PEF) pre-treatment for a convective two-step drying process. *Foods* **2020**, *9*, 512. [CrossRef]
136. Wu, Y.; Guo, Y.; Zhang, D. Study of the effect of high-pulsed electric field treatment on vacuum freeze-drying of apples. *Dry. Technol.* **2011**, *29*, 1714–1720. [CrossRef]
137. Lammerskitten, A.; Wiktor, A.; Siemer, C.; Toepfl, S.; Mykhailyk, V.; Gondek, E.; Rybak, K.; Witrowa-Rajchert, D.; Parniakov, O. The effects of pulsed electric fields on the quality parameters of freeze-dried apples. *J. Food Eng.* **2019**, *252*, 36–43. [CrossRef]
138. Fauster, T.; Giancaterino, M.; Pittia, P.; Jaeger, H. Effect of pulsed electric field pretreatment on shrinkage, rehydration capacity and texture of freeze-dried plant materials. *LWT* **2020**, *121*, 108937. [CrossRef]
139. Liu, C.; Pirozzi, A.; Ferrari, G.; Vorobiev, E.; Grimi, N. Effects of pulsed electric fields on vacuum drying and quality characteristics of dried carrot. *Food Bioprocess. Tech.* **2019**, *13*, 45–52. [CrossRef]
140. Huang, H.-W.; Wu, S.-J.; Lu, J.-K.; Shyu, Y.-T.; Wang, C.-Y. Current status and future trends of high-pressure processing in food industry. *Food Control.* **2017**, *72*, 1–8. [CrossRef]
141. Rastogi, N.K.; Angersbach, A.; Knorr, D. Synergistic effect of high hydrostatic pressure pretreatment and osmotic stress on mass transfer during osmotic dehydration. *J. Food Eng.* **2000**, *45*, 25–31. [CrossRef]
142. Eshtiaghi, M.N.; Stute, R.; Knorr, D. High-pressure and freezing pretreatment effects on drying, rehydration, texture and color of green beans, carrots and potatoes. *J. Food Sci.* **1994**, *59*, 1168–1170. [CrossRef]
143. Janowicz, M.; Lenart, A. The impact of high pressure and drying processing on internal structure and quality of fruit. *Eur. Food Res. Technol.* **2018**, *244*, 1329–1340. [CrossRef]
144. Yucel, U.; Alpas, H.; Bayindirli, A. Evaluation of high pressure pretreatment for enhancing the drying rates of carrot, apple, and green bean. *J. Food Eng.* **2010**, *98*, 266–272. [CrossRef]
145. Kingsly, A.R.P.; Balasubramaniam, V.M.; Rastogi, N.K. Effect of high-pressure processing on texture and drying behavior of pineapple. *J. Food Process. Eng.* **2009**, *32*, 369–381. [CrossRef]
146. George, J.M.; Sowbhagya, H.B.; Rastogi, N.K. Effect of high pressure pretreatment on drying kinetics and oleoresin extraction from ginger. *Dry. Technol.* **2017**, *36*, 1107–1116. [CrossRef]
147. Núñez-Mancilla, Y.; Vega-Gálvez, A.; Pérez-Won, M.; Zura, L.; García-Segovia, P.; Di Scala, K. Effect of osmotic dehydration under high hydrostatic pressure on microstructure, functional properties and bioactive compounds of strawberry (*Fragaria Vesca*). *Food Bioprocess. Tech.* **2013**, *7*, 516–524. [CrossRef]
148. Kim, K.W.; Kim, Y.-T.; Kim, M.; Noh, B.-S.; Choi, W.-S. Effect of high hydrostatic pressure (HHP) treatment on flavor, physico-chemical properties and biological functionalities of garlic. *LWT Food Sci. Technol.* **2014**, *55*, 347–354. [CrossRef]
149. Sampedro, F.; McAloon, A.; Yee, W.; Fan, X.; Geveke, D.J. Cost analysis and environmental impact of pulsed electric fields and high pressure processing in comparison with thermal pasteurization. *Food Bioprocess. Tech.* **2014**, *7*, 1928–1937. [CrossRef]
150. Pankaj, S.K.; Bueno-Ferrer, C.; Misra, N.N.; Milosavljević, V.; O'Donnell, C.P.; Bourke, P.; Keener, K.M.; Cullen, P.J. Applications of cold plasma technology in food packaging. *Trends Food Sci. Tech.* **2014**, *35*, 5–17. [CrossRef]
151. Niemira, B.A. Cold plasma decontamination of foods. *Annu. Rev. Food Sci. Technol.* **2012**, *3*, 125–142. [CrossRef]
152. Encinas, N.; Abenojar, J.; Martínez, M.A. Development of improved polypropylene adhesive bonding by abrasion and atmospheric plasma surface modifications. *Int. J. Adhes. Adhes.* **2012**, *33*, 1–6. [CrossRef]

153. Wiktor, A.; Hrycak, B.; Jasiński, M.; Rybak, K.; Kieliszek, M.; Kraśniewska, K.; Witrowa-Rajchert, D. Impact of atmospheric pressure microwave plasma treatment on quality of selected spices. *Appl. Sci.* **2020**, *10*, 6815. [CrossRef]
154. Bao, T.; Hao, X.; Shishir, M.R.I.; Karim, N.; Chen, W. Cold plasma: An emerging pretreatment technology for the drying of jujube slices. *Food Chem.* **2021**, *337*, 127783. [CrossRef]
155. Zhou, Y.-H.; Vidyarthi, S.K.; Zhong, C.-S.; Zheng, Z.-A.; An, Y.; Wang, J.; Wei, Q.; Xiao, H.-W. Cold plasma enhances drying and color, rehydration ratio and polyphenols of wolfberry via microstructure and ultrastructure alteration. *LWT* **2020**, *134*, 110173. [CrossRef]
156. Shishir, M.R.I.; Karim, N.; Bao, T.; Gowd, V.; Ding, T.; Sun, C.; Chen, W. Cold plasma pretreatment—A novel approach to improve the hot air drying characteristics, kinetic parameters, and nutritional attributes of shiitake mushroom. *Dry. Technol.* **2019**, *38*, 2134–2150. [CrossRef]
157. Li, S.; Chen, S.; Han, F.; Xv, Y.; Sun, H.; Ma, Z.; Chen, J.; Wu, W. Development and optimization of cold plasma pretreatment for drying on corn kernels. *J. Food Sci.* **2019**, *84*, 2181–2189. [CrossRef] [PubMed]
158. Zhang, X.-L.; Zhong, C.-S.; Mujumdar, A.S.; Yang, X.-H.; Deng, L.-Z.; Wang, J.; Xiao, H.-W. Cold plasma pretreatment enhances drying kinetics and quality attributes of chili pepper (*Capsicum annum* L.). *J. Food Eng.* **2019**, *241*, 51–57. [CrossRef]

Article

Effects of Osmotic Dehydration on the Hot Air Drying of Apricot Halves: Drying Kinetics, Mass Transfer, and Shrinkage

Ivan Pavkov¹, Milivoj Radojčin^{1,*}, Zoran Stamenković¹, Krstan Kešelj¹, Urszula Tylewicz², Péter Sipos³, Ondrej Ponjičan¹ and Aleksandar Sedlar¹

¹ Faculty of Agriculture, University of Novi Sad, Trg Dositeja Obradovića 8, 21000 Novi Sad, Serbia; ivan.pavkov@polj.uns.ac.rs (I.P.); zoran.stamenkovic@polj.uns.ac.rs (Z.S.); krstan.keselj@polj.uns.ac.rs (K.K.); ondrej.ponjican@polj.uns.ac.rs (O.P.); aleksandar.sedlar@polj.uns.ac.rs (A.S.)

² Department of Agricultural and Food Sciences, Alma Mater Studiorum-Università di Bologna, Piazza Goidanich 60, 47521 Cesena, Italy; urszula.tylewicz@unibo.it

³ Institute of Nutrition, Faculty of Agricultural and Food Sciences and Environmental Management, University of Debrecen, H-4032 Debrecen, Hungary; siposp@agr.unideb.hu

* Correspondence: milivoj.radojcin@polj.uns.ac.rs; Tel.: +381-21-485-3431

Abstract: This study aimed to determine the effects of osmotic dehydration on the kinetics of hot air drying of apricot halves under conditions that were similar to the industrial ones. The osmotic process was performed in a sucrose solution at 40 and 60 °C and concentrations of 50% and 65%. As expected increased temperatures and concentrations of the solution resulted in increased water loss, solid gain and shrinkage. The kinetics of osmotic dehydration were well described by the Peleg model. The effective diffusivity of water $5.50\text{--}7.387 \times 10^{-9} \text{ m}^2/\text{s}$ and solute $8.315 \times 10^{-10}\text{--}1.113 \times 10^{-9} \text{ m}^2/\text{s}$ was calculated for osmotic dehydration. Hot air drying was carried out at 40, 50, and 60 °C with air flow velocities of 1.0 m/s and 1.5 m/s. The drying time shortened with higher temperature and air velocity. The calculated effective diffusion of water was from $3.002 \times 10^{-10} \text{ m}^2/\text{s}$ to $1.970 \times 10^{-9} \text{ m}^2/\text{s}$. The activation energy was sensitive to selected air temperatures, so greater air velocity resulted in greater activation energy: 46.379–51.514 kJ/mol, and with the osmotic pretreatment, it decreased to 35.216–46.469 kJ/mol. Osmotic dehydration reduced the effective diffusivity of water during the hot air drying process. It also resulted in smaller shrinkage of apricot halves in the hot air drying process.

Keywords: apricot; osmotic dehydration; drying; kinetics; modeling; mass transfer; shrinkage

Citation: Pavkov, I.; Radojčin, M.; Stamenković, Z.; Kešelj, K.; Tylewicz, U.; Sipos, P.; Ponjičan, O.; Sedlar, A. Effects of Osmotic Dehydration on the Hot Air Drying of Apricot Halves: Drying Kinetics, Mass Transfer, and Shrinkage. *Processes* **2021**, *9*, 202. <https://doi.org/10.3390/pr9020202>

Academic Editors: Marek Markowski and Timothy Langrish

Received: 31 December 2020

Accepted: 19 January 2021

Published: 21 January 2021

Publisher's Note: MDPI stays neutral with regard to jurisdictional claims in published maps and institutional affiliations.



Copyright: © 2021 by the authors. Licensee MDPI, Basel, Switzerland. This article is an open access article distributed under the terms and conditions of the Creative Commons Attribution (CC BY) license (<https://creativecommons.org/licenses/by/4.0/>).

1. Introduction

Apricot (*Prunus armeniaca*) is one of the most valued stone fruit species grown in the temperate climate zone due to its attractive appearance and distinctive aroma. It is a rich source of antioxidants, minerals, and vitamins. In addition to its fresh use, it is used for various forms of processing (drying, freezing, gelled products, compotes, juices, and alcoholic beverages). The production of dried fruit in the world in 2019 amounted to 2.8 million tons, which is 16% higher than ten years ago. Compared to other fruits, dried apricot production has been recorded with the largest increase and a share of about 40%. The world's leading producer is Turkey, with 19% of total production, and the US with 12% [1–3]. In Serbia, the consumption of dried apricots has gradually increased over the last years, and most of it is imported from Turkey and Iran. Domestic production of dried apricots is rather small due to a lack of knowledge of adequate technology. Given the significant production of fresh apricots in Serbia and the economic justification of the drying process, further research on the drying of domestic varieties should be encouraged [4,5].

The common apricot drying technology includes a pre-treatment with sulfurization and hot air drying. Sulfurization slows down enzymatic and non-enzymatic reactions as well as microbiological spoilage during long storage. However, sulfurization and hot air drying affect the sensory, nutritional, and physical properties of dried apricots, and they

cause the reduction of phenolic compounds, carotenoids, and vitamin C [6–10]. Recently, there has been a growing demand in the world for dried sulfur-free apricots with better functional properties. Osmotic dehydration (OD) as a pre-treatment for hot air drying (HAD) offers less sulfur and improves the qualitative properties of dried fruit [11,12].

Osmotic dehydration is the process of removing water from tissue immersed in concentrated aqueous solutions. The difference in osmotic pressures causes mass transfer between the fruit tissue and the osmotic agent. Two opposite flows appear: diffusion of water from fruit cellular tissue (water loss, WL) and diffusion of osmotic agent into cells (solid gain, SG). The intensity of mass transfer depends on the type of osmotic agent, temperature, and concentration of the osmotic solution, agitation speed, size and shape of the fruit, fruit maturity, and fruit to osmotic agent mass ratio. Various osmotic agents can be used: sucrose, glucose, fructose, maltodextrin, sorbitol, sodium chloride, and their combinations [11–14]. The structure of fruit tissue cells plays a significant role in the rate of mass transfer [15,16]. Acceleration of osmotic dehydration via cell structure can be achieved by applying thermal pretreatments such as freezing and blanching. Recent research has focused on the application of non-thermal pretreatments such as high hydrostatic pressure (HHP), ultrasound (US), or pulsed electrical field (PEF) [15–18]. Both groups of pretreatments, thermal, and non-thermal, cause changes in the cell structure which is a limiting factor for mass transfer.

Osmotically-treated fruit has been proved to have a positive effect on the preservation of the content of total phenolic compounds and vitamin C compared to non-treated fruit. Apricot cubes osmotically treated in a sorbitol solution showed better color retention compared to the non-treated ones [12,19,20], as well as can help preserve the apricot shape, volume, and smooth surface during hot air drying [20]. Apricots treated osmotically in a sucrose solution presented lower water activity and lower glass transition temperature compared to untreated ones with the same water content [21]. In addition to the positive effects, OD also has some disadvantages. It requires an additional drying process, usually with hot air (HAD), to dry the product to a safe moisture content. The osmotic solution needs to be regenerated after some time. OD affects the reduction of the effective water diffusion coefficient in the additional drying process [20].

Literature data on the kinetics of OD and HAD of apricots refers to the pieces of small fruit cut into regular geometric shapes, cubes, slices, cylinders [11,13,14]. In industrial conditions, apricots are dried as a whole fruit or cut in half. Apricots up to 35 mm in diameter are dried as a whole fruit [22], and those with a diameter over 35 mm require cutting in halves or other shapes. To the best of our knowledge there is no data in literature describing the combination of OD and HAD of apricot fruits in the form of halves. Additionally, OD experiments are typically performed in small-volume vessels that cannot represent the real process of mass transfer, which is also the case with HAD experiments [13].

This study aims to determine the kinetics of OD as well as the influence of OD on mass transfer during HAD under conditions similar to the industrial ones. The research was performed on the apricot halves. During OD, the kinetics of water loss and solid gain, as well as the shrinkage by volume, length, width, and thickness were determined. Mathematical modeling of WL and SG kinetics was performed and the coefficients of effective diffusion of water and osmotic agent were calculated. During the HAD, mathematical modeling of the change in water content was done, the coefficients of effective water diffusion, activation energy, as well as the shrinkage of the volume, length, width, and thickness of apricot half were also determined.

2. Materials and Methods

2.1. Material

Fresh fruits of apricot (*Prunus armeniaca* L.) were harvested in the orchard of the University of Novi Sad, Faculty of Agriculture, Rimski šančevi (45°20' N and 19°50' E, 80 m a.s.l.), Serbia. The native variety from Novi Sad was chosen because of its presence in the domestic assortment [1,2]. The fruits were in full technological maturity with the

following characteristics (average values): moisture content of fresh fruit 7.45 ± 0.34 kg H₂O/kg d.m., length 50.9 ± 6.3 mm, width 49.0 ± 5.5 mm, thickness 44.7 ± 4.3 mm, whole fruit weight 60.6 ± 5.5 g, fruit strength 3.97 ± 0.32 kg/cm², pH value 3.03 ± 0.12 , and flesh ratio $94.49 \pm 1.16\%$. The picked fruits were stored in a cooling chamber at a temperature of 4 °C and relative air humidity of 75% for a maximum of 48 h.

2.2. Methods

2.2.1. Cutting in Halves and Sulfurization

The fruits were washed in tap water in the laboratory and then cut longitudinally into two halves with a metal blade. The average dimensions of apricot halves were: length $L_1 = 50.9 \pm 6.8$ mm, width $L_2 = 49.0 \pm 5.5$ mm, thickness $L_3 = 22.0 \pm 2.2$ mm, volume 27.58 ± 5.70 cm³. Characteristic dimensions, length, width, and thickness were measured with vernier caliper (0–190 mm, ± 0.05 mm, TMA MEBA, D-6-1, Prvomajska, Zagreb, Croatia). The halves were spread on plastic perforated trays $450 \times 250 \times 50$ mm in size. A stainless steel metal chamber $2000 \times 320 \times 510$ mm (or 0.327 m³) was used for dry sulfurization (SO₂). About 40 kg of apricot halves with a bulk porosity of 40% were placed in the chamber leaving 0.23 m³ of space. Powdered sulfur was used and 0.75 g of sulfur per one kilogram of apricot halves was burned for 2 h [6,22]. After sulfurization, the halves were osmotically dehydrated. The dry matter content was determined by drying the samples at 105 °C in an oven (Sterimatic, ST-11, Instrumentaria, Zagreb, Croatia) to constant weight.

2.2.2. Osmotic Dehydration

The osmotic dryer of 0.034 m³ volume was used with a circulation pump and a heat exchanger [23]. The working fluid was sucrose dissolved in distilled water [24,25]. To avoid a decrease in osmotic pressure because of the diluted solution, the ratio of osmotic solution/material was 10:1 [26]. Osmotic dehydration was performed at two temperatures, 40 and 60 °C, and two concentrations of sucrose, 50 and 65% (*w/w*). About 4 kg of sulfurized apricot halves were placed in a perforated metal basket and immersed in the osmotic solution. Drying lasted 3 h with a constant solution flow rate of 0.01033 m/s (ultrasonic flow meter, Krohne, UMF 600P, Sensor A, Beverly, MA, USA). Before the beginning of each osmotic dehydration experiment, 30 apricot halves were selected and their mass (m_0), length ($L_{1(0)}$), width ($L_{2(0)}$), thickness ($L_{3(0)}$), and volume (V_0) were measured. Every 20 min of the experiment, a sample of three halves was taken, the excess solution was carefully wiped with a paper towel, and then the measurements of mass (m_τ), length ($L_{1(\tau)}$), width ($L_{2(\tau)}$), thickness ($L_{3(\tau)}$), volume (V_τ), and dry matter content were taken. The weight of the sample was measured on an analytical balance (0–200 g, 0.01 g \pm 0.02 g, Kern, 440-33 N, Balingen, Germany). The dry matter content was determined by drying the samples at 105 °C in an oven (Sterimatic, ST-11, Instrumentaria, Zagreb, Croatia) to constant weight. The OD experiment was performed in three replicates of all factor combinations.

2.2.3. Hot Air Drying (HAD)

Pre-treatment samples OD1 (40 °C, 50%) OD2 (60 °C, 65%) and a control sample (without OD) were used to investigate the effect of OD on HAD. The prepared samples were placed in a tray-type tunnel dryer. The experiment of hot air drying was performed at 40, 50, 60 °C in a laboratory-scale dryer with 1.0 and 1.5 m/s air velocities. Two kilograms of apricot halves were arranged in a thin layer on four trays 440×290 mm in size. The specific load of the tray was 4 kg of apricot halves/m². The spherical part of the half was laid down facing the tray, and the cut part of the half was laid turned upwards. Inlet air was 25 ± 1.4 °C and the relative humidity was $42 \pm 7.8\%$. Before the experiment was started, the dryer was run empty for about 30 min to achieve the desired temperature and air velocity conditions. Drying with one combination of factors took 1380 min. Each combination of factors was repeated three times.

During the HAD process, the kinetics of the drying process was continuously measured and the following data were recorded: the mass of apricot halves, temperature of fruit, temperature of heated and surrounding air (dry and wet-bulb temperature). The change in the mass of the sample was measured using a mass sensor built into the dryer (HBM, Germany, model PW6CC3MR, measuring range 0–20 kg, accuracy ± 2 g). The temperature of apricot halves was measured by placing the tip of a thermocouple (J-type) 5 mm below the upper surface and it was measured on three halves. The temperature of the surrounding hot air was measured with thermocouples (J-type). Mass and temperature sensors were connected to a measurement acquisition (National Instruments, USA, model NI 622225) which recorded data every 60 s. Air velocity was measured using dynamic pressure that was measured by employing a pitot tube and a differential micro manometer (Testo 506, Germany, measuring range 0–100 hPa, accuracy ± 1 Pa). The dryer used in the experiment was described in detail in the previous paper [27]. At the beginning ($\tau = 0$ min) and at the end ($\tau = 1380$ min) of each HAD experiment, 10 apricot halves were selected and their mass (m_τ), length ($L_{1(\tau)}$), width ($L_{2(\tau)}$), thickness ($L_{3(\tau)}$), and volume (V_τ) were measured.

2.2.4. Measuring of Volume and Shrinkage

The volume of the apricot halves was measured by immersing the halves into 96% ethanol and calculating the volume according to the following equation [28]:

$$V_\tau = \frac{m_\tau - m}{\rho} \quad (1)$$

where V_τ is the volume of the half (cm^3), m_τ is the mass of the half and fluid (ethanol) (g), m is the fluid mass (g), ρ is fluid density (g/cm^3). One of the qualitative indicators of the drying process and the quality of the final product is the change in the volume and dimensions of the final product compared to the fresh material. Shrinkage of apricot halves was calculated with the following equations [26,29]:

$$S_{V(\tau)} = \frac{V_0 - V_\tau}{V_0} \quad (2)$$

$$S_{L_{1(\tau)}} = \frac{L_{1(0)} - L_{1(\tau)}}{L_{1(0)}}; \quad S_{L_{2(\tau)}} = \frac{L_{2(0)} - L_{2(\tau)}}{L_{2(0)}}; \quad S_{L_{3(\tau)}} = \frac{L_{3(0)} - L_{3(\tau)}}{L_{3(0)}} \quad (3)$$

where $S_{V(\tau)}$ is decrease in volume (-), V_0 initial volume of apricot half (cm^3), V_τ apricot half volume (cm^3) at time τ . $S_{L_{1(\tau)}}$ —shrinkage in length (-), $L_{1(0)}$, $L_{1(\tau)}$ —length (mm) at the beginning of process and at time τ , $S_{L_{2(\tau)}}$ —shrinkage in width (-), $L_{2(0)}$, $L_{2(\tau)}$ —width (mm) at the beginning of process and at time τ , $S_{L_{3(\tau)}}$ —shrinkage in thickness (-), $L_{3(0)}$, $L_{3(\tau)}$ —thickness (mm) at the beginning of process and at time τ .

2.2.5. Modeling of Osmotic Dehydration and Hot Air Drying

Following parameters describing the kinetics of the OD process were calculated [16]:

$$WL = \frac{m_0 X_0 - m_\tau X_\tau}{m_{d.m.(0)}} \quad (4)$$

$$SG = \frac{m_{d.m.(\tau)} - m_{d.m.(0)}}{m_{d.m.(0)}} \quad (5)$$

where WL is water loss (kg $\text{H}_2\text{O}/\text{kg}$ d.m.), SG is solid gain (kg d.m./kg i.d.m.; is initial dry matter), X_0 is initial water content (kg $\text{H}_2\text{O}/\text{kg}$ d.m.), X_τ is water content (kg $\text{H}_2\text{O}/\text{kg}$ d.m.) at time τ of the process, $m_{d.m.(0)}$ is the initial mass of dry matter (kg i.d.m.), $m_{d.m.(\tau)}$ is mass of dry matter (kg d.m.) at time τ of the process, m_0 is the initial mass of the sample (kg), and m_τ is mass of the sample (kg) at time τ of the process.

The Peleg model was used to describe the kinetics of OD based on WL and SG changes during the process [30]:

$$WL = \frac{\tau}{k_{w1} + k_{w2}\tau} \quad (6)$$

$$SG = \frac{\tau}{k_{s1} + k_{s2}\tau} \quad (7)$$

where τ is time (min) of drying, k_{w1} is Peleg's parameter (min kg d.m./kg H₂O), k_{w2} is Peleg's parameter (kg d.m./kg H₂O), k_{s1} is Peleg's parameter (min kg i.d.m./kg d.m.), k_{s2} is Peleg's parameter (kg d.m. initial/kg d.m.).

The moisture ratio (MR) and drying rate ($\Delta X/\Delta\tau$) were calculated using the following formulas to show the kinetics of the hot air drying process:

$$MR = \frac{X_\tau - X_{eq}}{X_0 - X_{eq}} \quad (8)$$

$$\frac{\Delta X}{\Delta\tau} = \frac{X_0 - X_\tau}{\tau - \tau_0} \quad (9)$$

where X_0 is the initial water content in the course of drying (kg H₂O/kg d.m.), X_τ is water content (kg H₂O/kg d.m.) at time τ of the process, X_{eq} —equilibrium water content (kg H₂O/kg d.m.), τ —drying time (min). The equilibrium water content for all experimental units was 0.1 kg H₂O/kg d.m. ($\approx 10\%$ wet base).

To select the best mathematical model that would describe the curves of hot air drying of apricot halves pretreated with osmotic dehydration, ten equations commonly used in literature were analyzed (Table 1).

Table 1. Mathematical models applied to hot air drying curves.

Model Number	Model Name	Model Equation	References
1	Newton ¹	$MR = \exp(-k\tau)$	[31]
2	Page	$MR = \exp(-k\tau^n)$	[32]
3	Modified Page	$MR = \exp(-(kt)^n)$	[33]
4	Logarithmic	$MR = a \exp(-k\tau) + b$	[34]
5	Henderson and Pabis	$MR = a \exp(-kt)$	[35]
6	Modified Henderson and Pabis	$MR = a \exp(-k_1\tau) + b \exp(-k_2\tau) + c \exp(-k_3\tau)$	[36]
7	Verma	$MR = a \exp(-k_1\tau) + (1 - a) \exp(-k_2\tau)$	[37]
8	Two Term	$MR = a \exp(-k_1\tau) + b \exp(-k_2\tau)$	[38]
9	Two Term Exponential	$MR = a \exp(-kt) + (1 - a) \exp(-kat)$	[39]
10	Diffusion Approach	$MR = a \exp(-kt) + (1 - a) \exp(-kbt)$	[40]

¹ k, k_1, k_2, k_3 —Drying constant (min^{-1}); a, b, c, n —Coefficients of the equations; τ —Time (min).

2.2.6. Determination of Water and Solute Diffusivities

The coefficient of effective diffusivity of water and solute during OD and HAD, obtained from the drying data, represents an overall mass transfer property of water or solute in the material, which may include liquid diffusion, vapor diffusion, hydrodynamic flow, and other possible mass transfer mechanisms. Analytical solutions of the equations representative of mass transfer in terms of Fick's law have been reported for geometrical shapes such as infinite slabs, infinite and finite cylinders, parallelepipeds, and spheres [41]. Nevertheless, several food products of hemispherical shape (mushrooms, coffee grains, halved potato, halved melons, halved apricots) are frequently modeled in this geometry [24,42]. For the hemispherical shape, more complex methods have been used based on finite element techniques to solve mass transfer in terms of Fick's law [43,44]. In this study, the diffusivities of water and osmotic agent was calculated by applying the analytical solution for a infinite slab geometry [24,25]. The solutions to the second Fick's law for infinite slab

and a working medium of limited volume are the following equations for diffusions of water and solute [25,41]:

$$\frac{WL}{WL_{eq}} \text{ or } \frac{SG}{SG_{eq}} = 1 - \sum_{i=1}^{\infty} C_i \cdot \exp\left(\frac{-q_i^2 \cdot D_e \tau}{l^2}\right) \quad (10)$$

$$C_i = \frac{2\alpha(\alpha + 1)}{1 + \alpha + q_i^2 \alpha^2} \quad (11)$$

where the q_i represents the non-zero roots of:

$$\tan q_i = -\alpha q_i \quad (12)$$

where WL_{eq} is water loss at equilibrium (kg H₂O/kg d.m.), SG_{eq} is solid gain at equilibrium (kg d.m./kg d.m.initial), l —half thickness of slab/sample (m), D_e is the effective diffusivity of the water or solute (m²/s), α is the ratio of solution/sphere volumes. The WL_{eq} and SG_{eq} values were determined experimentally. For all combinations, three apricot halves were placed in a 500 cm³ vessel with osmotic agent and placed in an incubator (Sterimatic, ST-05, Instrumentaria, Zagreb, Croatia). The mass was measured every 24 h until equilibrium was reached, and then the dry matter content was measured. The measurement was done in three replicates.

For diffusivity of a infinite slab, Fourier number $D_e \tau / l^2$ was set to be greater than 0.1; only the first term in Equation (10) is significant and other terms can be neglected, so Equation (10) can be, therefore, reduced to:

$$-\ln\left(\frac{1 - \left(\frac{WL}{WL_{eq}} \text{ or } \frac{SG}{SG_{eq}}\right)}{C_1}\right) = q_1^2 \left(\frac{D_e \tau}{l^2}\right) \quad (13)$$

The value D_e of water and solute can be determined from the slope of the linear regression plotting $-\ln((1 - WL/WL_{eq})/C_1)$ and $-\ln[(1 - SG/SG_{eq})/C_1]$ versus τ .

The solution to Fick's second law for the diffusion of an infinite slab in the media of unlimited volume resulted in the following equation for the transfer of water during hot air drying [41,42]:

$$MR = \frac{X_\tau - X_{eq}}{X_0 - X_{eq}} = \frac{8}{\pi^2} \sum_{i=0}^{\infty} \frac{1}{(2i + 1)^2} \cdot \exp\left(-\frac{(2i + 1)^2 \pi^2 D_{eff} \tau}{4l^2}\right) \quad (14)$$

where D_{eff} water diffusivity coefficient (m²/s). For long drying processes, only the first term on the right side of the equation is taken into consideration and then the equation takes the following form [41,42]:

$$MR = \frac{8}{\pi^2} \cdot \exp\left(-\frac{\pi^2 D_{eff} \tau}{4l^2}\right) \quad (15)$$

Only the first term in Equation (15) is significant and other terms can be neglected. The value D_{eff} of water can be determined from the slope of the linear regression plotting $\ln MR$ versus τ .

2.2.7. Determination of Activation Energy

Activation energy (E_a) shows the sensibility of the diffusivity (D_{eff}) to temperature. The greater value of E_a means more sensibility of diffusivity to temperature. The temperature dependence of effective diffusivity may be described by Arrhenius-type relationship as follows [44]:

$$D_{eff} = D_0 \exp\left(\frac{E_a}{RT}\right) \quad (16)$$

where E_a is activation energy (kJ/mol), D_0 is the Arrhenius factor that is generally defined as the infinitely high temperature (m^2/s), R is the universal gas constant (kJ/kmolK), and T is the absolute temperature (K). E_a is calculated using the right line that was obtained by linear regression between $\ln(D_{eff})$ and $(1/T)$.

2.2.8. Experimental Design and Statistical Analysis of the Results

In this study, a set of randomized 2×3 factorial experiments with three replicates was performed to investigate:

- effects of concentration and temperature of the osmotic solution on the drying behavior of apricot halves during OD, the kinetics of water loss, solid gain, shrinkage, and diffusivity coefficients;
- effects of the OD process parameters on the drying behavior of apricot halves during HAD, kinetics, shrinkage, diffusivity coefficients, and activation energy.

The data obtained from experiments were analyzed using “Statistica” software, version 13 (TIBCO Software Inc., Palo Alto, CA, USA). The analysis of variance (ANOVA) was used to evaluate the difference between mean values of response. The Duncan’s multiple range test was performed and significant differences were observed at $p < 0.05$. The drying constants and coefficients in the models were determined by performing a non-linear regression analysis. “Statistica” software version 13 (TIBCO Software Inc., Palo Alto, CA, USA) was used for statistical analysis. The determination coefficient (R^2), the root mean square error (RMSE), the reduced chi-squared (χ^2), and coefficient residual variation (CRV) were used to evaluate the fitness of the models [16]:

$$R^2 = \frac{\sum_{i=1}^N (MR_{i,p} - MR_e)^2}{\sum_{i=1}^N (MR_{i,e} - MR_p)^2} \quad (17)$$

$$RMSE = \sqrt{\frac{\sum_{i=1}^N (MR_{i,p} - MR_{i,e})^2}{N}} \quad (18)$$

$$\chi^2 = \sqrt{\frac{\sum_{i=1}^N (MR_{i,p} - MR_{i,e})^2}{N - n}} \quad (19)$$

$$CRV = 100\% \cdot \frac{\sqrt{\chi^2}}{Y} \quad (20)$$

where $MR_{i,p}$ is predicted dimensionless moisture ratio; $MR_{i,e}$ is experimental dimensionless moisture ratio; MR_e is experimental mean dimensionless moisture ratio; N is number of observations; n is number of constants in the model equation; Y mean experimental values of WL, SG or MR. High R^2 values, lower χ^2 , and RMSE indicate that the model fits well to the experimental data. The CRV values below 20% indicate that the model can be used for prediction.

3. Results

3.1. Osmotic Dehydration

Figure 1 shows the water loss (WL) of apricot halves during osmotic dehydration. After 180 min of process, the highest WL was recorded with the highest values of process parameters (60 °C, 65%) and it was 5.214 kg H₂O/kg d.m., and the lowest value was 3.832 kg H₂O/kg d.m. for the lowest temperature and smallest osmotic agent concentration (40 °C, 50%). During the first 60 min of the process, WL was most intense. Compared to the moisture content of apricot halves in the initial sample (8.304 kg H₂O/kg d.m.), 30–44% of water was lost, and for the remaining 120 min another 17–18% was lost. A total of 180 min of osmotic dehydration reduced moisture content in the range of 47–62%. Based on the osmotic drying curves and depending on the process parameters, the lowest moisture content was 3.187 kg H₂O/kg d.m. recorded after 180 min of the process

(Supplementary Figure S1). The evaluation of ANOVA (Table 2) showed the significance of both temperature and osmotic agent concentration for WL. The temperature of the solution had greater effect on WL, while the interaction of the factors was not statistically significant.

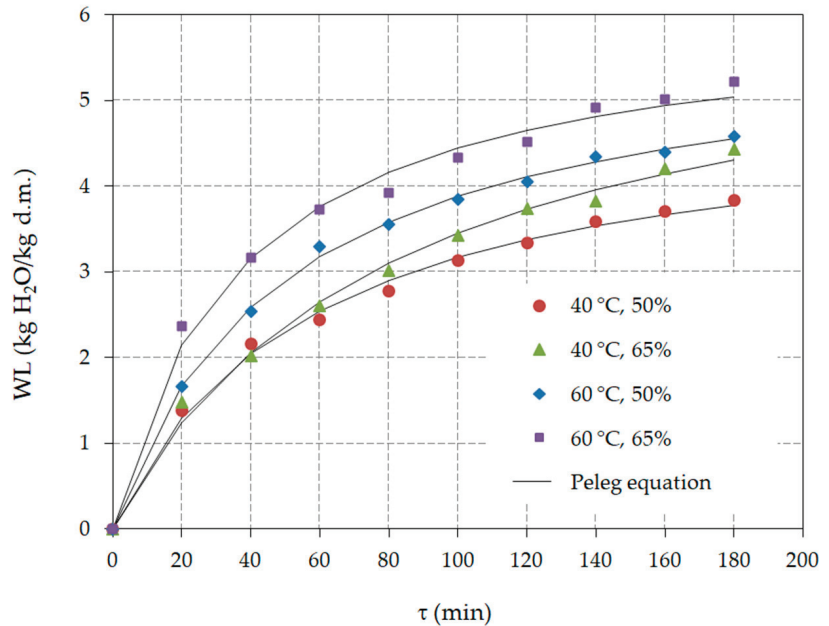


Figure 1. Water loss (WL) during the osmotic dehydration process (process predicted based on Equation (6)).

Table 2. Mass transfer parameters after 180 min of OD process.

¹ t (°C)	C (%)	WL (kg H ₂ O/kg d.m.)	SG (kg d.m./kg i.d.m.)	Ratio WL/SG (–)
40	50	3.832 ± 0.402 ^c	0.394 ± 0.004 ^b	9.711
40	65	4.429 ± 0.390 ^{bc}	0.478 ± 0.059 ^c	9.258
60	50	4.578 ± 0.441 ^{ba}	0.517 ± 0.017 ^{cb}	8.843
60	65	5.214 ± 0.018 ^a	0.568 ± 0.013 ^a	9.219

¹ t—temperature of osmotic solution. C—concentration of the osmotic agent. Data are mean ± standard deviation. The values marked with different letters (a, b, c) are significantly different ($p = 0.05$). WL—water loss. SG—solid gain.

Increase in solid gain (SG) is presented in Figure 2. After 180 min, depending on the process parameters, SG was: 0.565, 0.517, 0.478, 0.394 kg d.m./kg i.d.m., respectively, for samples treated at 60 °C, 65%, 60 °C, 50%, 40 °C, 65% and 40 °C, 50%. The highest SG was recorded in the first 40 min: 0.311, 0.222, 0.193, 0.166 kg d.m./kg i.d.m., respectively, for samples treated at 60 °C, 65%, 60 °C, 50%, 40 °C, 50%, and 40 °C, 65%. It continuously decreased until the end of the process.

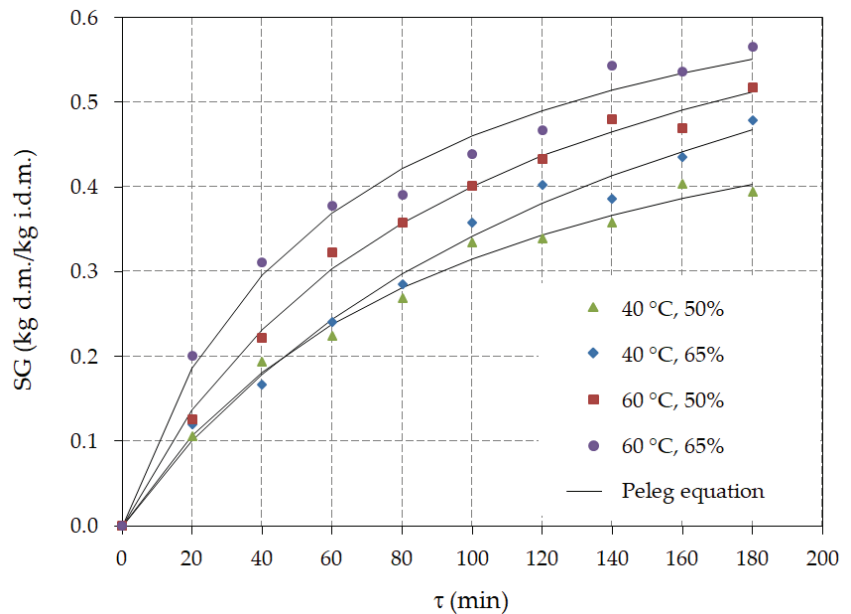


Figure 2. Solid gain (SG) during the osmotic dehydration process (process predicted based on Equation (7)).

The ANOVA results (Table 2) confirmed the significance of temperature and osmotic agent concentration for SG. Statistically, temperature was more significant, while the interaction of factors was statistically less significant. The average volume of apricot halves before the OD process was $27.58 \pm 5.71 \text{ cm}^3$. The highest decrease in volume, a value of 0.331, was observed in the samples that were treated at the highest temperature and osmotic agent concentration, followed by the values of 0.238 (40 °C, 65%) and 0.205 (60 °C, 55%), and the smallest decrease in volume was 0.157 (40 °C, 50%). The results of ANOVA (Table 2) showed that the factors are statistically significant, as well as their mutual interaction.

The volumetric shrinkage of apricot halves was approximately linear with the duration of the OD process (Supplementary Figure S2). The measured dimensions confirmed uneven shrinkage of apricot halves (Supplementary Table S1). The ANOVA results confirmed the significance of temperature and osmotic agent concentration for shrinkage. The largest shrinkage occurred in thickness ($S_{L3} = 0.226$), then width ($S_{L2} = 0.141$), and the smallest shrinkage was in length ($S_{L1} = 0.134$).

The mathematical modeling of each process allowed us to calculate the values of the required parameters for any observed time. Table 3 shows the results of osmotic dehydration constants of the Peleg model for WL and SG, as well as the results of statistical analysis of OD modeling. In general, the Peleg model with calculated drying constants shows good fitting with experimental data; R^2 is in the range of 0.9872–0.9985, and CRV is between 1.827 and 6.372%.

For WL models, the values of the Peleg model constants, k_{w1} and k_{w2} decrease with higher temperature, while higher osmotic agent concentration k_{w1} shows no dependence and the k_{w2} decreases. When modeling SG, the constants k_{s1} and k_{s2} decrease with increasing temperature, and the dependence was not determined with different concentrations. Fitting the WL with Equation (6) is shown in Figure 1, and SG with Equation (7) in Figure 2.

Table 3. Parameters of mathematical modeling used for the description of changes in WL (k_{w1} , k_{w2}) and SG (k_{s1} , k_{s2}) with statistical analysis.

Parameter	¹ t	C	k_{w1} or s_1	k_{w2} or s_2	R ²	RMSE	χ^2	CRV
WL	40	50	11.544	0.200	0.9955	0.0767	0.0073	3.258
		65	13.0325	0.1597	0.9937	0.0153	0.0135	4.055
	60	50	8.5438	0.1724	0.9985	0.0527	0.0034	1.827
		65	6.0601	0.1646	0.9916	0.1369	0.0234	4.188
SG	40	50	155.82	1.6133	0.9916	0.0114	0.0001	5.195
		65	176.64	1.1571	0.9889	0.0153	0.0002	6.372
	60	50	120.99	1.2826	0.9948	0.0115	0.0001	4.113
		65	80.298	1.3699	0.9872	0.0188	0.0044	5.851

¹ t (°C)—temperature of osmotic solution. C (%)—concentration of the osmotic agent. k_{w1} (min kg d.m./kg H₂O), k_{w2} (kg d.m./kg H₂O)—model constants for WL. k_{s1} (min kg i.d.m./kg d.m.), k_{s2} (kg d.m. initial/kg d.m.)—model constants for SG. CRV (%)—coefficient residual variation. WL—water loss. SG—solid gain.

Table 4 shows the values of diffusion coefficient of water (D_{ew}) and solute (D_{es}) calculated with Fick's model (Equations (10)–(13)). The D_{ew} values range from 5.50×10^{-9} m²/s to 7.387×10^{-9} m²/s. The coefficients of determination (R²) have values >0.9. The values of D_{es} range from 8.315×10^{-10} m²/s to 1.113×10^{-9} m²/s, and R² is within a range of 0.8831–0.9527. Higher temperature and osmotic agent concentration caused higher values of water and solute diffusivity.

Table 4. Water and solute diffusivities during osmotic dehydration calculated by Fick's model.

Osmotic Solution		Water Loss			Solid Gain		
¹ t (°C)	C (%)	D_{ew} (m ² /s)	R ²	WL _{eq} (kg H ₂ O/kg d.m.)	D_{es} (m ² /s)	R ²	SG _{eq} (kg d.m./kg i.d.m.)
40	50	5.500×10^{-9}	0.9337	7.11 ± 0.17	8.315×10^{-10}	0.9165	0.476 ± 0.051
	65	6.149×10^{-9}	0.9675	7.75 ± 0.36	1.00×10^{-9}	0.9527	0.593 ± 0.036
60	50	6.728×10^{-9}	0.9144	7.47 ± 0.21	1.076×10^{-9}	0.9131	0.562 ± 0.017
	65	7.387×10^{-9}	0.9183	7.93 ± 0.14	1.113×10^{-9}	0.8831	0.783 ± 0.044

¹ t—temperature of osmotic solution. C—concentration of the osmotic agent. D_{ew} —coefficient effective diffusivity of water. D_{es} —coefficient effective diffusivity of solute. WL_{eq}—water loss at equilibrium. SG_{eq}—solid gain at equilibrium.

3.2. Hot Air Drying

The moisture content of apricot halves in the control group was 8.295 kg H₂O/kg d.m. at the beginning of the drying process ($\tau = 0$ min), and in osmotically dehydrated samples it was 4.108 kg H₂O/kg d.m. (OD1) and 3.148 kg H₂O/kg d.m. (OD2). It was noticed that with increased air temperature and air velocity, the drying process was more intense for all experimental units. At the end of the hot air drying process, at $\tau = 1380$ min, the lowest recorded level of moisture content was achieved in the control sample 0.0751 kg H₂O/kg d.m. (60 °C, 1.5 m/s), as well as the smallest decrease in the moisture content, 1.050 kg H₂O/kg d.m. (40 °C, 1.0 m/s). In osmotically dehydrated samples, final moisture content in the range of 0.129–0.729 kg H₂O/kg d.m. (OD1) and 0.256–0.764 (OD2) was recorded (Supplementary Figures S3 and S4).

The hot air drying kinetics of untreated, OD1-treated and OD2-treated apricot halves are shown in the form of moisture ratio (MR) in Figures 3–5, respectively. The control sample (Figure 3) achieved the set equilibrium moisture ratio values at an air temperature of 60 °C and air velocity of 1.5 m/s for $\tau = 1230$ min. At the end of the process, at the same temperature and lower air velocity, 1.0 m/s, the sample needed only 1.2% of moisture ratio to reach the equilibrium value of the moisture content.

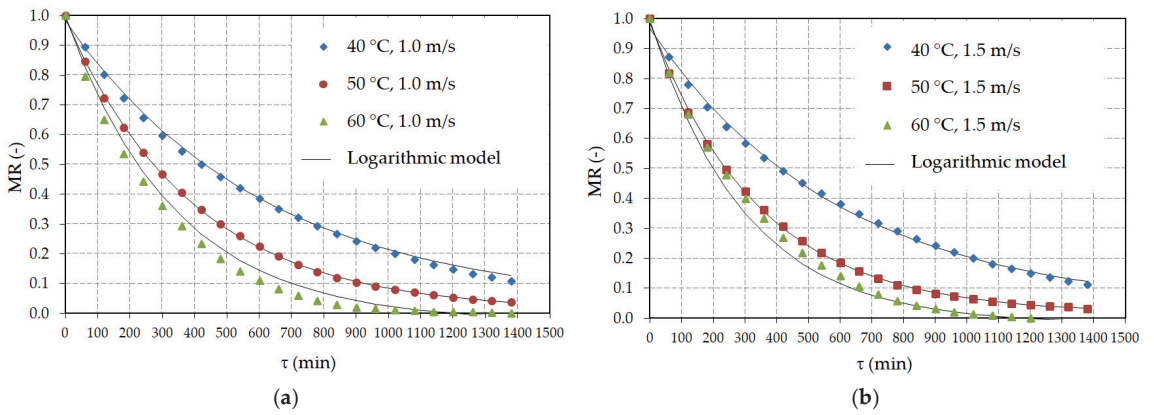


Figure 3. Drying curves of the hot air drying process of the control group (fresh apricot halves): (a) air velocity 1.0 m/s, (b) air velocity 1.5 m/s.

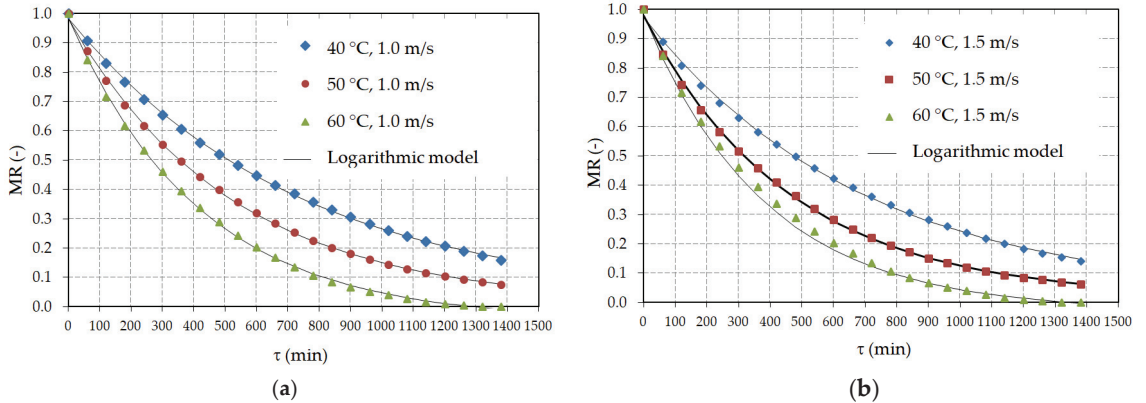


Figure 4. Drying curves of the hot air drying process of the apricot halves with osmotic pretreatment OD1 (40 °C, 50%): (a) air velocity 1.0 m/s, (b) air velocity 1.5 m/s.

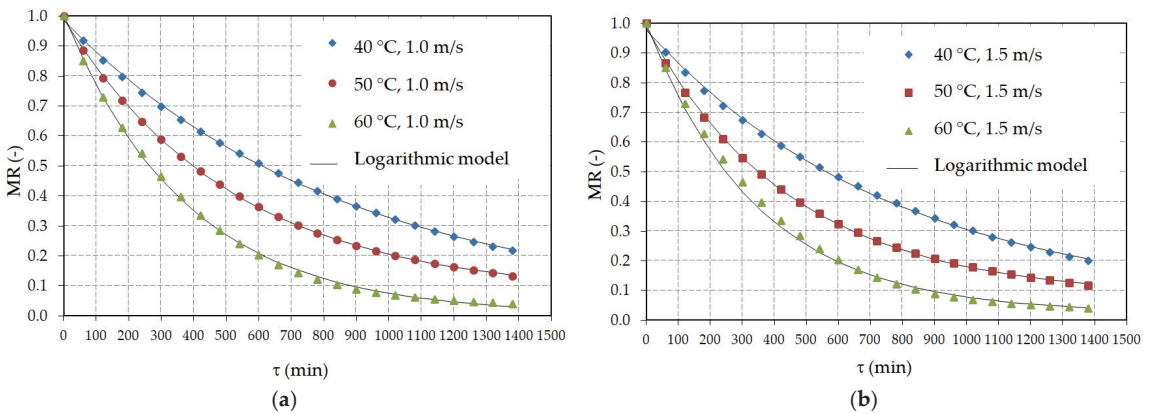


Figure 5. Drying curves of the hot air drying process of the apricot halves with osmotic pretreatment OD2 (60 °C, 65%): (a) air velocity 1.0 m/s, (b) air velocity 1.5 m/s.

Air temperature increase from 40 °C to 60 °C accelerates the drying process in the range of 11.72–17.70% in all experimental units. A particularly evident effect of air temperature on the drying speed was observed in osmotically dehydrated samples. As for the samples treated with OD2, increased air temperature reduced the water content from 15.38–17.70%, and for OD1, 13.34–15.82%. In the control group, the increase in temperature affected the rate of reaching the equilibrium moisture content of $\approx 11.72\%$.

Increased air velocity, from 1.0 to 1.5 m/s, accelerated the drying process by 0.41–1.80% for all experimental units. A slightly higher effect of air velocity on the drying rate was observed in osmotically-treated samples compared to the control group: 0.67–1.80% for OD1, 0.7–1.61% for OD2, and 0.41% for the control group.

Osmotic pretreatment slowed down the drying process of apricot halves. At the end of the hot air drying process, OD samples had smaller reduction in MR compared to the control group: 3.91–9.9% for OD2, and 0.07–4.04% for OD1. More pronounced slowing of the drying process was observed in the samples with OD2 pretreatment.

The decrease in shrinkage (S_v) of apricot halves was in the range of 0.628–0.903. The OD apricot halves exerted less shrinkage compared to the control group, 0.628–0.765 and 0.804–0.903, respectively. Shrinkage in size (S_{L1} , S_{L2} , S_{L3}) corresponds to the trend of S_v . It was observed that apricot halves shrank most in their width (S_{L3}), and least in the length (S_{L1}). It can be concluded that the drying air velocity is not statistically significant for shrinkage (Supplementary Table S2).

The influence of OD on the drying rate for the HAD process is shown in Figure 6 for the selected process parameters. With the same moisture content values, the most intensive drying rate was achieved with the control sample.

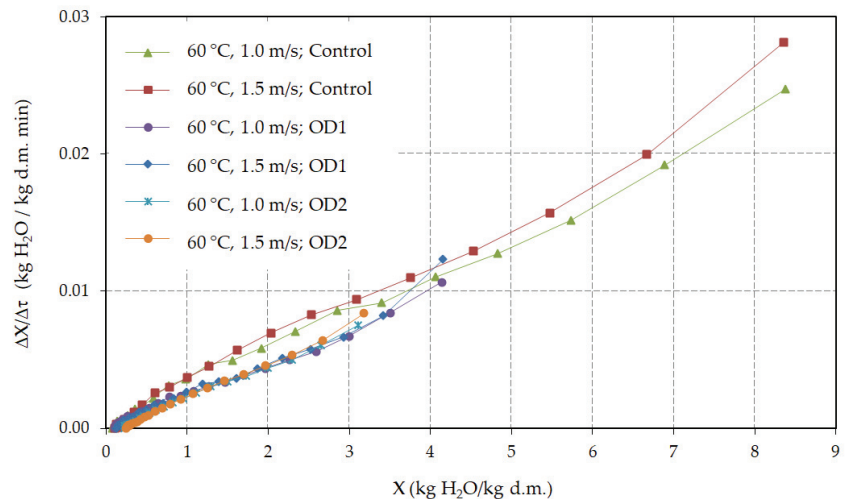


Figure 6. Drying rate of apricot halves during HAD for the air temperature of 60 °C; 1.0 and 1.5 m/s air velocity.

Drying speed for apricot halves with OD1 and OD2 pretreatments was approximately the same up to moisture content of ≈ 1.0 kg H₂O/kg d.m. ($\tau \approx 600$ min). However, in the later drying stage, the speed decreased in OD2 compared to OD1. The influence of air velocity on the drying kinetics was more pronounced in the control sample than in OD1 and OD2 up to a moisture content level of ≈ 1.0 kg H₂O/kg d.m., after which this influence was insignificant.

Figure 7 shows the temperatures of apricot halves (t_m) measured at a depth of ≈ 5 mm from the upper surface and for the selected HAD process parameters. There was a difference between temperature of the control and both OD1 and OD2 treated samples, even with the same material moisture content of the samples. Higher inner temperatures were achieved with the control sample. Temperature differences decreased as the moisture content reached equilibrium. Increased air velocity caused faster heating of the apricot halves.

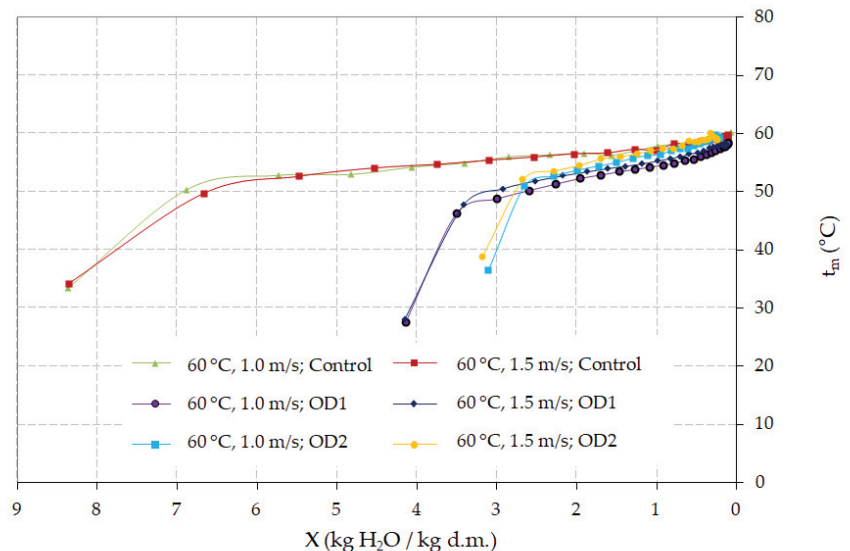


Figure 7. Temperature of apricot halves during HAD at 60 °C; 1.0 and 1.5 m/s air velocity.

The results of regression analysis of the ten studied models used to describe the kinetics of hot air drying of apricot halves with osmotic pretreatment, and the control group are summarized in Table 5 and Table S3. The analysis of results shows that all applied models have a good fit of the experimental results. The coefficient of determination (R^2) for all drying regimes is in the range from 0.9895–0.9999. The mean-square error (RMSE) and the values of the reduced test (χ^2) are small, 0.00119–0.02502, and 0.000002 and 0.00068, respectively. Additionally, the values of the coefficient of residual variation (CRV) are small for all regimes, 0.26–7.87%. The drying kinetics was, for standardization reasons, modeled with the logarithmic model, which gives the best overall results. For all experimental units, the logarithmic model gave results for the coefficient of determination (R^2) in the range of 0.9981–0.9999, a maximum mean-square error (RMSE) of 0.0108, and a reduced test of 0.00013 (Table 5).

In a few experiments had slightly better matching values that were obtained by using the Diffusion Approach and Page models. The coefficients of logarithmic model are given in Table 6, and other evaluated models are presented in Table S4 (Supplementary File, Tables S4–S12).

The results of effective moisture diffusivity (D_{eff}) of the apricot halves during the HAD process are shown in Table 7 together with the coefficient of determination (R^2), from 3.002×10^{-10} to 1.970×10^{-90} m^2/s and from 0.887 to 0.999, respectively. It can be concluded that the highest values of effective moisture diffusivity were achieved by the control samples, followed by the OD1 pretreated samples, and finally, the lowest value was recorded for OD2 ones. An increase in the value of the effective diffusivity of moisture was observed in all experimental units when the temperature and air velocity increased. The air temperature had a greater influence than air velocity on the increase in D_{eff} values.

Osmotic pretreatment influenced the decrease of D_{eff} values: higher values of osmotic dehydration, temperature, and concentration of the osmotic agent caused D_{eff} to decrease.

Table 5. Statistical analysis of logarithmic model used to describe the kinetics of hot air drying of fresh and osmotically-pretreated apricot halves.

Model	Pretreatment	Air Velocity (m/s)	Air Temperature (°C)	R ²	RMSE	χ^2	CRV (%)
Logarithmic	Control	1.0	40	0.9991	0.0073	0.00006	1.8987
			50	0.9998	0.0040	0.00002	1.4648
			60	0.9994	0.0071	0.00006	3.2927
		1.5	40	0.9981	0.0108	0.00013	2.8735
			50	0.9996	0.0055	0.00003	2.2259
			60	0.9991	0.0083	0.00008	4.2288
	OD1 ¹	1.0	40	0.9995	0.0053	0.00003	1.2226
			50	0.9996	0.0051	0.00003	1.5199
			60	0.9995	0.0062	0.00004	2.4909
		1.5	40	0.9989	0.0081	0.00008	1.9853
			50	0.9993	0.0070	0.00006	2.2776
			60	0.9992	0.0078	0.00007	3.2759
OD2	1.0	40	0.9996	0.0044	0.00002	0.9191	
		50	0.9999	0.0028	0.00001	0.7534	
		60	0.9994	0.0065	0.00005	2.4677	
	1.5	40	0.9991	0.0067	0.00005	1.4597	
		50	0.9997	0.0044	0.00002	1.2701	
		60	0.9997	0.0045	0.00002	1.7620	

OD1¹—Osmotic dehydration at temperature 40 °C and agent concentration 50%. OD2—Osmotic dehydration at temperature 60 °C and agent concentration 65%. R²—Determination coefficient, RMSE—Root mean square error, χ^2 —Reduced chi-squared, CRV—Coefficient residual variation.

Table 6. The coefficients of Logarithmic model used to describe the kinetics of hot air drying of fresh and osmotically-pretreated apricot halves.

Model	Pretreatment	Air Velocity (m/s)	Air Temperature (°C)	a ¹ (–)	b (–)	k (min ^{–1})
Logarithmic	Control	1.0	40	0.9558	0.0256	0.0016
			50	0.9828	0.0070	0.0025
			60	1.0250	–0.0287	0.0030
		1.5	40	0.9360	0.0313	0.0017
			50	0.9696	0.0155	0.0029
			60	1.0135	–0.0193	0.0034
	OD1	1.0	40	0.9649	0.0192	0.0014
			50	0.9747	0.0094	0.0019
			60	1.0349	–0.0474	0.0024
		1.5	40	0.9557	0.0178	0.0014
			50	0.9624	0.0146	0.0022
			60	1.0122	–0.0297	0.0026
OD2	1.0	40	0.9576	0.0279	0.0012	
		50	0.9193	0.0715	0.0019	
		60	0.9985	0.0050	0.0027	
	1.5	40	0.9268	0.0507	0.0013	
		50	0.9060	0.0797	0.0022	
		60	0.9756	0.0236	0.0029	

¹ a, b—Coefficients of the equation; k—Drying constant. OD1—Osmotic dehydration at temperature 40 °C and agent concentration 50%. OD2—Osmotic dehydration at temperature 60 °C and agent concentration 65%.

Table 7. The effective moisture diffusivity coefficients during hot air drying calculated by Fick's model.

Pretreatment	Air Velocity (m/s)	Air Temperature (°C)	D_{eff}^1 (m ² /s)	R ²
Control	1.0	40	5.431×10^{-10}	0.999
		50	8.933×10^{-10}	0.998
		60	1.585×10^{-9}	0.957
	1.5	40	5.984×10^{-10}	0.999
		50	9.328×10^{-10}	0.994
		60	1.970×10^{-9}	0.988
OD1	1.0	40	4.028×10^{-10}	0.999
		50	5.662×10^{-10}	0.999
		60	1.065×10^{-9}	0.887
	1.5	40	4.304×10^{-10}	0.999
		50	6.103×10^{-10}	0.999
		60	1.262×10^{-9}	0.987
OD2	1.0	40	3.002×10^{-10}	0.999
		50	4.198×10^{-10}	0.994
		60	6.777×10^{-10}	0.991
	1.5	40	3.019×10^{-10}	0.999
		50	4.513×10^{-10}	0.990
		60	7.259×10^{-10}	0.983

D_{eff}^1 —effective moisture diffusivity coefficients. OD1—Osmotic dehydration at temperature 40 °C and agent concentration 50%. OD2—Osmotic dehydration at temperature 60 °C and agent concentration 65%.

The activation energy for all experimental units is in the range of 35.216 kJ/mol to 51.514 kJ/mol (Table 8). Osmotic pretreatment lowered the activation energy value with respect to the control sample. Additionally, greater air velocity intensified the drying process, which led to higher activation energy.

Table 8. The activation energy for the apricot halves during the HAD process.

Pretreatment	Air Velocity (m/s)	E_a^1 (kJ/mol)	R ²
Control	1.0	46.379	0.996
	1.5	51.514	0.973
OD1	1.0	42.005	0.953
	1.5	46.469	0.974
OD2	1.0	35.216	0.985
	1.5	37.987	0.995

E_a^1 —activation energy. OD1—Osmotic dehydration at temperature 40 °C and agent concentration 50%. OD2—Osmotic dehydration at temperature 60 °C and agent concentration 65%.

4. Discussion

Increased temperatures and concentrations of the osmotic solution resulted in higher water loss and solid gain in the apricot halves. In fact, an increase in the solution concentration cause a rise in osmotic pressure, while an increase in the temperature of the osmotic agent can affected the permeability of the cell wall and the viscosity of water and osmotic agent, thus enabling water to pass more easily through the cell tissue and the agent to penetrate more easily into the apricot halves [15,16,25,45,46]. The measured values of WL and SG are in accordance with the results of other authors for the osmotic drying of apricot slices [25], apricot cubes [24], and apple cubes [30]. The results of the statistical analysis (Table 2) prove the influence of both factors on the rate of mass transfer,

but the temperatures of the osmotic agent gave a more significant difference. Khoyi and Hesari [25] points out that, for the mass transfer rate, the agent's temperature is statistically more significant than the concentration, when drying apricot slices in sucrose solution at a temperature from 30–60 °C and the concentration of 50–70%. Togrul and Ispir [46] came to the same conclusion when drying melon cubes.

The choice of process parameters depends on the WL/SG ratio (Table 2). Their ratio is chosen according to the desired characteristics of the finished product. In order to produce dried fruit with minimal addition of sugar, the most favorable ratio of the said process parameters for osmotic dehydration of apricot halves is 40 °C and 50% (WL/SG = 9.711). Khoyi and Hesari [25] recommend 50 °C temperature and 60% concentration for apricot slices drying due to high WL and low SG. They also point out better solution viscosity, lower production costs and less technical problems at the plant.

The calculated values of the effective diffusivity of water D_{ew} and solute D_{es} (Table 4), for WL and SG, are in agreement with the results of other authors who osmotically dehydrated the fruit in sucrose solution, at a similar range of temperatures and osmotic agent concentrations. The authors recorded the following values: apricot slices [25]: 0.61×10^{-10} – 4.06×10^{-10} m²/s for WL and 7.69×10^{-9} – 3.13×10^{-9} m²/s for SG; apricot halves [24]: 0.751×10^{-10} – 1.25×10^{-10} m²/s for WL and 0.69×10^{-10} – 1.21×10^{-9} m²/s for SG; apple cubes [30]: 1.98×10^{-10} – 2.48×10^{-9} m²/s for WL and 2.340×10^{-10} – 1.228×10^{-10} m²/s for SG; melon cubes [46]: 1.11×10^{-10} – 3.10×10^{-9} m²/s for WL and 1.02×10^{-10} – 2.46×10^{-10} m²/s for SG.

The greatest volumetric shrinkage was recorded in the samples dried at a temperature of 60 °C and osmotic agent concentration of 65%. The measured dimensions confirmed uneven shrinkage of apricot halves (Supplementary Table S1). The largest shrinkage occurred in thickness, then width, and the smallest shrinkage was observed in length. Figure 8 shows a cross-section of an apricot half with changes in size and mass transfer during OD. The solid and dotted lines indicate the dimensions before and after the OD process, respectively. As already mentioned, the intensity of WL and SG depends on the state of the cell wall [15,16,25,46]. When the apricot fruit was cut and stone removed, surfaces $F_{(1)}$ and $F_{(2)}$ were formed. The surface $F_{(1)}$ was with the damaged mesocarp tissue due to cutting, so the cells were more permeable for water and agent molecules. The surface $F_{(2)}$ consists of parenchyma cells and the cell wall is semi-permeable [47]. The $F_{(3)}$ surface contains cells of the epidermal tissue whose natural role is to protect the fruit from external influences. Uneven shrinkage in size ($S_{L1(0-\tau)} < S_{L2(0-\tau)} < S_{L3(0-\tau)}$) was a consequence of uneven water loss on the observed surfaces. The largest loss was marked on $F_{(1)}$, then $F_{(2)}$, and the smallest loss was on $F_{(3)}$, $WL_{(1)} > WL_{(2)} > WL_{(3)}$. Additionally, SG had the same trend: $SG_{(1)} > SG_{(2)} > SG_{(3)}$. Similar results have been reported by other researchers who discovered that the shrinkage was more pronounced in the cells that were closer to the surface of mass transfer and whose cell wall structure changed than inside the tissue [15,48–51].

The Peleg model was chosen to predict osmotic dehydration. High coefficients of determination (R^2) were obtained for both WL and SG, but the values were higher for WL due to the greater variability of experimental data in SG (Table 3). This was also reflected in higher values of the prediction error indicator (χ^2) of RMSE and CRV. Good matching of the data obtained with the Peleg model for the prediction of osmotic drying was also reported by other authors, for apricot slices [25], apple cubes [30], and melon cubes [46].

The drying rate was the highest for the control sample due to the difference in initial moisture content and the presence of osmotic agent in the treated samples (Figures 6, S3 and S4, Supplementary File). The figure (Figure 6) shows that the drying rate was not constant, and the speed was decreasing throughout the process. This indicates a dominant physical-mechanical diffusion of water in the fruit [22]. After OD1 lasting for 180 min, the moisture content in samples was 4.108 kg H₂O/kg d.m., while the control sample developed this moisture content in 220 min at 60 °C and air velocity of 1.0 m/s. After OD2, the samples had a moisture content of 3.148 kg H₂O/kg d.m., and the control sample achieved this moisture content in 315 min at 60 °C and air velocity of 1.0 m/s.

This means that osmotic dehydration had higher drying rate in the first 180 min of the process compared to HAD. The duration of the HAD process was affected more by higher temperature than air velocity. The results of other authors confirm this conclusion [22,52].

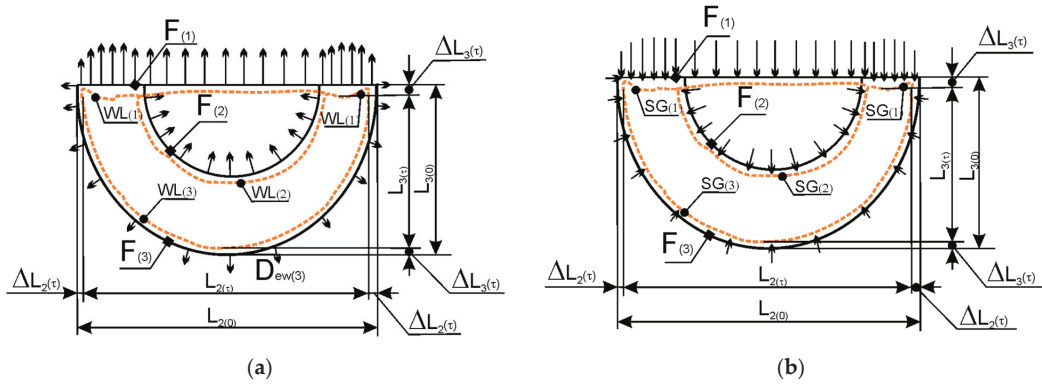


Figure 8. Cross-section of the apricot halves with shrinkage and mass transfer during osmotic dehydration: (a) Water loss (WL); (b) Solid gain (SG). $F_{(1)}$ —Surface after cutting; $F_{(2)}$ —Surface after the stone was removed; $F_{(3)}$ —Surface; $L_{2(0)}$, $L_{2(\tau)}$ —Width of apricot half at the beginning of process and at time τ ; $L_{3(0)}$, $L_{3(\tau)}$ —Thickness of apricot half at the beginning of process and at time τ ; $WL_{(1)}$, $WL_{(2)}$, $WL_{(3)}$ —Water loss through surfaces $F_{(1)}$, $F_{(2)}$, $F_{(3)}$; $SG_{(1)}$, $SG_{(2)}$, $SG_{(3)}$ —solid gain through surfaces $F_{(1)}$, $F_{(2)}$, $F_{(3)}$; Δ —difference; \rightarrow direction of water and solute diffusion, ----—dash line dimensions after OD.

The shrinkage measurement after HAD confirmed greater shrinkage of apricot halves in the control group compared to the osmotically-dehydrated samples (Table S2, Supplementary File). The authors [26,48] reported a positive effect of osmotic pretreatment on apple slices shrinkage; the treated samples shrank less than the control group after HAD. Figure 9 shows a cross-section of the apricot half with changes in size and mass transfer. The solid line shows the dimensions of the halves before HAD, and the dotted line shows dimensions after drying.

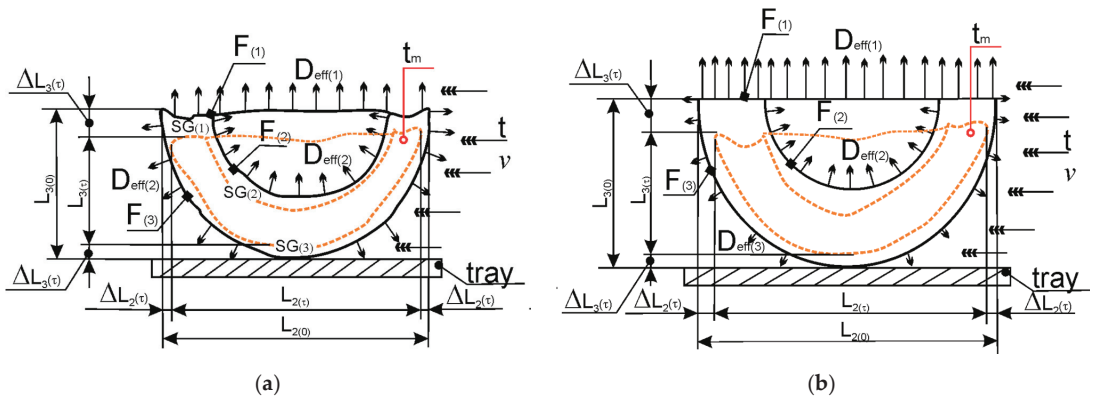


Figure 9. Cross-section of the apricot halves with shrinkage and mass transfer during HAD: (a) with OD pretreatment, (b) Control group. $F_{(1)}$ —Surface after cutting; $F_{(2)}$ —surface after the stone was removed; $F_{(3)}$ —Surface; $L_{2(0)}$, $L_{2(\tau)}$ —Width of apricot half at the beginning of the process and at time τ ; $L_{3(0)}$, $L_{3(\tau)}$ —Thickness of apricot half at the beginning of the process and at time τ ; $D_{eff(1)}$, $D_{eff(2)}$, $D_{eff(3)}$ —diffusion of water through surfaces $F_{(1)}$, $F_{(2)}$, $F_{(3)}$; Δ —difference; ----—dash line, dimensions after HAD; t_m —the temperature of apricot halves at a depth of 5 mm; t —hot air, v —air velocity; \leftarrow —airflow flow direction; \rightarrow direction of water diffusion on surfaces $F_{(1)}$, $F_{(2)}$, $F_{(3)}$.

During the HAD process, the transfer of moisture from the surface of apricot halves into the air and the diffusion of water molecules through the tissue and towards the transfer surface was more intense in the control sample (Figures 6 and 8b). The layers of cells that make up the surface $F_{(1)}$ had the highest transfer of moisture into the air, followed by the surface $F_{(2)}$, and the slowest transfer of moisture was from the surface $F_{(3)}$. In the control sample, at the beginning of the HAD process, due to the increased moisture content that was capillary bound, the evaporation process took place on the surfaces $F_{(1)}$, $F_{(2)}$, and $F_{(3)}$; during the evaporation process, it moved towards the interior of the apricot half. The layers of tissue cells that were closer to the surface were drier than the layers that were further away; the temperature of the material increased (Figure 7), and the volume decreased. The fast transition of the evaporation area towards the center caused the outer layers to dry out and the inner layers of the cells to be wetter, so an uneven field of moisture was formed in the material. Different moisture content between the cell layers that were made of surfaces $F_{(1)}$, $F_{(2)}$, and $F_{(3)}$ influenced the measured shrinkage intensity ($S_{L3(0-\tau)} > S_{L2(0-\tau)} > S_{L1(0-\tau)}$). Internal stresses were formed between the layers and greater deformation of the initial shape was observed in the control sample compared to the OD samples (Supplementary Table S2). More uniform drying of surfaces $F_{(1)}$, $F_{(2)}$, and $F_{(3)}$ was achieved in apricot halves pretreated with OD due to the presence of osmotic agent molecules in the tissue, in the order as follows $SG_{(1)} > SG_{(2)} > SG_{(3)}$ (Figure 8b). At the beginning of drying of OD samples, the halves that were smaller in size provided a shorter path for the diffusion of water molecules, which also affected the formation of a homogeneous moisture field inside the half. Consequently, the tissue temperature at a depth of 5 mm increased more slowly in the samples treated with OD compared to the control sample (Figure 7). The same results of temperature measuring were reported by the authors for drying apricots [22] and banana slices [53]. Over drying of surface layers was less pronounced in OD samples. The lower temperature of the material is a consequence of the heat consumption to break the newly formed bonds between the dry matter, osmotic agent, and moisture in the apricot tissue. This forms the moisture bound by adsorption whose higher share reduces the value of water activity [54].

Some semi-theoretical drying models that have been commonly used to describe the slow drying time in the literature are Newton, the Henderson and Pabis, the logarithmic, the Page model, and others (Table 1). These models are generally derived by simplifying general series solutions of Fick's second law and considering a direct relationship between the average water content and drying time [55–58]. They neglect the fundamentals of the drying process and their parameters have no physical meaning. The logarithmic model gives the highest values of R^2 and lowest of χ^2 , RMSE, and CRV (Table 5 and Supplementary File Table S3). It is also observed that the consistency of fitting the drying data into the model is very good for all of the experimental drying air conditions. Thus, the model can be assumed to represent the drying behavior of fresh and osmotically-treated apricot halves. The logarithmic model also describes the air drying curve of whole apricot [22] with a correlation coefficient of 0.991.

Within the scope of applied pretreatments, temperature, and drying air velocity, the calculated effective diffusion coefficient (D_{eff}) includes water diffusion in the tissue and external convective moisture transfer. The values obtained for all pretreatments, temperatures, and air velocities are given in Table 7. As the air temperature and velocity increased, the value of the effective diffusivity of water also increased. Osmotic pretreatment influences the reduction of the effective diffusion coefficient. The calculated effective water diffusion coefficients are in the range of the values reported by other authors. The diffusion coefficient for apricot halves dried with hot air at temperatures of 30–90 °C was 2.7×10^{-10} – 10.2×10^{-10} m²/s [44], for apricot halves without OD it was 1.47×10^{-9} – 6.56×10^{-9} m²/s, for whole apricot fruit, at 50–80 °C, it was 4.76×10^{-9} – 8.32×10^{-9} m²/s [22].

The calculated activation energy values (E_a) (Table 8) indicate the sensitivity of the effective water diffusion coefficient to the selected air temperature range. Increased air

velocity caused the value of E_a to increase as well. Osmotic pretreatment lowered the value of E_a , which may be an indication that the solute in the cells bound to water molecules, so energy is then needed to break these bonds. The E_a values obtained in this study are in the range of values obtained by other authors for HAD fruit 20.0–46.278 kJ/mol [22,44,57].

5. Conclusions

The kinetics of osmotic drying of apricot halves, water loss, and solid gain, are described using the Peleg model with satisfactory accuracy. The most favorable ratio of water loss and solid gain is with the osmotic agent temperature of 40 °C in the concentration of 50%. Cutting the apricot fruit in half disturbs its cellular structure and the shrinkage is then most evident in thickness and less in length. Higher parameters of the osmotic drying process intensify the mass transfer. The kinetics of hot air drying was described using the logarithmic model that approximated the experimental data over the entire time range with satisfactory accuracy. The model proved to be useful for predicting the kinetics of hot air drying of the apricot halves both for those which had the osmotic pretreatment and for those that did not.

Osmotic pretreatment slows down the kinetics of convective drying, reduces the water diffusion coefficient and activation energy. Osmotically-treated apricot halves shrank less in volume, length, thickness, and width than the control sample, which resulted in a better quality of the final product. The most favorable combinations of parameters of osmotic dehydration and hot air drying are: the temperature of 40 °C and 50% concentration of the osmotic agent, the temperature of 60 °C and air velocity of 1.0 m/s. Future research should focus on the energy consumption in hot air drying technology and comparison between the apricot halves with and without the osmotic pretreatment.

Supplementary Materials: The following are available online at <https://www.mdpi.com/2227-9717/9/2/202/s1>, Figure S1. Drying curves of the apricot halves during the osmotic dehydration process, Figure S2. Shrinkage of apricot halves (S_v) during the osmotic dehydration process, Figure S3. Drying curves of hot air drying apricot halves for air velocity 1.0 m/s, Figure S4. Drying curves of hot air drying apricot halves for air velocity 1.5 m/s, Table S1. Mean values of shrinkage for osmotic dehydrated samples after 180 min of process, Table S2. Mean values of shrinkage for hot air dried samples after 1380 min of process, Table S3. Statistical analysis of models used to describe the kinetics of hot air drying of fresh (control) and osmotically-pretreated apricot halves, Table S4. The coefficients of Newton model used to describe the kinetics of hot air drying of fresh (control) and osmotically-pretreated apricot halves, Table S5. The coefficients of Page model used to describe the kinetics of hot air drying of fresh (control) and osmotically-pretreated apricot halves, Table S6. The coefficients of Modified Page model used to describe the kinetics of hot air drying of fresh (control) and osmotically-pretreated apricot halves, Table S7. The coefficients of Henderson and Pabis model used to describe the kinetics of hot air drying of fresh (control) and osmotically-pretreated apricot halves, Table S8. The coefficients of Modified Henderson and Pabis model used to describe the kinetics of hot air drying of fresh (control) and osmotically-pretreated apricot halves, Table S9. The coefficients of Verma model used to describe the kinetics of hot air drying of fresh (control) and osmotically-pretreated apricot halves, Table S10. The coefficients of Two Term model used to describe the kinetics of hot air drying of fresh (control) and osmotically-pretreated apricot halves, Table S11. The coefficients of Two Term Exponential model used to describe the kinetics of hot air drying of fresh (control) and osmotically-pretreated apricot halves, Table S12. The coefficients of Diffusion Approach model used to describe the kinetics of hot air drying of fresh (control) and osmotically-pretreated apricot halves.

Author Contributions: Conceptualization: I.P. and M.R.; methodology: I.P.; contributions to sample and analysis experiments: I.P., M.R., Z.S., K.K., and O.P.; software: Z.S.; validation: U.T., and P.S.; investigation: A.S.; resources: A.S.; data curation: Z.S. and K.K.; writing—original draft preparation: I.P., M.R., Z.S., U.T., and P.S.; writing—review and editing: I.P., M.R., and P.S.; visualization: K.K.; supervision: M.R., P.S., and U.T.; project administration: Z.S. All authors have read and agreed to the published version of the manuscript.

Funding: This research was funded by Ministry of Education, Science and Technology, Republic of Serbia, grant number 451-03-68/2020-14/200125.

Institutional Review Board Statement: Not applicable.

Informed Consent Statement: Not applicable.

Data Availability Statement: The data presented in this study are available on request from the corresponding author. The data are not publicly available due to unpublished results.

Conflicts of Interest: The authors declare no conflict of interest.

References

- Miodragović, M.; Magazin, N.; Keserović, N.; Milić, B.; Popović, B.; Blagojević, B.; Klajdžić, J. The Early Performance and Fruit Properties of Apricot Cultivars Grafted on *Prunus spinosa* L. Interstock. *Sci. Hortic.* **2019**, *250*, 199–206. [CrossRef]
- Miodragović, M.; Keserović, Z.; Milić, B.; Dorić, M.; Magazin, N. Physical and Chemical Fruit Properties of Apricot Cultivars and Selections from Novi Sad within High-Density Growing System. *J. Pomol.* **2015**, *49*, 37–42. (In Serbian)
- Vukoje, V.; Pavkov, I.; Miljatić, A. Economic Aspects of Dried Fruit Production by Combined Technology. *Econ. Agric.* **2018**, *65*, 1031–1044. [CrossRef]
- Vukoje, V.; Pavkov, I. Analysis of Economic Justification of Drying of Apricots by Combined Technology. *J. Process. Energy Agric.* **2010**, *14*, 40–43. Available online: <https://scindeks-clanci.ceon.rs/data/pdf/1821-4487/2010/1821-44871001040V.pdf> (accessed on 17 November 2020).
- Keserović, Z.; Magazin, N.; Milić, B.; Igić, M.; Miodragović, M.; Kalajdžić, J. New Apricot Cultivar—“Buda”. *J. Pomol.* **2018**, *52*, 27–31.
- Karabulut, I.; Tugca, B.; Sislioglu, K.; Gokbulut, I.; Ozdemir, I.S.; Seyhan, F.; Ozturk, K. Chemical Composition of Apricots Affected by Fruit Size and Drying Methods. *Dry. Technol.* **2018**, *36*, 1937–1948. [CrossRef]
- Türkyılmaz, M.; Tağı, S.; Özkan, M. Changes in Chemical and Microbial Qualities of Dried Apricots Containing Sulphur Dioxide at Different Levels During Storage. *Food Bioprocess Technol.* **2013**, *6*, 1526–1538. [CrossRef]
- Sağırlı, F.; Tağı, S.; Özkan, M.; Yemiş, O. Chemical and Microbial Stability of High Moisture Dried Apricots During Storage. *J. Sci. Food Agric.* **2008**, *88*, 858–869. [CrossRef]
- Madrau, M.C.; Piscopo, A.; Sanguinetti, A.M.; Del Caro, A.; Poiana, M.; Romeo, F.V.; Piga, A. Effect of Drying Temperature on Polyphenolic Content and Antioxidant Activity of Apricots. *Eur. Food Res. Technol.* **2009**, *228*, 441–448. [CrossRef]
- Mir, M.A.; Hussain, P.R.; Fouzia, S.; Rather, A.H. Effect of Sulphiting and Drying Methods on Physico-Chemical and Sensorial Quality of Dried Apricots During Ambient Storage. *Int. J. Food Sci. Technol.* **2009**, *44*, 1157–1166. [CrossRef]
- Torreggiani, D.; Bertolo, G. Osmotic Pre-treatment in Fruit Processing: Chemical, Physical and Structural Effects. *J. Food Eng.* **2001**, *49*, 247–253. [CrossRef]
- Sakooei-Vayghan, R.; Peighambaroust, S.H.; Hesari, J.; Peressini, D. Effects of Osmotic Dehydration (with and without sonication) and Pectinbased Coating Pretreatments on Functional Properties and Color of Hot-Air Dried Apricot Cubes. *Food Chem.* **2020**, *311*, 125978. [CrossRef] [PubMed]
- Ispir, A.; Togrul, I.T. The Influence of Application of Pretreatment on the Osmotic Dehydration of Apricots. *J. Food Process. Preserv.* **2009**, *33*, 58–74. [CrossRef]
- Ciurzynska, A.; Kowalska, H.; Czajkowska, K.; Lenart, A. Osmotic Dehydration in Production of Sustainable and Healthy Food. *Trends Food Sci. Technol.* **2016**, *59*, 186–192. [CrossRef]
- Rastogi, N.K.; Niranjan, K. Enhanced Mass Transfer During Osmotic Dehydration of High Pressure Treated Pineapple. *J. Food Sci.* **1998**, *63*, 508–511. [CrossRef]
- Wiktor, A.; Sledz, M.; Nowacka, M.; Chudoba, T.; Witrowa-Rajchert, D. Pulsed Electric Field Pretreatment for Osmotic Dehydration of Apple Tissue: Experimental and Mathematical Modeling Studies. *Dry. Technol.* **2014**, *32*, 408–417. [CrossRef]
- Nowacka, M.; Wiktor, A.; Sledz, M.; Jurek, N.; Witrowa-Rajchert, D. Drying of Ultrasound Pretreated Apple and its Selected Physical Properties. *J. Food Eng.* **2012**, *113*, 427–433. [CrossRef]
- Vega-Galaves, A.; Uribe, E.; Perez, M.; Tabilo-Munizaga, G.; Vegara, J.; Garcia-Segovia, P.; Lara, E.; Di Scala, K. Effect of High Hydrostatic Pressure Pretreatment on Drying Kinetics, Antioxidant Activity, Firmness and Microstructure of Aloe Vera (*Aloe barbadensis* Miller) gel. *LWT* **2011**, *44*, 384–391. [CrossRef]
- Rodríguez, M.M.; Rodríguez, A.; Mascheroni, R.H. Color, Texture, Rehydration Ability and Phenolic Compounds of Plums Partially Osmodehydrated and Finish-Dried by Hot Air. *J. Food Process. Preserv.* **2015**, *39*, 2647–2662. [CrossRef]
- Riva, M.; Campolongo, S.; Leva, A.A.; Maestrelli, A.; Torreggiani, D. Structure–Property Relationships in Osmo-Air-Dehydrated Apricot Cubes. *Food Res. Int.* **2005**, *38*, 533–542. [CrossRef]
- Mrad, N.D.; Bonazzi, B.; Boudhrioua, N.; Kechaou, N.; Courtois, F. Influence of Sugar Composition on Water Sorption Isotherms and on Glass Transition in Apricots. *J. Food Eng.* **2012**, *111*, 403–411. [CrossRef]
- Kešelj, K.; Babić, M.; Pavkov, I.; Radojčin, M.; Stamenković, Z.; Tekić, D.; Ivanišević, M. Effects of Storage and Sulfurization with Sulfur Dioxide of Different Concentration on Changes in the Color of Cried Apricots. *J. Process. Energy Agric.* **2019**, *23*, 190–194. [CrossRef]

23. Pavkov, I.; Babić, L.; Babić, M. Mathematical Model of the Apricot Kinetic Osmotic Drying. *J. Process. Energy Agric.* **2007**, *11*, 98–101. (In Serbian). Available online: <https://scindeks.ceon.rs/article.aspx?artid=1450-50290703098P> (accessed on 7 December 2020).
24. Ispir, A.; Togrul, I.T. Osmotic Dehydration of Apricot: Kinetics and the Effect of Process Parameters. *Chem. Eng. Res. Des.* **2009**, *87*, 166–180. [CrossRef]
25. Khoyi, M.R.; Hesari, J. Osmotic Dehydration Kinetics of Apricot Using Sucrose Solution. *J. Food Eng.* **2007**, *78*, 1355–1360. [CrossRef]
26. Rahimi, J.; Singh, A.; Adewale, P.O.; Adedeji, A.A.; Ngadi, M.O.; Raghavan, V. Effect of Carboxymethyl Cellulose Coating and Osmotic Dehydration on Freeze Drying Kinetics of Apple Slice. *Foods* **2013**, *2*, 170–182. [CrossRef] [PubMed]
27. Pavkov, I.; Babić, L.; Babić, M.; Radojčin, M. Kinetics of the Combined Drying Technology of Pear Slice (Pyrus). *J. Process. Energy Agric.* **2009**, *13*, 111–116. Available online: <https://scindeks.ceon.rs/article.aspx?artid=1821-44871104217P> (accessed on 10 December 2020).
28. Mohsenin, N.N. *Physical Properties of Plant and Animal Materials*; Gordon and Breach Sci. Publ.: New York, NY, USA, 1986; pp. 23–25.
29. Radojčin, M.; Babić, M.; Pavkov, I.; Stamenković, Z. Osmotic Drying Effects on the Mass Transfer and Shrinkage of Quince tissue. *J. Process. Energy Agric.* **2015**, *19*, 113–119. Available online: <https://scindeks.ceon.rs/article.aspx?artid=1821-44871503113R> (accessed on 10 December 2020).
30. Assis, F.R.; Morais, R.M.S.C.; Morais, A.M.M.B. Mathematical Modeling of Osmotic Dehydration Kinetics of Apple Cubes. *J. Food Process. Preserv.* **2017**, *41*, 1–16. [CrossRef]
31. Lewis, W.K. The Rate of Drying of Solid Materials. *ACES* **1921**, *13*, 427–432. [CrossRef]
32. Page, C. Factors Influencing the Maximum Rates of Air Drying of Shelled Corn in Thin Layer. Master's Thesis, Purdue University, Lafayette, IN, USA, 1949. Unpublished work.
33. Overhults, D.G.; White, H.E.; Hamilton, H.E.; Ross, I.J. Drying Soybeans With Heated Air. *Trans. ASAE* **1973**, *16*, 112–113. [CrossRef]
34. Yagcioglu, A.; Degirmencioglu, A.; Cagatay, F. Drying Characteristics of Laurel Leaves Under Different Drying Conditions. In Proceedings of the 7th International Congress on Agricultural Mechanization and Energy, Adana, Turkey, 26–27 May 1999; pp. 565–569.
35. Henderson, S.M.; Pabis, S. Grain drying theory I. Temperature Effect on Drying Coefficient. *J. Agric. Eng. Res.* **1961**, *6*, 169–174.
36. Karathanos, V.T.; Belessiotis, V.G. Application of a Thin Layer Equation to Drying Data of Fresh and Semi-Dried Fruits. *J. Agric. Eng. Res.* **1999**, *74*, 355–361. [CrossRef]
37. Verma, L.R.A.; Bucklin, J.B.; Endan, F.T.W. Effects of Drying Air Parameters on Rice Drying Models. *Trans. ASABE* **1985**, *28*, 296–301. [CrossRef]
38. Henderson, S.M. Progress in Developing the Thin Layer Drying Equation. *Trans. ASABE* **1974**, *17*, 1167–1172. [CrossRef]
39. Yaldız, O.; Ertekin, C. Thin Layer Solar Drying Some Different Vegetables. *Dry. Technol.* **2001**, *19*, 583–596. [CrossRef]
40. Kassem, A.S. Comparative Studies on Thin Layer Drying Models for Wheat. In *Proceedings of the 13th International Congress on Agricultural Engineering, Rabat, Morocco, 2–6 February 1998*; Bartali, E.H., Ed.; ANAFIDE: Rabat, Morocco, 1998.
41. Crank, J. *Mathematics of Diffusion*, 2nd ed.; Clarendon Press: Oxford, UK, 1975; pp. 24–68.
42. Kayran, S.; Doymaz, I. Infrared Drying and Effective Moisture Diffusivity of Apricot Halves: Influence of Pretreatment and Infrared Power. *J. Food Process. Preserv.* **2017**, *41*, 1–8. [CrossRef]
43. Ruiz-Lopez, I.I.; Ruiz-Espinosa, H.; Luna-Guevara, M.L.; Garcia-Alvarado, M.A. Modeling and Simulation of Heat and Mass Transfer During Drying of Solids With Hemispherical Shell Geometry. *Comput. Chem. Eng.* **2011**, *35*, 191–199. [CrossRef]
44. Bon, J.; Simal, S.; Rossello, C.; Mulet, A. Drying Characteristic of Hemispherical Solids. *J. Food Eng.* **1997**, *34*, 109–122. [CrossRef]
45. Togrul, I.T.; Ispir, A. Effect on Effective Diffusion Coefficients and Investigation of Shrinkage During Osmotic Dehydration of Apricot. *Energy Convers. Manag.* **2007**, *48*, 2611–2621. [CrossRef]
46. Junior, J.L.B.; Mancini, M.C.; Hubinger, M.D. Mass Transfer Kinetics and Mathematical Modeling of the Osmotic Dehydration of Orange-Fleshed Honeydew Melon in Corn Syrup and Sucrose Solutions. *Int. J. Food Sci. Technol.* **2013**, *48*, 2463–2473. [CrossRef]
47. Archibald, R.; Melton, L. The Anatomy of the Fleshy Pericarp of Maturing Moorpac Apricots, *Prunus Armeniaca*. *N. Z. J. Bot.* **1987**, *25*, 181–184. [CrossRef]
48. Mandala, I.G.; Anagnostaras, E.F.; Oikonomou, C.K. Influence of Osmotic Dehydration Conditions on Apple Air Drying Kinetics and their Quality Characteristics. *J. Food Eng.* **2005**, *69*, 307–316. [CrossRef]
49. Barat, J.M.; Fito, P.; Chiralt, A. Modeling of Simultaneous Mass Transfer and Structural Changes in Fruit Tissues. *J. Food Eng.* **2001**, *49*, 77–85. [CrossRef]
50. Yang, J.; Di, Q.; Jiang, Q.; Zhao, J. Application of Pore Size Analyzers in Study of Chinese Angelica Slices Drying. *Dry. Technol.* **2010**, *28*, 214–221. [CrossRef]
51. Guine, R.P.F.; Castro, J.A.A.M. Pear Drying Process Analysis: Drying Rates and Evaluation of Water and Sugar Concentrations in Space and Time. *Dry. Technol.* **2002**, *20*, 1515–1526. [CrossRef]
52. Bozkir, O. Thin-layer Drying and Mathematical Modeling for Washed Dry Apricots. *J. Food Eng.* **2006**, *77*, 146–151. [CrossRef]
53. Sankat, C.K.; Castaigne, F.; Maharaj, R. The Air Drying Behaviour of Fresh and Osmotically Dehydrated Banana Slices. *Int. J. Food Sci. Technol.* **1996**, *3*, 123–135. [CrossRef]

54. Azoubel, P.M.; El-Aouar, A.A.; Tonon, R.V.; Kurozawa, L.M.; Graziella, C.A.; Murr, F.E.X.; Park, K.J. Effect of Osmotic Dehydration on the Drying Kinetics and Quality of Cashew Apple. *Int. J. Food Sci. Technol.* **2009**, *44*, 980–986. [CrossRef]
55. Igual, M.; Garcia-Martinez, E.; Martina-Espraza, M.E.; Martinez-Navarrete, N. Effect of Processing on the Drying Kinetics and Functional Value of Dried Apricot. *Food Res. Int.* **2012**, *47*, 284–290. [CrossRef]
56. Doymaz, I. Effect of Pre-treatments Using Potassium Metabisulphide and Alkaline Ethyl Oleate on the Drying Kinetics of Apricots. *Biosyst. Eng.* **2004**, *89*, 281–287. [CrossRef]
57. Bon, J.; Rossello, C.; Femenia, A.; Eim, V.; Simal, S. Mathematical Modeling of Drying Kinetics for Apricots: Influence of the External Resistance to Mass Transfer. *Dry. Technol.* **2007**, *25*, 1829–1835. [CrossRef]
58. Krzykowski, A.; Dziki, D.; Rudy, S.; Gawlik-Dziki, U.; Janiszewska-Turak, E.; Biernacka, B. Wild Strawberry *Fragaria vesca* L.: Kinetics of Fruit Drying and Quality Characteristics of the Dried Fruits. *Processes* **2020**, *8*, 1265. [CrossRef]

The Changes of Flavonoids in Honey during Storage

Goran Šarić ^{1,*}, Nada Vahčić ², Danijela Bursać Kovačević ² and Predrag Putnik ^{2,*}

¹ Department of Food Technology, Karlovac University of Applied Sciences, Trg J. J. Strossmayera 9, 47000 Karlovac, Croatia

² Faculty of Food Technology and Biotechnology, University of Zagreb, Pierottijeva 6, 10000 Zagreb, Croatia; nvahcic@pbf.hr (N.V.); dbursac@pbf.hr (D.B.K.)

* Correspondence: gsaric@vuka.hr (G.Š.); pputnik@alumni.uconn.edu (P.P.)

Received: 3 July 2020; Accepted: 31 July 2020; Published: 6 August 2020

Abstract: The purpose of this study was to determine the changes in the contents of flavonoids that were the most prevalent in acacia and multifloral honey during one year of storage. Samples were stored in transparent glass containers, at room temperature, on open shelves exposed to light during daytime. Eight individual flavonoids identified and quantified using HPLC-Diode Array Detector (DAD) belongs to three subgroups: flavonols (quercetin, luteolin, kaempferol and galangin), total flavanons (hesperetin and pinocembrin) and total flavones (apigenin and chrysin). Obtained results revealed that multifloral honey had more total flavonoids than acacia samples did. On average from all of the samples, multifloral honey had more of quercetin, hesperetin, luteolin, kaempferol and apigenin than acacia honey did. Content of flavonoids increased in samples between the 1st and 6th month of storage and then started to decrease until the 9th month, when they remained relatively constant all the way until the 12th month of storage. In conclusion, acacia and multifloral honey after one-year of storage still can be a valuable source of flavonoids.

Keywords: honey; flavonoids; storage; HPLC; marker; floral origin

1. Introduction

Chemically, honey is quite a complex mixture of more than 70 different compounds. Some of them are added by honeybees, some come from the nectar producing plants, while some during ripening of honey in honeycombs [1]. Despite the rapid development of various analytical methods, composition of honey is still not completely elucidated [2–4]. In some ways, this is not an issue as not knowing all the ingredients prevents artificial industrial production and adulterations. That way honey maintains its properties of a natural product, produced solely by the honeybees. Perhaps the most important property by which the chemical composition of honey can be described is variability hence there are virtually no two exactly the same honey samples. Different honey types, as well as honeys within those varieties, differ in their chemical composition depending on their botanical and geographical origins, climate conditions, honeybee breed and skillfulness of the beekeepers [5,6]. The most represented compounds in honey are water and carbohydrates, mostly fructose and glucose, which together make 99% of the honey. The rest includes proteins (including enzymes), minerals, vitamins, organic acids, phenolic compounds, volatile compounds (aroma substances) and various chlorophyll derivatives. Although the share of those compounds is very small, they are greatly responsible for sensory and nutritive properties of honey [7,8].

It was proven that honey has medicinal benefits and for centuries, or even millenniums, it was used as a sweetener (food) and a medicine. Until 1800s, honey was the only easily available sweetener used for human nutrition, when it was replaced with industrial made sugar. Over the last 20 years, a new branch of medicine was developed, called “apitherapy” that relies on medicines based on honey

and other bee products for different diseases. Today, for medicinal purposes, honey is mainly used to treat wounds, burns and infections [9].

Phenolic compounds are one of the numerous groups of compounds from honey where a large portion falls to flavonoids, mainly in the form of glycosides [10]. Usually detected flavonoids from honey originate from propolis, while pollen is not a good source of such compounds, as their content is quite low in there. Characteristic flavonoids found in propolis are chrysin, galangin, tektorizin, pinocembrin and pinobanksin. As flavonoids and other phenolic compounds come exclusively from plants, it is clear that their content will be defined by botanical origins of honey [9], however storage conditions also have an important effect [11].

There are several reports, which confirmed that phenolic and flavonoid profiles determined in investigated honey samples, as well as their antioxidant activities, could be used as markers for honey identification, mainly due to the prevalence of some specific compounds [12–14]. For instance, 52 Spanish honey samples from different botanical origins were analyzed with the aim to determine their botanical origins according to the flavonoid and phenolic acid contents. Additional to the other honey types, authors also analyzed seven acacia samples where they found 0.06–5.11 mg kg⁻¹ of quercetin, 2.30–18.69 mg kg⁻¹ of pinocembrin and 0.39–4.36 mg kg⁻¹ of chrysin, while luteolin (0.06–0.32 mg kg⁻¹) and kaempferol (0.35–0.37 mg kg⁻¹) were detected only in two of the samples [15]. Results from this study also showed that phenolic compounds are potential markers for the floral origins for some honey types (e.g., useful for the heather, chestnut, eucalyptus, rapeseed and lime-tree); while they cannot be used for others due to the absence of their floral specificity (e.g., lavender and acacia). Furthermore, Akbari et al. analyzed a total of 60 samples from 6 different types of honey with respect to phenolic acids and flavonoids. Here, the flavonol quercetin, p-coumaric acid, caffeic acid, flavone chrysin and flavanone hesperetin were detected in all honey samples. In acacia honey, authors found 22.54 ± 7.1 µg/100 g of chrysin and 8.04 ± 4.37 µg/100 g honey of hesperetin, while quercetin was not detected. Among all investigated types, jujube and thyme had the highest total flavonoid aglycone contents [14].

Although there are various papers associating the contents of different phenolic compounds in the honey samples with the floral origin [11,16,17], with over addressing the health benefits of phenolics [18], still there is scarcity of reports that deal with the stability and/or changes of the single flavonoids during prolonged storage. Honey is quite a stable food with the ability to stay unspoiled over longer time due to its high sugar and low water contents, however native flavonoid content may be degraded by the storage. Therefore, phenolics markers have limited usefulness as indicators for determining botanical origins of the samples, as honey is often stored for longer periods before consumption. Consequently, this study aimed to highlight the quality of the samples in terms of individual flavonoids during one year of storage.

2. Materials and Methods

2.1. Honey Samples

Twenty acacia and twenty multifloral honey samples ($n = 40$) from Varaždin county in Croatia were used in this study. Five different samples of each honey type were collected from each of the four regions of Varaždin County. They were stored for one year in transparent glass containers, at room temperature, on shelves exposed to indirect sunlight. These conditions were chosen because they correspond very well to the average conditions and storage period of honey in households and food markets.

To confirm their botanical origin, all of the samples were subjected to melisopalynological analysis, which was done by counting the pollen grains by a microscope. Briefly, honey samples were diluted in distilled water (5 g in 10 mL), and after thorough mixing they were centrifuged at 3000 rpm for 5 min. The supernatant was discarded while the residue was mixed with glacial acetic acid and centrifuged again. The obtained residue was then mixed with acetolysis mixture (1 mL sulfuric acid mixed with

9 mL acetic anhydride), boiled in a water bath at 85 °C for 3 min, again centrifuged and decanted. The residue was thoroughly washed with distilled water, centrifuged, decanted and mixed with liquid glycerin. The obtained sample was then used for microscopic analysis, which was done by an optical microscope at 400×. Pollen grains were identified using the relevant literature [19].

2.2. Chemicals

Methanol HPLC and p.a. grade (Panreac, Barcelona, Spain); Amberlite XAD-2 (Supelco, Sigma-Aldrich, Steinheim, Germany); formic acid 98–100%, p.a. grade (Sigma-Aldrich, Steinheim, Germany); hydrochloric acid 37% analytical reagent grade (Fisher Scientific, Loughborough, UK) and diethyl-ether Reag. Ph. Eur. (Panreac, Barcelona, Spain). For quantification and identification of individual flavonoids in honey samples, pure compounds of analytical grade were used as internal standards: quercetin (3,3',4',5,7-pentahydroxyflavone), hesperetin (3',5,7-Trihydroxy-4'-methoxyflavone), luteolin (3',4',5,7-tetrahydroxyflavone), kaempferol (3,4',5,7-tetrahydroxyflavone), apigenin (4',5,7-trihydroxyflavone), pinocembrin (5,7-dihydroxyflavanone), chrysin (5,7-dihydroxyflavone) and galangin (3,5,7-trihydroxyflavone) were supplied by Sigma-Aldrich Chemie GmbH (Steinheim, Germany).

2.3. Sample Preparation

The mass of 50 g of honey was weighed in a 400 mL glass and was dissolved in 250 mL of acidified distilled water (pH = 2, using HCl, 37% p.a.; total of 350 mL of acidified water was prepared per sample), which was then flown through a glass column filled with Amberlite XAD-2 filler. Flow speed was 9.5–11 mL/min, so there was no loss of phenolic compounds due to leakage through a layer of absorbent. In this phase, various phenolic compounds were bind to filler particles, while sugars and other polar compounds were washed away from the column by water solvent. After that, the same flow rate was maintained, the column was rinsed with an additional 100 mL of previously prepared acidified distilled water, and 300 mL of distilled water until the pH value of the eluate was 7. Using a specially designed pump, residual water was forced out of the column to shorten the time of the following evaporation process.

The total phenolic fraction was rinsed away from the filler by 300 mL of methanol at an elution speed of 2.5 mL/min. Methanol was than evaporated in a low-pressure atmosphere at 40 °C. Dry residue was diluted in 5 mL of distilled water and extracted three times per 5 mL of diethyl-ether. All three etheric extracts were combined together and again evaporated until dry in a low-pressure atmosphere at 40 °C. Before HPLC analysis, dry residue was diluted in 0.5 mL of methanol and filtered through the syringe filter with the pore size of 0.45 µm.

Flavonoid analyses were conducted on six occasions during one year, after one, three, six, nine and twelve months of storage. Each honey sample was analyzed in two parallels.

2.4. HPLC-DAD Analysis

Prior injection to HPLC apparatus, dry flavonoid fraction was prepared and dissolved in 0.5 mL of methanol and filtered through the syringe filter (Cameo, 17F Syringe filter, Teflon, 0.45 µm pore size, 17 mm diameter). The detector used for the HPLC (Shimadzu, Kyoto, Japan) analysis was DAD (Diode Array Detector) and wavelengths were between 290 and 340 nm, depending on the specific flavonoid. The LiChrospher 100 RP-18 (Merck; 12.5 cm × 0.4 cm; 5 µm particle size) column was used for the separation of the compounds. Acidified demineralized water-3% formic acid (mobile phase A) and methanol-HPLC grade (mobile phase B) were used in gradient flow mode. Gradient program was: from 0 to 15 min—30% methanol; at 20 min—40% methanol; at 30 min—45% methanol; at 50 min—60% methanol and at 52 min 80% methanol until the end of 60 min. The operating conditions included an injection volume of $V = 20 \mu\text{L}$ and the flow rate of the 1 mL/min [20]. Individual flavonoids were identified by comparing the obtained chromatographic data (the retention times and the UV spectra)

with the data obtained from the analysis of internal standards. Quantification was performed through external calibration data with the same compounds.

2.5. Statistical Analysis

Descriptive statistic was used to assess the basic information about the experimental dataset (e.g., to obtain a sample basic metrics, check for the normality of distribution). As recommended by the literature [21], continuous variables were tested by the multivariate analysis of variance (two-way ANOVA). The significance levels for all tests were at $p \leq 0.05$. Dependent variables were grouped and individual flavonoids, while independent variables included types of honey and lengths of storage in months with their interactions. Statistical analyses were performed with IBM SPSS Statistics (v.20), and by Statgraphics Centurion (StatPoint Technologies, Inc., Warrenton, VA, USA).

3. Results and Discussion

Results of the quantitative analysis of individual phenolic compounds regarded as the sum of total flavonols (quercetin, luteolin, kaempferol and galangin), total flavanones (hesperetin and pinocembrin) and total flavones (apigenin and chrysin) are presented in Table 1.

Table 1. The changes in total flavonols, flavanones, flavones and flavonoids in acacia and multifloral honey samples during 1, 3, 6, 9 and 12 months of storage.

Source of Variation	<i>n</i>	Total Flavonols	Total Flavanones	Total Flavones	Σ Total Flavonoid Content (TFC)
Honey type		$p \leq 0.01^\dagger$	$p = 0.07^\ddagger$	$p \leq 0.01^\dagger$	$p \leq 0.01^\dagger$
Acacia Honey	20	1.07 ± 0.14^b	0.70 ± 0.10^a	0.73 ± 0.09^b	2.50 ± 0.28^b
Multifloral Honey	20	2.60 ± 0.14^a	0.97 ± 0.10^a	1.58 ± 0.09^a	5.15 ± 0.28^a
Shelf life		$p \leq 0.01^\dagger$	$p \leq 0.01^\dagger$	$p \leq 0.01^\dagger$	$p \leq 0.01^\dagger$
1 month	8	1.58 ± 0.22^b	0.42 ± 0.16^b	0.66 ± 0.15^b	2.65 ± 0.45^c
3 months	8	2.38 ± 0.22^a	0.79 ± 0.16^b	1.18 ± 0.15^c	4.34 ± 0.45^b
6 months	8	2.57 ± 0.22^a	1.43 ± 0.16^a	1.64 ± 0.15^a	5.63 ± 0.45^a
9 months	8	1.14 ± 0.22^b	0.84 ± 0.16^b	$0.95 \pm 0.15^{b,c}$	2.92 ± 0.45^c
12 months	8	1.52 ± 0.22^b	0.72 ± 0.16^b	$1.36 \pm 0.15^{a,c}$	$3.59 \pm 0.45^{b,c}$
Honey type by Shelf life		$p = 0.28^\ddagger$	$p = 0.30^\ddagger$	$p = 0.66^\ddagger$	$p = 0.52^\ddagger$
Acacia Honey	4	0.98 ± 0.31^a	0.13 ± 0.23^a	0.24 ± 0.21^a	1.34 ± 0.63^a
3 months	4	1.37 ± 0.31^a	0.70 ± 0.23^a	0.70 ± 0.21^a	2.76 ± 0.63^a
6 months	4	1.56 ± 0.31^a	1.44 ± 0.23^a	1.21 ± 0.21^a	4.21 ± 0.63^a
9 months	4	0.70 ± 0.31^a	0.88 ± 0.23^a	0.71 ± 0.21^a	2.29 ± 0.63^a
12 months	4	0.77 ± 0.31^a	0.35 ± 0.23^a	0.81 ± 0.21^a	1.92 ± 0.63^a
Multifloral Honey	4	2.18 ± 0.31^a	0.71 ± 0.23^a	1.08 ± 0.21^a	3.97 ± 0.63^a
3 months	4	3.38 ± 0.31^a	0.87 ± 0.23^a	1.67 ± 0.21^a	5.92 ± 0.63^a
6 months	4	3.58 ± 0.31^a	1.41 ± 0.23^a	2.06 ± 0.21^a	7.04 ± 0.63^a
9 months	4	1.58 ± 0.31^a	0.79 ± 0.23^a	1.20 ± 0.21^a	3.56 ± 0.63^a
12 months	4	2.27 ± 0.31^a	1.09 ± 0.23^a	1.91 ± 0.21^a	5.26 ± 0.63^a
SAMPLE MEAN	40	1.83 ± 0.10	0.84 ± 0.07	1.16 ± 0.07	3.83 ± 0.20

* Results are expressed as mean \pm standard error in mg kg^{-1} of honey. † Values represented with different letters are statistically different at $p \leq 0.05$; ‡ not statistically significant at $p \leq 0.05$.

Eight flavonoid aglycone compounds were identified and quantified and total flavonoid aglycone content (TFC) was calculated as the sum of all individual flavonoids. In general, multifloral honey had twice more total flavonoids than acacia honey samples (5.15 vs. 2.50 mg kg^{-1}). Moreover, multifloral honey contained significantly higher amounts of total flavonols and total flavones as compared to acacia honey samples. Furthermore, total flavanones were not significantly different with respect to investigated honey samples.

The content of TFC increased in the samples between the 1st and the 6th month of the storage and then started to decline at the 9th month, when it remained relatively constant until the 12th month. In other words, they returned to the values from the start of the study or to the 1st month of the storage.

This way flavonoids lost 48% and 36%, respectively from the maximum measured value obtained in the 6th month as compared to the contents measured after the 9th and 12th months of storage (see Table 1). The largest losses from the maximum measured values were obtained in the 6th month for flavonols (56% and 41% for the 9th and the 12th month, respectively) and flavanones (41% and 50% for the same respective storage times). The contents of flavones also declined by the 42% and 17% for the 9th and 12th month, respectively. This trend was the same for both honey types. Our results showed that storage had significant impacts on flavonoids and botanical origin of honey that is contrary to the findings from Maurya et al., who stated that storage had only minor influences on phenolics in the honey [22]. Authors also claimed that the botanical origin played predominant roles in changes of antioxidants and phenolics in honey. On the other hand, Brudzynski and Kim (2011) concluded that storage had adverse effects on the antibacterial activity of honeys. Dietary phenolics are known antimicrobial agents [23], and similar to our results the antibacterial activity of the honey samples was rapidly reduced during the storage. For instance, the 50% decreased activity was observed in the first 3–6 months of storage and further reduction was gradually identified over the period of 12–36 months. These findings implicated that the compounds responsible for the microbial inhibition were chemically unstable during the storage [24]. Furthermore, Sousa et al. concluded that the honey samples showed high antibacterial activities due to unique phenolic profile, including flavonoids [25]. Hence, it can be concluded that determination of instability of honey flavonoids during storage is of great importance for the evaluation of the botanical origins, antioxidant and antibacterial activities that change during the storage.

On average in all of the samples, multifloral honey had higher contents of quercetin, hesperetin, luteolin, kaempferol and apigenin than acacia honey did. However, at the beginning of the storage multifloral honey had only hesperetin, luteolin and apigenin in higher concentrations than acacia. No differences in contents of pinocembrin, chrysin and galangin among different types of honey samples were observed. Stability of polyphenols during the length of shelf life followed various patterns for different compounds. Hesperetin content increased in the samples by 1.5 times from the initial measurements in the 1st month and until the 6th month of storage, and then stabilized thorough the end of the study. Pinocembrin, chrysin and galangin increased in content by the 6th month of storage and then started to decline by the end of the study. Quercetin and kaempferol contents remained more or less the same during storage of honey over 12 months, while luteolin and apigenin followed a trend similar for hesperetin with a difference for the 9th month of storage when their contents experienced sharp drop, only to be back to a constant value in the 12th month of storage. The type of honey did not have an influence on stability of the most polyphenols. Hesperetin content only increased in multifloral honey during storage but remained constant in acacia samples. Data strongly indicated that in order to retain the most of the polyphenols as markers for botanical origins, honey should not be tested later than 6 months from the initial harvest and flavonoids content will be equally well preserved in both types of honey samples.

The average values of individual flavonoids obtained after one month of storage in acacia honey were somewhat lower than the ones determined in multifloral honey samples (Table 2). Figures 1 and 2 show the typical HPLC chromatograms of eight identified and quantified flavonoids detected in both honey samples. Considering that eight identified flavonoids represent a smaller part of the total flavonoid content in honey samples, the trends in changes of individual flavonoids might be compared with the trends in changes of total flavonoids during a prolonged storage. Similarly, our previous research reported that total flavonoids, total phenolic content and corresponding antioxidant activity decreased during one year of storage [26].

Table 2. The changes in individual flavonoids in acacia and multifloral honey samples during 1, 3, 6, 9 and 12 months of storage.

Source of Variation	n	Total Flavonols				Total Flavonones				Total Flavones		
		Quercetin	Galangin	Luteolin	Kaempferol	Hesperetin	Pinocembrin	Chrysin	Apigenin			
Honey type		$p \leq 0.01$ †	$p = 0.05$ †	$p \leq 0.01$ †	$p \leq 0.01$ †	$p \leq 0.01$ †	$p = 0.97$ †	$p = 0.51$ †	$p \leq 0.01$ †			
Acacia Honey	20	0.20 ± 0.02 b	0.55 ± 0.10 a	0.10 ± 0.03 b	0.22 ± 0.06 b	0.06 ± 0.02 b	0.64 ± 0.10 a	0.44 ± 0.06 a	0.29 ± 0.05 b			
Multifloral Honey	20	0.52 ± 0.02 a	0.82 ± 0.10 a	0.39 ± 0.03 a	0.86 ± 0.06 a	0.34 ± 0.02 a	0.64 ± 0.01 a	0.50 ± 0.06 a	1.08 ± 0.05 a			
Shelf life		$p = 0.06$ †	$p \leq 0.01$ †	$p \leq 0.01$ †	$p = 0.49$ †	$p \leq 0.01$ †	$p \leq 0.01$ †	$p \leq 0.01$ †	$p \leq 0.01$ †			
1 month	8	0.37 ± 0.04 a	0.60 ± 0.15 ab	0.18 ± 0.04 ab	0.42 ± 0.09 a	0.14 ± 0.02 b	0.28 ± 0.16 b	0.18 ± 0.10 b	0.47 ± 0.08 c			
3 months	8	0.45 ± 0.04 a	0.98 ± 0.15 a	0.33 ± 0.04 a	0.62 ± 0.09 a	0.16 ± 0.02 b	0.62 ± 0.16 ab	0.44 ± 0.10 b	0.74 ± 0.08 b			
6 months	8	0.49 ± 0.04 a	1.15 ± 0.15 a	0.29 ± 0.04 a	0.63 ± 0.09 a	0.21 ± 0.02 a	1.22 ± 0.16 a	0.84 ± 0.10 a	0.80 ± 0.08 b			
9 months	8	0.18 ± 0.04 a	0.35 ± 0.15 b	0.10 ± 0.04 b	0.51 ± 0.09 a	0.27 ± 0.02 a	0.56 ± 0.16 ab	0.52 ± 0.10 ab	0.43 ± 0.08 c			
12 months	8	0.33 ± 0.04 a	0.34 ± 0.15 b	0.33 ± 0.04 a	0.51 ± 0.09 a	0.21 ± 0.02 a	0.51 ± 0.16 b	0.37 ± 0.10 b	0.99 ± 0.08 a			
Honey type by Shelf life		$p = 0.73$ †	$p = 0.29$ †	$p = 0.06$ †	$p = 0.97$ †	$p = 0.04$ †	$p = 0.19$ †	$p = 0.76$ †	$p = 0.08$ †			
1 month	4	0.24 ± 0.05 a	0.51 ± 0.21 a	0.07 ± 0.06 a	0.16 ± 0.13 a	0.06 ± 0.03 a	0.07 ± 0.23 a	0.06 ± 0.14 a	0.17 ± 0.11 a			
3 months	4	0.27 ± 0.05 a	0.68 ± 0.21 a	0.15 ± 0.06 a	0.27 ± 0.13 a	0.06 ± 0.03 a	0.64 ± 0.23 a	0.42 ± 0.14 a	0.27 ± 0.11 a			
6 months	4	0.29 ± 0.05 a	0.82 ± 0.21 a	0.15 ± 0.06 a	0.29 ± 0.13 a	0.06 ± 0.03 a	1.39 ± 0.23 a	0.90 ± 0.14 a	0.31 ± 0.11 a			
9 months	4	0.11 ± 0.05 a	0.34 ± 0.21 a	0.06 ± 0.06 a	0.18 ± 0.13 a	0.08 ± 0.03 a	0.80 ± 0.23 a	0.51 ± 0.14 a	0.20 ± 0.11 a			
12 months	4	0.12 ± 0.05 a	0.40 ± 0.21 a	0.07 ± 0.06 a	0.18 ± 0.13 a	0.05 ± 0.03 a	0.30 ± 0.23 a	0.31 ± 0.14 a	0.49 ± 0.11 a			
1 month	4	0.51 ± 0.05 a	0.69 ± 0.21 a	0.30 ± 0.06 a	0.68 ± 0.13 a	0.23 ± 0.05 b	0.48 ± 0.23 a	0.30 ± 0.14 a	0.78 ± 0.11 a			
3 months	4	0.63 ± 0.05 a	1.29 ± 0.21 a	0.50 ± 0.06 a	0.97 ± 0.13 a	0.27 ± 0.05 b	0.61 ± 0.23 a	0.46 ± 0.14 a	1.20 ± 0.11 a			
6 months	4	0.69 ± 0.05 a	1.48 ± 0.21 a	0.44 ± 0.06 a	0.97 ± 0.13 a	0.36 ± 0.05 a	1.05 ± 0.23 a	0.78 ± 0.14 a	1.28 ± 0.11 a			
9 months	4	0.24 ± 0.05 a	0.36 ± 0.21 a	0.14 ± 0.06 a	0.83 ± 0.13 a	0.46 ± 0.05 a	0.33 ± 0.23 a	0.53 ± 0.14 a	0.66 ± 0.11 a			
12 months	4	0.54 ± 0.05 a	0.29 ± 0.21 a	0.59 ± 0.06 a	0.84 ± 0.13 a	0.36 ± 0.05 a	0.73 ± 0.23 a	0.42 ± 0.14 a	1.48 ± 0.11 a			
SAMPLE MEAN	40	0.36 ± 0.02	0.69 ± 0.07	0.25 ± 0.02	0.54 ± 0.04	0.20 ± 0.01	0.64 ± 0.07	0.47 ± 0.04	0.69 ± 0.04			

* Results are expressed as mean \pm standard error in mg kg⁻¹ of honey. † Values represented with different letters are statistically different at $p \leq 0.05$; ‡ not statistically significant at $p \leq 0.05$.

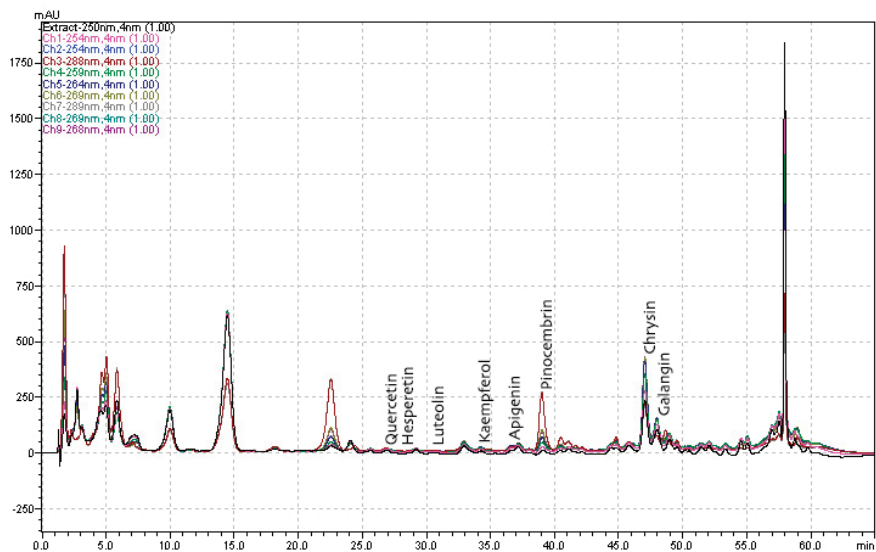


Figure 1. A typical chromatogram of acacia honey.

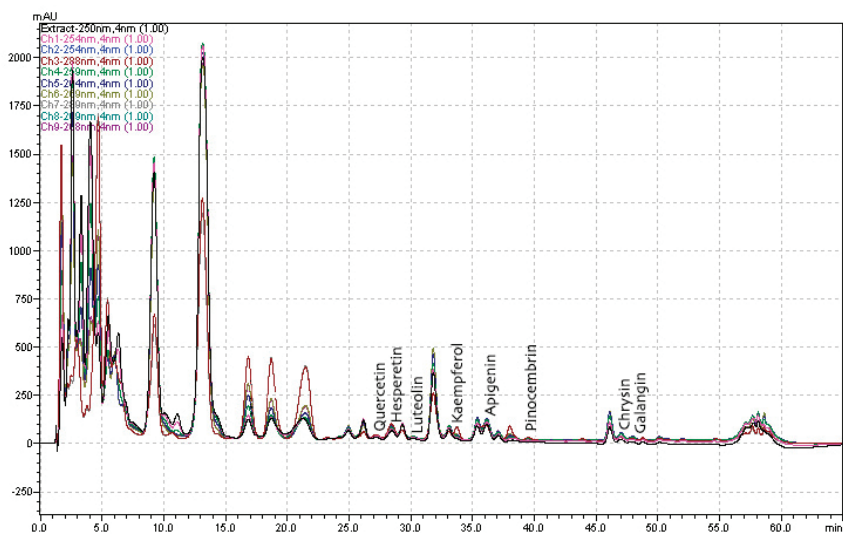


Figure 2. A typical chromatogram of multifloral honey.

The results for acacia samples from the 1st month of our study had fifteen times lower contents of hesperetin (0.004 vs. 0.06 mg kg^{-1}), eight times less apigenin (0.021 vs. 0.17 mg kg^{-1}), three times lower content of pinocembrin (0.027 vs. 0.07 mg kg^{-1}) and quercetin (0.077 vs. 0.24 mg kg^{-1}), while contents of luteolin, chrysin and kaempferol were very similar (0.07 vs. 0.04 mg/kg , 0.06 vs. 0.04 mg kg^{-1} and 0.17 vs. 0.16 mg kg^{-1} , respectively) in comparison to those found in literature [27].

A research on honey samples harvested from three different geographic regions in Argentina was conducted with the aim to evaluate the changes in the flavonoids content. Contents of three individual flavonoids were determined with the average values for all three regions: myricetin ($1.9\text{--}5.8 \text{ mg kg}^{-1}$), quercetin ($3.8\text{--}10.2 \text{ mg kg}^{-1}$) and luteolin ($1.8\text{--}4.3 \text{ mg kg}^{-1}$) [28]. These values were slightly higher than the ones obtained in our research and there are two possible reasons for this discrepancy. The most

likely is that the authors used different types of honey that originated from different geographical and climatic conditions, and the second reason is possibly due to the use of different sample preparation and flavonoid determination procedures.

Results from another study revealed in acacia honey 0.19 mg kg⁻¹ of apigenin, 1.56 mg kg⁻¹ of chrysin, 0.42 mg kg⁻¹ of hesperetin, 0.38 mg kg⁻¹ of kaempferol, 6.00 mg kg⁻¹ of pinocembrin and 2.95 mg kg⁻¹ of quercetin. These results were similar to the ones that were obtained in our research, although there were some significant differences regarding the contents of several flavonoids namely chrysin (0.064 mg kg⁻¹ vs. 1.56 mg kg⁻¹) and pinocembrin (0.073 mg kg⁻¹ vs. 6.00 mg kg⁻¹) [29].

Due to considerably larger varieties of herbal nectars from the nature that bees use to make floral honeys commonly, its chemical compositions and corresponding flavonoid contents are typically very different from that in acacia honey. Additionally, one has to bear in mind that these differences are strongly dependent on the percentage of different plant nectars that are present in multifloral samples. In line with this, by using a pollen analysis, it was found that the samples of acacia honey had 34.0% of pollen grains of acacia (*Robinia pseudoacacia* L.), 29.0% of pollen from rose family plants (*Rosaceae*), 16.0% from legumes family (*Fabaceae*), 11.0% from the crucifers (*Brassicaceae*) and 1.5% from plant species of the *Asteraceae* family. On the other hand, the mean percentage values of the most represented pollen grains in multifloral honey samples used in this research were: 45.2% of pollen from rose family plants (*Rosaceae*); 16.3% from the crucifers (*Brassicaceae*); 9.8% from willow (*Sallix* sp.); 7.1% from acacia (*Robinia pseudoacacia*); 6.8% from sweet chestnut (*Castanea sativa*); 5.3% from legumes family (*Fabaceae*) and 2.7% from amorphia (*Amorpha fruticosa*). Other research suggested that the variation in the pollen composition during different times of acacia honey harvest plays a significant role in the total flavonoid contents [27].

All of the various compounds potentially have different influences on each other, which might be a possible reason for differences in flavonoid stability and changes in their content during storage [30]. Scripca et al. [31] determined the contents of twelve phenolic compounds in various honey types, including acacia and floral samples. The contents of total polyphenols measured in acacia honey (0.08–0.06 mg/100 g) against the floral honey (9.13–1.84 mg/100 g) showed quite a large difference. Interestingly, authors did not find any amounts of myricetin, quercetin, luteolin or kaempferol in acacia honey samples, which differ from the results obtained in our current research.

Content of the most investigated flavonoids for the both honey types was the highest in the middle of a storage period (i.e., 6th–9th month of storage). To the best of our knowledge, there are no available scientific papers that explained what exactly influenced flavonoids or similar molecules in honey during prolonged periods of storage, but it is possible to speculate several possibilities. For instance, the results from a recent study pointed out that chemical reactions in honey could spontaneously produce new compounds from the existing substrates with no impact of the botanical source during the extended storage under the UV absorbance [24]. Moreover, it is possible that enzymatic activity caused changes in molecular structure of flavonoids or they were resynthesized after initial degradation, or storage temperature might affect their stability (as it was not controlled). Moreover, flavonoids occur mainly as *O*-glycosides in plants, thus, most flavonoid aglycones in plants originate from flavonoid glycosides produced by enzymatic hydrolysis by enzymes in honey or microorganisms [10]. In fact, flavonoid glycosides are widespread in honey and it is therefore likely that the honey samples in this investigation also contained flavonoid glycosides.

Connection of temperature and antioxidant activity was investigated by Turkmen et al., who studied the effects of elevated heating on antioxidant activity on the color of honey. They discovered that the biggest changes for both investigated parameters occurred at 70 °C, while they were less pronounced at 50 and 60 °C. Authors demonstrated that there is a strong correlation between antioxidant activities and increased browning of honey. So, even though, Turkish honey was exposed to much higher temperatures than the samples from our study, still the influence of temperature on our samples might be similar but more spread over the longer period of storage.

Wang et al. analyzed the effects of processing and storage on antioxidant capacity of honey by determining the contents of some flavonoids among other parameters. The obtained results after six months of storage showed that contents of all investigated flavonoids remained virtually constant. Another study confirmed that thermal treatment of honey does not have a significant impact on flavonoid profiles in investigated honey samples [13] or antioxidant activity after short thermal treatment of honey [26].

Finally, analyzed data suggested that honey samples should be stored no longer than 6 months to retain most of the flavonoids contents while they will be equally well preserved regardless of the honey type. Meaning that botanical origin will not have large influence on the stability of flavonoids, which is a good characteristic for potential markers. Hence, determining the changes of individual flavonoids in honey during storage has great potential, aligned with the recent attempts to use these individual compounds as floral markers. This is additional to the possibility to securely and accurately determine and predict the antioxidative activity of honey and potential health benefits.

4. Conclusions

In general, it was found that multifloral honey samples had higher contents of total aglycone flavonoids as compared to acacia honey samples. On the other hand, the changes among their contents during storage were very similar. The content of flavonoids increased in the samples between the 1st and the 6th month of storage and then started to decline at the 9th month, when it remained almost constant up until the 12th month of storage. The reasons behind an initial increase of the flavonoids and the subsequent drop to initial values were not fully clear. However, flavonoids showed the potential to be used as markers for botanical origin of honey, but they should be best used before the end of the six months of storage. Anyhow, more research should be done on this topic to further elucidate the changes that might be occurring in the honey during the storage and/or processing, as honey is an important commodity on food markets.

Author Contributions: Conceptualization, G.Š., and N.V.; methodology, G.Š., and N.V.; formal analysis, G.Š.; investigation, G.Š., N.V., P.P., D.B.K.; data curation, P.P.; writing—original draft preparation, G.Š., P.P., D.B.K.; writing—review and editing, G.Š., P.P., D.B.K. All authors have read and agreed to the published version of the manuscript.

Funding: This paper was produced as part of a project co-financed by the European Union from the European Regional Development Fund and the Operational Program Competitiveness and Cohesion 2014–2020.

Conflicts of Interest: The authors declare no conflict of interest.

References

1. Krell, R. Value-added products from beekeeping. In *FAO Agricultural Services Bulletin No. 124*; Food and Agriculture Organization of the United Nations: Rome, Italy, 1996.
2. Guellis, C.; Valério, D.C.; Bessegato, G.G.; Boroski, M.; Dragunski, J.C.; Lindino, C.A. Non-targeted method to detect honey adulteration: Combination of electrochemical and spectrophotometric responses with principal component analysis. *J. Food Compos. Anal.* **2020**, *89*, 103466. [CrossRef]
3. Guo, N.; Zhao, L.; Zhao, Y.; Li, Q.; Xue, X.; Wu, L.; Gomez Escalada, M.; Wang, K.; Peng, W. Comparison of the chemical composition and biological activity of mature and immature honey: An HPLC/QTOF/MS-based metabolomic approach. *J. Agric. Food Chem.* **2020**, *68*, 4062–4071. [CrossRef]
4. Schievano, E.; Sbrizza, M.; Zuccato, V.; Piana, L.; Tessari, M. NMR carbohydrate profile in tracing acacia honey authenticity. *Food Chem.* **2020**, *309*, 125788. [CrossRef] [PubMed]
5. Škenderov, S.; Ivanov, C. *Bee Products and their Use*; Nolit: Beograd, Serbia, 1986.
6. Önür, İ.; Misra, N.N.; Barba, F.J.; Putnik, P.; Lorenzo, J.M.; Gökmen, V.; Alpas, H. Effects of ultrasound and high pressure on physicochemical properties and HMF formation in Turkish honey types. *J. Food Eng.* **2018**, *219*, 129–136. [CrossRef]
7. Singhal, R.S.; Kulkarni, P.R.; Rege, D.V. *Handbook of Indices of Food Quality*; Woodhead Publishing Limited: Cambridge, UK, 1997; pp. 358–379.

8. Cebrero, G.; Sanhueza, O.; Pezoa, M.; Báez, M.E.; Martínez, J.; Báez, M.; Fuentes, E. Relationship among the minor constituents, antibacterial activity and geographical origin of honey: A multifactor perspective. *Food Chem.* **2020**, *315*, 126296. [CrossRef] [PubMed]
9. Šedík, P.; Pocol, C.B.; Horská, E.; Fiore, M. Honey: Food or medicine? A comparative study between Slovakia and Romania. *Br. Food J.* **2019**, *121*, 1281–1297. [CrossRef]
10. Truchado, P.; Ferreres, F.; Tomas-Barberan, F.A. Liquid chromatography–tandem mass spectrometry reveals the widespread occurrence of flavonoid glycosides in honey, and their potential as floral origin markers. *J. Chromatogr. A* **2009**, *1216*, 7241–7248. [CrossRef]
11. Cheung, Y.; Meenu, M.; Yu, X.; Xu, B. Phenolic acids and flavonoids profiles of commercial honey from different floral sources and geographic sources. *Int. J. Food Prop.* **2019**, *22*, 290–308. [CrossRef]
12. Shen, S.; Wang, J.; Zhuo, Q.; Chen, X.; Liu, T.; Zhang, S.-Q. Quantitative and discriminative evaluation of contents of phenolic and flavonoid and antioxidant competence for chinese honeys from different botanical origins. *Molecules* **2018**, *23*, 1110. [CrossRef]
13. Escriche, I.; Kadar, M.; Juan-Borrás, M.; Domenech, E. Suitability of antioxidant capacity, flavonoids and phenolic acids for floral authentication of honey. Impact of industrial thermal treatment. *Food Chem.* **2014**, *142*, 135–143. [CrossRef]
14. Akbari, E.; Baigbabaie, A.; Shahidi, M. Determination of the floral origin of honey based on its phenolic profile and physicochemical properties coupled with chemometrics. *Int. J. Food Prop.* **2020**, *23*, 506–519. [CrossRef]
15. Tomás-Barberán, F.A.; Martos, I.; Ferreres, F.; Radovic, B.S.; Anklam, E. HPLC flavonoid profiles as markers for the botanical origin of European unifloral honeys. *J. Sci. Food Agric.* **2001**, *81*, 485–496. [CrossRef]
16. NĪsbet, C.; Aker, D. Antioxidant activities, total phenolic and flavonoid contents of honey collected from different botanical origins. *Ank. Üniversitesi Vet. Fakültesi Derg.* **2020**. [CrossRef]
17. Ciucure, C.T.; Geană, E.I. Phenolic compounds profile and biochemical properties of honeys in relationship to the honey floral sources. *Phytochem. Anal.* **2019**, *30*, 481–492. [CrossRef]
18. Cianciosi, D.; Forbes-Hernández, T.; Afrin, S.; Gasparrini, M.; Reboredo-Rodríguez, P.; Manna, P.; Zhang, J.; Bravo Lamas, L.; Martínez Flórez, S.; Agudo Toyos, P.; et al. Phenolic compounds in honey and their associated health benefits: A review. *Molecules* **2018**, *23*, 2322. [CrossRef]
19. Von der Ohe, K.; Von der Ohe, W. *Celle's Mellisopalynological Collection*; Niedersächsisches Landesinstitut für Bienenkunde: Celle, Germany, 2003.
20. Kenjeric, D.; Mandic, M.; Primorac, L.; Bubalo, D.; Perl, A. Flavonoid profile of Robinia honeys produced in Croatia. *Food Chem.* **2007**, *102*, 683–690. [CrossRef]
21. Granato, D.; Putnik, P.; Kovačević, D.B.; Santos, J.S.; Calado, V.; Rocha, R.S.; Cruz, A.G.D.; Jarvis, B.; Rodionova, O.Y.; Pomerantsev, A. Trends in Chemometrics: Food Authentication, Microbiology, and Effects of Processing. *Compr. Rev. Food Sci. Food Saf.* **2018**, *17*, 663–677. [CrossRef]
22. Maurya, S.; Kushwaha, A.K.; Singh, S.; Singh, G. An overview on antioxidative potential of honey from different flora and geographical origins. *Indian J. Nat. Prod. Resour.* **2014**, *5*, 9–19.
23. Takó, M.; Kerekes, E.B.; Zambrano, C.; Kotogán, A.; Papp, T.; Krisch, J.; Vágvolgyi, C. Plant Phenolics and Phenolic-Enriched Extracts as Antimicrobial Agents against Food-Contaminating Microorganisms. *Antioxidants* **2020**, *9*, 165. [CrossRef]
24. Brudzynski, K.; Kim, L. Storage-induced chemical changes in active components of honey de-regulate its antibacterial activity. *Food Chem.* **2011**, *126*, 1155–1163. [CrossRef]
25. Sousa, J.M.; de Souza, E.L.; Marques, G.; Meireles, B.; de Magalhães Cordeiro, Â.T.; Gullón, B.; Pintado, M.M.; Magnani, M. Polyphenolic profile and antioxidant and antibacterial activities of monofloral honeys produced by Meliponini in the Brazilian semi-arid region. *Food Res. Int.* **2016**, *84*, 61–68. [CrossRef]
26. Šarić, G.; Marković, K.; Vukičević, D.; Lež, E.; Hruškar, M.; Vahčić, N. Changes of antioxidant activity in honey after heat treatment. *Czech. J. Food Sci.* **2013**, *31*, 601–606. [CrossRef]
27. Moniruzzaman, M.; Sulaiman, S.; Azlan, S.; Gan, S. Two-year variations of phenolics, flavonoids and antioxidant contents in acacia honey. *Molecules* **2013**, *18*, 14694–14710. [CrossRef] [PubMed]
28. Iurlina, M.O.; Saiz, A.I.; Fritz, R.; Manrique, G.D. Major flavonoids of Argentinean honeys. Optimisation of the extraction method and analysis of their content in relationship to the geographical source of honeys. *Food Chem.* **2009**, *115*, 1141–1149. [CrossRef]

29. Pulcini, P.; Allegrini, F.; Festuccia, N. Fast SPE extraction and LC-ESI-MS-MS analysis of flavonoids and phenolic acids in honey. *Apiacta* **2006**, *41*, 17–21.
30. Jibril, F.I.; Hilmi, A.B.M.; Manivannan, L. Isolation and characterization of polyphenols in natural honey for the treatment of human diseases. *Bull. Natl. Res. Cent.* **2019**, *43*, 1–9. [CrossRef]
31. Scripcă, L.A.; Norocel, L.; Amariei, S. Comparison of physicochemical, microbiological properties and bioactive compounds content of grassland honey and other floral origin honeys. *Molecules* **2019**, *24*, 2932. [CrossRef]



© 2020 by the authors. Licensee MDPI, Basel, Switzerland. This article is an open access article distributed under the terms and conditions of the Creative Commons Attribution (CC BY) license (<http://creativecommons.org/licenses/by/4.0/>).

Article

Accelerated Solvent Extraction as a Green Tool for the Recovery of Polyphenols and Pigments from Wild Nettle Leaves

Maja Repajić ^{1,*}, Ena Cegledi ¹, Valentina Kruk ¹, Sandra Pedisić ¹, Firat Çınar ²,
Danijela Bursać Kovačević ¹, Ivanka Žutić ³ and Verica Dragović-Uzelac ¹

¹ Faculty of Food Technology and Biotechnology, University of Zagreb, Pierottijeva 6, 10000 Zagreb, Croatia; eceglei@pbf.hr (E.C.); vkruk@pbf.hr (V.K.); spedisc@pbf.hr (S.P.); dbursac@pbf.hr (D.B.K.); vdragov@pbf.hr (V.D.-U.)

² Faculty of Engineering, University of Mersin, Çiftlikköy Kampüsü, 33343 Yenişehir, Mersin, Turkey; firatcinar@mersin.edu.tr

³ Faculty of Agriculture, University of Zagreb, Svetošimunska cesta 25, 10000 Zagreb, Croatia; izutic@agr.hr

* Correspondence: maja.repajic@pbf.unizg.hr

Received: 22 June 2020; Accepted: 7 July 2020; Published: 9 July 2020

Abstract: This study aimed to investigate the performance of accelerated solvent extraction (ASE) as a green approach for the recovery of polyphenols and pigments from wild nettle leaves (NL). ASE was operated at different temperatures (20, 50, 80 and 110 °C), static times (5 and 10 min) and cycle numbers (1–4) using ethanol (96%) as an extraction solvent. In order to compare the efficiency of ASE, ultrasound assisted extraction (UAE) at 80 °C for 30 min was performed as a referent. Polyphenol and pigment analyses were carried out by HPLC and antioxidant capacity was assessed by ORAC. Seven polyphenols from subclasses of hydroxycinnamic acids and flavonoids, along with chlorophylls *a* and *b* and their derivatives and six carotenoids and their derivatives were identified and quantified. Chlorogenic acid was the most abundant polyphenol and chlorophyll *a* represented the dominant pigment. ASE conditions at 110 °C/10 min/3 or 4 cycles proved to be the optimal for achieving the highest yields of analyzed compounds. In comparison with UAE, ASE showed better performance in terms of yields and antioxidants recovery, hence delivering extract with 60% higher antioxidant capacity. Finally, the potential of NL as a functional ingredient from natural sources can be successfully accessed by ASE.

Keywords: *Urtica dioica* L.; nettle leaves; accelerated solvent extraction; polyphenols; chlorophylls; carotenoids; HPLC; ORAC

1. Introduction

Nettle (*Urtica dioica* L.) is a herbaceous and perennial wild plant for which numerous studies show that almost every part of it (stem, flowers, leaves, roots and seeds) has a significant content of various bioactive compounds with corresponding antioxidant capacity (polyphenols, carotenoids, chlorophyll, phytosterols, etc.) [1–3]. Therefore, different parts of this plant may have different applications for functional food production due to its valuable nutritional and biological composition [4–7]. In particular, aerial parts of the nettle are good sources of polyphenols [8–10] and pigments [11,12] with different pharmacological and medicinal properties [13–15]. Dried nettle extract has already been used as commercially formulated food supplement that may have positive effects on reducing osteoarthritis symptoms [16]. Consumer preferences are driving rapidly towards the natural products, hence, the interest of the industry in the production and application of natural extracts is constantly growing as they show multiple benefits and could represent a valuable ingredient of functional foods, food supplements and nutraceuticals [17,18].

Nettle extracts are the most common form of its application in the industry, where for each individual species, as well as its part, optimal extraction conditions should be determined with an emphasis on maximum process efficiency and selective isolation of target compounds [19]. Conventional extraction techniques, such as maceration and solvent extraction, use large amounts of solvent, are long-lasting and ultimately do not result in extracts of adequate quality and yield. Therefore, currently priority is given to green extraction techniques that enable fast and environmentally friendly efficient extraction with less energy and solvent consumption [20]. Among these techniques, Accelerated Solvent Extraction (ASE) is highly appreciated for its effectiveness, easy use and fully automated process [21]. The ASE is carried out with a liquid solvent in a combination of elevated temperature and elevated pressure. The method is suitable for the extraction of bioactive compounds sensitive to oxygen and heat [22]. The great advantage of this technique is the ability to work with a larger number of extraction cycles, which significantly contributes to a higher extraction yield [23]. Other benefits of ASE include better diffusion of solvent into the sample due to cell-wall disruption upon high pressure, reduced viscosity of the solvent at elevated pressure and temperature resulting in better solubility, advanced mass transfer, and reduced extraction time [24]. However, ASE may be incomplete due to the limited volume of the solvent and also lower extraction yields of thermolabile components can be reached due to elevated temperatures [24]. Nevertheless, as each extraction parameter can have a significant effect on the extraction efficiency of target compounds, ASE should be optimized in order to maximize its potential [25].

Novel green solvent extraction approaches follow the requirements of being free of toxic solvents. Also, to be performed in miniaturized [26] and automated [27] fashion, are other features of greenness of analytical chemistry. Although the ASE system has been successfully used for isolation of bioactive compounds from various plant material, studies investigating the application of ASE for the isolation of bioactive compounds from nettle are very scarce. Only one research was conducted with aim to investigate ASE extracts of nettle roots, stems, leaves and flowers with respect to anti-inflammatory activity [28]. The extraction methodology was taken from the publication of Johnson et al. [29] and included temperature (22–27 °C and 100 °C), static time 5 min, flushing volume 50%, nitrogen purge time 100 s, and number of cycles 3. Nevertheless, the aim of this work was to investigate the anti-inflammatory and cytotoxic effects of obtained nettle extracts, therefore, did not give a conclusion about the efficiency of ASE in terms of the influence of its process parameters on bioactives recovery. In conclusion, authors stated that further chemical investigation of ASE extracts of nettle is required to identify the individual bioactive compounds responsible for their observed therapeutic potential [28].

Therefore, the aim of this study was to investigate the potential of ASE as a green strategy for the recovery of hydrophilic and lipophilic antioxidants such as polyphenols and pigments (chlorophylls and carotenoids) from wild nettle (*Urtica dioica* L.). As a referent extraction technique for the comparison with ASE efficiency, ultrasound assisted extraction (UAE) was also performed. Moreover, ASE parameters such as extraction temperature, static time and cycle number were optimized with respect to the highest recovery of target bioactive compounds and antioxidant capacity.

2. Materials and Methods

2.1. Chemicals

HPLC grade acetonitrile was purchased from J.T. Baker Chemicals (Deventer, Netherlands). Water was purified in a ableMilli-Q water purification system (Millipore, Burlington, MA, USA). Ethanol (96%) was obtained from Gram–mol d.o.o. (Zagreb, Croatia) and formic acid (98–100%) from T.T.T. d.o.o. (Sveta, Nedelja, Croatia). Chlorogenic acid ($\geq 95\%$), *p*-coumaric acid ($\geq 98\%$), ferulic acid ($\geq 99\%$), quercetin-3-glucoside ($\geq 99\%$), (–)- β -carotene, α -carotene, chlorophyll *a* (from *Anacystis nidulans* algae), chlorophyll *b* (from spinach) and 2,2'-Azobis (2-amidinopropane) dihydrochloride were obtained from Sigma-Aldrich (St. Louis, MO, USA). Fluorescein sodium salt was purchased from Honeywell

Fluka™ (Seelze, Germany) and Trolox (6-hydroxy-2,5,7,8-tetramethylchroman-2-carboxylic acid) from Acros Organics (Geel, Belgium).

2.2. Plant Material

Wild nettle (*Urtica dioica* L.) was collected in April 2019 in Sela Žakanjska, Croatia (altitude 244 m, latitude 45°36′27.8″ N, longitude 15°20′38.2″ E). Immediately after harvesting, nettle leaves (NL) were separated from stalks and freeze-dried (Alpha 1-4 LSCPlus, Martin Christ Gefriertrocknungsanlagen GmbH, Osterode am Harz, Germany). Afterwards, dry leaves were grinded using a mortar and obtained powder was instantly used for the extraction. Dry matter content of nettle powders was determined by drying at 103 ± 2 °C to constant mass [30].

2.3. Extraction Procedures

2.3.1. Accelerated Solvent Extraction

Polyphenols and pigments of NL were isolated using Accelerated Solvent Extraction (ASE) (Dionex™ ASE™ 350 Accelerated Solvent Extractor, Thermo Fisher Scientific Inc., Sunnyvale, CA, USA). Extractions were performed in 34 mL stainless steel cells fitted with two cellulose filters (Dionex™ 350/150 Extraction Cell Filters, Thermo Fisher Scientific Inc., Sunnyvale, CA, USA) containing 1 g of the sample mixed with 2 g of diatomaceous earth. In order to establish the highest extraction efficiency, extractions were performed under different extraction conditions as follows: extraction temperatures (20, 50, 80 and 110 °C), static extraction times (5 and 10 min) and extraction cycles (1, 2, 3 and 4), while all other parameters remained constant: 10.34 MPa, 30 s of purge with nitrogen and 50% volume flush. Ethanol (96%) was used as the extraction solvent and obtained extracts were collected in 250 mL glass vial with Teflon septa, transferred into 50 mL volume flask and made up to volume with the extraction solvent.

2.3.2. Ultrasound Assisted Extraction

In order to compare ASE efficiency, an ultrasound assisted extraction (UAE) of NL polyphenols and pigments was simultaneously conducted at previously optimized conditions. Briefly, sample (0.5 g) was put into a sealed test tube (50 mL) and 25 mL of ethanol (96%) was added and homogenized on the Vortex ZX3 (Velp Scientifica Srl, Usmate (MB), Italy). The test tube was placed in an ultrasound bath with frequency of 40 kHz (Bandelin electronic GmbH & Co., Berlin, Germany) at 80 °C for 30 min. Afterwards, the suspension was centrifuged (Z 206 A, Hermle Labortechnik GmbH, Wehingen, Germany) at 6000 rpm for 15 min. The supernatant was filtered using Whatman No. 4 filter into 25 mL volumetric flasks, and made up to volume with the extraction solvent.

Experiential setup is shown in Figure 1. All extracts were prepared in duplicate. Extracts were stored at −18 °C in inert gas atmosphere and filtered through a 0.45 µm membrane filter (Macherey-Nagel GmbH, Düren, Germany) prior to HPLC analysis.

2.4. HPLC Analysis

Separation and quantification of polyphenols and pigments were performed using HPLC analysis with Agilent 1260 Infinity quaternary LC system (Agilent Technologies, Santa Clara, CA, USA) equipped with photodiode array detector (PDA), an automatic injector and ChemStation software. The separation of phenolic compounds was performed on a Nucleosil 100-5C18, 5 mm (250 mm × 4.6 mm i.d.) column (Macherey-Nagel, GmbH, Düren, Germany). The composition of solvents and gradient elution conditions were previously described by [31]. For gradient elution, mobile phase A contained 3% of formic acid in water (*v/v*), while mobile phase B contained 3% of formic acid in 100% acetonitrile (*v/v*). The used elution program commenced with 10% A in B, raising to 40% A after 25 min, then to 70% A after 30 min and then to 10% A after 35 min. Operating conditions were as follows: column temperature 20 °C, injection volume 20 µL and the flow rate was 0.9 mL min^{−1}. Detection was

performed with UV/VIS–PDA detector by scanning from 220 to 360 nm. Identification was assessed by comparing retention times and spectral data with those of authentic standards (phenolic acids were identified at 280 nm and flavonol glycosides at 360 nm) and previous literature reports [1,32–34]. Quantitative determinations were carried out using external standard method.

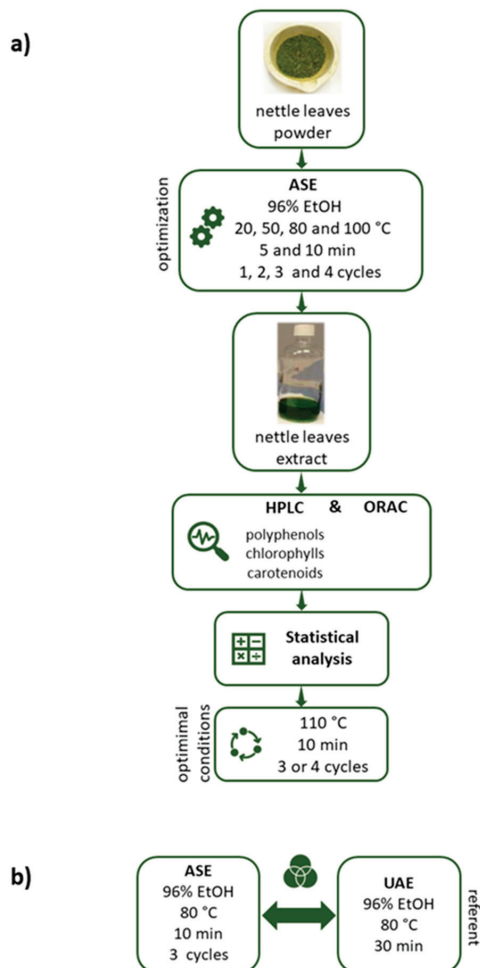


Figure 1. Experimental setup: (a) optimization of ASE conditions, (b) comparison of ASE and UAE efficiency. (ASE = accelerated solvent extraction, UAE = ultrasound assisted extraction).

For HPLC analysis of carotenoids and chlorophylls, Phenomenex Develosil RP-Aqueous C 30, 3 μm , (250 \times 4.6 mm i.d.) (Phenomenex, Torrance, CA, USA) column was used. The solvent composition and the used gradient conditions were described previously by Castro-Puyana et al. [35]. The mobile phase consisted of a mixture of MeOH: Methyl tert-butyl ether (MTBE): water (90:7:3, *v/v/v*) as mobile phase A and MeOH: MTBE (10:90, *v/v*), as mobile phase B. The flow rate was 0.8 mL min^{-1} and the injection volume 10 μL . The chromatogram was monitored by scanning from 240 to 770 nm and the signal intensities detected at 450 nm and 660 nm were used for carotenoid and chlorophyll quantitation. Identification was carried out by comparing retention times and spectral data with those of the authentic standards (α - and β -carotene, chlorophyll *a* and *b*) or in case of unavailability of standards by comparing the absorption spectra reported in the literature [36,37]. Quantifications were made by the external standard calculation, using calibration curves of the standards β -carotene, α -carotene, chlorophyll *a* and chlorophyll *b*. The quantification of individual carotenoid compounds (neoxantine, violaxantine, lutein and its derivatives, derivative of zeaxantine and lycopene) was calculated as β -carotene equivalents and derivatives of chlorophylls as chlorophyll *a* and *b* equivalents using the equation based on the calibration curves, respectively. The concentrations of analyzed compounds were expressed as mg 100 g^{-1} of dry matter, as mean values \pm SD (N = 4).

2.5. Antioxidant Capacity

The antioxidant capacity of the extracts was assessed by the oxygen radical absorbance capacity (ORAC) assay according to the study of Prior et al. [38] and Bender et al. [39] with minor modifications. The ORAC procedure used an automated plate reader (BMG LABTECH, Offenburg, Germany) with 96-well plates and data were analyzed by MARS 2.0 software. The 2,2'-Azobis radical (2-amidinopropane) dihydrochloride (AAPH), fluorescein solution, different dilutions of 6-hydroxy-2,5,7,8-tetramethylchroman-2-carboxylic acid (Trolox) and samples were prepared in 75 μM phosphate buffer (pH 7.4). Briefly, 25 mL of appropriate diluted samples were added in a 96-well black plate containing 150 μL of fluorescein solution (70.3 nM). The plate was incubated for 30 min at 37 $^{\circ}\text{C}$ and after the first three cycles (representing the baseline signal), AAPH (240 mM) was injected into each well to initiate the peroxy radical generation. On each plate, different dilutions of Trolox (3.37–107.88 μM) were used as a reference standard. Fluorescence intensity (excitation at 485 nm and emission at 528 nm) was monitored every 90 s over a total measurement period of 120 min. The measurements were performed in duplicates and results are expressed as mmol of Trolox equivalents (TE) 100 g^{-1} of dry matter, as mean values \pm SD (N = 4).

2.6. Statistical Analysis

Statistical analysis was carried out using Statistica ver. 10.0 software (Statsoft Inc., Tulsa, OK, USA). Experimental part was designed as full factorial randomized design and descriptive statistic was assessed for the basic evaluation of the data. Multivariate analysis of variance (MANOVA) was used for the analysis of continuous variables (polyphenols, pigments and antioxidant capacity) and marginal mean values were compared with Tukey's HSD test. Obtained results are expressed as mean \pm SE. Relationships between antioxidant capacity and determined compounds were tested by calculation of Pearson's correlation coefficient. All tests were carried out at the significance level $p \leq 0.05$.

3. Results and Discussion

3.1. Influence of Accelerated Solvent Extraction on Polyphenols Recovery

ASE of NL was performed using 96% ethanol as solvent. The reason for choosing this solvent is that ethanol has a GRAS status ("Generally Recognized as Safe"), so it meets one of the criteria of green chemistry, i.e., green extraction [40] that coupled with ASE might be an efficient green tool for bioactives recovery. Therefore, in order to achieve the maximum efficiency of the extraction process and to provide a high extraction yield of target compounds, the extraction operating parameters need to be

optimized [41]. Therefore, present study involved the optimization of the ASE operating conditions in terms of temperature (20, 50, 80 and 110 °C), static time (5 and 10 min) and number of extraction cycles (1–4) for NL polyphenols and pigments extraction. In obtained extracts various polyphenols have been identified and quantified by HPLC analysis: chlorogenic acid (ChA), *p*-coumaric acid (*p*-CA), ferulic acid (FA) and chicoric acid (CA) belonging to the group of hydroxycinnamic acids (HCA) and flavonoids (F) quercetin-3-glucoside (Q-3-G), kaempferol-3-rutinoside (K-3-R) and luteolin (LTL) (Table 1). As it can be observed, the most abundant polyphenol was ChA with the highest content of 278.14 mg 100 g⁻¹ dm at 110 °C/10 min/2 cycles. CA was the least represented compound, detected only at 110 °C/10 min/2–4 cycles. Similar polyphenols profile in NL was found by other authors [2,9,10,34,42,43]. Carvalho et al. [10] studied the polyphenols composition in leaves of three nettle species (*Urtica dioica* L., *Urtica membranacea* Poir and *Urtica urens* L.), where *Urtica dioica* L. had the highest concentration of polyphenols and HCA were the most dominant, especially derivatives of caffeic and *p*-CA. In accordance, Vajić et al. [42] identified two groups of polyphenols in NL, HCA and F, among which the most dominant were 2-*O*-caffeoyl malic acid, ChA and rutin. Orčić et al. [9] reported that neochlorogenic acid was the most abundant compound in overground parts of nettle, consisting up to 3.6% of the extract by weight. The following most represented components were quercetin-3-*O*-rhamnosylglucoside and Q-3-G. Slight differences in composition of polyphenols could be due to the type and various extraction conditions, as well as the pre-harvest and post-harvest conditions [1,2,44,45]. In study of Pinelli et al. [34] ChA and 2-*O*-caffeoylmalic acids represented 71.5 and 76.5 % of total polyphenols (TP) in cultivated and wild NL, respectively. However, CA was not reported in previous research, while in our study it was identified only at the highest applied conditions (110 °C/10 min/2–4 cycles), pointing ASE as very efficient for the isolation of bioactive polyphenolic compounds.

The influence of ASE parameters (temperature, static time and cycle number) on yield of NL polyphenols are presented in Table 2. The sum of TP includes determined total HCA (THCA) and total F (TF). As it can be seen, the effect of temperature, static time and cycle number had a significant influence ($p < 0.01$) on all polyphenols groups as well as on TP, except THCA were not significantly affected by the cycle number ($p = 0.19$). The increase of temperature from 20 to 110 °C resulted with significantly higher THCA, ranging from 16.87 to 255.51 mg 100 g⁻¹ dm, TF (from 3.67 to 80.16 mg 100 g⁻¹ dm) and TP (from 20.54 to 335.67 mg 100 g⁻¹ dm). These results are in accordance with the findings of Zgórka (2009) [46] who reported that the concentration of isoflavone from clover increased with temperature increase (75–125 °C) during ASE and there was no degradation of the analyzed compounds. Increase of the temperature during ASE increases the solubility of the compounds, diffusion rate and mass transfer, enhances the penetration of the solvents into the matrix and thus affects the extraction efficiency [47]. However, Erdogan and Erdemoglu [48] reported that optimum temperature for ASE of polyphenols from apricots was 60 °C, above which the amount of polyphenols decreased due to the possible degradation, which accents the need for the adjustment of proper temperature depending on the used matrix. Considering static time, all polyphenol groups showed the highest content at static time of 10 min (THCA = 164.31 mg 100 g⁻¹ dm, TF = 50.47 mg 100 g⁻¹ dm, TP = 214.78 mg 100 g⁻¹ dm) (Table 2). It is evident that longer static time (10 vs. 5 min) promoted almost double yields of all compound groups. Regarding the cycle number, results revealed that the highest yields of polyphenols were achieved during the third cycle, with an increase of 42–58% when compared to the initial cycle number (1). The same trend was observed by Gomes et al. [49] where the maximum of studied ASE conditions (80 °C/10 min/5 cycles) resulted in highest polyphenols yields. Moreover, Mottaleb and Sarker [21] confirmed the significance of the combined effects of static time and number of cycles in the recovery of natural products.

Table 1. Nettle leaves polyphenols (mg 100 g⁻¹ dm) and ORAC values (mmol TE 100 g⁻¹ dm) in extracts obtained at ASE different conditions.

Temperature (°C)	Static Time (min)	Cycle Number	ChA	p-CA	FA	CA	Q-3-G	K-3-R	LTL	ORAC	
20	5	1	6.69 ± 0.05	1.33 ± 0.02	nd	nd	nd	nd	nd	2.66 ± 0.01	
		2	8.63 ± 0.31	1.73 ± 0.04	nd	nd	nd	nd	nd	3.08 ± 0.03	
		3	9.03 ± 0.34	1.51 ± 0.20	nd	nd	nd	nd	nd	nd	2.42 ± 0.04
		4	10.53 ± 0.17	1.76 ± 0.08	nd	nd	nd	nd	nd	nd	2.96 ± 0.14
20	10	1	10.14 ± 6.63	1.75 ± 1.10	nd	nd	5.41 ± 0.04	nd	nd	5.37 ± 0.07	
		2	19.74 ± 0.80	2.82 ± 0.57	nd	nd	7.32 ± 0.52	nd	nd	7.54 ± 0.06	
		3	24.09 ± 1.01	3.61 ± 0.33	nd	nd	8.27 ± 0.67	nd	nd	nd	10.22 ± 0.02
		4	27.65 ± 1.00	3.95 ± 0.12	nd	nd	8.32 ± 0.42	nd	nd	nd	9.91 ± 0.05
50	5	1	10.08 ± 0.25	1.82 ± 0.23	nd	nd	6.57 ± 0.27	nd	nd	4.61 ± 0.02	
		2	13.00 ± 0.24	1.63 ± 0.22	nd	nd	3.84 ± 0.16	nd	nd	4.77 ± 0.04	
		3	13.70 ± 0.72	1.55 ± 0.32	nd	nd	4.69 ± 0.40	nd	nd	nd	3.53 ± 0.04
		4	15.56 ± 0.53	1.55 ± 0.37	nd	nd	4.80 ± 0.20	nd	nd	nd	3.43 ± 0.06
50	10	1	23.36 ± 0.94	4.01 ± 0.73	nd	nd	5.63 ± 0.55	nd	nd	7.50 ± 0.04	
		2	31.13 ± 1.47	4.89 ± 0.79	nd	nd	7.17 ± 0.98	nd	nd	10.08 ± 0.01	
		3	37.35 ± 1.70	6.14 ± 1.01	nd	nd	8.67 ± 1.16	nd	nd	nd	10.74 ± 0.06
		4	51.01 ± 0.54	7.14 ± 0.87	nd	nd	11.71 ± 1.93	2.62 ± 3.70	nd	nd	12.53 ± 0.05
80	5	1	74.73 ± 2.56	45.79 ± 1.78	nd	nd	29.48 ± 4.99	10.13 ± 1.05	1.61 ± 0.36	14.13 ± 0.03	
		2	72.28 ± 1.76	26.68 ± 10.49	nd	nd	39.24 ± 10.96	10.66 ± 1.11	2.06 ± 0.72	13.43 ± 0.02	
		3	150.77 ± 41.24	30.19 ± 7.08	1.81 ± 0.00	nd	30.93 ± 9.27	9.14 ± 0.80	1.28 ± 0.39	13.24 ± 0.07	
		4	109.74 ± 31.04	17.70 ± 2.30	1.55 ± 0.03	nd	34.49 ± 10.31	9.57 ± 0.85	1.37 ± 0.34	13.67 ± 0.03	
80	10	1	154.35 ± 19.17	54.71 ± 20.50	2.07 ± 0.05	nd	50.73 ± 11.06	13.02 ± 0.21	1.86 ± 0.21	14.26 ± 0.06	
		2	188.32 ± 6.66	104.22 ± 3.84	2.60 ± 0.09	nd	73.60 ± 10.53	17.88 ± 1.05	2.75 ± 0.21	21.11 ± 0.03	
		3	231.86 ± 37.64	68.26 ± 16.06	2.49 ± 0.04	nd	68.51 ± 8.61	17.12 ± 0.70	2.45 ± 0.22	22.07 ± 0.03	
		4	173.65 ± 7.56	47.85 ± 8.91	3.18 ± 0.02	nd	64.14 ± 9.80	15.82 ± 0.87	2.21 ± 0.18	21.71 ± 0.02	
110	5	1	83.78 ± 13.87	29.49 ± 6.89	1.31 ± 0.10	nd	31.04 ± 3.17	9.81 ± 0.40	0.89 ± 0.05	14.51 ± 0.05	
		2	134.55 ± 23.01	39.40 ± 9.57	1.89 ± 0.06	nd	40.48 ± 10.86	12.76 ± 0.27	1.31 ± 0.06	14.52 ± 0.02	
		3	163.61 ± 23.95	52.84 ± 3.21	2.41 ± 0.05	nd	48.66 ± 7.59	14.86 ± 0.19	1.14 ± 0.05	14.05 ± 0.02	
		4	143.13 ± 6.73	52.59 ± 1.18	2.35 ± 0.10	nd	51.42 ± 8.06	14.85 ± 0.50	1.84 ± 0.70	14.52 ± 0.02	
110	10	1	174.46 ± 2.09	57.49 ± 22.23	1.94 ± 0.05	nd	55.63 ± 13.15	16.81 ± 0.75	1.14 ± 0.24	14.34 ± 0.03	
		2	278.14 ± 55.96	76.83 ± 19.23	4.26 ± 0.00	4.34 ± 0.03	71.22 ± 16.81	21.87 ± 0.81	3.20 ± 2.30	16.71 ± 0.04	
		3	251.58 ± 38.79	104.56 ± 16.76	5.91 ± 0.00	6.07 ± 0.04	94.67 ± 8.87	24.22 ± 0.98	6.76 ± 4.89	17.78 ± 0.04	
		4	248.49 ± 38.24	105.96 ± 3.42	8.22 ± 0.03	8.47 ± 0.08	87.14 ± 4.84	23.34 ± 0.90	6.25 ± 4.63	17.50 ± 0.05	

ASE = accelerated solvent extraction, ChA = chlorogenic acid, p-CA = p-coumaric acid, FA = ferulic acid, CA = chiroic acid, Q-3-G = quercetin-3-glucoside, K-3-R = kaempferol-3-rutinoside, LTL = luteolin. nd = not detected. Results are expressed as mean ± SD.

Table 2. The influence of ASE conditions on yield of nettle leaves polyphenols (mg 100 g⁻¹ dm), pigments (mg 100 g⁻¹ dm) and ORAC values (mmol TE 100 g⁻¹ dm).

Source of Variation	THCA	TF	TP	TCH	TCAR	TPG	ORAC
Temperature (°C)	<i>p</i> < 0.01 *	<i>p</i> < 0.01 *	<i>p</i> < 0.01 *	<i>p</i> < 0.01 *	<i>p</i> < 0.01 *	<i>p</i> < 0.01 *	<i>p</i> < 0.01 *
20	16.87 ± 3.72a	3.67 ± 1.70a	20.54 ± 4.23a	464.37 ± 2.25a	31.48 ± 0.01a	495.85 ± 2.25a	5.52 ± 0.01a
50	27.99 ± 3.72a	6.96 ± 1.70a	34.95 ± 4.23a	678.60 ± 2.25b	44.07 ± 0.01b	722.67 ± 2.25b	7.15 ± 0.01b
80	195.60 ± 3.72b	63.76 ± 1.70b	259.35 ± 4.23b	1070.63 ± 2.25c	64.74 ± 0.01c	1135.38 ± 2.25c	16.70 ± 0.01d
110	255.51 ± 3.72c	80.16 ± 1.70c	335.67 ± 4.23c	1075.25 ± 2.25c	65.81 ± 0.01d	1141.06 ± 2.25c	15.49 ± 0.01c
Static time (min)	<i>p</i> < 0.01 *	<i>p</i> < 0.01 *	<i>p</i> < 0.01 *	<i>p</i> < 0.01 *	<i>p</i> < 0.01 *	<i>p</i> < 0.01 *	<i>p</i> < 0.01 *
5	83.67 ± 2.63a	26.81 ± 1.21a	110.48 ± 2.99a	709.20 ± 1.59a	45.52 ± 0.00a	754.71 ± 1.59a	8.72 ± 0.01a
10	164.31 ± 2.63b	50.47 ± 1.21b	214.78 ± 2.99b	935.23 ± 1.59b	57.54 ± 0.00b	992.77 ± 1.59b	13.71 ± 0.01b
Cycle number	<i>p</i> < 0.01 *	<i>p</i> < 0.01 *	<i>p</i> < 0.01 *	<i>p</i> < 0.01 *	<i>p</i> < 0.01 *	<i>p</i> < 0.01 *	<i>p</i> < 0.01 *
1	92.41 ± 3.72a	29.97 ± 1.70a	122.38 ± 4.23a	746.06 ± 2.25a	47.31 ± 0.01a	793.37 ± 2.25a	9.67 ± 0.01a
2	127.13 ± 3.72b	39.42 ± 1.70b	166.55 ± 4.23b	829.68 ± 2.25b	52.60 ± 0.01c	882.28 ± 2.25b	11.41 ± 0.01b
3	146.17 ± 3.72c	42.67 ± 1.70b	188.84 ± 4.23c	838.54 ± 2.25c	51.94 ± 0.01b	890.48 ± 2.25b	11.76 ± 0.01c
4	130.25 ± 3.72b	42.49 ± 1.70b	172.74 ± 4.23b	874.57 ± 2.25d	54.26 ± 0.01d	928.82 ± 2.25c	12.03 ± 0.01d
Grand mean	123.99	38.64	162.63	822.21	51.53	873.74	11.22

ASE = accelerated solvent extraction, THCA = total hydroxycinnamic acids, TF = total flavonoids, TP = total phenols, TCH = total chlorophylls, TCAR = total carotenoids, TPG = total pigments. * Statistically significant variable at *p* ≤ 0.05. Results are expressed as mean ± SE. Values with different letters within column are statistically different at *p* ≤ 0.05.

The purpose of the extraction cycles is to introduce a fresh solvent during the extraction with the aim to maintain a favorable extraction balance. This could be useful for samples with a high concentration of analytes or for samples where it is difficult for solvent to penetrate in the pores of matrix. However, extraction cycles need to be adequately combined with static extraction time for the most efficient extraction [21].

Currently, UAE performed by using an ultrasound bath operating at a frequency between 37 and 45 kHz represents an easy and low-cost extraction process used to obtain high valuable compounds from natural products [50]. In line with this, ASE (80 °C/10 min/3 cycles) was compared with UAE under previously optimized conditions (80 °C/30 min). The polyphenols concentrations obtained at UAE optimal conditions are shown in Table 3. Comparing the yields of both techniques obtained at similar setups, ASE outputs are generally three-fold higher for most of the analyzed polyphenols. Zengin et al. [51] reported that ASE accomplished the highest yields of TP content (65.05 mg GAE g⁻¹) of *Tanacetum parthenium* extracts in comparison with other four different extraction techniques, among which UAE was also studied.

Table 3. Nettle leaves polyphenols (mg 100 g⁻¹ dm), pigments (mg 100 g⁻¹ dm) and ORAC values (mmol TE 100 g⁻¹ dm) in UAE extracts obtained at optimal extraction conditions (80 °C/30 min).

Compounds		Concentration
Polyphenols	ChA	76.84 ± 3.32
	<i>p</i> -CA	53.23 ± 1.07
	Q-3-G	19.02 ± 2.77
	K-3-R	5.18 ± 0.45
Chlorophylls	CHL <i>b</i> der 1	8.42 ± 0.06
	CHL <i>a</i> der 1	36.65 ± 2.10
	CHL <i>a</i> der 2	38.62 ± 2.44
	CHL <i>b</i>	230.46 ± 15.17
	CHL <i>a</i>	589.04 ± 22.36
	CHL <i>a</i> der 5	5.07 ± 0.02
Carotenoids	VIOLAX der	1.17 ± 0.10
	NEOX	2.38 ± 0.15
	VIOLAX	1.10 ± 0.08
	13'- <i>cis</i> -LUT	2.38 ± 0.06
	LUT 5,6-ep	1.10 ± 0.09
	NEOX der	0.67 ± 0.02
	LUT	21.25 ± 1.04
	ZEAX der	1.02 ± 0.03
	9'- <i>cis</i> -LUT	1.78 ± 0.11
	α-CAR	6.12 ± 0.41
β-CAR	14.14 ± 1.03	
LYC der 10	0.32 ± 0.01	
Antioxidant capacity		
ORAC		13.26 ± 0.05

UAE = ultrasound assisted extraction, ChA = chlorogenic acid, *p*-CA = *p*-coumaric acid, Q-3-G = quercetin-3-glucoside, K-3-R = kaempferol-3-rutinoside, CHL *b* der 1 = chlorophyll *b* derivative 1, CHL *a* der 1 = chlorophyll *a* derivative 1, CHL *a* der 2 = chlorophyll *a* derivative 2, CHL *b* = chlorophyll *b*, CHL *a* = chlorophyll *a*, CHL *a* der 5 = chlorophyll *a* derivative 5, VIOLAX der = violaxanthin derivative, NEOX = neoxanthin, VIOLAX = violaxanthin, 13'-*cis*-LUT = 13'-*cis*-lutein, LUT 5,6-ep = lutein 5,6-epoxide, NEOX der = neoxanthin derivative, LUT = lutein, ZEAX der = zeaxanthin derivative, 9'-*cis*-LUT = 9'-*cis*-lutein, α-CAR = α-carotene, β-CAR = β-carotene, LYC der 10 = lycopene derivative 10. Results are expressed as mean ± SD.

In their study, UAE yielded 30% less of polyphenols in comparison with ASE, showing its lower efficiency, which is similarly to our results. ASE also showed the best performance for polyphenols extraction in other studies [47,51,52]. Summarizing the obtained results, ASE proved to be effective green technique for recovery of NL polyphenols, whereas conditions 110 °C/10 min/3 cycles showed the highest polyphenols yield. It was shown that temperature presents one of the most important factors among the examined conditions, where generally, application of higher temperature results in higher yields of polyphenols.

3.2. Influence of Accelerated Solvent Extraction on Chlorophylls and Carotenoids Recovery

Chlorophylls and carotenoids are pigments responsible for plant color [53], but they also possess antioxidant properties [54,55], therefore promoting health effects [56]. Along with phenols, NL extracts were also analyzed for the pigment content and the obtained results are given in Tables 4 and 5. HPLC analysis revealed eight chlorophylls including chlorophyll *a* (CHL *a*), chlorophyll *b* (CHL *b*) and their derivatives (Table 4). CHL *a* was the most abundant component ranging between 167.41 and 871.33 mg 100 g⁻¹ dm, where the highest level was obtained at 80 °C/10 min/2 cycles. The following component was CHL *b* in a ratio of 1:3 when compared to the amount of CHL *a*, which had been previously confirmed in other studies [12,44]. The component with the lowest concentration was CHL *a* derivative 2 in the range of 1.06–3.70 mg 100 g⁻¹ dm obtained only at 50 and 80 °C. Concentrations of other identified chlorophylls were much lower. Identified carotenoids were as follows: violaxanthin derivative (VIOLAX der), neoxanthin (NEOX), violaxanthin (VIOLAX), 13'-*cis*-lutein (13'-*cis*-LUT), lutein 5,6-epoxide (LUT 5,6-ep), neoxanthin derivative (NEOX der), lutein (LUT), zeaxanthin (ZEAX), 9'-*cis*-lutein (9'-*cis*-LUT), α -carotene (α -CAR), β -carotene (β -CAR) and lycopene derivative 10 (LYC der 10) (Table 5). The most dominant carotenoid was LUT ranging from 5.52 to 30.16 mg 100 g⁻¹ dm with the highest yield achieved at 110 °C/10 min/2 cycles. β -CAR was the following carotenoid with a maximum value of 19.02 mg 100 g⁻¹ dm, while the least present carotenoid was LYC der 10 (0.32–0.85 mg 100 g⁻¹ dm) and it was detected only at higher temperatures (80 and 110 °C). With respect to carotenoids composition, our results are in agreement with the findings from the study of Guil-Guerrero et al. [11] where total of nine carotenoids were identified in NL extracts being LUT, β -CAR and their isomers 60% of total carotenoids (TCAR). However, carotenoids in our study were found in higher concentrations, probably due to the application of different extraction technique and conditions. When supercritical and liquid CO₂ extraction were used to characterize NL chlorophylls and carotenoids, it was revealed that chlorophylls content was lower (CHL *a* 73 mg 100 g⁻¹ dm, CHL *b* 100 100 g⁻¹ dm), while LUT and β -CAR contents were higher (LUT 39 mg 100 g⁻¹ dm, β -CAR 24 mg 100 g⁻¹ dm) in comparison with our results [57]. Moreover, it can be observed that the chlorophylls levels are much higher compared to the levels of carotenoids (Tables 4 and 5), which is in accordance with previous studies, where NL extracts had four-fold higher concentrations of chlorophylls in comparison with carotenoids [2,44].

Table 4. Nettle leaves chlorophylls (mg100 g⁻¹ dm) in extracts obtained at ASE different conditions.

Temperature (°C)	Static Time (min)	Cycle Number	CHL <i>b</i> der 1	CHL <i>a</i> der 1	CHL <i>a</i> der 2	CHL <i>b</i>	CHL <i>a</i> der 3	CHL <i>a</i> der 4	CHL <i>a</i>	CHL <i>a</i> der 5
20	5	1	nd	nd	nd	50.13 ± 3.21	2.32 ± 0.14	nd	167.41 ± 10.10	nd
		2	nd	nd	nd	52.20 ± 1.96	2.80 ± 0.09	nd	201.34 ± 1.36	nd
		3	nd	nd	nd	64.08 ± 5.47	2.98 ± 0.25	1.81 ± 0.11	218.83 ± 19.03	nd
		4	nd	nd	nd	76.86 ± 4.49	4.06 ± 0.31	2.53 ± 0.14	266.62 ± 22.25	nd
20	10	1	nd	nd	nd	149.34 ± 11.54	5.77 ± 0.11	6.27 ± 0.02	486.82 ± 30.11	9.71 ± 0.66
		2	nd	nd	nd	124.02 ± 9.65	4.23 ± 0.32	4.75 ± 0.33	420.08 ± 3.56	5.63 ± 0.41
		3	nd	nd	nd	144.32 ± 3.63	5.42 ± 0.25	5.31 ± 0.25	493.82 ± 14.79	7.12 ± 0.22
		4	nd	nd	nd	164.12 ± 12.09	6.08 ± 0.04	5.97 ± 0.19	546.09 ± 21.45	6.14 ± 0.31
50	5	1	nd	nd	nd	128.14 ± 2.55	5.28 ± 0.06	2.79 ± 0.08	410.82 ± 9.96	2.15 ± 0.06
		2	nd	nd	nd	118.76 ± 4.58	5.96 ± 0.14	3.81 ± 0.20	405.97 ± 37.05	1.84 ± 0.25
		3	nd	nd	nd	118.89 ± 8.85	5.29 ± 0.24	3.79 ± 0.27	399.27 ± 16.16	2.15 ± 1.04
		4	nd	nd	nd	127.24 ± 4.30	7.26 ± 0.57	5.12 ± 0.15	444.73 ± 7.86	1.86 ± 0.77
50	10	1	nd	nd	nd	149.14 ± 6.98	6.13 ± 0.48	5.75 ± 0.43	480.65 ± 25.52	4.90 ± 0.13
		2	nd	2.07 ± 0.03	1.86 ± 0.07	186.43 ± 14.74	9.64 ± 0.08	6.35 ± 0.23	576.32 ± 5.93	6.71 ± 0.52
		3	nd	1.90 ± 0.16	2.34 ± 0.11	199.60 ± 8.55	10.89 ± 0.87	7.97 ± 0.50	618.59 ± 50.38	8.20 ± 0.74
		4	nd	2.61 ± 0.23	3.70 ± 0.18	220.30 ± 18.18	11.09 ± 0.66	6.55 ± 0.42	691.27 ± 7.45	6.74 ± 0.30
80	5	1	nd	4.60 ± 0.33	1.06 ± 0.05	223.73 ± 15.02	8.95 ± 0.73	3.06 ± 0.27	672.71 ± 49.12	8.13 ± 0.18
		2	nd	4.97 ± 0.12	3.59 ± 0.09	250.17 ± 21.37	8.70 ± 0.55	2.96 ± 0.02	722.10 ± 60.17	12.55 ± 1.09
		3	nd	4.52 ± 0.06	2.87 ± 0.14	253.59 ± 7.58	9.23 ± 0.32	2.84 ± 0.03	721.07 ± 58.77	21.77 ± 1.11
		4	nd	5.03 ± 0.11	nd	253.75 ± 8.64	11.06 ± 0.86	3.11 ± 0.18	736.72 ± 8.72	21.21 ± 2.04
80	10	1	nd	5.03 ± 0.07	nd	253.75 ± 10.54	11.06 ± 0.74	3.11 ± 0.08	736.72 ± 3.66	21.21 ± 1.45
		2	nd	7.47 ± 0.37	nd	301.80 ± 26.44	10.89 ± 0.71	2.94 ± 0.22	871.33 ± 52.30	13.63 ± 0.99
		3	nd	7.60 ± 0.22	nd	280.77 ± 14.73	8.81 ± 0.42	3.20 ± 0.17	850.56 ± 30.47	15.20 ± 0.56
		4	11.91 ± 0.42	8.92 ± 0.44	nd	239.99 ± 20.19	13.05 ± 0.24	4.39 ± 0.36	860.70 ± 13.96	10.98 ± 0.87
110	5	1	nd	4.23 ± 0.06	nd	217.77 ± 5.66	7.33 ± 0.09	2.55 ± 0.14	660.54 ± 28.87	7.48 ± 0.63
		2	nd	4.82 ± 0.01	nd	259.70 ± 17.05	9.86 ± 0.05	3.40 ± 0.11	739.60 ± 15.47	11.11 ± 1.04
		3	nd	4.70 ± 0.10	nd	280.66 ± 23.56	11.64 ± 0.60	4.13 ± 0.35	714.51 ± 41.41	22.89 ± 1.52
		4	7.20 ± 0.15	4.36 ± 0.08	nd	271.95 ± 3.72	12.57 ± 1.03	4.43 ± 0.40	768.41 ± 1.22	22.19 ± 2.07
110	10	1	7.45 ± 0.02	4.16 ± 0.28	nd	233.27 ± 5.27	10.29 ± 0.08	3.89 ± 0.23	756.26 ± 31.28	26.66 ± 1.95
		2	nd	2.42 ± 0.02	nd	308.74 ± 19.54	11.05 ± 1.07	4.89 ± 0.13	775.16 ± 26.55	152.85 ± 12.12
		3	nd	5.05 ± 0.09	nd	255.42 ± 7.46	8.36 ± 0.54	3.06 ± 0.21	821.35 ± 3.33	35.94 ± 3.02
		4	nd	4.68 ± 0.15	nd	271.74 ± 22.47	8.31 ± 0.11	2.97 ± 0.05	793.09 ± 54.06	36.89 ± 0.98

ASE = accelerated solvent extraction, CHL *b* der 1 = chlorophyll *b* derivative 1, CHL *a* der 1 = chlorophyll *a* derivative 1, CHL *a* der 2 = chlorophyll *a* derivative 2, CHL *b* = chlorophyll *b*, CHL *a* der 3 = chlorophyll *a* derivative 3, CHL *a* der 4 = chlorophyll *a* derivative 4, CHL *a* = chlorophyll *a*, CHL *a* der 5 = chlorophyll *a* derivative 5. nd = not detected. Results are expressed as mean ± SD.

Table 5. Nettle leaves carotenoids (mg 100 g⁻¹ dm) in extracts obtained at ASE different conditions.

Temperature (°C)	Static Time (min)	Cycle Number	VIOLAX der	NEOX	VIOLAX	13'-cis-LUT	LUT 5,6-ep	NEOX der	LUT	ZEAX	9'-cis-LUT	α-CAR	β-CAR	LYC der 10
20	5	1	0.60 ± 0.02	0.70 ± 0.05	2.14 ± 0.14	nd	nd	0.30 ± 0.01	5.52 ± 0.21	nd	0.54 ± 0.03	1.45 ± 0.07	4.23 ± 0.22	nd
		2	0.63 ± 0.01	0.83 ± 0.01	2.48 ± 0.21	nd	0.33 ± 0.01	0.35 ± 0.00	6.39 ± 0.45	0.28 ± 0.00	0.57 ± 0.00	1.80 ± 0.11	5.11 ± 0.01	nd
		3	0.65 ± 0.02	0.90 ± 0.03	2.65 ± 0.23	0.21 ± 0.01	0.35 ± 0.01	0.35 ± 0.01	6.91 ± 0.44	0.30 ± 0.02	0.58 ± 0.01	1.59 ± 0.16	5.66 ± 0.51	nd
		4	0.81 ± 0.05	1.06 ± 0.05	3.11 ± 0.17	0.30 ± 0.01	0.41 ± 0.02	0.44 ± 0.03	8.28 ± 0.66	0.37 ± 0.01	0.74 ± 0.02	2.28 ± 0.03	6.75 ± 0.55	nd
10	4	1	1.01 ± 0.07	1.90 ± 0.12	3.65 ± 0.30	1.55 ± 0.10	0.30 ± 0.00	0.52 ± 0.01	15.71 ± 1.02	0.54 ± 0.03	1.72 ± 0.01	3.71 ± 0.25	12.40 ± 1.02	nd
		2	0.84 ± 0.06	1.76 ± 0.12	3.45 ± 0.32	1.02 ± 0.03	0.10 ± 0.00	1.06 ± 0.01	13.16 ± 1.10	0.45 ± 0.03	1.52 ± 0.05	3.18 ± 0.24	10.82 ± 0.87	nd
		3	1.11 ± 0.10	1.92 ± 0.01	3.24 ± 0.26	1.54 ± 0.06	0.00 ± 0.00	0.66 ± 0.04	15.27 ± 0.96	0.53 ± 0.01	1.98 ± 0.07	3.61 ± 0.16	12.59 ± 0.99	nd
		4	1.16 ± 0.08	2.29 ± 0.17	4.81 ± 0.41	1.30 ± 0.09	0.13 ± 0.00	1.53 ± 0.09	17.51 ± 1.20	0.67 ± 0.04	1.12 ± 0.06	5.29 ± 0.41	13.87 ± 1.05	nd
50	5	1	0.99 ± 0.08	1.89 ± 0.10	4.40 ± 0.39	0.58 ± 0.01	0.62 ± 0.02	0.51 ± 0.01	12.71 ± 0.95	0.19 ± 0.01	0.91 ± 0.02	3.82 ± 0.12	9.22 ± 0.04	nd
		2	0.92 ± 0.03	2.01 ± 0.15	4.66 ± 0.44	0.45 ± 0.01	0.63 ± 0.03	0.42 ± 0.03	12.95 ± 0.96	0.19 ± 0.00	0.79 ± 0.03	3.87 ± 0.12	9.38 ± 0.23	nd
		3	0.95 ± 0.07	1.85 ± 0.12	4.18 ± 0.32	0.60 ± 0.03	0.60 ± 0.02	0.43 ± 0.02	12.49 ± 0.87	0.20 ± 0.01	0.80 ± 0.03	3.88 ± 0.05	9.38 ± 0.00	nd
		4	1.14 ± 0.05	2.17 ± 0.20	5.00 ± 0.47	0.60 ± 0.05	0.70 ± 0.05	0.52 ± 0.02	14.30 ± 0.56	0.65 ± 0.05	1.02 ± 0.08	4.34 ± 0.33	10.44 ± 0.21	nd
10	3	1	1.05 ± 0.06	1.89 ± 0.13	3.29 ± 0.15	1.34 ± 0.11	0.65 ± 0.05	0.40 ± 0.01	14.76 ± 1.11	0.26 ± 0.01	1.03 ± 0.07	4.76 ± 0.45	11.83 ± 0.66	nd
		2	1.23 ± 0.01	2.20 ± 0.17	3.73 ± 0.29	1.67 ± 0.10	0.77 ± 0.04	0.46 ± 0.02	17.67 ± 0.85	0.84 ± 0.06	1.24 ± 0.09	5.74 ± 0.55	14.10 ± 0.36	nd
		3	1.36 ± 0.10	2.21 ± 0.07	3.76 ± 0.21	1.93 ± 0.15	0.89 ± 0.01	0.69 ± 0.04	18.49 ± 0.84	0.89 ± 0.07	1.59 ± 0.10	5.88 ± 0.21	14.56 ± 0.74	nd
		4	1.80 ± 0.13	2.67 ± 0.09	5.38 ± 0.11	1.87 ± 0.06	1.13 ± 0.09	0.92 ± 0.08	21.88 ± 1.57	1.05 ± 0.09	1.76 ± 0.09	6.30 ± 0.11	15.84 ± 0.77	nd
80	5	1	2.07 ± 0.14	2.39 ± 0.13	6.10 ± 0.50	1.48 ± 0.03	1.08 ± 0.08	1.20 ± 0.10	20.38 ± 1.66	0.72 ± 0.05	1.99 ± 0.11	5.13 ± 0.26	14.83 ± 0.91	nd
		2	1.99 ± 0.15	2.71 ± 0.22	5.82 ± 0.33	2.00 ± 0.17	1.13 ± 0.09	1.13 ± 0.08	21.93 ± 2.00	0.82 ± 0.04	3.99 ± 0.12	5.62 ± 0.09	15.54 ± 1.21	0.36 ± 0.01
		3	2.01 ± 0.16	2.78 ± 0.26	5.57 ± 0.45	1.93 ± 0.18	1.14 ± 0.01	1.03 ± 0.07	21.25 ± 1.52	0.29 ± 0.01	3.93 ± 0.06	5.42 ± 0.49	15.64 ± 1.20	0.34 ± 0.00
		4	1.70 ± 0.09	3.12 ± 0.24	5.11 ± 0.28	2.25 ± 0.08	1.08 ± 0.08	0.85 ± 0.07	22.29 ± 0.98	0.82 ± 0.05	3.82 ± 0.14	5.90 ± 0.27	15.35 ± 0.59	0.35 ± 0.01
10	3	1	1.70 ± 0.09	3.12 ± 0.12	5.11 ± 0.24	2.25 ± 0.10	1.08 ± 0.07	0.85 ± 0.06	22.29 ± 0.58	0.82 ± 0.05	3.82 ± 0.20	5.90 ± 0.35	15.35 ± 0.85	0.35 ± 0.02
		2	1.19 ± 0.011	3.47 ± 0.21	6.67 ± 0.52	2.38 ± 0.07	1.32 ± 0.07	1.17 ± 0.11	25.40 ± 2.21	0.88 ± 0.06	4.50 ± 0.23	6.59 ± 0.24	17.55 ± 0.24	0.41 ± 0.01
		3	2.12 ± 0.18	3.28 ± 0.25	5.86 ± 0.23	2.49 ± 0.22	1.24 ± 0.10	1.10 ± 0.05	24.30 ± 0.33	0.87 ± 0.04	4.57 ± 0.17	6.37 ± 0.24	17.00 ± 1.05	0.44 ± 0.02
		4	2.45 ± 0.21	3.09 ± 0.11	6.03 ± 0.36	2.17 ± 0.14	1.26 ± 0.12	1.13 ± 0.09	24.40 ± 2.08	0.85 ± 0.03	4.48 ± 0.31	6.35 ± 0.52	16.56 ± 0.74	nd
110	5	1	1.69 ± 0.012	2.87 ± 0.06	5.91 ± 0.35	1.79 ± 0.17	1.00 ± 0.05	0.67 ± 0.02	20.89 ± 0.78	0.65 ± 0.03	2.90 ± 0.18	5.51 ± 0.31	14.72 ± 0.47	nd
		2	1.72 ± 0.14	3.50 ± 0.014	6.16 ± 0.41	2.18 ± 0.20	1.18 ± 0.09	0.82 ± 0.02	23.52 ± 0.32	0.92 ± 0.07	3.25 ± 0.22	6.21 ± 0.20	16.00 ± 1.25	0.32 ± 0.00
		3	1.77 ± 0.13	3.62 ± 0.22	5.94 ± 0.35	2.44 ± 0.19	0.98 ± 0.07	0.81 ± 0.05	23.20 ± 1.47	0.87 ± 0.06	3.57 ± 0.09	6.12 ± 0.54	16.41 ± 1.26	0.34 ± 0.01
		4	1.74 ± 0.14	3.43 ± 0.30	5.26 ± 0.47	2.50 ± 0.23	1.09 ± 0.06	0.74 ± 0.03	23.23 ± 0.88	0.76 ± 0.06	3.63 ± 0.16	5.77 ± 0.20	15.71 ± 0.93	0.36 ± 0.01
10	3	1	1.93 ± 0.15	3.40 ± 0.24	4.68 ± 0.43	2.65 ± 0.24	1.08 ± 0.06	0.73 ± 0.04	22.98 ± 1.26	0.81 ± 0.02	3.70 ± 0.08	5.83 ± 0.17	15.53 ± 0.88	0.43 ± 0.03
		2	2.04 ± 0.11	4.33 ± 0.36	2.50 ± 0.21	4.35 ± 0.37	0.95 ± 0.07	0.59 ± 0.03	30.16 ± 2.11	1.07 ± 0.01	4.54 ± 0.25	7.03 ± 0.66	19.02 ± 1.52	0.85 ± 0.04
		3	1.97 ± 0.05	3.45 ± 0.15	4.71 ± 0.12	3.00 ± 0.28	1.13 ± 0.03	0.80 ± 0.07	24.18 ± 1.45	0.90 ± 0.07	3.72 ± 0.15	6.19 ± 0.62	16.29 ± 0.62	0.55 ± 0.03
		4	1.77 ± 0.07	3.17 ± 0.27	3.93 ± 0.33	2.72 ± 0.18	0.97 ± 0.02	0.71 ± 0.06	23.07 ± 0.63	0.74 ± 0.06	3.74 ± 0.10	5.59 ± 0.47	15.80 ± 0.14	0.58 ± 0.04

ASE = accelerated solvent extraction, VIOLAX der = violaxanthin derivative, NEOF = neoxanthin, VIOLAX = violaxanthin, 13'-cis-LUT = 13'-cis-lutein, LUT 5,6-ep = lutein 5,6-epoxide, NEOF der = neoxanthin derivative, LUT = lutein, ZEAX = zeaxanthin, 9'-cis-LUT = 9'-cis-lutein, α-CAR = α-carotene, β-CAR = β-carotene, LYC der 10 = lycopene derivative 10, nd = not detected. Results are expressed as mean ± SD.

Table 2 provides the results of ASE conditions' impact on the yield of NL pigments. The sum of total pigments (TPG) includes total chlorophylls (TCH) and TCAR. The results showed that the temperature, static time and number of cycles significantly affected ($p < 0.01$) content of all analyzed pigments. TCH and TCAR increased two-fold with an increase in temperature (TCH 464.37 vs. 1075.25 mg 100 g⁻¹ dm, TCAR 31.48 vs. 65.81 mg 100 g⁻¹ dm). Nevertheless, it can be observed that several chlorophylls and carotenoids achieved maximum yield at 80 °C, while at 110 °C a decrease in yield was recorded (Tables 4 and 5). Considering static time, all pigments showed higher content at static time of 10 min and as for cycle number, it can be observed that the highest yields of pigments were achieved at the maximum cycle number (Table 2). Finally, the highest TPG was obtained at 110 °C (1141.06 mg 100 g⁻¹ dm), at the static time of 10 min (992.77 mg 100 g⁻¹ dm) and at the fourth cycle of extraction (928.82 mg 100 g⁻¹ dm) with temperature being dominant for influencing the extraction yield. Temperature increase affects the viscosity and solubility of the solvent, but degradation of the components can also occur if the applied temperature is too high [58]. Optimization of ASE parameters for carotenoids extraction (LUT and β -CAR) from carrot was also conducted by Saha et al. [58] by variation of temperature (40, 50 and 60 °C) and static time (5, 10 and 15 min). An increase in extraction yield for 4–8% was recorded by increasing the time for 5 min at 60 °C, but extraction efficiency was not observed when more than three cycles were carried out, giving 60 °C/15 min/3 cycles as optimal conditions. Furthermore, Cha et al. [59] investigated the effect of temperature (50, 105 and 160 °C) and static time (8, 19 and 30 min) on content of chlorophylls and carotenoids from algae *Chlorella vulgaris* and also concluded that temperature had the strongest influence on pigment extraction. They reported maximum yields of CHL *a* and *b* at the highest temperatures (150–160 °C), while β -CAR showed temperature sensitivity since its yield decreased at temperatures between 120 and 160 °C. Kim et al. [60] characterized twelve carotenoids from different varieties of paprika isolated using ASE at optimal conditions of 100 °C/5 min/3 cycles, and Mustafa et al. [56] reported 60 °C/2 min/5 cycles as the highest efficiency ASE conditions for carotenoids extraction from carrot by-products. They recorded a decrease of α - and β -CAR at temperatures above 120 °C, which is explainable by the thermo-sensitivity of carotenoids. They also proposed the use of several cycles, since some carotenoids are beginning to release during longer extraction time. Hojnik et al. [12] believe that for the extraction of chlorophylls it is necessary to conduct at least 2 extraction cycles in order to obtain a high yield, while Rafajlovska et al. [61] showed that multiple cycle extraction is better technique than one long cycle extraction. Although they applied different technique (supercritical CO₂ extraction), the levels of CHL *a* + *b* and β -CAR in NL significantly raised with the application of several steps of extraction. Further, chlorophylls dissolved better at higher pressure and temperature (210 bar, 50 °C) compared to the carotenoids (140 bar, 40 °C).

Comparing the pigment yields between ASE and UAE (Tables 3–5), it is evident that ASE yielded higher amounts of almost all pigments, especially the dominant ones. Research of Plaza et al. [62] also compared ASE and UAE for the extraction of chlorophylls and carotenoids from the algae *Chlorella*. It was concluded that ASE accomplished higher yields of pigments along with being a faster and more controlled technique. Moreover, Koo et al. [63] achieved a seven-fold higher amount of zeaxanthin from *Chlorella* in ASE extract compared to the extracts obtained with UAE. Based on the above results, ASE is a technique that executes higher yields of targeted compounds and protects sensitive compounds from light and oxygen under controlled conditions of temperature, pressure and extraction time [64].

3.3. Influence of Accelerated Solvent Extraction on Antioxidant Capacity

As already mentioned, it is well established that antioxidants prevent the oxidation of other substances and, in biological systems, they neutralize reactive free radicals, thus protect the body from various diseases. Since NL extracts already proved to be a very rich source of natural antioxidants, antioxidant capacity (AC) in obtained extracts was documented by the ORAC method (Table 1). ORAC values ranged from 2.42 to 22.07 mmol TE 100 g⁻¹ dm. The highest value was determined in extract obtained at 80 °C/10 min/3 cycles, after which a decline was recorded. Similar ORAC levels

were recorded by Moldovan et al. [8]. High AC of nettle was also confirmed in Skapska et al. [65] and Tian et al. [66] research.

Considering ASE conditions, temperature, static time and cycle number had a significant influence ($p < 0.01$) on the AC. The most suitable combination of ASE parameters for achieving the extract with the highest ORAC value was 80 °C/10 min/4 cycles, as presented in Table 2. Regarding temperature, AC of the extracts was three-fold higher at 80 °C (16.70 mmol TE 100 g⁻¹ dm) compared to the value at the initial temperature (5.52 mmol TE 100 g⁻¹ dm) and afterwards it slightly decreased. This points that analyzed compounds of NL extracts were stable at 80 °C. This is in accordance with previously discussed results since the increase of AC derives from the abundant presence of bioactive molecules at higher temperatures as a consequence of the cell-wall disruption and increased mass transfer from the sample to the pressurized solvent. Accordingly, Howard et al. [67] reported an increase of spinach extracts AC combined with elevated temperature as well as Benchikh and Louailèche [68] in study of carob pulp polyphenols.

Calculated correlation coefficients showed a very strong correlation ($r = 0.86$ – 0.94) between the analyzed compounds and ORAC levels (Table 6), showing that NL THCA and TF as well as pigments significantly contribute to its antioxidant potential. Previous research showed that phenolic acids and flavonoids are significant antioxidants [69–71] as well as chlorophylls [54] and carotenoids [72–75].

Table 6. Pearson's correlations between nettle leaves polyphenols (mg 100 g⁻¹ dm), pigments (mg 100 g⁻¹ dm) and ORAC values (mmol TE 100 g⁻¹ dm) in ASE extracts.

Parameter	ORAC
THCA	0.86 *
TF	0.87 *
TP	0.87 *
TCH	0.94 *
TCAR	0.92 *
TPG	0.92 *

ASE = accelerated solvent extraction, THCA = total hydroxycinnamic acids, TF = total flavonoids, TP = total phenols, TCH = total chlorophylls, TCAR = total carotenoids, TPG = total pigments. * $p \leq 0.05$.

When comparing AC between ASE and UAE extracts, the higher ORAC values were observed in ASE compared to UAE extracts (22.07 vs. 13.26 mmol TE 100 g⁻¹ dm) (Tables 1 and 3), confirming that ASE is more efficient for achieving high valuable extracts. Similarly, Hossain et al. [47] reported 77.52% higher AC in rosemary ASE extract in comparison with conventional extract, as a result of more efficient ASE of antioxidant phenolic compounds. Other authors also reported similar findings [51].

From all of the above, NL certainly represents a great source of various antioxidants (hydrophilic and lipophilic), where generally all analyzed compounds strongly contribute to AC. Moreover, ASE provides higher extraction yields of bioactive antioxidants in comparison with UAE; thus, it could be considered as an efficient green tool for the production of highly valuable nettle extracts for further industrial use.

4. Conclusions

Due to the increased interest in the industry for application of natural extracts in functional food production, the obtained results clearly demonstrate that ASE nettle extracts could be considered as green extracts for potential further use. Wild NL extracts were shown as a valuable natural source of structurally diverse bioactive compounds, polyphenols and pigments. Moreover, high efficiency for obtaining valuable NL extracts has been successfully obtained by ASE at optimized conditions of 110 °C, 10 min of static time and three or four cycles. Among the bioactive components that contribute to the biological value of NL, seven polyphenols belonging to the groups of hydroxycinnamic acids and flavonoids, chlorophylls *a* and *b* along with six of their derivatives and twelve carotenoids were present. Quantitatively, ChA was the most abundant polyphenol and CHL *a* represented the dominant pigment,

followed by CHL *b*, LUT and β -CAR. Furthermore, ASE showed better performance in comparison with UAE, obtaining higher yields of antioxidant compounds and 60% higher antioxidant capacity. Results of this study are fundamental for future research involving spray-drying of NL extracts and further implementation of the obtained NL powder into various food products.

Author Contributions: Conceptualization, M.R. and D.B.K.; Data curation, M.R., E.C., S.P. and F.Ç.; Formal analysis, V.K., S.P. and F.Ç.; Methodology, M.R., S.P. and D.B.K.; Project administration, V.D.-U.; Resources, I.Ž.; Supervision, V.D.-U.; Writing—original draft, M.R., E.C. and D.B.K.; Writing—review & editing, V.D.-U. All authors have read and agreed to the published version of the manuscript.

Funding: This work was supported by the Croatian Science Foundation project (grant number IP-01-2018-4924).

Conflicts of Interest: The authors declare no conflict of interest. The funders had no role in the design of the study; in the collection, analyses, or interpretation of data; in the writing of the manuscript, or in the decision to publish the results.

References

- Otles, S.; Yalcin, B. Phenolic compounds analysis of root, stalk, and leaves of nettle. *Sci. World J.* **2012**, *2012*, 1–12. [CrossRef] [PubMed]
- Durović, S.; Pavlič, B.; Šorgić, S.; Popov, S.; Savić, S.; Petronijević, M.; Radojković, M.; Cvetanović, A.; Zeković, Z. Chemical composition of stinging nettle leaves obtained by different analytical approaches. *J. Funct. Foods* **2017**, *32*, 18–26. [CrossRef]
- Grauso, L.; de Falco, B.; Lanzotti, V.; Motti, R. Stinging nettle, *Urtica dioica* L.: Botanical, phytochemical and pharmacological overview. *Phytochem. Rev.* **2020**. [CrossRef]
- Durović, S.; Vujanović, M.; Radojković, M.; Filipović, J.; Filipović, V.; Gašić, U.; Tešić, Ž.; Mašković, P.; Zeković, Z. The functional food production: Application of stinging nettle leaves and its extracts in the baking of a bread. *Food Chem.* **2020**, *312*. [CrossRef] [PubMed]
- Tomczyk, M.; Zaguła, G.; Dżugan, M. A simple method of enrichment of honey powder with phytochemicals and its potential application in isotonic drink industry. *Lwt* **2020**, *125*. [CrossRef]
- Hayward, L.; Wedel, A.; McSweeney, M.B. Acceptability of beer produced with dandelion, nettle, and sage. *Int. J. Gastron. Food Sci.* **2019**, *18*. [CrossRef]
- Marchetti, N.; Bonetti, G.; Brandolini, V.; Cavazzini, A.; Maietti, A.; Meca, G.; Mañes, J. Stinging nettle (*Urtica dioica* L.) as a functional food additive in egg pasta: Enrichment and bioaccessibility of Lutein and β -carotene. *J. Funct. Foods* **2018**, *47*, 547–553. [CrossRef]
- Moldovan, L.; Gaspar, A.; Toma, L.I.A.N.A.; Craciunescu, O.A.N.A.; Saviuc, C.R.I.N.A. Comparison of polyphenolic content and antioxidant capacity of five Romanian traditional medicinal plants. *Revista de Chimie -Buchar.* **2011**, *62*, 299–303.
- Orčić, D.; Francišковиć, M.; Bekvalac, K.; Svirčev, E.; Beara, I.; Lesjak, M.; Mimica-Dukić, N. Quantitative determination of plant phenolics in *Urtica dioica* extracts by high-performance liquid chromatography coupled with tandem mass spectrometric detection. *Food Chem.* **2014**, *143*, 48–53. [CrossRef]
- Carvalho, A.R.; Costa, G.; Figueirinha, A.; Liberal, J.; Prior, J.A.V.; Lopes, M.C.; Cruz, M.T.; Batista, M.T. *Urtica* spp.: Phenolic composition, safety, antioxidant and anti-inflammatory activities. *Food Res. Int.* **2017**, *99*, 485–494. [CrossRef]
- Guil-Guerrero, J.L.; Rebolloso-Fuentes, M.M.; Torija Isasa, M.E. Fatty acids and carotenoids from Stinging Nettle (*Urtica dioica* L.). *J. Food Compos. Anal.* **2003**, *16*, 111–119. [CrossRef]
- Hojnik, M.; Škerget, M.; Knez, Ž. Isolation of chlorophylls from stinging nettle (*Urtica dioica* L.). *Sep. Purif. Technol.* **2007**, *57*, 37–46. [CrossRef]
- Ibrahim, M.; Rehman, K.; Razzaq, A.; Hussain, I.; Farooq, T.; Hussain, A.; Akash, M.S.H. Investigations of phytochemical constituents and their pharmacological properties isolated from the genus *urtica*: Critical review and analysis. *Crit. Rev. Eukaryotic Gene Expr.* **2018**, *28*, 25–66. [CrossRef]
- Martínez-Aledo, N.; Navas-Carrillo, D.; Orenes-Piñero, E. Medicinal plants: Active compounds, properties and antiproliferative effects in colorectal cancer. *Phytochem. Rev.* **2020**, *19*, 123–137. [CrossRef]
- Ziaei, R.; Foshati, S.; Hadi, A.; Kermani, M.A.H.; Ghavami, A.; Clark, C.C.T.; Tarrahi, M.J. The effect of nettle (*Urtica dioica*) supplementation on the glycemic control of patients with type 2 diabetes mellitus: A systematic review and meta-analysis. *Phytother. Res.* **2019**, *34*, 282–294. [CrossRef]

16. Jacquet, A.; Girodet, P.-O.; Pariente, A.; Forest, K.; Mallet, L.; Moore, N. Phytalgic®, a food supplement, vs placebo in patients with osteoarthritis of the knee or hip: A randomised double-blind placebo-controlled clinical trial. *Arthritis Res. Ther.* **2009**, *11*. [CrossRef]
17. Cencic, A.; Chingwaru, W. The role of functional foods, nutraceuticals, and food supplements in intestinal health. *Nutrients* **2010**, *2*, 611–625. [CrossRef]
18. Granato, D.; Barba, F.J.; Bursać Kovačević, D.; Lorenzo, J.M.; Cruz, A.G.; Putnik, P. Functional foods: Product development, technological trends, efficacy testing, and safety. *Annu. Rev. Food Sci. Technol.* **2020**, *11*, 93–118. [CrossRef]
19. Stanojević, L.P.; Stanković, M.Z.; Cvetković, D.J.; Cakić, M.D.; Ilić, D.P.; Nikolić, V.D.; Stanojević, J.S. The effect of extraction techniques on yield, extraction kinetics, and antioxidant activity of aqueous-methanolic extracts from nettle (*Urtica dioica* L.) leaves. *Sep. Sci. Technol.* **2016**, *51*, 1817–1829. [CrossRef]
20. Chemat, F.; Vian, M.A.; Cravotto, G. Green extraction of natural products: Concept and principles. *Int. J. Mol. Sci.* **2012**, *13*, 8615–8627. [CrossRef]
21. Mottaleb, M.A.; Sarker, S.D. Accelerated Solvent Extraction for Natural Products Isolation. In *Natural Products Isolation*, 3rd ed.; Sarker, S.D., Nahar, L., Eds.; Springer: New York, NY, USA, 2012; pp. 75–88. [CrossRef]
22. Putnik, P.; Barba, F.J.; Španić, I.; Zorić, Z.; Dragović-Uzelac, V.; Bursać Kovačević, D. Green extraction approach for the recovery of polyphenols from Croatian olive leaves (*Olea europea*). *Food Bioprod. Process* **2017**, *106*, 19–28. [CrossRef]
23. Bursać Kovačević, D.; Barba, F.J.; Granato, D.; Galanakis, C.M.; Herceg, Z.; Dragović-Uzelac, V.; Putnik, P. Pressurized Hot Water Extraction (PHWE) for the green recovery of bioactive compounds and steviol glycosides from *Stevia rebaudiana* Bertoni Leaves. *Food Chem.* **2018**. [CrossRef]
24. Ameer, K.; Shahbaz, H.M.; Kwon, J.-H. Green extraction methods for polyphenols from plant matrices and their byproducts: A Review. *Compr. Rev. Food Sci. F* **2017**, *16*, 295–315. [CrossRef]
25. Jentzer, J.-B.; Alignan, M.; Vaca-Garcia, C.; Rigal, L.; Vilarem, G. Response surface methodology to optimise accelerated solvent extraction of steviol glycosides from *Stevia rebaudiana* Bertoni leaves. *Food Chem.* **2015**, *166*, 561–567. [CrossRef] [PubMed]
26. Pena-Pereira, F.; Lavilla, I.; Bendicho, C. Miniaturized preconcentration methods based on liquid–liquid extraction and their application in inorganic ultratrace analysis and speciation: A review. *Spectrochim. Acta Part B* **2009**, *64*, 1–15. [CrossRef]
27. Alexovič, M.; Dotsikas, Y.; Bober, P.; Sabo, J. Achievements in robotic automation of solvent extraction and related approaches for bioanalysis of pharmaceuticals. *J. Chromatogr. B* **2018**, *1092*, 402–421. [CrossRef] [PubMed]
28. Johnson, T.A.; Sohn, J.; Inman, W.D.; Bjeldanes, L.F.; Rayburn, K. Lipophilic stinging nettle extracts possess potent anti-inflammatory activity, are not cytotoxic and may be superior to traditional tinctures for treating inflammatory disorders. *Phytomedicine* **2013**, *20*, 143–147. [CrossRef]
29. Johnson, T.A.; Morgan, M.V.C.; Aratow, N.A.; Estee, S.A.; Sashidhara, K.V.; Loveridge, S.T.; Segraves, N.L.; Crews, P. Assessing Pressurized Liquid Extraction for the high-throughput extraction of marine-sponge-derived natural products. *J. Nat. Prod.* **2010**, *73*, 359–364. [CrossRef]
30. AOAC. *Official Methods of Analysis: Changes in Official Methods of Analysis Made at the Annual Meeting*, 15th ed.; Association of Official Analytical Chemists: Rockville, Maryland, 1990; Volume I, pp. 40–64.
31. Dent, M.; Dragović-Uzelac, V.; Penić, M.; Brnčić, M.; Bosiljkov, T.; Levaj, B. The effect of extraction solvents, temperature and time on the composition and mass fraction of polyphenols in dalmatian wild sage (*Salvia officinalis* L.) extracts. *Food Technol. Biotech.* **2013**, *51*, 84–91.
32. Akbay, P.; Basaran, A.A.; Undeger, U.; Basaran, N. *In vitro* immunomodulatory activity of flavonoid glycosides from *Urtica dioica* L. *Phytother. Res.* **2003**, *17*, 34–37. [CrossRef] [PubMed]
33. Farag, M.A.; Weigend, M.; Luebert, F.; Brokamp, G.; Wessjohann, L.A. Phytochemical, phylogenetic, and anti-inflammatory evaluation of 43 *Urtica* accessions (stinging nettle) based on UPLC–Q-TOF-MS metabolomic profiles. *Phytochemistry* **2013**, *96*, 170–183. [CrossRef] [PubMed]
34. Pinelli, P.; Ieri, F.; Vignolini, P.; Bacci, L.; Baronti, S.; Romani, A. Extraction and HPLC analysis of phenolic compounds in leaves, stalks, and textile fibers of *Urtica dioica* L. *J. Agric. Food Chem.* **2008**, *56*, 9127–9132. [CrossRef]

35. Castro-Puyana, M.; Pérez-Sánchez, A.; Valdés, A.; Ibrahim, O.H.M.; Suarez-Álvarez, S.; Ferragut, J.A.; Micol, V.; Cifuentes, A.; Ibáñez, E.; García-Cañas, V. Pressurized liquid extraction of *Neochloris oleoabundans* for the recovery of bioactive carotenoids with anti-proliferative activity against human colon cancer cells. *Food Res. Int.* **2017**, *99*, 1048–1055. [CrossRef]
36. Gupta, P.; Sreelakshmi, Y.; Sharma, R. A rapid and sensitive method for determination of carotenoids in plant tissues by high performance liquid chromatography. *Plant. Methods* **2015**, *11*, s13007–s13015. [CrossRef] [PubMed]
37. Sözgen Başkan, K.; Tütem, E.; Özer, N.; Apak, R. Spectrophotometric and chromatographic assessment of contributions of carotenoids and chlorophylls to the total antioxidant capacities of plant foods. *J. Agric. Food Chem.* **2013**, *61*, 11371–11381. [CrossRef] [PubMed]
38. Prior, R.L.; Wu, X.L.; Schaich, K. Standardized methods for the determination of antioxidant capacity and phenolics in foods and dietary supplements. *J. Agric. Food Chem.* **2005**, *53*, 4290–4302. [CrossRef]
39. Bender, C.; Graziano, S.; Zimmerman, B.F.; Weidlich, H.H. Antioxidant potential of aqueous plant extracts assessed by the cellular antioxidant activity assay. *Am. J. Biol. Life Sci.* **2014**, *2*, 72–79.
40. Rodríguez-Rojo, S.; Visentin, A.; Maestri, D.; Cocero, M.J. Assisted extraction of rosemary antioxidants with green solvents. *J. Food Eng.* **2012**, *109*, 98–103. [CrossRef]
41. Carabias-Martínez, R.; Rodríguez-Gonzalo, E.; Revilla-Ruiz, P.; Hernández-Méndez, J. Pressurized liquid extraction in the analysis of food and biological samples. *J. Chromatogr. A* **2005**, *1089*, 1–17. [CrossRef]
42. Vajić, U.-J.; Grujić-Milanović, J.; Živković, J.; Šavikin, K.; Godevac, D.; Miloradović, Z.; Bugarški, B.; Mihailović-Stanojević, N. Optimization of extraction of stinging nettle leaf phenolic compounds using response surface methodology. *Ind. Crops Prod.* **2015**, *74*, 912–917. [CrossRef]
43. Moreira, S.A.; Silva, S.; Costa, E.M.; Saraiva, J.A.; Pintado, M. Effect of high hydrostatic pressure extraction on biological activities of stinging nettle extracts. *Food Funct.* **2020**, *11*, 921–931. [CrossRef] [PubMed]
44. Zeipina, S.; Alsina, I.; Lepse, L. Stinging nettle—the source of biologically active compounds as sustainable daily diet supplement. *Res. Rural. Dev.* **2014**, *20*, 34–38.
45. Ciulu, M.; Quirantes-Piné, R.; Spano, N.; Sanna, G.; Borrás-Linares, I.; Segura-Carretero, A. Evaluation of new extraction approaches to obtain phenolic compound-rich extracts from *Stevia rebaudiana* Bertoni leaves. *Ind. Crops Prod.* **2017**, *108*, 106–112. [CrossRef]
46. Zgórká, G. Pressurized liquid extraction versus other extraction techniques in micropreparative isolation of pharmacologically active isoflavones from *Trifolium* L. species. *Talanta* **2009**, *79*, 46–53. [CrossRef] [PubMed]
47. Hossain, M.B.; Barry-Ryan, C.; Martin-Diana, A.B.; Brunton, N.P. Optimisation of accelerated solvent extraction of antioxidant compounds from rosemary (*Rosmarinus officinalis* L.), marjoram (*Origanum majorana* L.) and oregano (*Origanum vulgare* L.) using response surface methodology. *Food Chem.* **2011**, *126*, 339–346. [CrossRef]
48. Erdoğan, S.; Erdemoğlu, S. Evaluation of polyphenol contents in differently processed apricots using accelerated solvent extraction followed by high-performance liquid chromatography–diode array detector. *Int. J. Food Sci. Nutr.* **2011**, *62*, 729–739. [CrossRef]
49. Gomes, S.V.F.; Portugal, L.A.; dos Anjos, J.P.; de Jesus, O.N.; de Oliveira, E.J.; David, J.P.; David, J.M. Accelerated solvent extraction of phenolic compounds exploiting a Box-Behnken design and quantification of five flavonoids by HPLC-DAD in *Passiflora* species. *Microchem. J.* **2017**, *132*, 28–35. [CrossRef]
50. Esclapez, M.D.; García-Pérez, J.V.; Mulet, A.; Cárcel, J.A. Ultrasound-Assisted Extraction of natural products. *Food Eng. Rev.* **2011**, *3*, 108–120. [CrossRef]
51. Zengin, G.; Cvetanović, A.; Gašić, U.; Stupar, A.; Bulut, G.; Şenkardes, I.; Dogan, A.; Ibrahim Sinan, K.; Uysal, S.; Aumeeruddy-Elalfi, Z.; et al. Modern and traditional extraction techniques affect chemical composition and bioactivity of *Tanacetum parthenium* (L.) Sch.Bip. *Ind. Crops Prod.* **2020**, *146*. [CrossRef]
52. Barros, F.; Dykes, L.; Awika, J.M.; Rooney, L.W. Accelerated solvent extraction of phenolic compounds from sorghum brans. *J. Cereal Sci.* **2013**, *58*, 305–312. [CrossRef]
53. Alkema, J.; Seager, S.L. The chemical pigments of plants. *J. Chem. Educ.* **1982**, *59*. [CrossRef]
54. Ferruzzi, M.G.; Bohm, V.; Courtney, P.D.; Schwartz, S.J. Antioxidant and antimutagenic activity of dietary chlorophyll derivatives determined by radical scavenging and bacterial reverse mutagenesis assays. *J. Food Sci.* **2002**, *67*, 2589–2595. [CrossRef]

55. Jaime, L.; Rodríguez-Meizoso, I.; Cifuentes, A.; Santoyo, S.; Suarez, S.; Ibáñez, E.; Señorans, F.J. Pressurized liquids as an alternative process to antioxidant carotenoids' extraction from *Haematococcus pluvialis* microalgae. *Lwt Food Sci. Technol.* **2010**, *43*, 105–112. [CrossRef]
56. Mustafa, A.; Trevino, L.M.; Turner, C. Pressurized hot ethanol extraction of carotenoids from carrot by-products. *Molecules* **2012**, *17*, 1809–1818. [CrossRef]
57. Sovová, H.; Sajfrtová, M.; Bártlová, M.; Opletal, L. Near-critical extraction of pigments and oleoresin from stinging nettle leaves. *J. Supercrit. Fluids* **2004**, *30*, 213–224. [CrossRef]
58. Saha, S.; Walia, S.; Kundu, A.; Sharma, K.; Paul, R.K. Optimal extraction and fingerprinting of carotenoids by accelerated solvent extraction and liquid chromatography with tandem mass spectrometry. *Food Chem.* **2015**, *177*, 369–375. [CrossRef]
59. Cha, K.H.; Lee, H.J.; Koo, S.Y.; Song, D.-G.; Lee, D.-U.; Pan, C.-H. Optimization of Pressurized Liquid Extraction of carotenoids and chlorophylls from *Chlorella vulgaris*. *J. Agric. Food Chem.* **2010**, *58*, 793–797. [CrossRef]
60. Kim, J.-S.; An, C.G.; Park, J.-S.; Lim, Y.P.; Kim, S. Carotenoid profiling from 27 types of paprika (*Capsicum annuum* L.) with different colors, shapes, and cultivation methods. *Food Chem.* **2016**, *201*, 64–71. [CrossRef]
61. Rafajlovska, V.; Djarmati, Z.; Najdenova, V.; Cvetkov, L. Extraction of stinging nettle (*Urtica dioica* L.) with supercritical carbon dioxide. *Balikesir Üniversitesi Fen Bilimleri Enstitüsü Dergisi* **2016**, *4*, 49–52.
62. Plaza, M.; Santoyo, S.; Jaime, L.; Avalo, B.; Cifuentes, A.; Reglero, G.; García-Blairsy Reina, G.; Señorans, F.J.; Ibáñez, E. Comprehensive characterization of the functional activities of pressurized liquid and ultrasound-assisted extracts from *Chlorella vulgaris*. *Lwt-Food Sci. Technol.* **2012**, *46*, 245–253. [CrossRef]
63. Koo, S.Y.; Cha, K.H.; Song, D.-G.; Chung, D.; Pan, C.-H. Optimization of pressurized liquid extraction of zeaxanthin from *Chlorella ellipsoidea*. *J. Appl. Phycol.* **2011**, *24*, 725–730. [CrossRef]
64. Cheng, S.H.; Khoo, H.E.; Kong, K.W.; Prasad, K.N.; Galanakis, C.M. Extraction of carotenoids and applications. In *Carotenoids: Properties, Processing and Applications*; Galanakis, C.M., Ed.; Academic Press: New York, NY, USA, 2020; pp. 259–288. [CrossRef]
65. Skapska, S.; Marszałek, K.; Woźniak, L.; Zawada, K.; Wawer, I. Aronia dietary drinks fortified with selected herbal extracts preserved by thermal pasteurization and high pressure carbon dioxide. *Lwt-Food Sci. Technol.* **2017**, *85*, 423–426. [CrossRef]
66. Tian, Y.; Pughanen, A.; Alakomi, H.-L.; Uusitupa, A.; Saarela, M.; Yang, B. Antioxidative and antibacterial activities of aqueous ethanol extracts of berries, leaves, and branches of berry plants. *Food Res. Int.* **2018**, *106*, 291–303. [CrossRef]
67. Howard, L.; Pandjaitan, N. Pressurized Liquid Extraction of flavonoids from spinach. *J. Food Sci.* **2008**, *73*, C151–C157. [CrossRef]
68. Benchikh, Y.; Louailèche, H. Effects of extraction conditions on the recovery of phenolic compounds and in vitro antioxidant activity of carob (*Ceratonia siliqua* L.) pulp. *Acta Botanica Gallica* **2014**, *161*, 175–181. [CrossRef]
69. Četković, G.; Čanadanović-Brunet, J.; Djilas, S.; Tumbas, V.; Markov, S.; Cvetković, D. Antioxidant potential, lipid peroxidation inhibition and antimicrobial activities of *Satureja montana* L. subsp. *kitaibelii* extracts. *Int. J. Mol. Sci.* **2007**, *8*, 1013–1027. [CrossRef]
70. Miguel, M.G. Antioxidant activity of medicinal and aromatic plants. A review. *Flavour Fragr. J.* **2010**, *25*, 291–312. [CrossRef]
71. Zenão, S.; Aires, A.; Dias, C.; Saavedra, M.J.; Fernandes, C. Antibacterial potential of *Urtica dioica* and *Lavandula angustifolia* extracts against methicillin resistant *Staphylococcus aureus* isolated from diabetic foot ulcers. *J. Herbal Med.* **2017**, *10*, 53–58. [CrossRef]
72. Böhm, V.; Puspitasari-Nienaber, N.L.; Ferruzzi, M.G.; Schwartz, S.J. Trolox equivalent antioxidant capacity of different geometrical isomers of α -carotene, β -carotene, lycopene, and zeaxanthin. *J. Agric. Food Chem.* **2002**, *50*, 221–226. [CrossRef]
73. Ben-dor, A.; Steiner, M.; Gheber, L.; Danilenko, M.; Dubi, N.; Linnewiel, K.; Zick, A.; Sharoni, Y.; Levy, J. Carotenoids activate the antioxidant response element transcription system. Carotenoids activate the antioxidant response element transcription system. *Mol. Cancer Ther.* **2005**, *4*, 177–186. [PubMed]

74. Dewick, P.M. *Medicinal Natural Products: A Biosynthetic Approach*; John Wiley & Sons Ltd.: Chichester, UK, 2009.
75. Yunbo, L. Carotenoids. In *Antioxidants in Biology and Medicine: Essentials, Advances, and Clinical Applications*; Tsisana Shartava, M.D., Tbilisi, G., Eds.; Nova Science Publishers Inc.: New York, NY, USA, 2011.



© 2020 by the authors. Licensee MDPI, Basel, Switzerland. This article is an open access article distributed under the terms and conditions of the Creative Commons Attribution (CC BY) license (<http://creativecommons.org/licenses/by/4.0/>).

Article

Production of Liquid Milk Protein Concentrate with Antioxidant Capacity, Angiotensin Converting Enzyme Inhibitory Activity, Antibacterial Activity, and Hypoallergenic Property by Membrane Filtration and Enzymatic Modification of Proteins

Arijit Nath ^{1,*}, Burak Atilla Eren ¹, Attila Csighy ¹, Klára Pásztorné-Huszár ², Gabriella Kiskó ³, László Abrankó ⁴, Attila Tóth ⁵, Emőke Szerdahelyi ⁶, Zoltán Kovács ⁷, András Koris ¹ and Gyula Vatai ^{1,*}

¹ Department of Food Engineering, Faculty of Food Science, Szent István University, Ménési st 44, HU-1118 Budapest, Hungary; Eren.Burak.Atilla@hallgato.uni-szie.hu (B.A.E.); Attila.Csighy@phd.uni-szie.hu (A.C.); Koris.Andras@etk.szie.hu (A.K.)

² Department of Refrigeration and Livestock Products Technology, Faculty of Food Science, Szent István University, Ménési út 43-45, HU-1118 Budapest, Hungary; pasztorne.huszar.klara@etk.szie.hu

³ Department of Food Microbiology and Biotechnology, Faculty of Food Science, Szent István University, Somlói st 14–16, HU-1118 Budapest, Hungary; Kisko.Gabriella@etk.szie.hu

⁴ Department of Applied Chemistry, Faculty of Food Science, Szent István University, Villányi út 29-43, HU-1118 Budapest, Hungary; Abranko.Laszlo@etk.szie.hu

⁵ Division of Clinical Physiology, Department of Cardiology, Faculty of Medicine, University of Debrecen, Móricz Zsigmond Str 22, HU-4032 Debrecen, Hungary; atitoth@med.unideb.hu

⁶ Department of Biology, National Agricultural Research and Innovation Center, Food Science Research Institute, Herman Ottó út 15, HU-1022 Budapest, Hungary; szerdahelyi.emoke@eki.naik.hu

⁷ Department of Physics and Control, Faculty of Food Science, Szent István University, Somlói street 14-16, HU-1118 Budapest, Hungary; Kovacs.Zoltan3@etk.szie.hu

* Correspondence: arijit0410@gmail.com (A.N.); Vatai.Gyula@etk.szie.hu (G.V.); Tel.: +36-1-305-7110 (A.N.); +36-1-305-7115 (G.V.)

Received: 3 June 2020; Accepted: 10 July 2020; Published: 18 July 2020

Abstract: Liquid milk protein concentrate with different beneficial values was prepared by membrane filtration and enzymatic modification of proteins in a sequential way. In the first step, milk protein concentrate was produced from ultra-heat-treated skimmed milk by removing milk serum as permeate. A tubular ceramic-made membrane with filtration area $5 \times 10^{-3} \text{ m}^2$ and pore size 5 nm, placed in a cross-flow membrane house, was adopted. Superior operational strategy in filtration process was herein: trans-membrane pressure 3 bar, retention flow rate $100 \text{ L} \cdot \text{h}^{-1}$, and implementation of a static turbulence promoter within the tubular membrane. Milk with concentrated proteins from retentate side was treated with the different concentrations of trypsin, ranging from $0.008\text{--}0.064 \text{ g} \cdot \text{L}^{-1}$ in individual batch-mode operations at temperature $40 \text{ }^\circ\text{C}$ for 10 min. Subsequently, inactivation of trypsin in reaction was done at a temperature of $70 \text{ }^\circ\text{C}$ for 30 min of incubation. Antioxidant capacity in enzyme-treated liquid milk protein concentrate was measured with the Ferric reducing ability of plasma assay. The reduction of angiotensin converting enzyme activity by enzyme-treated liquid milk protein concentrate was measured with substrate (Abz-FRK(Dnp)-P) and recombinant angiotensin converting enzyme. The antibacterial activity of enzyme-treated liquid milk protein concentrate towards *Bacillus cereus* and *Staphylococcus aureus* was tested. Antioxidant capacity, anti-angiotensin converting enzyme activity, and antibacterial activity were increased with the increase of trypsin concentration in proteolytic reaction. Immune-reactive proteins in enzyme-treated liquid milk protein concentrate were identified with clinically proved milk positive pooled human serum and peroxidase-labelled anti-human Immunoglobulin E. The reduction of allergenicity in milk protein concentrate was enzyme dose-dependent.

Keywords: liquid milk protein concentrate; antioxidant capacity; angiotensin converting enzyme inhibitory activity; antibacterial activity; hypoallergenic property

1. Introduction

For years, different types of non-fermented and fermented dairy-based food formulas are received great attention among different communities. As time progressed, dairy industries tried their best to improve the quality of dairy-based formulas to fulfill the expectations of consumers [1]. For industrial production of fermented dairy products, milk with a standardized amount of protein is necessary to maintain the quality of products [2,3]. Different dairy-based protein concentrates, such as milk protein concentrate, milk protein isolate, whey protein concentrate, whey protein isolate, micellar casein concentrate, micellar casein isolate, whey concentrate, and selectively demineralized whey concentrate are widely used in the food and biopharmaceutical industries [4]. Milk protein concentrate is well accepted among all communities because it is an abundant source of the various kinds of proteins, including micellar casein, whey proteins, and glycomacropeptide, and has significantly lower amounts of lactose and fat compared to whey protein concentrate and whole milk protein concentrate, respectively [5]. Therefore, it is popularly used to prepare infant formula, protein bar, yogurt, recombined cheese, cultured product, frozen dessert, weight management products, and sports formulas [6]. To produce dairy-based protein concentrate, large-scale production plants with different unit operations are requirement. It may be noted that production of milk varies throughout the year. During the spring season, milk production is quite high compared to the fall season. To balance economic competitiveness, small-scale and medium-scale dairy industries avoid expensive processing steps, such as evaporation and drying to prepare dairy-based protein concentrate in powder form, and prefer to use liquid milk protein concentrate for manufacturing fresh cultured-food products [7,8].

In the dairy industry, application of membrane technology is noteworthy. Membrane technology is used for preparing concentrated milk proteins, fractionation of dairy proteins, demineralization of whey, and removal of microbial count in milk [9–11]. In some cases, ultrafiltration or nanofiltration operated with diafiltration mode was adopted to achieve high protein concentrate and avoid membrane fouling [12–14]. Some limitations in this context are reported. The limitations are (a) development of gel layer (concentration polarization) on the membrane surface and subsequent membrane fouling, and (b) high energy consumption. During filtration, due to deposition of solute molecules on the membrane surface, concentration polarization take place on the membrane surface. Because of this, permeate flux is reduced in drastic way [15–17]. However, increase of trans-membrane pressure (TMP) or fluid flow through a mechanical pump reduces the development of gel layer on the membrane surface; there is a debating issue about high energy consumption [18,19]. Therefore, it may feel that an efficient membrane separation process and its operational strategy are needed to explore to produce liquid milk protein concentrate.

However, milk has gained a great attention around the globe due to the presence of the different types of proteins (α_{S1} -casein, α_{S2} -casein, β -casein, κ -casein, γ -casein, immunoglobulin, bovine serum albumin, lactoferrin, α -lactalbumin, and β -lactoglobulin), lactose, vitamins (vitamin A, vitamin E, ascorbic acid, riboflavin, vitamin B6, nicotinic acid, pantothenic acid, and thiamin) and minerals (calcium, magnesium, phosphorus, potassium, selenium, and zinc) [20]. The milk sensitive community frequently experiences with the symptoms of immunoglobulin-mediated milk protein allergies, in some cases [21,22]. Due to the presence of Immunoglobulin E- and Immunoglobulin G- binding epitopes, milk proteins are listed among the “big 8” allergens [23,24]. Milk allergens provoke mild symptoms to life-threatening biochemical outcomes, including severe enterocolitis atopic eczema and immediate immunoglobulin-mediated systematic multisystem reactions [25]. Milk is not recommended in the diet chart due to the presence of saturated fatty acids—those contribute heart disease [26,27], type 2 diabetes, and Alzheimer’s disease [28,29]. Furthermore, due to the absence of lactase, a hydrolytic

enzyme in brush border of epithelial cells in the small intestine, the milk sensitive community frequently suffers with symptoms of lactose maldigestion [20,21]. However, concentrations of lactose and fat in milk protein concentrate are significantly low; in some cases, food formulas fortified with milk protein concentrate offer immunoglobulin-mediated allergies among people of all ages [30,31]. A plethora of literature about thermal and non-thermal processing technologies have been adopted to combat milk protein allergens [32,33]. The reduction in protein allergenicity in the molecular basis is the destruction of structure of epitopes. Applications of high pressure- [34,35], heat- [36–38], microwave- [39], and membrane bioreactors [40,41] were implemented for the reduction of allergenic sequences in milk proteins. In some cases, physical- [42–44] and enzymatic- [45–48] modifications of proteins have been adopted for a similar objective. Furthermore, combined physical and biochemical technologies have been adopted for the reduction of milk protein allergens [49–56]. In some cases, new epitopes (neoepitopes) or hidden epitopes may even be produced during cow milk processing due to denaturation of native allergen (cryptotopes) [57]. Realizing advantages and disadvantages of mentioned technologies, it may feel that enzymatic hydrolysis of allergenic epitopes in protein sequences may be an effective attempt to reduce milk protein allergens. Besides the elimination of their allergenic potentiality, modification of milk proteins through enzymatic routes may alter their functional properties, because peptides with unique amino acids in C- and N- terminal positions are produced through enzymatic hydrolysis of peptide bonds in milk proteins. Furthermore, the enzymatic modification of milk proteins may generate new antigenic substances, which may offer immunomodulation, and provide extra health benefits [58]. However, lots of information about the reduction of allergenic epitopes in milk proteins through an enzymatic route are stored in scholarly databases; its production in industrial scale is limited [59]. The challenging issues in enzyme-mediated process are (a) high cost of enzymes, and (b) find out suitable operating process parameters in enzyme-mediated processes. Therefore, it can feel that an investigation is needed to find out the minimum amount of enzymes, which is responsible for reducing a significant amount (>99.9%) of the allergenic sequence and improve the functional activities of milk protein concentrate. Trypsin is an endopeptidase generally found in the pancreas of mammals, and cleaves at the carboxyl terminal side of arginine and lysine amino acid residues, except arginyl-proline and lysyl-proline bonds. It is popularly used for preparation of dairy formulations with lower antigenic activities [60,61]. As the catalytic activity of trypsin is quite high (relative activity 99%) at pH 7 and may be able to change the biological activity of proteins and peptides [62–64], it was used in this investigation.

From the above discussion, one can realize that efforts are needed to reduce the limitations of milk protein concentrate production and dairy product consumption. In this investigation, an attempt was considered to develop liquid milk protein concentrate from ultra-heat-treated skimmed milk with antioxidant capacity, angiotensin converting enzyme inhibitory activity, antibacterial activity, and hypoallergenic property by membrane filtration and enzymatic modification of proteins in a sequential way. In the present investigation, membrane filtration process was adopted to increase the protein concentration in milk by reducing the milk serum as permeate and, subsequently, trypsin was adopted to hydrolyze the concentrated liquid milk proteins, obtained at the retentate side. Membrane filtration process itself cannot change the structural and biological activities of milk proteins. Peptides, produced by enzymatic hydrolysis of milk proteins with unique C- and N-terminal amino acids, peptide length, and amino acid sequence, offer distinguishing biological activities. Furthermore, allergenic activity of proteins is reduced due to enzymatic cleavage in allergenic epitopes within the amino acid sequence in protein.

2. Materials and Methods

2.1. Chemicals and Reagents

Lyophilized trypsin (≥ 27.78 units per mg of solid at temperature 25 °C) from bovine pancreas, Bradford reagent, bovine serum albumin, casein, α -lactalbumin and β -lactoglobulin from bovine milk,

Abz-FRK(Dnp)-P, peroxidase-labelled anti-human Immunoglobulin E, 2,4,6-Tris(2-pyridyl)-s-triazine ($\geq 98\%$), 4-chloronaphtol ($\geq 98\%$), hydrogen peroxide ($\geq 98\%$), ethanol ($\geq 99\%$), and phosphate buffered saline solution were purchased from the Sigma-Aldrich (Sigma-Aldrich, Schnellendorf, Germany). Ultrasil P3-11 was purchased from Ecolab-Hygiene Kft (Ecolab-Hygiene Kft, Budapest, Hungary). Citric acid (99%), hydrochloric acid ($\geq 99\%$), urea ($\geq 99\%$), dithiothreitol (DTT) and sodium hydroxide ($\geq 99\%$) were purchased from Reanal Kft (Reanal Kft, Budapest, Hungary). Ferric chloride ($\geq 99\%$), sodium acetate (anhydrous, $\geq 99\%$), sodium chloride ($\geq 99\%$), zinc chloride ($\geq 99\%$), bacteriological agar powder, soybean casein digestive medium and ascorbic acid (99.7%) were procured from Merck (Merck, Darmstadt, Germany). Sodium-dodecyl sulphate ($\geq 99\%$), acrylamide ($\geq 99\%$), ammonium persulfate ($\geq 99\%$), bis-acrylamide ($\geq 99\%$), tetramethylethylenediamine ($\geq 99\%$), tris(hydroxymethyl)aminomethane hydrochloride (TRIS HCl), ethyl alcohol ($\geq 99\%$), glycine ($\geq 99\%$), coomassie blue stain R250 ($\geq 99\%$), acetic acid ($\geq 99\%$), glycerol ($\geq 99\%$), isopropanol ($\geq 99\%$), 2 β -mercaptoethanol ($\geq 99\%$), and bromophenol blue ($\geq 99\%$) were procured from Bio-Rad (Bio-Rad, Hercules, USA). High performance liquid chromatography mass spectrometry (HPLC-MS)-grade acetonitrile, formic acid, and trisodium citrate ($\geq 99\%$) were purchased from VWR International Ltd. (VWR International Ltd., Debrecen, Hungary). Recombinant angiotensin converting enzyme was kindly provided by Division of Clinical Physiology, Institute of Cardiology, University of Debrecen (University of Debrecen, Debrecen, Hungary). *Bacillus cereus* and *Staphylococcus aureus* ATCC 6538 were collected from the Strain collection unit of Szent István University (Szent István University, Budapest, Hungary). Milli-Q ultrapure deionized water (18.2 M Ω ·cm) was obtained from Milli-Q Synergy/Elix water purification system (Merck-Millipore, Molsheim, France) and used throughout the experiment.

2.2. Ultra-Heat-Treated Skimmed Cow Milk

Ultra-heat-treated skimmed cow milk was procured from local supermarkets, in and around Budapest, Hungary. Concentrations of protein, lactose, and fat in milk were in average $31 \pm 0.16 \text{ g}\cdot\text{L}^{-1}$, $47 \pm 0.15 \text{ g}\cdot\text{L}^{-1}$ and $1 \pm 0.02 \text{ g}\cdot\text{L}^{-1}$, respectively. Average pH of milk was 6.8. Milk was stored in a refrigerator at temperature 10 °C.

2.3. Production of Hypoallergenic Liquid Milk Protein Concentrate with Functional Values

An attempt was considered to develop a process to produce allergen-free liquid milk protein concentrate with functional values, such as antioxidant capacity, angiotensin converting enzyme inhibitory activity, and antibacterial activity. Combination of different physical- and biochemical-based technologies were adopted for this purpose (Figure 1).

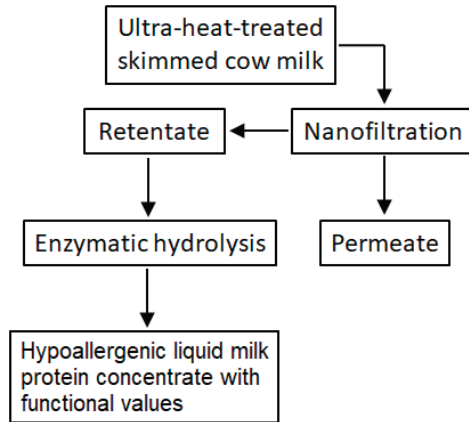


Figure 1. Experimental steps for preparing hypoallergenic liquid milk protein concentrate with functional values (antioxidant capacity, angiotensin converting enzyme inhibitory activity, and antibacterial activity).

2.3.1. Concentrate Milk Proteins in Ultra-Heat-Treated Skimmed Milk by Membrane Technology

De-watering (remove of milk serum) of ultra-heat-treated skimmed milk was performed by a tubular nanofiltration membrane with active filtration area $5 \times 10^{-3} \text{ m}^2$ and pore size 5 nm (Pall Corporation, Crailsheim, Germany), placed in a stainless steel-made cross-flow membrane module (Figure 2). The active layer, support layer, length, inner diameter, and outer diameter of the membrane were titanium oxide, aluminum oxide, 250 mm, 7 mm, and 10 mm, respectively. In the membrane module, feed flow rate was controlled by a centrifugal pump (Verder Hungary Kft, Budapest, Hungary). Flow rate of fluid (milk, water) in the membrane module was also controlled by a rotameter at a retentate flow channel and a bypass channel at the inlet channel of the membrane module. TMP of the membrane module was controlled by pressure gauges, fitted at inlet and retentate flow channels of the membrane module. A mechanical agitator was fitted inside of the storage tank of the membrane module. Temperature in the storage tank of the membrane module was maintained by a temperature sensor and automated circulation of warm/cold water within the water jacket.

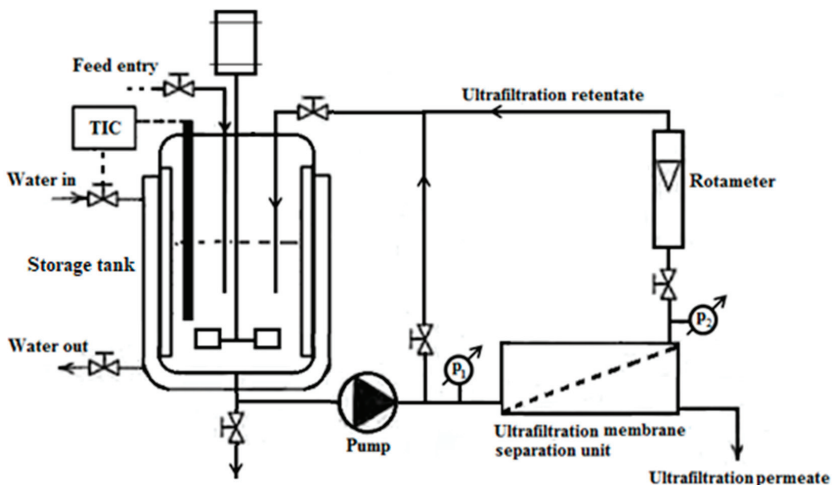


Figure 2. Schematic diagram of the cross-flow membrane module.

A mechanical device, known as static turbulence promoter, made of stainless steel (SS316), was inserted within the membrane tube. Detailed geometry of the static turbulence promoter is mentioned in an earlier publication [65]. To investigate the effects of process parameters in filtration process, different TMPs, such as 2 bar and 3 bar, and retention flow rates (RFRs), such as 100 L·h⁻¹ and 200 L·h⁻¹, were used with or without the static turbulence promoter. Each membrane filtration experiment started with 1 L of ultra-heat-treated skimmed milk, and volume reduction factor 2 was considered. Membrane filtration process was performed with a batch recirculation mode. Constant volume of permeate from the membrane was collected at different time fractions and permeate flux (J) was calculated with the following equation.

$$J = V/(A \times t) \quad (1)$$

where, J = permeate flux during filtration (L m⁻²·h⁻¹), V = volume of permeate (L), A = active membrane filtration area (m²) and t = filtration time (h) [66].

In the feed tank, after 50% reduction of volume (volume reduction factor 2), reduction of permeate flux (ΔJ) was calculated from initial permeate flux with Equation (2).

$$\Delta J (\%) = (J_{initial} - J_{final}) \times 100/J_{initial} \quad (2)$$

where, ΔJ = reduction of permeate flux (-), $J_{initial}$ = initial permeate flux (L m⁻²·h⁻¹) and J_{final} = final permeate flux (L m⁻²·h⁻¹) [65].

During filtration, pressures at inlet and retentate flow channels of the membrane module were recorded. Specific energy consumption (E_s) was calculated with Equation (3).

$$E_s = (RFR \times \Delta p)/(J_{initial} \times A) \quad (3)$$

where, E_s = specific energy consumption (kWh·m⁻³), Q_R = retention flow rate (L·h⁻¹), Δp = difference of pressure (Newton·m⁻²), A = active membrane filtration area (m²) and $J_{initial}$ = initial permeate flux (L m⁻²·h⁻¹) [65].

After removing the milk serum, membrane cleaning was performed with 1% ultrasil and 1% citric acid in a sequential way with intermediate water cleaning. During cleaning with ultrasil and citric acid, TMP 0.8 bar and RFR 200 L h⁻¹ were used. During cleaning with water, TMP 4 bar and RFR 200 L h⁻¹ were used. Prior to removing the milk serum, membrane compaction was performed with de-ionized water to achieve the steady state water permeate flux. For that purpose, TMP 4 bar and RFR 200 L·h⁻¹ were used [67].

2.3.2. Enzymatic Hydrolysis of Concentrated Proteins in Milk

Milk with concentrated proteins was collected from the storage tank of the membrane module. Prior to enzymatic reaction, milk with concentrated proteins, pH 7 was pre-incubated until the temperature reached 40 °C in a laboratory-scale well-controlled jacketed bioreactor, working volume 0.6 L and aspect ratio H/D* 2:1 (Solida Biotech, München, Germany). After pre-incubation of milk with concentrated proteins, it was treated with different concentrations of trypsin, such as 0.008 g·L⁻¹, 0.016 g·L⁻¹, 0.032 g·L⁻¹, and 0.064 g·L⁻¹. Individual batch-mode experiments were performed for protein hydrolysis process. For that purpose, 450 µL, 900 µL, 1.8 mL, and 3.6 mL of trypsin solution from stock solution (concentration of trypsin 0.009 g·mL⁻¹) were injected through 0.22 µm of polytetrafluoroethylene (PTFE) syringe filter (VWR International, Pennsylvania, USA) to 500 mL of milk with concentrated proteins in bioreactor [67]. Enzymatic reaction was performed at a temperature of 40 °C for 10 min [68,69]. During enzymatic reaction, agitation speed in the bioreactor was maintained, 175 rpm, and the pH of milk in the bioreactor was controlled, 6.8, by automated addition of 2.0 N of sodium hydroxide or hydrochloric acid [67]. After 10 min of enzymatic reaction, 20 mL of sample was collected by a syringe from the bioreactor and kept in a sample tube. Activity of

trypsin in enzymatic reaction was stopped by heat treatment. For that purpose, sample tubes were immediately placed in a water bath at temperature 70 °C for 30 min because denaturation temperatures of bovine α -lactalbumin and β -lactoglobulin are ~75 °C [70–72]. Two control samples (without enzyme treatment) were considered in the experiment: control 1: ultra-heat-treated skimmed milk was heated at temperature 40 °C for 10 min and subsequently placed at temperature 70 °C for 30 min; control 2: milk with concentrated protein was heated at temperature 40 °C for 10 min and subsequently placed at temperature 70 °C for 30 min. After inactivation of trypsin, the temperature of samples (reaction mixture) was reduced to ambient temperature (~25 °C) and freshly prepared samples were used for all kinds of biochemical assay, described in Section 2.4.

2.4. Analytical Method

2.4.1. Understanding of Molecular Weight of Proteins in Concentrated Milk

Molecular weight of proteins in concentrated milk was determined by liquid chromatography-electrospray ionization time-of-flight mass spectrometry (LC-ESI-TOF-MS) (Agilent Technologies, Santa Clara, CA, USA). Sample preparation was performed according to the protocol, mentioned by Rauh et al., 2015 [73]. Briefly, 200 μ L of concentrated milk was treated with 20 μ L of 0.5 M DTT, 1 mL of 100 mM trisodium citrate, and 6 M urea at temperature 30 °C for 1 h in a thermostat. Subsequently, a sample was centrifuged at 9500 g for 20 min at temperature 4 °C by a laboratory centrifuge (HERMLE Labortechnik, Wehingen, Germany). Aliquot of the clear phase was collected aseptically and used for LC-MS analysis. Chromatographic separation was achieved by an XBridge BEH300 C4 column with particle size: 3.5 μ m, and inner diameter \times length: 2.1 mm \times 150 mm (Waters, Milford, USA), placed in an Agilent 1200 HPLC system (Agilent Technologies, Santa Clara, CA, USA). The column temperature was 30 °C during chromatographic separation. The binary mobile phase consisted of Milli-Q ultrapure deionized water with 0.1% formic acid (eluent A), and acetonitrile (eluent B) was used for that purpose. The flow rate was set to 0.5 mL \cdot min⁻¹. Gradient separation started at 3% B and linearly increased to reach 90% in 9 min. The eluent was kept constant at 90% B until 11 min and then the column was re-equilibrated at the initial conditions for 8 min. A UV signal was recorded at 280 nm using the diode-array detector (DAD) in the LC system and the effluent was connected to an Agilent 6530 high-resolution, accurate-mass, quadrupole time-of-flight mass spectrometry system equipped with a dual sprayer electrospray ion source. The mass spectrometry was run with full scan, MS-only mode (2 GHz, extended dynamic range setup) scanning in the range of 50–3200 m/z in positive ionization mode. A continuous reference mass correction was applied using purine and HP-921 (Hexakis(1H,1H,3H-perfluoropropoxy)phosphazene) as reference substances. The ion source temperature was maintained at 325 °C, and capillary and fragmentor voltages were set to –4000 V and 140 V, respectively. The Mass Hunter (MH) Workstation software package (version B02.01) and MH BioConfirm (version B 09.00) (Agilent Technologies, Santa Clara, CA, USA) were used for data acquisition and data evaluation, respectively. For raw mass spectrum deconvolution, the maximum entropy algorithm was used with automatic mass range detection (for intact protein), and for multiply charged ions, 500–3000 m/z limited range was considered.

2.4.2. Understanding of Hydrolysis of Liquid Milk Protein Concentrate

Molecular weight of proteins in ultra-heat-treated skimmed milk, milk with concentrated proteins, and enzyme-treated milks was determined by the sodium dodecyl sulfate polyacrylamide gel electrophoresis (SDS-PAGE) method. For this purpose, a vertical electrophoresis system (Bio-Rad Mini Protean Tetra system) and standard protein marker (precision plus protein standards) from Bio-Rad (Bio-Rad, Hercules, CA, USA) were used. In the SDS-PAGE method, concentration of stacking gel and running gel were 6% and 15%, respectively. The Laemmli sample buffer with 2-mercaptoethanol was used for dilution of samples and 10 μ L of appropriate diluted sample was loaded into the respective wells. 0.2% Coomassie Brilliant Blue R250 was used for gel staining. After 30 min of gel staining,

de-staining of gel was performed with 50% (volume basis) of methanol-water and 10% (volume basis) of acetic acid. Gel image was captured using a Gel Doc XR+ System (Bio-Rad, Hercules, USA) and the molecular weight of bands were determined using Quantity One software program (version 4.6) (Bio-Rad, Hercules, CA, USA) [74].

2.4.3. Immunoblotting of Concentrated Milk Proteins

Proteins from SDS-PAGE gel were transferred onto a 0.45 μm of polyvinylidene difluoride (PVDF) membrane (Merck-Millipore, Molsheim, France) by a trans blot semi-dry transfer cell (Bio-Rad, Hercules, CA, USA). It was operated with 0.25 V and 0.08 mA/cm^2 for 60 min. Immune-reactive proteins were identified with clinically proved milk positive pooled human serum and peroxidase-labelled anti-human Immunoglobulin E. The binding patterns were visualized using a substrate solution containing 4-chloronaphthol, hydrogen peroxide, and ethanol in phosphate buffered saline solution. Image analysis of blots was carried out with Gel Doc 2000 system (Bio-Rad, Hercules, CA, USA) [75].

2.4.4. Determination of Antioxidant Capacity

Antioxidant capacity of ultra-heat-treated skimmed milk, milk with concentrated proteins and enzyme-treated milks was measured using the Ferric reducing ability of plasma method with respect of ascorbic acid [76]. Appropriate diluted 100 μL of all kinds of milk samples with 2.9 mL of reagent (20 mM of ferric chloride: 10 mM of 2,4,6-Tris(2-pyridyl)-s-triazine with 40 mM of hydrochloric acid: 300 mM of acetate buffer, pH 3.6 = 1:1:10 (volume basis)) were incubated at temperature $\sim 35^\circ\text{C}$ for 30 min in a water bath. Colorimetric determination was performed in room temperature ($\sim 25^\circ\text{C}$) with a UV-Vis spectrophotometer (Thermo ScientificTM, Waltham MA, USA). Spectrophotometric measurement was performed with wavelength 593 nm.

2.4.5. Estimation of Angiotensin-Converting-Enzyme Inhibitory Activity

Enzymatic reaction mixture (final volume 200 μL in each well), consisted of 50 mM of sodium chloride, 100 mM of TRIS HCl (pH 7), 10 μM of zinc chloride, 15 μM of substrate Abz-FRK(Dnp)-P, recombinant angiotensin converting enzyme, and milk samples (in a dilution range of 10-fold to 10^6 -fold) was used in investigation. The amount of the recombinant angiotensin converting enzyme was chosen to result in about 10-fold activity than that in the human serum (dilution was 200 to 400-fold from the stock). Reaction was initiated by the addition of substrate. Changes in fluorescent intensities were recorded in each 2–3 min and then changes were plotted as the function of time. These plots were fitted by a linear fit, and the slope was used to estimate enzyme activity (slope represents the change in fluorescent intensity in one minute). Activities in the absence of milk samples (uninhibited samples) were used as controls. The level of inhibition was calculated as % of uninhibited activity in each plate. Measurements were performed in a fluorescent plate reader (BMG Labtech, Ortenberg, Germany) at temperature 37°C in Corning 96 wells black and flat bottom plates (Corning, New York, USA). Changes in optical density were measured with wavelength 340 nm for at least 90 min with 5 min intervals [77].

2.4.6. Determination of Protein Concentration

Concentration of protein in ultra-heat-treated skimmed milk, milk with concentrated proteins, and enzyme-treated milks were determined by the Bradford assay. Appropriate dilution of 100 μL of all kinds of milk samples with 3 mL of Bradford reagent were incubated at room temperature ($\sim 25^\circ\text{C}$) for 30 min in a water bath. Colorimetric determination was performed with wavelength 280 nm in a UV-Vis spectrophotometer (Thermo ScientificTM, Waltham, MA, USA). Assay was performed in room temperature ($\sim 25^\circ\text{C}$) and bovine serum albumin as a standard was used in assay [78].

2.4.7. Microbiological Assay

Antibacterial activity of ultra-heat-treated skimmed milk, milk with concentrated proteins, and enzyme-treated milks against *Bacillus cereus* and *Staphylococcus aureus* ATCC 6538 were investigated. Antibacterial activity was measured by agar well diffusion method. Sterile soybean casein digestive agar medium was used in the investigation. Freshly prepared (overnight grown culture) each culture was diluted with maximum recovery diluent (MRD) solution (8.5 g sodium chloride + 1 g peptone in 1 L of de-ionized water) to reach the bacterial concentration 10^6 colony-forming units mL^{-1} in respective agar plate [79]. Bacterial culture was spread on solidified agar in respective petri plates (pour plated) and agar wells with diameter 5 mm were filled with 100 μL of control milk and enzyme-treated milk samples. Petri plates were incubated at temperature 37°C for 48 h in a biological incubator (HACH, Düsseldorf, Germany) [65,67]. The diameter of zone of inhibitions in microbial plates were measured by excluding the diameter of wells (5 mm) using a digital Vernier caliper (UEMATSU SHOKAI CO., LTD., Sendai, Japan).

2.5. Statistical Analysis

All experiments were performed at three times (technical triplicate). The mean value and standard deviation were calculated by Microsoft Excel (version 2013) (Microsoft Corporation, Washington, DC, USA). Subsequently, one-way analysis of variance method followed by the Tukey's post hoc test were performed to understand the significant difference ($P < 0.05$) between different groups. SPSS 15.0 (version 25.0) (IBM, Armonk, NY, USA) was used for statistical analysis.

3. Results and Discussion

3.1. Concentrate Milk Proteins in Skimmed Milk by Membrane Filtration

A ceramic tubular membrane with active filtration area $5 \times 10^{-3} \text{ m}^2$ and pore size 5 nm was used to concentrate milk proteins in ultra-heat-treated skimmed milk by removing milk serum as a permeate. At room temperature and $\text{pH} \sim 7$, casein micelle may have a mean radius of 50 nm, whereas, the radius of whey proteins, such as α -lactalbumin, β -lactoglobulin, bovine serum albumin, and tetrad immunoglobulin are $\sim 1.8 \text{ nm}$, $\sim 1.8 \text{ nm}$, $\sim 4 \text{ nm}$, and $\sim 6 \text{ nm}$, respectively [80]. Typically, ultra-heat-treated milk is prepared with temperature $135\text{--}145^\circ\text{C}$ and treatment exposure time 1–8 s [81]. Due to heat treatment with high temperature, beside the Maillard reaction, sizes of proteins in milk are changed compared to their conventional sizes. When milk is heated at a temperature above 80°C , the tertiary structure of whey protein turns to unfold [82]. It has been reported that at a temperature higher than 80°C , denaturation rate of α -lactalbumin is faster than β -lactoglobulin's and denaturation of α -lactalbumin is faster when β -lactoglobulin is present [83,84]. Subsequently, intramolecular highly reactive thiol groups, broken hydrophobic, and disulphide bonds may bind with covalent and hydrophobic bonds among themselves or with casein molecules, especially with κ -casein, present in periphery of casein micelle [85–87]. Furthermore, some whey proteins with sulfur containing thiol group (R-SH) can bind with other proteins by covalent bonds. Bovine serum albumin and β -lactoglobulin [88,89], and κ -casein and β -lactoglobulin [90–92] may bind together due to heat treatment. However, α -lactalbumin does not contain -SH group, it may conjugate with caseins in presence of β -lactoglobulin [93]. In addition, heat treatment may promote the formation of isopeptide bond between lysine and glutamine (N- ϵ -(γ -glutamyl)-lysine) or asparagine (N- ϵ -(β -aspartyl)-lysine) among different proteins, present in liquid milk protein concentrate [94–96]. Due to faster thermodenaturation of α -lactalbumin in presence of β -lactoglobulin, it may completely conjugate with casein micelle [80]. Therefore, it might expect that most of whey proteins have chance to conjugate with casein and the size of casein micelle might increase. On the other hand, due to intermolecular conjugation of whey proteins, the size of whey proteins might increase. Because of it, most of the proteins might reject by the nanofiltration membrane and residual (unbounded) whey proteins and lactose might permeate with milk serum through membrane pores during nanofiltration.

As nanofiltration is a pressure-driven membrane separation process, a gel layer is developed on the membrane surface during separation process. A detailed investigation was performed to reduce the development of gel layer on the membrane surface by changing TMP and RFR. In Table 1, initial permeate flux and percentage change of permeate flux for different TMPs and RFRs are reported.

Table 1. Difference of pressure, initial permeate flux and percentage change of permeate flux for different trans-membrane pressures (TMPs) and retention flow rates (RFRs) in absence and presence of static turbulence promoter. Results are represented by mean value with standard deviation (\pm values). In superscript, dissimilar alphabet represents the significant difference between results, evaluated by the Tukey's post hoc method.

TMP (Bar)	RFR (L·h ⁻¹)	Without Static			With Static		
		Δp (Bar)	$J_{initial}$ (L·h ⁻¹ ·m ⁻²)	ΔJ (%)	Δp (Bar)	$J_{initial}$ (L·h ⁻¹ ·m ⁻²)	ΔJ (%)
2	100	0.1	8.06 \pm 1 ^a	41.69 \pm 1.27 ^a	0.3	15.58 \pm 1.1 ^a	32.33 \pm 1.25 ^a
2	200	0.1	8.2 \pm 1.2 ^a	37.39 \pm 2.35 ^{a,b}	0.7	15.88 \pm 1 ^a	31.70 \pm 2.5 ^a
3	100	0.1	13.45 \pm 1.1 ^b	36.95 \pm 1.55 ^{a,b}	0.3	34.22 \pm 1.08 ^b	24.01 \pm 1.19 ^b
3	200	0.1	18 \pm 3.9 ^b	33.33 \pm 2.79 ^b	0.7	34.55 \pm 1.02 ^b	23.61 \pm 2.31 ^b

It is observed that permeate flux of serum was increased with the increase of TMP, because TMP provided driving force on the membrane surface. At higher TMP, the formation of gel layer on membrane surface was reduced and convective flux of serum increased due to the driving force on the membrane surface. For a similar reason, the percentage change of permeate flux decreased with the increase of TMP. As an outcome, concentration of protein in retentate side of the membrane, increased. As an example, after volume reduction 2, concentrations of protein in storage tank of the membrane module were 59.2 g·L⁻¹ and 42 g·L⁻¹, when filtration process was performed with TMP 3 bar, RFR 100 L·h⁻¹ and 2 bar, RFR 100 L·h⁻¹, respectively. At constant TMP, permeate flux was increased at higher RFR; however, results were not statistically significant. The tubular membrane had the lower surface area to volume ratio and, therefore, high feed flow rate promoted permeation. In cross-flow module, fluid on the membrane surface flowed with horizontal direction on the membrane surface with higher velocity and created more turbulence at higher RFR. Due to the sweeping action of fluid on the membrane surface, the deposition of solute molecules on the membrane surface reduced. Lower deposition of solute molecules on the membrane surface reduced the formation of concentration polarization and gel layer resistance, accompanied by the increase rate of permeation. Moreover, it was found that rate of flux declination was lower when the static turbulence promoter was used in the filtration process. The static turbulence promoter offered tangential velocity of fluid across the membrane surface, which created turbulence and vorticity of fluid on the membrane surface. Furthermore, the static turbulence promoter provided centrifugal force on the fluid, which contributed driving force on the membrane surface. All these factors reduced the deposition of solute molecules on the membrane surface and membrane gel layer resistance, which offered higher permeate flux in filtration process. As permeate flux was significantly higher in the static turbulence promoter-implemented filtration process, specific energy consumption was studied with different TMPs and RFRs in static turbulence promoter-implemented filtration process (Figure 3).

At constant TMP, values of specific energy consumption in filtration process were significantly low at lower RFR. When RFR was 200 L·h⁻¹, permeate flux was not significantly increased compared to 100 L·h⁻¹ because RFR could not provide driving force on the membrane surface. Therefore, permeate flux was not significantly increased compared to pressure drop at two opposite ends of the membrane. Filtration process with static turbulence promoter, higher TMP and lower RFR, tangential velocity of fluid across the membrane surface, driving, and centrifugal force on the fluid were generated. As an outcome, permeate flux was increased and pressure drop was reduced. Protein concentration in the retentate side of the membrane is also represented in Figure 3. It is noted that concentration of

protein in the retentate side was higher with TMP 3 bar compared to TMP 2 bar. Protein concentration increased due to higher permeation of serum through membrane pores at higher TMP. Concentration of protein in retentate was not significantly increased at RFR 200 L·hh⁻¹ compared to 100 L·hh⁻¹, because RFR could not generate the driving force on the membrane surface and osmotic pressure. In Figure 4, time histories of the permeate flux, without and with the static turbulence promoter, are presented.

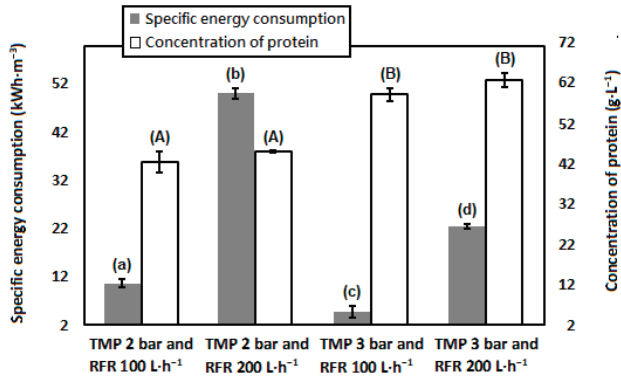


Figure 3. Specific energy consumption and concentration of protein in the retentate side of membrane for different trans-membrane pressures (TMPs) and retention flow rates (RFRs) in static turbulence promoter-implemented filtration process. Results are represented by mean value with standard deviation (\pm values). In superscript, dissimilar alphabet represents the significant difference between results, evaluated by the Tukey’s post hoc method.

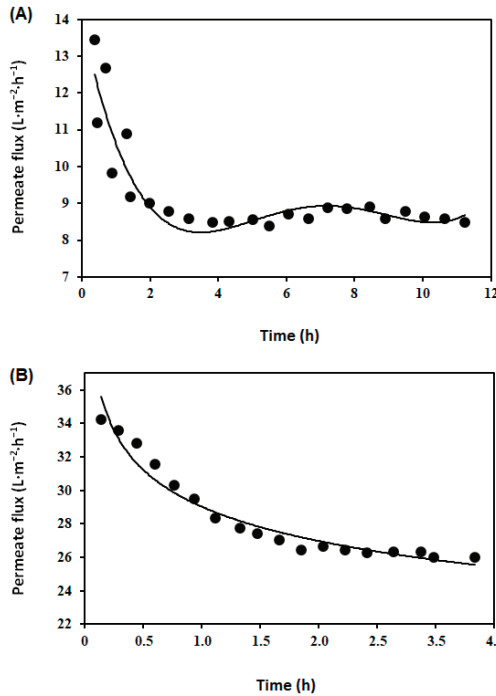


Figure 4. Time history of permeate flux without the static turbulence promoter (A) and with the static turbulence promoter (B).

It was noted that when the static turbulence promoter was used in membrane filtration process, rate of flux declination and filtration time were reduced because the formation of gel layer was reduced in the presence of static turbulence promoter inside of tubular membrane.

3.2. Molecular Weight of Different Proteins in Concentrated Milk and Their Enzymatic Hydrolysis

Analysis of molecular weight of different proteins in concentrated milk was performed using UV chromatogram, total ion chromatogram (TIC), and deconvoluted mass spectrum of observed protein spectra (Figure 5).

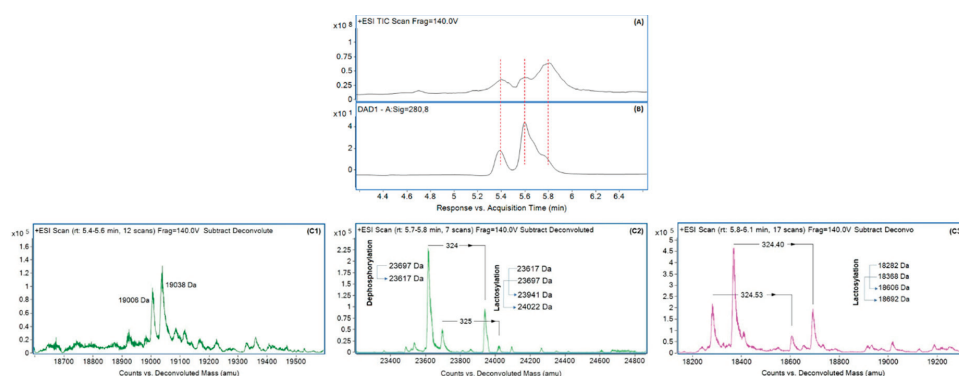


Figure 5. Results of liquid chromatography-mass spectrometry; (A) UV chromatogram of proteins in concentrated milk, (B) total ion chromatogram of proteins in concentrated milk, (C) deconvoluted mass spectra of different proteins, peaks appear at retention time 5.4 min (C1), 5.6 min (C2), and 5.8 min (C3).

Major proteins provided pronounced UV signal at 280 nm. In that UV wavelength, three peaks at 5.4 min, 5.6 min, and 5.8 min retention times were detected. Corresponding MS (TIC) signals are fully matched with UV peaks and deconvolution of each chromatographic peak spectrum was performed. Deconvoluted mass spectrum of proteins appeared in the retention time 5.4 min is provided in Figure 5(C1). In this figure, it is noted that there are two major deconvoluted masses, such as 19006 Da and 19038 Da. According to the previously published results, they might represent κ -casein. Deconvoluted mass spectrum of proteins appeared in retention time 5.6 min is provided in Figure 5(C2). In this figure, two major deconvoluted masses, such as 23617 Da and 23697 Da are observed. Comparing with the previously published results, they might represent α -casein [97]. Protein with molecular mass 23617 Da might be dephosphorylated form of α -casein (-80 Da mass shift from 23697 Da). Different types of caseins have a high degree of phosphorylation, which is generally affected by high temperature treatment during milk processing [98]. Interestingly, two protein with molecular mass shift $+324$ Da were observed in Figure 5(C2). These proteins with molecular mass 23941 Da and 24022 Da might be the lactosylated form of their original protein. Lactosylation of protein took place due to heat treatment during ultra-heat-treated milk production and, subsequently, their storage. The Amadori product ϵ -lactulosyllysine is produced by free ϵ -amino group of lysine in protein chain and milk sugar lactose [99]. It has been reported that protein become more hydrophilic due to addition of lactose in its structure, which results a shift to lower retention time [100,101]. Deconvoluted mass spectrum of proteins appeared in retention time 5.8 min is provided in Figure 5(C3). In this figure, two major deconvoluted masses, such as 18282 Da and 18368 Da, along with their lactosylated form with molecular mass 18606 Da and 18692 Da are observed. According to the already published results, the original protein might represent β -lactoglobulin [97]. According to the electrophoretic pattern, represented in Figure 6, ultra-heat-treated skimmed milk and milk with concentrated proteins may have had immunoglobulin, lactoferrin, lactoperoxidase, bovine serum albumin, α -casein, conjugated β -lactoglobulin, and α -lactalbumin or dimer β -lactoglobulin, β -casein,

γ -casein, κ -casein, β -lactoglobulin, and α -lactalbumin with molecular weight ~ 150 kDa, ~ 80 kDa, ~ 78 kDa, ~ 66 kDa, ~ 35 kDa, ~ 34 kDa, ~ 25 kDa, ~ 22 kDa, ~ 20 kDa, ~ 18 kDa, and ~ 14 kDa, respectively. Some other investigators also published similar results [83,102–104].

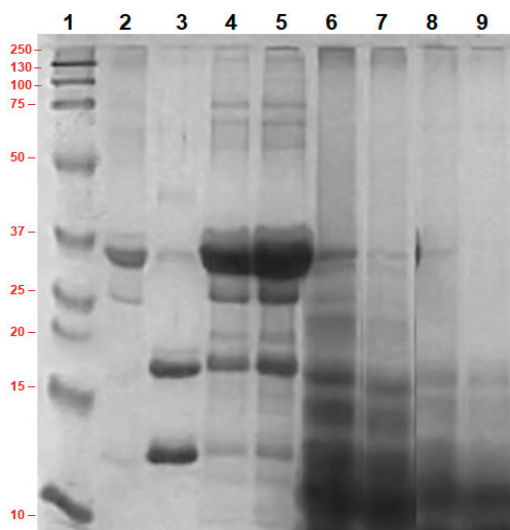


Figure 6. Sodium dodecyl sulfate polyacrylamide gel electrophoresis (SDS-PAGE) image of ultra-heat-treated skimmed milk, milk with concentrated proteins and milk with concentrated proteins after enzyme treatment; lane 1: marker protein, lane 2: standard casein, lane 3: standard α -lactalbumin and β -lactoglobulin, lane 4: ultra-heat-treated skimmed milk, lane 5: concentrated ultra-heat-treated skimmed milk, lane 6: concentrated liquid milk protein treated with 0.008 g L^{-1} of trypsin, lane 7: concentrated liquid milk protein treated with 0.016 g L^{-1} of trypsin, lane 8: concentrated liquid milk protein treated with 0.032 g L^{-1} of trypsin, lane 9: concentrated liquid milk protein treated with 0.064 g L^{-1} of trypsin.

In the PAGE image, hydrophobic protein conjugate with molecular weight ~ 34 kDa is clearly visualized. It was reported that due to heat treatment of skimmed milk, sometimes β -lactoglobulin and α -lactalbumin might participate in intermolecular thiol-disulphide bond interchange to produce covalently bonded hydrophobic aggregates [105]. Another group of investigators reported that at temperature more than 90°C , β -lactoglobulin might present with disulphide-bonded dimer with molecular weight ~ 34 kDa and monomer [106]. However, some researchers reported about the formation of dimer α -lactalbumin with molecular weight ~ 28 kDa [107], but it was not found in our investigation. From the above discussion, it may say that the molecular weight of casein in concentrated milk, determined by SDS-PAGE and mass-spectroscopy is not directly comparable. It may explain by the fact that the electrophoretic mobility of caseins in electrophoresis gel is lower than expected from their molar mass [108]. It may be justified by the fact that phosphorylation [109] and lactosylation of caseins [73] change the migration of casein molecules in electrophoresis gel. However, in SDS-PAGE, several protein aggregates were present, they were absent in mass-spectrum. The possible reason is that dissociation of protein molecules and disruption of any type of protein aggregate might done by reducing agents DTT and chaotropic agent urea in sample preparation for mass-spectroscopy [110].

Without any contradiction, it was found that the numbers of peptide bands were increased due to tryptic digestion of milk proteins (lane 6–9). The hydrolysis of concentrated milk proteins was dose-dependent because it was noted that band numbers with lower molecular weight were increased gradually with increase of enzyme concentration in hydrolysis reaction. Immunoglobulin were hydrolyzed at more than 99% when concentration of trypsin was increased from 0.016 g L^{-1} to

0.032 g·L⁻¹. Lactoferrin, lactoperoxidase, and bovine serum albumin were hydrolyzed at more than 99% due to treatment with 0.008 g·L⁻¹ of trypsin. Furthermore, κ -casein and β -casein were hydrolyzed at more than 99% when concentration of trypsin was increased from 0.008 g·L⁻¹ to 0.016 g·L⁻¹, whereas α -casein was retained. α -casein was hydrolyzed at more than 99% with 0.064 g·L⁻¹ of trypsin. This can be justified by the fact that α -casein might have less chance to participate in enzymatic reaction because in the interior part of casein micelle, calcium phosphate clusters bind with the phosphoserine residues of α_s -casein and β -casein, whereas κ -casein was present in the periphery of casein micelle and received chance to participate in enzymatic reaction [111]. Due to partial hydrolysis of β -casein with 0.008 g·L⁻¹ of trypsin, some peptone and γ -casein with molecular weight ~22 kDa might produce and they were hydrolyzed when milk with concentrated proteins was treated with 0.032 g·L⁻¹ of trypsin. Dimer β -lactoglobulin with molecular weight ~32 kDa was hydrolyzed when trypsin was increased from 0.016 g·L⁻¹ to 0.032 g·L⁻¹.

3.3. Antioxidant Capacity

Antioxidant capacity of milk with concentrated proteins was 167.35 ± 9.8 mg equivalent ascorbic acid L⁻¹ and it was increased after enzyme treatment. In Figure 7, it is noted that change of antioxidant capacity in enzyme-treated milks was dose-dependent. Similar types of findings were also published by other researchers [62,63].

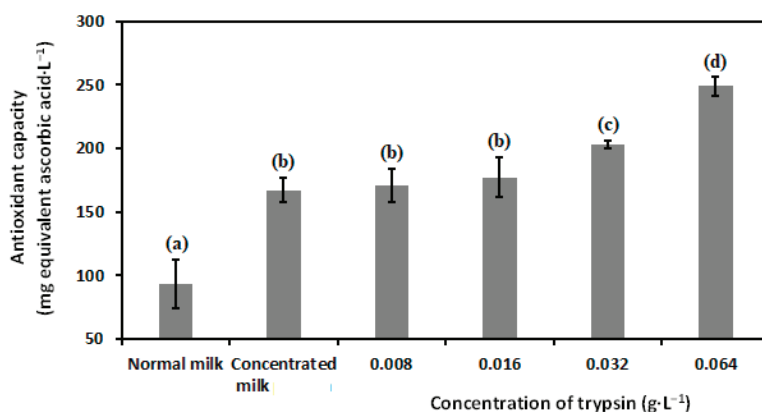


Figure 7. Antioxidant capacity of ultra-heat-treated skimmed milk, milk with concentrated proteins, and milk with concentrated proteins after enzyme treatment. Results are represented by mean value with standard deviation (\pm values). In superscript, dissimilar alphabet represents the significant difference between results, evaluated by the Tukey's post hoc method.

Trypsin is a serine endopeptidase, consisting of three amino acids, such as His 57, Ser 195, and Asp 102 in catalytic triad. In amino acid sequence, trypsin cleaves between the carboxyl group of basic amino acid lysine or arginine in N terminal position and the amino group of the adjacent amino acid with hydrophobic side chain in C terminal position. This cleavage does not occur when lysine or arginine is followed by proline. Adjacent hydrophobic amino acid, such as alanine, isoleucine, leucine, methionine, phenylalanine, valine, proline, and glycine in peptide chain, derived from milk proteins by tryptic hydrolysis, offered reducing activity towards ferric ion [64,112,113].

3.4. Angiotensin Converting Enzyme-Inhibitory Activity

Angiotensin converting enzyme inhibitory activity of ultra-heat-treated skimmed milk and milk with concentrated proteins was negligible. Inhibitions of angiotensin converting enzyme were ~15% and ~6% for ultra-heat-treated skimmed milk and milk with concentrated proteins, respectively (Figure 8A). Our finding was similar in accordance with other researchers [114,115].

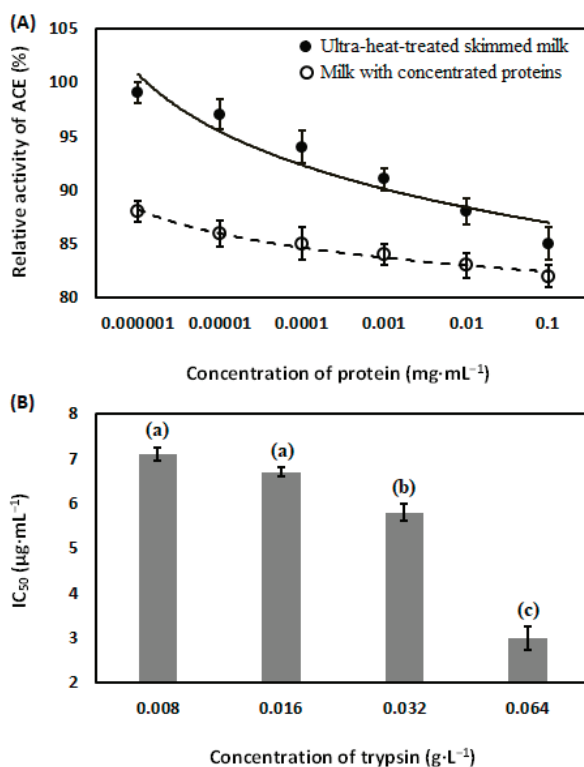


Figure 8. Angiotensin converting enzyme (ACE)-inhibitory activity of ultra-heat-treated skimmed milk and milk with concentrated proteins (A), and values of IC₅₀ in milk with concentrated proteins after enzyme treatment (B). Results are represented by mean value with standard deviation (\pm values). In superscript, dissimilar alphabet represents the significant difference between results, evaluated by the Tukey's post hoc method.

It can be justified by the fact that interaction between active side of angiotensin converting enzyme and native milk proteins might not be facilitated, because steric hindrance might present [116]. Angiotensin converting enzyme in concentrated milk proteins significantly increased after trypsin treatment. Similar types of findings were reported by other investigators [117,118]. Changes of IC₅₀ value in liquid milk protein concentrate due to enzyme treatment were dose-dependent (Figure 8B). Because of tryptic hydrolysis of milk proteins, active sides in low molecular weight peptides were exposed and interaction with angiotensin converting enzyme was facilitated. It was reported that peptides with hydrophobic amino acids, such as proline, tryptophan, tyrosine, and phenylalanine at C-terminal position, are able to bind with angiotensin converting enzyme [119,120]. In our investigation, more than 95% inhibition was not achieved. This can be justified by the fact that angiotensin converting enzyme inhibitory peptides, produced by tryptic hydrolysis of milk proteins might change the structural configuration of angiotensin converting enzyme, which might not favorable for interaction between substrate and angiotensin converting enzyme [121].

3.5. Antibacterial Activity

Antibacterial activity (represented in zone of inhibition) of enzyme-treated liquid milk protein concentrate towards *Bacillus cereus* and *Staphylococcus aureus* was proven. No zone of inhibition was found when milk with concentrated proteins was tested. In Figure 9, radius of zone of inhibition

represented the antibacterial activity of milk with concentrated proteins after enzyme treatment is mentioned.

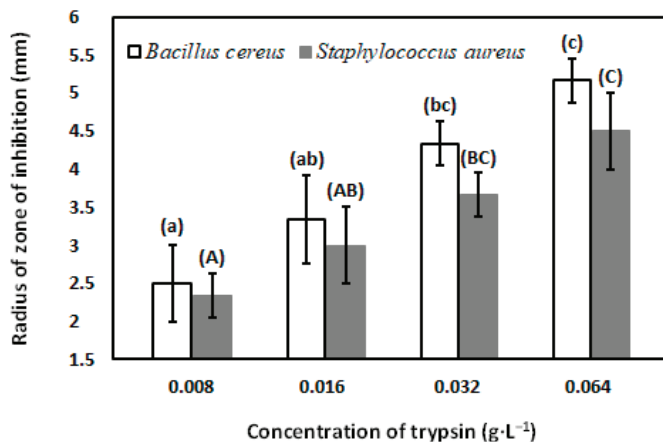


Figure 9. Antibacterial activity of milk with concentrated proteins after enzyme treatment. Results are represented by mean value with standard deviation (\pm values). Superscript dissimilar alphabet represents the significant difference between results, evaluated by the Tukey's post hoc method.

Zone of inhibition (radius of inhibition zone) was significantly increased when concentration of trypsin was increased from 0.008 g·L⁻¹ to 0.032 g·L⁻¹ during hydrolysis of liquid milk protein concentrate. It was found that for *Bacillus cereus*, values of zone of inhibition (radius of inhibition zone) were 2.5 \pm 0.5 mm and 5.2 \pm 0.3 mm, when concentrated milk protein was treated with 0.008 g·L⁻¹ and 0.064 g·L⁻¹ of trypsin, respectively. For *Staphylococcus aureus*, values of zone of inhibition (radius of inhibition zone) were 2.3 \pm 0.03 mm and 4.5 \pm 0.5 mm when concentrated milk protein was treated with 0.008 g·L⁻¹ and 0.064 g·L⁻¹ of trypsin, respectively. Several biochemical mechanisms about antibacterial activity of enzyme-treated liquid milk protein concentrate were reported. Trypsin cleaves the peptide bond at the C-terminus of lysin and arginine, when the N terminus is not a proline. Several peptides with hydrophobic, hydrophilic or amphipathic amino acids, produced due to tryptic hydrolysis of milk proteins. These peptides may interact with peptidoglycan in bacterial cell membrane, create a complex with bacterial cell wall components, and, subsequently, create pores in bacterial cell membrane. These pores might expedite the permeabilization of cellular contents to the abiotic environment and subsequently, destruction of cell. It has been also reported that interaction between bacterial cell membrane with antibacterial peptides frequently leads to lipid segregation in the cell membrane. It leads to delocalization of essential membrane proteins, increase membrane permeability, inhibit cell division, followed by cellular death [122,123].

3.6. Allergenicity

Immunoblotting, a combination of gel electrophoresis and antigen-antibody reaction was performed with positive pooled human sera to understand the allergenic potentiality of proteins, present in liquid milk protein concentrate. It was reported that major cow milk allergens belong to the casein fraction (α_{S1} -, α_{S2} -, β -, and κ -casein), and whey proteins α -lactalbumin and β -lactoglobulin; however, lactoferrin, bovine serum albumin and immunoglobulins, which are present with lower quantities in cow milk, have importance in allergenic reaction [22]. In present investigation, it was noted that however, immunoglobulin, lactoferrin, lactoperoxidase, bovine serum albumin, and casein had strong interaction with antibody, monomeric β -lactoglobulin had weak interaction, and monomeric α -lactalbumin had no detectable interaction (Figure 10).

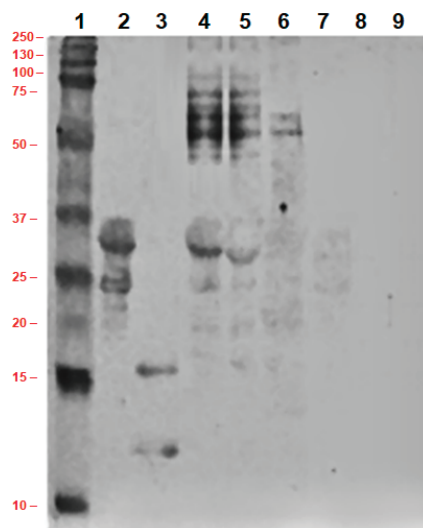


Figure 10. Immunoblot of ultra-heat-treated skimmed milk, milk with concentrated proteins and milk with concentrated proteins after enzyme treatment; lane 1: marker protein, lane 2: standard casein, lane 3: standard α -lactalbumin and β -lactoglobulin, lane 4: ultra-heat-treated skimmed milk, lane 5: concentrated ultra-heat-treated skimmed milk, lane 6: concentrated liquid milk protein treated with $0.008 \text{ g}\cdot\text{L}^{-1}$ of trypsin, lane 7: concentrated liquid milk protein treated with $0.016 \text{ g}\cdot\text{L}^{-1}$ of trypsin, lane 8: concentrated liquid milk protein treated with $0.032 \text{ g}\cdot\text{L}^{-1}$ of trypsin, lane 9: concentrated liquid milk protein treated with $0.064 \text{ g}\cdot\text{L}^{-1}$ of trypsin.

This result can be explained by the following justifications. As the experiment was performed with ultra-heat-treated skimmed milk, due to heat treatment most of α -lactalbumin and β -lactoglobulin were unfolded, and allergenic epitopes in α -lactalbumin and β -lactoglobulin were destroyed [104,124]. Allergenic epitopes in higher molecular weight proteins, such as bovine serum albumin, lactoperoxidase, conjugated α -lactalbumin, and β -lactoglobulin or α -casein were not fully affected during heat treatment because their denaturation temperatures were quite high [104,125]. In an investigation with 20 children (median age 4 months), it was also found that, however, α_{S1} -casein, α_{S2} -casein, β -casein, κ -casein, bovine serum albumin, Immunoglobulin-G heavy chain, and lactoferrin had allergenic cross-linking, α -lactalbumin did not have any allergenic activity [126]. However, all proteins in concentrated milk, except α -lactalbumin, were immunoreactive; they lost allergenic activity due to enzymatic hydrolysis. Residual immunoreactivity of caseins and dimeric β -lactoglobulin or conjugated α -lactalbumin- β -lactoglobulin were still present at $0.016 \text{ g}\cdot\text{L}^{-1}$ of trypsin treatment. They lost allergenic potentiality when $0.032 \text{ g}\cdot\text{L}^{-1}$ of trypsin was used in enzymatic reaction.

3.7. Superiority of the Process

After skillful experiment to prepare liquid skimmed milk protein concentrate, the superior operation strategy was trans-membrane pressure 3 bar, retention flow rate $100 \text{ L}\cdot\text{h}^{-1}$, and implementation of a static turbulence promoter within a tubular ceramic membrane with pore size 5 nm and filtration area $5 \times 10^{-3} \text{ m}^2$. In the present investigation, a cross-flow membrane module was adopted and batch-mode filtration was performed with volume reduction factor 2. To prepare milk protein concentrate, polymeric spiral wound [19,127,128], single flat sheet [13,129,130], and tubular [131] membranes were used. Furthermore, ceramic tubular membrane was used to prepare milk protein concentrate by several investigators [132–136]. Single stage membrane filtration [19,127,129,131,136] and ultrafiltration with diafiltration were used by several investigators to prepare milk protein

concentrate [137,138]. Both continuous and discontinuous diafiltration were adopted to reduce major whey proteins, such as α -lactalbumin and β -lactoglobulin from casein fraction by ultrafiltration or nanofiltration membrane. In continuous diafiltration process, sterilize water was added to the feed tank to maintain the feed volume, whereas discontinuous diafiltration was introduced in the process when the feed concentration reached to a certain level to overcome the high viscosity of feed and protect the membrane by fouling. However, milk protein concentrate was prepared by both polymeric and ceramic membrane; flux declination is a considerable drawback. To overcome this issue, stepwise increase of TMP was adopted in sometimes [131,134] and it may feel that in respect of energy consumption, this approach is not appreciable. In our investigation, due to application of the static turbulence promoter reduction of permeate flux was remarkably low. The experiment was started with 1 L of milk in the feed tank and after volume reduction factor 2 without diafiltration, initial permeate flux $34 \text{ L}\cdot\text{m}^{-2}\cdot\text{h}^{-1}$ reduced to $26 \text{ L}\cdot\text{m}^{-2}\cdot\text{h}^{-1}$, i.e., only 24% reduction in permeate flux. During filtration, consumption of mechanical energy, contributed by fluid flow rate and TMP was 4.9 kWh m^{-3} . However, in SDS-PAGE image all proteins in concentrated milk were clearly visualized, but in immunoblot it was found that monomeric α -lactalbumin and β -lactoglobulin did not offer allergenicity, due to change of their structural configuration during heat treatment. Hence, diafiltration was not required to fulfil the objective of present investigation. Filtration process without diafiltration might be reduced the water consumption and process time. According to our experimental finding, application of $0.032 \text{ g}\cdot\text{L}^{-1}$ of trypsin to liquid milk protein concentrate at temperature 40°C for 10 min can delete allergenic epitopes and increase the antioxidant capacity, anti-angiotensin enzyme activity, and antibacterial activity compared to native milk protein concentrate. According to the literature review, it may be considered that it is the first approach in the context of development of dairy-based hypoallergenic functional food by membrane- and enzyme- based technologies.

4. Conclusions

In the present investigation, liquid milk protein concentrate with antioxidant capacity, anti-angiotensin activity, antibacterial activity, and allergen-free was produced from ultra-heat-treated skimmed milk by combination of membrane- and enzyme- based technologies. A ceramic-made tubular nanofiltration membrane with pore size 5 nm, placed in a cross-flow membrane house, was used for the production of liquid milk protein concentrate by reducing milk serum as a permeate. As the mean radius of casein micelle and their conjugated form with whey proteins in ultra-heat-treated skimmed milk were quite high compared to the pore size of the nanofiltration membrane, they were almost rejected by the membrane. Membrane filtration process alone cannot change the biological activities of milk proteins. Biological activities of protein derivatives, i.e., peptides offer antioxidant capacity, angiotensin converting enzyme inhibitory activity, and antibacterial activity. Therefore, milk with concentrated proteins from the retentate side of the membrane was treated with the different concentrations of trypsin, such as $0.008 \text{ g}\cdot\text{L}^{-1}$, $0.016 \text{ g}\cdot\text{L}^{-1}$, $0.032 \text{ g}\cdot\text{L}^{-1}$, and $0.064 \text{ g}\cdot\text{L}^{-1}$ in individual batch-mode experiments. Hydrolysis of milk protein was enzyme dose dependent because trypsin cleaves the peptide bond at the C-terminus of lysin and arginine in specific way. Antioxidant capacity, angiotensin converting enzyme inhibitory activity, and antibacterial activity of liquid milk protein concentrate were increased depending on the enzymatic hydrolysis of milk proteins. Trypsin concentration $0.032 \text{ g}\cdot\text{L}^{-1}$ was able to reduce allergenic epitopes at more than 99.9% in liquid milk protein concentrate.

After summarizing all experimental results, one may believe that the proposed technology may reduce the limitations of milk protein concentrate production and increase the consumption of dairy products. To the best of our knowledge, this is the first attempt to produce liquid milk protein concentrate with antioxidant capacity, angiotensin converting enzyme inhibitory activity, antibacterial activity, and hypoallergenic property by membrane filtration and enzymatic modification of proteins. In general, small-scale and medium-scale dairy plants prefer to use liquid milk protein concentrate for preparing cultured-dairy products instead of using dried milk protein concentrate for economical issue. Therefore, to implement this process in industrial scale, further systematic investigation with

techno-economical viewpoint is a prerequisite. However, in the present investigation molecular weight of peptides derived from concentrated milk proteins were determined by SDS-PAGE; more accurate results about molecular mass distribution of peptides and their sequences may be determined by a LC-ESI-Q-TOF-MS-based bottom-up sequencing in future research. In the groundbreaking research area of food biotechnology, one may expect that the proposed research may receive attention from academic and industrial sectors.

Author Contributions: A.N. was involved in performing the experiment, evaluating the results, and writing the whole manuscript. B.A.E. and A.C. were involved in assisting with the experiments, preparing graphs, and tables. G.K. was involved in the microbiological assay. L.A., A.T., E.S., and A.K. were involved in performing the biochemical assay. Z.K. was involved in statistical analysis. K.P.-H. and G.V. were involved in cross checking results and correcting the whole manuscript. All authors have read and agreed to the published version of the manuscript.

Funding: This research received no external funding.

Acknowledgments: Authors acknowledge the support from the European Union project (grant agreement no. EFOP-3.6.3-VEKOP-16-2017-00005). A. Csighy acknowledges Doctoral School of Food Science, Szent István University, Hungary. Z. Kovacs acknowledges the support of the New National Excellence Program of the Ministry for Innovation and Technology (ÚNKP-19-4-SZIE-27) and the Bolyai János Scholarship from the Hungarian Academy of Sciences. L. Abrankó is grateful for the János Bolyai Research Scholarship from the Hungarian Academy of Sciences. This research was supported by the Higher Education Institutional Excellence Program (FEKUTSTRAT) awarded by the Ministry of Human Capacities within the framework of plant breeding and plant protection researches of Szent István University, Budapest, Hungary.

Conflicts of Interest: The authors declare no conflict of interest.

References

1. St-Onge, M.-P.; Farnworth, E.R.; Jones, P.J. Consumption of fermented and nonfermented dairy products: Effects on cholesterol concentrations and metabolism. *Am. J. Clin. Nutr.* **2000**, *71*, 674–681. [CrossRef] [PubMed]
2. Guinee, T.P.; O’Kennedy, B.T.; Kelly, P.M. Effect of Milk Protein Standardization Using Different Methods on the Composition and Yields of Cheddar Cheese. *J. Dairy Sci.* **2006**, *89*, 468–482. [CrossRef]
3. Amatayakul, T.; Sherkat, F.; Shah, N.P. Syneresis in set yogurt as affected by EPS starter cultures and levels of solids. *Int. J. Dairy Technol.* **2006**, *59*, 216–221. [CrossRef]
4. Schuck, P.; Jeantet, R.; Bhandari, B.; Chen, X.D.; Perrone, Í.T.; De Carvalho, A.F.; Fenelon, M.; Kelly, P. Recent advances in spray drying relevant to the dairy industry: A comprehensive critical review. *Dry. Technol.* **2016**, *34*, 1773–1790. [CrossRef]
5. Ur Rehman, S.; Farkye, N.Y.; Considine, T.; Schaffner, A.; Drake, M.A. Effects of Standardization of Whole Milk with Dry Milk Protein Concentrate on the Yield and Ripening of Reduced-Fat Cheddar Cheese. *J. Dairy Sci.* **2003**, *86*, 1608–1615. [CrossRef]
6. Meena, G.S.; Singh, A.K.; Panjagari, N.R.; Arora, S. Milk protein concentrates: Opportunities and challenges. *J. Food Sci. Technol.* **2017**, *54*, 3010–3024. [CrossRef]
7. Amelia, I.; Barbano, D.M. Production of an 18% protein liquid micellar casein concentrate with a long refrigerated shelf life. *J. Dairy Sci.* **2013**, *96*, 3340–3349. [CrossRef]
8. Henriques, M.H.F.; Gomes, D.M.G.S.; Pereira, C.J.D.; Gil, M.H.M. Effects of Liquid Whey Protein Concentrate on Functional and Sensorial Properties of Set Yogurts and Fresh Cheese. *Food Bioprocess Technol.* **2013**, *6*, 952–963. [CrossRef]
9. Rosenberg, M. Current and future applications for membrane processes in the dairy industry. *Trends Food Sci. Technol.* **1995**, *6*, 12–19. [CrossRef]
10. Pouliot, Y. Membrane processes in dairy technology—From a simple idea to worldwide panacea. *Int. Dairy J.* **2008**, *18*, 735–740. [CrossRef]
11. Kumar, P.; Sharma, N.; Ranjan, R.; Kumar, S.; Bhat, Z.F.; Jeong, D.K. Perspective of Membrane Technology in Dairy Industry: A Review. *Asian Australas. J. Anim. Sci.* **2013**, *26*, 1347. [CrossRef] [PubMed]
12. Li, H.; Hsu, Y.-C.; Zhang, Z.; Dharsana, N.; Ye, Y.; Chen, V. The influence of milk components on the performance of ultrafiltration/diafiltration of concentrated skim milk. *Sep. Sci. Technol.* **2017**, *52*, 381–391. [CrossRef]

13. Arunkumar, A.; MR, E. Milk Protein Concentration Using Negatively Charged Ultrafiltration Membranes. *Foods* **2018**, *7*, 134. [CrossRef] [PubMed]
14. Gavazzi-April, C.; Benoit, S.; Doyen, A.; Britten, M.; Pouliot, Y. Preparation of milk protein concentrates by ultrafiltration and continuous diafiltration: Effect of process design on overall efficiency. *J. Dairy Sci.* **2018**, *101*, 9670–9679. [CrossRef] [PubMed]
15. Ng, K.S.Y.; Haribabu, M.; Harvie, D.J.E.; Dunstan, D.E.; Martin, G.J.O. Mechanisms of flux decline in skim milk ultrafiltration: A review. *J. Membr. Sci.* **2017**, *523*, 144–162. [CrossRef]
16. Bacchin, P.; Aimar, P.; Field, R.W. Critical and sustainable fluxes: Theory, experiments and applications. *J. Membr. Sci.* **2006**, *281*, 42–69. [CrossRef]
17. Marshall, A.D.; Munro, P.A.; Trägårdh, G. The effect of protein fouling in microfiltration and ultrafiltration on permeate flux, protein retention and selectivity: A literature review. *Desalination* **1993**, *91*, 65–108. [CrossRef]
18. Bahnasawy, A.H.; Shenana, M.E. Flux behavior and energy consumption of ultrafiltration (UF) process of milk. *Aust. J. Agric. Eng.* **2010**, *1*, 54–65.
19. Méthot-Hains, S.; Benoit, S.; Bouchard, C.; Doyen, A.; Bazinet, L.; Pouliot, Y. Effect of transmembrane pressure control on energy efficiency during skim milk concentration by ultrafiltration at 10 and 50 °C. *J. Dairy Sci.* **2016**, *99*, 8655–8664. [CrossRef]
20. Guetouache, M.; Guessas, B.; Medjekal, S. Composition and nutritional value of raw milk 2014. *Bio. Sci. Pharm. Res.* **2014**, *2*, 115–122.
21. Walsh, J.; Meyer, R.; Shah, N.; Quekett, J.; Fox, A.T. Differentiating milk allergy (IgE and non-IgE mediated) from lactose intolerance: Understanding the underlying mechanisms and presentations. *Br. J. Gen. Pract.* **2016**, *66*, e609–e611. [CrossRef] [PubMed]
22. Lifschitz, C.; Szajewska, H. Cow's milk allergy: Evidence-based diagnosis and management for the practitioner. *Eur. J. Pediatrics* **2015**, *174*, 141–150. [CrossRef] [PubMed]
23. Sicherer, S.H.; Sampson, H.A. Food allergy: Epidemiology, pathogenesis, diagnosis, and treatment. *J. Allergy Clin. Immunol.* **2014**, *133*, 291–307. [CrossRef]
24. US Food and Drug Administration. Food Allergen Labeling and Consumer Protection Act of 2004 (FALCPA). *J. Acad. Nutr. Diet.* **2004**, *106*, 1742–1744.
25. Sackesen, C.; Altintas, D.U.; Bingol, A.; Bingol, G.; Buyuktiryaki, B.; Demir, E.; Kansu, A.; Kuloglu, Z.; Tamay, Z.; Sekerel, B.E.; et al. Current Trends in Tolerance Induction in Cow's Milk Allergy: From Passive to Proactive Strategies. *Front. Pediatrics* **2019**, *7*, 372. [CrossRef]
26. Forouhi, N.G.; Krauss, R.M.; Taubes, G.; Willett, W. Dietary fat and cardiometabolic health: Evidence, controversies, and consensus for guidance. *BMJ* **2018**, *361*. [CrossRef]
27. Lordan, R.; Tsoupras, A.; Mitra, B.; Zabetakis, I. Dairy Fats and Cardiovascular Disease: Do We Really Need to be Concerned? *Foods* **2018**, *7*, 29. [CrossRef]
28. Ferreira, L.S.S.; Fernandes, C.S.; Vieira, M.N.N.; De Felice, F.G. Insulin Resistance in Alzheimer's Disease. *Front. Neurosci.* **2018**, *12*. [CrossRef]
29. Lee, H.J.; Seo, H.I.; Cha, H.Y.; Yang, Y.J.; Kwon, S.H.; Yang, S.J. Diabetes and Alzheimer's Disease: Mechanisms and Nutritional Aspects. *Clin. Nutr. Res.* **2018**, *7*, 229–240. [CrossRef]
30. Xu, Q.; Shi, J.; Yao, M.; Jiang, M.; Luo, Y. Effects of heat treatment on the antigenicity of four milk proteins in milk protein concentrates. *Food Agric. Immunol.* **2016**, *27*, 401–413. [CrossRef]
31. Villa, C.; Costa, J.; Mafra, I. Detection and Quantification of Milk Ingredients as Hidden Allergens in Meat Products by a Novel Specific Real-Time PCR Method. *Biomolecules* **2019**, *9*, 804. [CrossRef] [PubMed]
32. Villa, C.; Costa, J.; Oliveira, M.B.P.P.; Mafra, I. Bovine Milk Allergens: A Comprehensive Review. *Compr. Rev. Food Sci. Food Saf.* **2018**, *17*, 137–164. [CrossRef]
33. Bu, G.; Luo, Y.; Chen, F.; Liu, K.; Zhu, T. Milk processing as a tool to reduce cow's milk allergenicity: A mini-review. *Dairy Sci. Technol.* **2013**, *93*, 211–223. [CrossRef] [PubMed]
34. Kleber, N.; Maier, S.; Hinrichs, J. Antigenic response of bovine β -lactoglobulin influenced by ultra-high pressure treatment and temperature. *Innov. Food Sci. Emerg. Technol.* **2007**, *8*, 39–45. [CrossRef]
35. Chicón, R.; Belloque, J.; Alonso, E.; López-Fandiño, R. Immunoreactivity and digestibility of high-pressure-treated whey proteins. *Int. Dairy J.* **2008**, *18*, 367–376. [CrossRef]
36. Kleber, N.; Hinrichs, J. Antigenic response of β -lactoglobulin in thermally treated bovine skim milk and sweet whey. *Milchwissenschaft* **2007**, *62*, 121–124.

37. Fiocchi, A.; Restani, P.; Riva, E.; Mirri, G.P.; Santini, I.; Bernardo, L.; Galli, C.L. Heat treatment modifies the allergenicity of beef and bovine serum albumin. *Allergy* **2008**, *53*, 798–802. [CrossRef]
38. Bu, G.; Luo, Y.; Zheng, Z.; Zheng, H. Effect of heat treatment on the antigenicity of bovine α -lactalbumin and β -lactoglobulin in whey protein isolate. *Food Agric. Immunol.* **2009**, *20*, 195–206. [CrossRef]
39. Ismahan, B.D.; Hanane, K.; Omar, K.; Djamel, S. Microwave irradiation of bovine milk reduces allergic response in mouse model of food allergy. *Front. Immunol.* **2014**, *10*. [CrossRef]
40. Cheison, S.C.; Wang, Z.; Xu, S.-Y. Preparation of Whey Protein Hydrolysates Using a Single- and Two-Stage Enzymatic Membrane Reactor and Their Immunological and Antioxidant Properties: Characterization by Multivariate Data Analysis. *J. Agric. Food Chem.* **2007**, *55*, 3896–3904. [CrossRef]
41. Guadix, A.; Camacho, F.; Guadix, E.M. Production of whey protein hydrolysates with reduced allergenicity in a stable membrane reactor. *J. Food Eng.* **2006**, *72*, 398–405. [CrossRef]
42. Kobayashi, K.; Hirano, A.; Ohta, A.; Yoshida, T.; Takahashi, K.; Hattori, M. Reduced Immunogenicity of β -Lactoglobulin by Conjugation with Carboxymethyl Dextran Differing in Molecular Weight. *J. Agric. Food Chem.* **2001**, *49*, 823–831. [CrossRef]
43. Bu, G.; Lu, J.; Zheng, Z.; Luo, Y. Influence of Maillard reaction conditions on the antigenicity of bovine α -lactalbumin using response surface methodology. *J. Sci. Food Agric.* **2009**, *89*, 2428–2434. [CrossRef]
44. Bu, G.; Luo, Y.; Lu, J.; Zhang, Y. Reduced antigenicity of β -lactoglobulin by conjugation with glucose through controlled Maillard reaction conditions. *Food Agric. Immunol.* **2010**, *21*, 143–156. [CrossRef]
45. Pahud, J.J.; Monti, J.C.; Jost, R. Allergenicity of whey protein: Its modification by tryptic in vitro hydrolysis of the protein. *J. Pediatric Gastroenterol. Nutr.* **1985**, *4*, 408–413. [CrossRef]
46. Nakamura, T.; Sado, H.; Syukunobe, Y.; Hirota, T. Antigenicity of whey protein hydrolysates prepared by combination of two proteases. *Milchwissenschaft* **1993**, *48*, 667–670.
47. Wroblewska, B.; Karamac, M.; Amarowicz, R.; Szymkiewicz, A.; Troszynska, A.; Kubicka, E. Immunoreactive properties of peptide fractions of cow whey milk proteins after enzymatic hydrolysis. *Int. J. Food Sci. Technol.* **2004**, *39*, 839–850. [CrossRef]
48. Ena, J.M.; Berestejn, E.C.H.; Robben, A.J.P.M.; Schmidt, D.G. Whey Protein Antigenicity Reduction by Fungal Proteinases and a Pepsin/Pancreatin Combination. *J. Food Sci.* **1995**, *60*, 104–110. [CrossRef]
49. Chicón, R.; Belloque, J.; Recio, I.; López-Fandiño, R. Influence of high hydrostatic pressure on the proteolysis of β -lactoglobulin A by trypsin. *J. Dairy Res.* **2006**, *73*, 121–128. [CrossRef]
50. Bonomi, F.; Fiocchi, A.; Frøkiær, H.; Gaiaschi, A.; Iametti, S.; Poiesi, C.; Rasmussen, P.; Restani, P.; Rovere, P. Reduction of immunoreactivity of bovine β -lactoglobulin upon combined physical and proteolytic treatment. *J. Dairy Res.* **2003**, *70*, 51–59. [CrossRef]
51. Beran, M.; Klubal, R.; Molik, P.; Strohalm, J.; Urban, M.; Klaudyova, A.A.; Prajzlerova, K. Influence of high-hydrostatic pressure on tryptic and chymotryptic hydrolysis of milk proteins. *High Press. Res.* **2009**, *29*, 23–27. [CrossRef]
52. El Mecherfi, K.E.; Saidi, D.; Kheroua, O.; Boudraa, G.; Touhami, M.; Rouaud, O.; Curet, S.; Choiset, Y.; Rabesona, H.; Chobert, J.-M.; et al. Combined microwave and enzymatic treatments for β -lactoglobulin and bovine whey proteins and their effect on the IgE immunoreactivity. *Eur. Food Res. Technol.* **2011**, *233*, 859–867. [CrossRef]
53. Izquierdo, F.J.; Alli, I.; Yaylayan, V.; Gomez, R. Microwave-assisted digestion of β -lactoglobulin by pronase, α -chymotrypsin and pepsin. *Int. Dairy J.* **2007**, *17*, 465–470. [CrossRef]
54. Izquierdo, F.J.; Peñas, E.; Baeza, M.L.; Gomez, R. Effects of combined microwave and enzymatic treatments on the hydrolysis and immunoreactivity of dairy whey proteins. *Int. Dairy J.* **2008**, *18*, 918–922. [CrossRef]
55. Yang, W.; Tu, Z.; Wang, H.; Zhang, L.; Kaltashov, I.A.; Zhao, Y.; Niu, C.; Yao, H.; Ye, W. The mechanism of reduced IgG/IgE-binding of β -lactoglobulin by pulsed electric field pretreatment combined with glycation revealed by ECD/FTICR-MS. *Food Funct.* **2018**, *9*, 417–425. [CrossRef]
56. Quintieri, L.; Monaci, L.; Baruzzi, F.; Giuffrida, M.G.; De Candia, S.; Caputo, L. Reduction of whey protein concentrate antigenicity by using a combined enzymatic digestion and ultrafiltration approach. *J. Food Sci. Technol.* **2017**, *54*, 1910–1916. [CrossRef]
57. El Mecherfi, K.E.; Curet, S.; Lupi, R.; Larré, C.; Rouaud, O.; Choiset, Y.; Rabesona, H.; Haertlé, T. Combined microwave processing and enzymatic proteolysis of bovine whey proteins: The impact on bovine β -lactoglobulin allergenicity. *J. Food Sci. Technol.* **2019**, *56*, 177–186. [CrossRef]
58. Spies, J.B. Milk Allergy. *Milk Food Technol.* **1973**, *36*, 225–231. [CrossRef]

59. El-Agamy, E.I. The challenge of cow milk protein allergy. *Small Rumin. Res.* **2007**, *68*, 64–72. [CrossRef]
60. Kim, S.B.; Ki, K.S.; Khan, M.A.; Lee, W.S.; Lee, H.J.; Ahn, B.S.; Kim, H.S. Peptic and Tryptic Hydrolysis of Native and Heated Whey Protein to Reduce Its Antigenicity. *J. Dairy Sci.* **2007**, *90*, 4043–4050. [CrossRef]
61. Ahmad, N.; Imran, M.; Khan, M.K.; Nisa, M.U. Degree of hydrolysis and antigenicity of buffalo alpha S1 casein and its hydrolysates in children with cow milk allergy. *Food Agric. Immunol.* **2016**, *27*, 87–98. [CrossRef]
62. Abd El-Fattah, A.M.; Sakr, S.S.; El-Dieb, S.M.; Elkashef, H.A.S. Bioactive peptides with ACE-I and antioxidant activity produced from milk proteolysis. *Int. J. Food Prop.* **2017**, *20*, 3033–3042. [CrossRef]
63. Luo, Y.; Pan, K.; Zhong, Q. Physical, chemical and biochemical properties of casein hydrolyzed by three proteases: Partial characterizations. *Food Chem.* **2014**, *155*, 146–154. [CrossRef] [PubMed]
64. Bamdad, F.; Shin, S.H.; Suh, J.-W.; Nimalaratne, C.; Sunwoo, H. Anti-Inflammatory and Antioxidant Properties of Casein Hydrolysate Produced Using High Hydrostatic Pressure Combined with Proteolytic Enzymes. *Molecules* **2017**, *22*, 609. [CrossRef] [PubMed]
65. Nath, A.; Szécsi, G.; Csehi, B.; Mednyánszky, Z.; Kiskó, G.; Bányai, É.; Dernovics, M.; Koris, A. Production of Hypoallergenic Antibacterial Peptides from Defatted Soybean Meal by a Membrane Associated Bioreactor: A Bioprocess Engineering Study with Comprehensive Product Characterization. *Food Technol. Biotechnol.* **2017**, *55*, 308–324. [CrossRef] [PubMed]
66. Nath, A.; Chakraborty, S.; Bhattacharjee, C.; Chowdhury, R. Studies on the separation of proteins and lactose from casein whey by cross-flow ultrafiltration. *Desalin. Water Treat.* **2015**, *54*, 481–501. [CrossRef]
67. Nath, A.; Kailo, G.G.; Mednyánszky, Z.; Kiskó, G.; Csehi, B.; Pásztor-Huszár, K.; Gerencsér-Berta, R.; Galambos, I.; Pozsgai, E.; Bánvölgyi, S.; et al. Antioxidant and Antibacterial Peptides from Soybean Milk through Enzymatic- and Membrane-Based Technologies. *Bioengineering* **2019**, *7*, 5. [CrossRef]
68. Nongonierma, A.B.; Paoletta, S.; Mudgil, P.; Maqsood, S.; FitzGerald, R.J. Dipeptidyl peptidase IV (DPP-IV) inhibitory properties of camel milk protein hydrolysates generated with trypsin. *J. Funct. Foods* **2017**, *34*, 49–58. [CrossRef]
69. Cheison, S.C.; Schmitt, M.; Leeb, E.; Letzel, T.; Kulozik, U. Influence of temperature and degree of hydrolysis on the peptide composition of trypsin hydrolysates of β -lactoglobulin: Analysis by LC–ESI-TOF/MS. *Food Chem.* **2010**, *121*, 457–467. [CrossRef]
70. Elfagm, A.A.; Wheelock, J.V. Interaction of Bovine α -Lactalbumin and β -Lactoglobulin during Heating. *J. Dairy Sci.* **1978**, *61*, 28–32. [CrossRef]
71. De Wit, J.; Klarenbeek, B. Effects of Various Heat Treatments on Structure and Solubility of Whey Proteins. *J. Dairy Sci.* **1984**, *67*, 2701–2710. [CrossRef]
72. Cassiani, D.M.; Yamul, D.K.; Conforti, P.A.; Pérez, V.A.; Lupano, C.E. Structure and Functionality of Whey Protein Concentrate-Based Products with Different Water Contents. *Food Bioprocess Technol.* **2013**, *6*, 217–227. [CrossRef]
73. Rauh, V.M.; Johansen, L.B.; Bakman, M.; Ipsen, R.; Paulsson, M.; Larsen, L.B.; Hammershøj, M. Protein lactosylation in UHT milk during storage measured by Liquid Chromatography-Mass Spectrometry and quantification of furosine. *Int. J. Dairy Technol.* **2015**, *68*, 486–494. [CrossRef]
74. Csehi, B.; Szerdahelyi, E.; Pásztor-Huszár, K.; Salamon, B.; Tóth, A.; Zeke, I.; Jónás, G.; Friedrich, L. Changes of protein profiles in pork and beef meat caused by high hydrostatic pressure treatment. *Acta Aliment.* **2016**, *45*, 565–571. [CrossRef]
75. Hajós, G.; Polgár, M.; Farkas, J. High-pressure effects on IgE immunoreactivity of proteins in a sausage batter. *Innov. Food Sci. Emerg. Technol.* **2004**, *5*, 443–449. [CrossRef]
76. Benzie, I.F.F.; Strain, J.J. The Ferric Reducing Ability of Plasma (FRAP) as a Measure of “Antioxidant Power”: The FRAP Assay. *Anal. Biochem.* **1996**, *239*, 70–76. [CrossRef]
77. Fagyas, M.; Úri, K.; Siket, I.M.; Daragó, A.; Boczán, J.; Bányai, E.; Édes, I.; Papp, Z.; Tóth, A. New Perspectives in the Renin-Angiotensin-Aldosterone System (RAAS) I: Endogenous Angiotensin Converting Enzyme (ACE) Inhibition. *PLoS ONE* **2014**, *9*, e87843. [CrossRef]
78. Bradford, M.M. A rapid and sensitive method for the quantitation of microgram quantities of protein utilizing the principle of protein-dye binding. *Anal. Biochem.* **1976**, *72*, 248–254. [CrossRef]
79. Hussein, K.; Friedrich, L.; Kisko, G.; Ayari, E.; Nemeth, C.; Dalmadi, I. Use of allyl-isothiocyanate and carvacrol to preserve fresh chicken meat during chilling storage. *Czech J. Food Sci.* **2019**, *37*, 417–424. [CrossRef]

80. De Wit, J.N. Nutritional and Functional Characteristics of Whey Proteins in Food Products. *J. Dairy Sci.* **1998**, *81*, 597–608. [CrossRef]
81. Penfield, M.P.; Campbell, A.M.; Penfield, M.P.; Campbell, A.M. Chapter 8—Milk and Milk Products. In *Food Science and Technology*, 3rd ed.; Penfield, M.P., Campbell, A.M.B.T.-E.F.S., Eds.; Academic Press: San Diego, CA, USA, 1990; pp. 162–183, ISBN 978-0-12-157920-3.
82. Relkin, P.; Mulvihill, D.M. Thermal unfolding of β -lactoglobulin, α -lactalbumin, and bovine serum albumin. A thermodynamic approach. *Crit. Rev. Food Sci. Nutr.* **1996**, *36*, 565–601. [CrossRef] [PubMed]
83. Lee, Y.-R.; Hong, Y.-H. Electrophoretic Behaviors of α -Lactalbumin and β -Lactoglobulin Mixtures Caused by Heat Treatment. *Asian Australas. J. Anim. Sci.* **2003**, *16*, 1041–1045. [CrossRef]
84. Manderson, G.A.; Hardman, M.J.; Creamer, L.K. Effect of Heat Treatment on the Conformation and Aggregation of β -Lactoglobulin A, B, and C. *J. Agric. Food Chem.* **1998**, *46*, 5052–5061. [CrossRef]
85. Law, A.J.R.; Horne, D.S.; Banks, J.M.; Leaver, J. Heat-induced changes in the whey proteins and caseins. *Milchwissenschaft* **1994**, *49*, 125–129.
86. Dannenberg, F.; Kessler, H.-G. Reaction Kinetics of the Denaturation of Whey Proteins in Milk. *J. Food Sci.* **1988**, *53*, 258–263. [CrossRef]
87. Dannenberg, F.; Kessler, H.G. Thermodynamic approach to kinetics of β -lactoglobulin denaturation in heated skim milk and sweet whey. *Milchwissenschaft* **1988**, *43*, 139–142.
88. Dalglish, D.G. Denaturation and aggregation of serum proteins and caseins in heated milk. *J. Agric. Food Chem.* **1990**, *38*, 1995–1999. [CrossRef]
89. Gezimati, J.; Singh, H.; Creamer, L.K. Heat-Induced Interactions and Gelation of Mixtures of Bovine β -Lactoglobulin and Serum Albumin. *J. Agric. Food Chem.* **1996**, *44*, 804–810. [CrossRef]
90. Sawyer, W.H. Complex Between β -Lactoglobulin and κ -Casein. A Review. *J. Dairy Sci.* **1969**, *52*, 1347–1355. [CrossRef]
91. Sawyer, W.H.; Coulter, S.T.; Jenness, R. Role of Sulfhydryl Groups in the Interaction of κ -Casein and β -Lactoglobulin. *J. Dairy Sci.* **1963**, *46*, 564–565. [CrossRef]
92. Jang, H.; Swaisgood, H. Disulfide Bond Formation Between Thermally Denatured β -Lactoglobulin and κ -Casein in Casein Micelles. *J. Dairy Sci.* **1990**, *73*, 900–904. [CrossRef]
93. Morr, C.V.; Ha, E.Y.W. Whey protein concentrates and isolates: Processing and functional properties. *Crit. Rev. Food Sci. Nutr.* **1993**, *33*, 431–476. [CrossRef] [PubMed]
94. Buchert, J.; Ercili Cura, D.; Ma, H.; Gasparetti, C.; Monogioudi, E.; Faccio, G.; Mattinen, M.; Boer, H.; Partanen, R.; Selinheimo, E.; et al. Crosslinking Food Proteins for Improved Functionality. *Annu. Rev. Food Sci. Technol.* **2010**, *1*, 113–138. [CrossRef]
95. Gerrard, J.A. Protein–protein crosslinking in food: Methods, consequences, applications. *Trends Food Sci. Technol.* **2002**, *13*, 391–399. [CrossRef]
96. Singh, H. Modification of food proteins by covalent crosslinking. *Trends Food Sci. Technol.* **1991**, *2*, 196–200. [CrossRef]
97. Miranda, G.; Bianchi, L.; Krupova, Z.; Trossat, P.; Martin, P. An improved LC–MS method to profile molecular diversity and quantify the six main bovine milk proteins, including genetic and splicing variants as well as post-translationally modified isoforms. *Food Chem. X* **2020**, *5*, 100080. [CrossRef]
98. Singh, H. Heat stability of milk. *Int. J. Dairy Technol.* **2004**, *57*, 111–119. [CrossRef]
99. Kastrup Dalsgaard, T.; Holm Nielsen, J.; Bach Larsen, L. Proteolysis of milk proteins lactosylated in model systems. *Mol. Nutr. Food Res.* **2007**, *51*, 404–414. [CrossRef]
100. Czerwenka, C.; Maier, I.; Pittner, F.; Lindner, W. Investigation of the lactosylation of whey proteins by liquid chromatography—Mass spectrometry. *J. Agric. Food Chem.* **2006**, *54*, 8874–8882. [CrossRef]
101. Losito, I.; Carbonara, T.; Monaci, L.; Palmisano, F. Evaluation of the thermal history of bovine milk from the lactosylation of whey proteins: An investigation by liquid chromatography—Electrospray ionization mass spectrometry. *Anal. Bioanal. Chem.* **2007**, *389*, 2065–2074. [CrossRef]
102. Almaas, H.; Cases, A.-L.; Devold, T.; Holm, H.; Langsrud, T.; Aabakken, L.; Aadnoy, T.; Vegarud, G. In vitro digestion of bovine and caprine milk by human gastric and duodenal enzymes. *Int. Dairy J.* **2006**, *16*, 961–968. [CrossRef]

103. Costa, F.F.; Vasconcelos Paiva Brito, M.A.; Moreira Furtado, M.A.; Martins, M.F.; Leal de Oliveira, M.A.; Mendonça De Castro Barra, P.; Amigo Garrido, L.; Siqueira De Oliveira Dos Santos, A. Microfluidic chip electrophoresis investigation of major milk proteins: Study of buffer effects and quantitative approaching. *Anal. Methods* **2014**, *6*, 1666–1673. [CrossRef]
104. Wróblewska, B.; Kaliszewska, A. Cow's Milk Proteins Immunoreactivity and Allergenicity in Processed Food. *Czech J. Food Sci.* **2012**, *30*, 211–219. [CrossRef]
105. Hong, Y.-H.; Creamer, L.K. Changed protein structures of bovine β -lactoglobulin B and α -lactalbumin as a consequence of heat treatment. *Int. Dairy J.* **2002**, *12*, 345–359. [CrossRef]
106. Dunnill, P.; Green, D.W. Sulphydryl groups and the N \rightleftharpoons R conformational change in β -lactoglobulin. *J. Mol. Biol.* **1966**, *15*, 147–151. [CrossRef]
107. Havea, P.; Singh, H.; Creamer, L.K. Characterization of heat-induced aggregates of β -lactoglobulin, α -lactalbumin and bovine serum albumin in a whey protein concentrate environment. *J. Dairy Res.* **2001**, *68*, 483–497. [CrossRef]
108. Raak, N.; Abbate, R.; Lederer, A.; Rohm, H.; Jaros, D. Size Separation Techniques for the Characterisation of Cross-Linked Casein: A Review of Methods and Their Applications. *Separations* **2018**, *5*, 14. [CrossRef]
109. Wu, Z.; Tiambeng, T.N.; Cai, W.; Chen, B.; Lin, Z.; Gregorich, Z.R.; Ge, Y. Impact of Phosphorylation on the Mass Spectrometry Quantification of Intact Phosphoproteins. *Anal. Chem.* **2018**, *90*, 4935–4939. [CrossRef]
110. Bobe, G.; Beitz, D.C.; Freeman, A.E.; Lindberg, G.L. Sample Preparation Affects Separation of Whey Proteins by Reversed-Phase High-Performance Liquid Chromatography. *J. Agric. Food Chem.* **1998**, *46*, 1321–1325. [CrossRef]
111. Cheema, M.; Mohan, M.S.; Campagna, S.R.; Jurat-Fuentes, J.L.; Harte, F.M. The association of low-molecular-weight hydrophobic compounds with native casein micelles in bovine milk. *J. Dairy Sci.* **2015**, *98*, 5155–5163. [CrossRef]
112. Assem, F.M.; Abd El-Gawad, M.A.M.; Kassem, J.M.; Abd El-Salam, M.H. Proteolysis and antioxidant activity of peptic, tryptic and chymotryptic hydrolysates of cow, buffalo, goat and camel caseins. *Int. J. Dairy Technol.* **2018**, *71*, 236–242. [CrossRef]
113. Power, O.; Jakeman, P.; FitzGerald, R.J. Antioxidative peptides: Enzymatic production, in vitro and in vivo antioxidant activity and potential applications of milk-derived antioxidative peptides. *Amino Acids* **2013**, *44*, 797–820. [CrossRef] [PubMed]
114. Manso, M.A.; López-Fandiño, R. Angiotensin I converting enzyme-inhibitory activity of bovine, ovine, and caprine kappa-casein macropeptides and their tryptic hydrolysates. *J. Food Prot.* **2003**, *66*, 1686–1692. [CrossRef]
115. Vermeirssen, V.; Van Camp, J.; Decroos, K.; Van Wijmelbeke, L.; Verstraete, W. The Impact of Fermentation and In Vitro Digestion on the Formation of Angiotensin-I-Converting Enzyme Inhibitory Activity from Pea and Whey Protein. *J. Dairy Sci.* **2003**, *86*, 429–438. [CrossRef]
116. Wang, C.; Tu, M.; Wu, D.; Chen, H.; Chen, C.; Wang, Z.; Jiang, L. Identification of an ACE-Inhibitory Peptide from Walnut Protein and Its Evaluation of the Inhibitory Mechanism. *Int. J. Mol. Sci.* **2018**, *19*, 1156. [CrossRef] [PubMed]
117. Pihlanto-Leppälä, A.; Rokka, T.; Korhonen, H. Angiotensin I converting enzyme inhibitory peptides derived from bovine milk proteins. *Int. Dairy J.* **1998**, *8*, 325–331. [CrossRef]
118. Abubakar, A.; Saito, T.; Kitazawa, H.; Kawai, Y.; Itoh, T. Structural Analysis of New Antihypertensive Peptides Derived from Cheese Whey Protein by Proteinase K Digestion. *J. Dairy Sci.* **1998**, *81*, 3131–3138. [CrossRef]
119. López-Fandiño, R.; Otte, J.; Van Camp, J. Physiological, chemical and technological aspects of milk-protein-derived peptides with antihypertensive and ACE-inhibitory activity. *Int. Dairy J.* **2006**, *16*, 1277–1293. [CrossRef]
120. Cheung, H.S.; Wang, F.L.; Ondetti, M.A.; Sabo, E.F.; Cushman, D.W. Binding of peptide substrates and inhibitors of angiotensin-converting enzyme. Importance of the COOH-terminal dipeptide sequence. *J. Biol. Chem.* **1980**, *255*, 401–407.
121. Medeiros, V.; Rainha, N.; Paiva, L.; Lima, E.; Baptista, J. Bovine Milk Formula Based on Partial Hydrolysis of Caseins by Bromelain Enzyme: Better Digestibility and Angiotensin-Converting Enzyme-Inhibitory Properties. *Int. J. Food Prop.* **2014**, *17*, 806–817. [CrossRef]

122. Malanovic, N.; Lohner, K. Antimicrobial Peptides Targeting Gram-Positive Bacteria. *Pharmaceuticals* **2016**, *9*, 59. [CrossRef] [PubMed]
123. Travkova, O.G.; Moehwald, H.; Brezesinski, G. The interaction of antimicrobial peptides with membranes. *Adv. Colloid Interface Sci.* **2017**, *247*, 521–532. [CrossRef] [PubMed]
124. Qian, F.; Sun, J.; Cao, D.; Tuo, Y.; Jiang, S.; Mu, G. Experimental and Modelling Study of the Denaturation of Milk Protein by Heat Treatment. *Korean J. Food Sci. Anim. Resour.* **2017**, *37*, 44. [CrossRef] [PubMed]
125. Abe, S.; Kabashima, K.; Moriyama, T.; Tokura, Y. Food-dependent anaphylaxis with serum IgE immunoreactive to dairy products containing high-molecular-weight proteins. *J. Dermatol. Sci.* **2010**, *57*, 137–140. [CrossRef]
126. Natale, M.; Bisson, C.; Monti, G.; Peltran, A.; Perono Garoffo, L.; Valentini, S.; Fabris, C.; Bertino, E.; Coscia, A.; Conti, A.; et al. Cow's milk allergens identification by two-dimensional immunoblotting and mass spectrometry. *Mol. Nutr. Food Res.* **2004**, *48*, 363–369. [CrossRef]
127. Meyer, P.; Petermeier, J.; Hartinger, M.; Kulozik, U. Concentration of Skim Milk by a Cascade Comprised of Ultrafiltration and Nanofiltration: Investigation of the Nanofiltration of Skim Milk Ultrafiltration Permeate. *Food Bioprocess Technol.* **2017**, *10*, 469–478. [CrossRef]
128. Mistry, V.V.; Hassan, H.N. Delactosed, High Milk Protein Powder. 1. Manufacture and Composition. *J. Dairy Sci.* **1991**, *74*, 1163–1169. [CrossRef]
129. Luo, X.; Ramchandran, L.; Vasiljevic, T. Lower ultrafiltration temperature improves membrane performance and emulsifying properties of milk protein concentrates. *Dairy Sci. Technol.* **2015**, *95*, 15–31. [CrossRef]
130. Rinaldoni, A.N.; Tarazaga, C.C.; Campderrós, M.E.; Padilla, A.P. Assessing performance of skim milk ultrafiltration by using technical parameters. *J. Food Eng.* **2009**, *92*, 226–232. [CrossRef]
131. Grandison, A.S.; Youravong, W.; Lewis, M.J. Hydrodynamic factors affecting flux and fouling during ultrafiltration of skimmed milk. *Le Lait* **2000**, *80*, 165–174. [CrossRef]
132. Meena, G.S.; Singh, A.K.; Arora, S.; Borad, S.; Sharma, R.; Gupta, V.K. Physico-chemical, functional and rheological properties of milk protein concentrate 60 as affected by disodium phosphate addition, diafiltration and homogenization. *J. Food Sci. Technol.* **2017**, *54*, 1678–1688. [CrossRef]
133. Meena, G.S.; Singh, A.K.; Gupta, V.K.; Borad, S.; Parmar, P.T. Effect of change in pH of skim milk and ultrafiltered/diafiltered retentates on milk protein concentrate (MPC70) powder properties. *J. Food Sci. Technol.* **2018**, *55*, 3526–3537. [CrossRef] [PubMed]
134. Meyer, P.; Mayer, A.; Kulozik, U. High concentration of skim milk proteins by ultrafiltration: Characterisation of a dynamic membrane system with a rotating membrane in comparison with a spiral wound membrane. *Int. Dairy J.* **2015**, *51*, 75–83. [CrossRef]
135. Samuelsson, G.; Dejmek, P.; Trägårdh, G.; Paulsson, M. Minimizing whey protein retention in cross-flow microfiltration of skim milk. *Int. Dairy J.* **1997**, *7*, 237–242. [CrossRef]
136. Pompei, C.; Resmini, P.; Peri, C. Skim Milk Protein Recovery and Purification by Ultrafiltration Influence of Temperature on Permeation Rate and Retention. *J. Food Sci.* **1973**, *38*, 867–870. [CrossRef]
137. Meena, G.S.; Singh, A.K.; Gupta, V.K.; Borad, S.; Arora, S.; Tomar, S.K. Effect of pH adjustment, homogenization and diafiltration on physicochemical, reconstitution, functional and rheological properties of medium protein milk protein concentrates (MPC70). *J. Food Sci. Technol.* **2018**, *55*, 1376–1386. [CrossRef]
138. Meena, G.S.; Singh, A.K.; Gupta, V.K.; Borad, S.G.; Arora, S.; Tomar, S.K. Alteration in physicochemical, functional, rheological and reconstitution properties of milk protein concentrate powder by pH, homogenization and diafiltration. *J. Food Sci. Technol.* **2019**, *56*, 1622–1630. [CrossRef]



© 2020 by the authors. Licensee MDPI, Basel, Switzerland. This article is an open access article distributed under the terms and conditions of the Creative Commons Attribution (CC BY) license (<http://creativecommons.org/licenses/by/4.0/>).

Review

Modifying Effects of Physical Processes on Starch and Dietary Fiber Content of Foodstuffs

Róbert Nagy¹, Endre Máthé¹, János Csapó^{2,3} and Péter Sipos^{1,*}

¹ Faculty of Agricultural and Food Sciences and Environmental Management, Institute of Nutrition, University of Debrecen, 138 Böszörményi Street, 4032 Debrecen, Hungary; nagy.robert@agr.unideb.hu (R.N.); endre.mathe64@gmail.com (E.M.)

² Faculty of Agricultural and Food Sciences and Environmental Management, Institute of Food Technology, University of Debrecen, 138 Böszörményi Street, 4032 Debrecen, Hungary; csapo.janos@gmail.hu

³ Department of Food Science, Faculty of Miercurea Ciuc, SAPIENTIA Hungarian University of Transylvania, Piata Libertatii 1, RO-4100, 530104 Miercurea Ciuc, Romania

* Correspondence: siposp@agr.unideb.hu

Abstract: Carbohydrates are one of the most important nutrients in human consumption. The digestible part of carbohydrates has a significant role in maintaining the energy status of the body and the non-digestible parts like dietary fibers have specific nutritional functions. One of the key issues of food processing is how to influence the technological and nutritional properties of carbohydrates to meet modern dietary requirements more effectively, considering particularly the trends in the behavior of people and food-related health issues. Physical processing methods have several advantages compared to the chemical methods, where chemical reagents, such as acids or enzymes, are used for the modification of components. Furthermore, in most cases, there is no need to apply them supplementarily in the technology, only a moderate modification of current technology can result in significant changes in dietary properties. This review summarizes the novel results about the nutritional and technological effects of physical food processing influencing the starch and dietary fiber content of plant-derived foodstuffs.

Keywords: dietary fibers; starch; physical food processing; technological properties of carbohydrates

Citation: Nagy, R.; Máthé, E.; Csapó, J.; Sipos, P. Modifying Effects of Physical Processes on Starch and Dietary Fiber Content of Foodstuffs. *Processes* **2021**, *9*, 17. <https://dx.doi.org/10.3390/pr9010017>

Received: 9 November 2020

Accepted: 11 December 2020

Published: 23 December 2020

Publisher's Note: MDPI stays neutral with regard to jurisdictional claims in published maps and institutional affiliations.



Copyright: © 2020 by the authors. Licensee MDPI, Basel, Switzerland. This article is an open access article distributed under the terms and conditions of the Creative Commons Attribution (CC BY) license (<https://creativecommons.org/licenses/by/4.0/>).

1. Introduction

Carbohydrates produced by plants are a main energy source for all living organisms, though their bioavailability could feature some species-specific characteristics among animals and humans. In the context of human nutrition, carbohydrates can be rendered into digestible and non-digestible categories based upon the properties of carbohydrate utilization by the human digestive system. The non-digestible carbohydrates like dietary fibers on chemical grounds could be considered as three types: (i) non-starch type of polysaccharides like cellulose, hemicellulose, and arabinoxylan; (ii) non-digestible oligosaccharides, and (iii) resistant starch. Dietary fibers have an important role in the formation of the structure of foodstuffs, while their relevance in the prevention of numerous chronic diseases, such as type 1 or 2 diabetes, colon cancer, high blood pressure and cholesterol level, and different cardiovascular diseases has been demonstrated [1–4]. On the other hand, digestible carbohydrates, such as starch and its sugar monomers, provide energy, but also have a significant role in gel formation and water absorption and influence the viscosity, adhesion, and strength of binding amongst molecules. Starch is commonly used in several food processing technologies (e.g., in baking for crumb softening and as a food thickener and water binder), but other industries can also take advantage of its beneficial physical properties [5]. Starch does not swell in cold water, but forms a colloidal solution, gelatinizes when cooked, and retrogrades after cooling down, suggesting that such plausible modifications could widen its food-based technological range of application.

It is noteworthy that the modifications of starch could influence its solubility, digestibility, and absorption, affecting its nutritional value. Moreover, certain physical and chemical treatments could inflict changes on the non-digestible carbohydrates, influencing their technological properties and nutritional values. The current review intends to summarize the physical processes specific to the food industry with respect to the modifications of starch and dietary fibers affecting their technological parameters, together with some nutritional considerations.

2. Role of Carbohydrates in Nutrition and Food Processing

Oversimplifying the nutritional importance of carbohydrates would emphasize their energy-providing role for animals and humans. Nevertheless, a more careful analysis would reveal a fairly versatile functional spectrum of carbohydrates, including the synthesis of fatty acids, amino acids, nucleotides, glycolipids, glycoproteins, and vitamins, affecting cellular metabolism, the cytoskeleton, and redox regulation. Based on the digestibility of starch, it can be classified into rapidly and slowly digestible starch categories (see Figure 1). The former's digestion to glucose is initiated in the buccal cavity, and it is completed in the upper portion of the small intestine. The slowly digestible starch is digested and absorbed gradually after ingestion in the intestinal tract, resulting in a slower and more even glucose absorption, playing an important role in regulating blood insulin level, which helps in treating type 1 and 2 diabetes, cardiovascular diseases, and obesity [4,6].

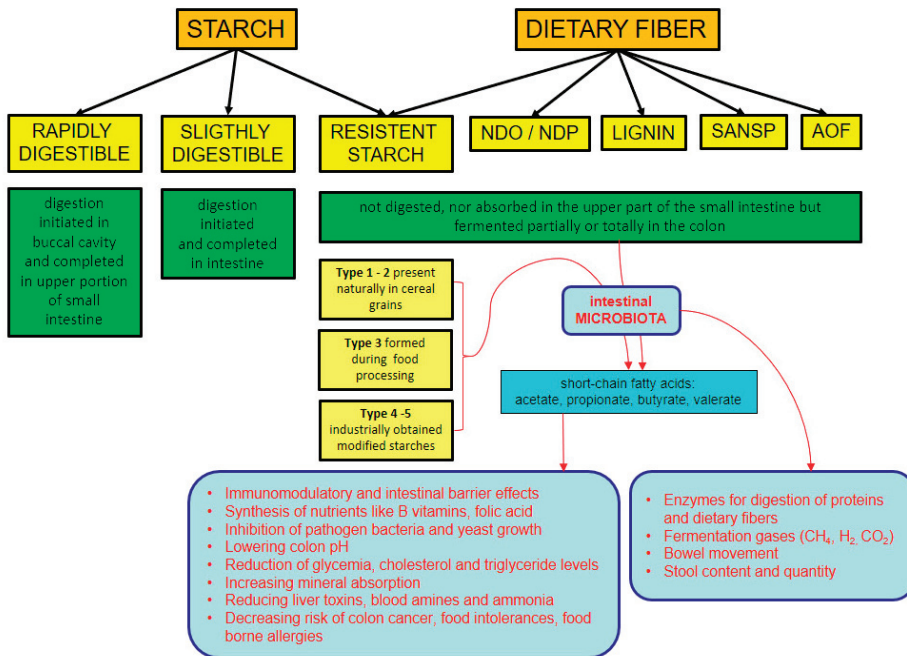


Figure 1. The comparison of some starch and dietary fiber-related properties. Note: NDO—non-digestible oligosaccharide; NDP—non-digestible polysaccharide (cellulose, hemicellulose, polyfructoses, gums, mucilages, pectins); SANSP—substances associated with non-starch polysaccharides (waxes, cutin, suberin); AOF—animal origin fiber (chitin, chitosan, chondroitin).

The third kind of starch is the so-called resistant type, which is neither digested nor absorbed in the upper part of the small intestine of healthy humans, therefore, it could be classified as dietary fiber. The resistant starch could be divided into five subgroups based on the origin of its resistance to digestion. Type 1 and 2 are present naturally in cereal grains,

while type 3 is formed during food processing. Type 4 and 5 are industrially obtained modified starches that cannot be obtained naturally. The resistant starch passing through the human digestive tract without digestion and absorption is utilized by the gastrointestinal microbiota through fermentation, resulting in useful short-chain fatty acids such as propionic acid or butyric acid that play an important role in maintaining the health status. It was suggested that the digestive system of humans constantly faces mild inflammation, and the abovementioned microbiota produced fatty acids helping to reduce this inflammation, as well as the other chronic diseases associated with inflammation. In addition to its anti-inflammatory and antimicrobial effects against *Salmonella typhimurium*, propionic acid was suggested to increase insulin sensitivity [4,7]. Furthermore, the ingestion of resistant starch would reduce calorie intake, and therefore could exert a preventive role regarding excessive caloric intake, obesity, and metabolic syndrome, and might reduce the risk of colon cancer and high blood sugar level [4].

In contrast with starch, dietary fibers have been defined as plant-derived carbohydrates that are resistant to digestion and absorption in the human small intestine and reaching the colon would provide some health-promoting effects [8]. Carbohydrate-based dietary fibers of animal origin, like chitin, chitosan, and chondroitin, have also been identified, but collagen protein was also included in the dietary fiber category due to its physical properties.

Among the dietary fibers, the non-digestible oligosaccharides (NDOs) and polysaccharides (NDPs) are partially or completely fermented by the microbiome of the digestive apparatus of humans, and do play a major role in the regulation of technological and sensory parameters of foods, with some of them acting like mucus substances and gel-forming agents. The NDOs and NDPs are based on principal groupings like cellulose, hemicellulose, polyfructoses, pectins, gums, and mucilages. Most of the NDOs and NDPs are not or only slightly soluble in water, but they absorb a significant amount of water, hence, they could affect the structure of foods. In several cases, the incorporation of NDOs, like cyclodextrins, fructooligosaccharides, or galactooligosaccharides, and NDPs, like hemicellulose, pectin, or beta-glucan, into recipes would positively modify texture, color, taste, viscosity, and the shelf life of foodstuff [2,9–12]. The fibers in question, besides their emulsifying properties, could absorb antioxidant compounds like phenolic compounds or vitamins, providing protection against the oxidation and rancidity of foods with a high fat content and increase product shelf life [12,13]. Moreover, such fibers could also bind different kinds of compounds, such as macronutrients, fat, and metal ions, and generate complex matrices within foodstuffs [12].

The dietary fibers exert a significant influence on the gastrointestinal tract, most particularly on the microbiome of the large intestine of humans, depending on a plethora of variables like their fermentation ability and dosage, together with the meal-specific matrix composition and structure [8]. Further to the concentration and composition of partially and/or highly fermentable dietary fibers present in the entire fiber-containing meal, and together with the consumer-specific physiological properties, the emerging physiological effects look rather complicated to study. Nevertheless, some physiological effects, like the absorption of nutrients, carbohydrate/fat, and sterol metabolisms, together with the colonic fermentation-related barrier and immune functions, and the production of stools, are intensively investigated in the case of healthy individuals and those with chronic diseases. The colonic microbiota produces enzymes to further assist the digestion of proteins, and to ferment dietary fibers, producing gases (methane, hydrogen, carbon dioxide), short chain fatty acids (SCFAs, C2–C5 organic acid-derived acetate, propionate, butyrate, valerate), and substantial amounts of lifeless bacterial mass that contributes to stool bulk. The extent of dietary fiber fermentation depends primarily upon its physicochemical nature, so that in the context of a cellulose–amylose–oat beta glucan–inulin–pea starch–potato starch comparison, increasing yields of acetate were observed, while the propionate and butyrate levels showed significant variation, and the valerate levels were mostly reduced [14]. Several studies are indicating the health-promoting effects of fermentable dietary fibers,

though the mechanisms are still poorly understood [15]. The anticancer effect was suggested to be related to the decreased synthesis of carcinogenic substances by rebalancing the colon microbiome and reducing the number of pathogenic bacteria [16] and/or the anti-inflammatory and anti-apoptotic effects of colonic bacteria-derived metabolites [17]. The link between increased dietary fiber intake and decreased risk or alleviation of diabetes was attributed to well-fermented and viscous fibers that seemed to reduce the glycemic response and to increase insulin sensitivity. Several experimental datasets indicate that well-fermented and viscous dietary fibers derived from oats, psyllium, pectin, and guar gum can lower blood cholesterol levels and might play a role in reducing the risk of cardiovascular diseases. Other highly fermented fibers, like inulin and fructooligosaccharides, promote calcium, magnesium, and iron absorption in the colon, and are essential for the integrity of the intestinal barrier, preventing many gastrointestinal diseases.

It is worth mentioning that even poorly fermented dietary fibers can have health-promoting effects since they could facilitate stool laxation by decreasing the colon-specific transition time, and they also bind substances such as bile acids and carcinogens, lowering the risk of colon cancer and cholesterol pathologies. Poorly or unfermented dietary fibers will slow down the absorption of other food components and could increase the feeling of satiety, making them suitable for anti-obesity diets [10,18]. Despite all the progress made in explaining the dietary fiber-specific health-associated effects, there is an urgent need for studies addressing their physical and technological properties to explain the relevant cause–effect type of correlations.

3. The Modification of Carbohydrates and Their Properties

Carbohydrates are one of the most common macronutrients of food, while the preferences of consumers seem to change with respect to high-sugar-containing foods. The consumption of bread, cakes, doughnuts and other flour products, and refined sugar-containing foods and drinks is declining, while the intake of whole grain cereals, legumes, and fruits, as well as candy, ice cream, and frozen yogurt increased in recent decades [19]. As the number of people who make health-conscious food choices is growing, the food industry has to find new processes to increase the health-promoting effects of newly developed foodstuffs. On the other hand, in several cases, the natural properties of carbohydrates do not meet the requirements of the production of a special product and, consequently, they need to be modified to provide better solubility for starch in cold water, slower retrogradation, or higher efficiency in releasing antioxidants from fibers. The range of gluten-free products must be diversified due to the increasing number of gluten allergies, and special lifestyle or diet trends of consumers, who seem to fully appreciate previously encountered taste, appearance, and other sensory and nutritional properties [20]. To give an example, wheat gluten has a unique property that makes it suitable to confer a unique stable structure to food products, which generally characterizes bakery and pasta products [21–23]. In the case of gluten-free products, fibers and other carbohydrates have to substitute for these functions that can be further improved by modifications to their properties [24–26]. The methods used for the modification of fibers and other carbohydrates depend on the nature and properties of such raw materials, paying attention to the anticipated effect. Generally, physical, chemical, and biological methods, and their various combinations, can be applied to reach the proposed quality parameters, like solubility, swelling properties, water- and oil-binding capacity, or free radical scavenging capacity [5,10,12,25]. Currently, the physical methods are of special interest to us as they are generally much faster than the chemical and microbiological ones, and do not make use of chemicals, which makes them safe and much more accepted by the consumers. In the current paper, we review the relevant physical processing methods used in food production that can have an effect on the nutritional properties of carbohydrates, increasing or decreasing their digestibility and influencing the technological behavior of starch and fiber (e.g., modifying solubility, swelling power, and structure-forming properties) (see Table 1). The general physical processes for these modifications are size reduction and heat and pressure treatment, but irradiation and the

use of cold or non-thermal plasma for the modification of carbohydrate properties also seem to be often applied in manufacturing practice and have an influence on carbohydrate properties.

Table 1. Physical processing-induced nutritional modifications of carbohydrates.

Physical Processes	Effects on Carbohydrate Properties
Size reduction	Increase in fiber solubility [27]
Heat treatment	Modified starch formation [5,28,29] Starch damage [30] Modification of resistant content formation [25,31,32] Starch complex formation [30,33–35] Increase in fiber solubility [36,37] Changes in the starch digestibility time [29,38]
	Superheating Heat moisture treatment Annealing Drying
Combined high temperature and pressure treatment	Increase in the starch digestibility time [39] Change in glycemic index [39]
	High hydrostatic pressure, autoclaving, steam explosion
	Extrusion
Cold plasma treatment	Increase in starch solubility [41] Increase in resistant starch content [32,42] Increase in fiber solubility [1,43]
	Increase in resistant starch content [44–46]
Radiation	Changes in amylose–amylopectin ratios [47–49]

3.1. Size Reduction

Size reduction is a basic method for the processing of cereals and pulse grains. Based on particle size, different kinds of fractions can be separated into bran, shorts, and flour [50] and these fractions differ not only in size but composition and, therefore, in nutritional and techno-functional properties. Size influences water-binding capacity for both starch and fibers, due to an increase in surface area and pore volume upon grinding [51]. Milling also influences the amount of soluble fiber and arabinoxylan content. Zheng et al. found more than 10% arabinoxylan in hull-less bran, less than its shorts content of 50% and its flour content of one third. The result of size reduction depends on the applied method, and ball milling, rotor, impact and jet milling, cyclone milling, and roller milling have different effects on the properties of the milled product [33,50]. Craeyveld et al. evaluated dry ball milling and found a significant increase in water-extractable arabinoxylan oligomer content of pericarp-enriched wheat and rye bran as an effect of the increase in the jar volume capacity (from 16 to 50%) and milling time (24 and 120 h). On the other hand, yield showed a negative correlation to jar volume capacity [27]. Noort et al. compared rotor, impact, and jet milling in the decrease in average bran particle size from 831.1 μm to 47.9 μm for pure bran, while bran contained an aleurone layer from 205.6 μm to 46.5 μm and the different sized bran fractions were used for bread making. This size reduction strongly influenced water-binding capacity, as fibers bind water by capillary forces, which has a strong connection with the particle size. Water-binding capacity decreased from more than 500% to under 300% due to intensive milling [52]. The addition of a finely ground bran fraction to bread doughs and pasta results in a decrease in product size, darker color, and unfavorable sensory properties, and also makes the dough structure, baking, and pasting properties worse [3,33,53,54]. Coda et al. evaluated the effect of the fermentation of brans with different particle sizes (750, 400, 150, and 50 μm) by *Lactobacillus brevis* and *Kazachastania exigua* and found that a smaller than average particle size improves fermentation and the addition of carbohydrase enzyme further increased the effect [55].

3.2. Heat Treatment

Heat treatment is a widely used food processing application including several dry and wet techniques to reach goals like enzyme inactivation or roasting. The aforementioned techniques have benefits and disadvantages that must be carefully balanced with respect to the proposed goals. Dry heat treatment is found to be milder, but can result in drastic changes by increasing the temperature, while the wet heat treatment, performed in fluid or by steam, has a larger influence on chemical composition and, therefore, could influence the bioavailability of biologically active compounds [34]. The starch-related effects of the increased temperature are relatively well documented. By heating in the presence of water, starch undergoes a structural transformation and gelatinization, its crystal structure disintegrates, and its solubility, together with the rheological properties, are modified. With superheating, a dry high temperature will also produce modified starches that are soluble and swellable in cold water. On the other hand, using high pressure and wet heat treatments, the gelatinization parameters of starch could change, and it retains its original structure even at higher temperatures [5,28]. Chi et al. evaluated the combined effect of dry heating and annealing on corn and potato starches, and found that dry heat treatment resulted in shorter starch chains that were more prone to being rearranged into crystal structures during annealing. The combined application of these technological processes caused increased order in the structure of the double helix and in the crystal structure of starch, which influenced pasting properties and decreased digestibility [38]. Marston et al. evaluated the functional effects of dry heat treatments of 95 °C and 125 °C on sorghum flour, and observed promising results related on the volume and sensory properties of breads and cakes. These effects are due to the modified gelatinization properties of starch and increased ability to absorb water [38].

Drying has a special importance for pasta production, as the technological processing temperature strongly affects the properties of the product (fracture resistance, strength, elasticity, leaching losses) influenced by carbohydrate–protein and carbohydrate–carbohydrate reactions. Padalino et al. evaluated the effect of a drying temperature at 50 °C, 65 °C, 75 °C, 80 °C, and 90 °C on durum pasta, and observed better pasta properties as the temperature increased. The high drying temperature denatured proteins, partially gelatinized starch, and inactivated amylase enzymes, which reduced the amount of damaged starch in the doughs, as well as the amount of amylose, and resulted in less leaching into the cooking water. Furthermore, it also enhanced the formation of amylose–lipid complexes, and 90% of the free lipids were in a bound form, which inhibited swelling and resulted in less sticky doughs. Denaturation of the proteins produced a structure reinforced with tighter S-S bridges, which inhibited starch swelling and amylose leaching. The only negative effect of the high temperature was the required cooking time that increased with the increase in drying heat [30]. Hot air drying also forms starch–protein complexes in the case of Chinese yam, influencing its functional properties, including solubility and swelling power, gelatinization parameters, pasting characteristics, and rheological properties [35]. Bucsell et al. also found that the combined dry and wet heat treatment helped to form protein–carbohydrate–lipid complexes, leading to increased water-soluble carbohydrate content, stronger dough structure, and increased dough development time [34].

Hydrothermal processing is one of the food manufacturing methods based on heat treatment, and the thermochemical conversion is based upon the heat–moisture treatment (HMT) or annealing that would yield more valuable food products. In the case of HMT, the applied moisture content is less than 35% and the temperature is between 80 and 140 °C, while a higher moisture content (but less than 65%) and lower, under gelatinization, temperature is typical for annealing. Annealing produces partial gelatinization and would increase the starting temperature of gelatinization up to 14 °C as compared to the native starch, because of the structural changes of granules and increasing amount of crystallized polymers. Besides gelatinization, the HMT influences crystallinity, recrystallization, enzymatic hydrolysis, and the freeze–thaw stability of starch. In the case of potato starch, decreased viscosity and pasting temperature were observed, while the breakdown viscosity

diminished, showing higher resistance to heat and mechanical treatments. HMT also produced slower and less swelling [56,57]. In the case of banana starch, both treatments increased the pasting temperature, but the effects were much more significant for HMT (12 °C) compared to annealing treatment (1 °C) [58]. The ratio of short sweet potato amylopectin chains was increased as a result of these treatments, and the kind of starch crystalline pattern was also modified from type 3 to type 1 [29]. In contrast, Hung et al. did not observe morphological changes in the HMT of unpolished rice, but found starch swelling and degradation to be inhibited, and the amount of resistant starch was also significantly increased [25,31]. The wheat bran hydrothermal treatments made a significant proportion of the arabinoxylan become water soluble, and improved the extraction of non-soluble fractions. A large fraction of fibers became soluble too: about 40% at 180 °C and 51% at 200 °C of hemicellulose and 10 and 15% of lignin, respectively [36].

Roasting and steaming are also performed at temperatures higher than 100 °C, as for HMT. Their combined application of wheat bran improved the rheological properties when 30% was added to wheat flour. Combined with the untreated bran–flour mixture, increased water absorption capacity, better farinograph quality, and increased amylograph viscosity values were obtained, while the dough developmental time became longer. Lipase activity was also decreased, having favorable consequences in the terms of shelf life, and the formation of sterol–starch complexes was also observed [29,59,60]. Steam treatment also influenced the water soluble arabinoxylan, and decreased sugar content positively [37].

Powder drying leads to the fast evaporation of water from starch without influencing its structure, therefore, it has only a negligible effect on its properties [25]. However, freeze drying, the gentlest drying method, does affect the characteristics of starch. It has been found in several studies that the high pressure and low temperature could modify the starch structure, and induce amylopectin degradation, lower molecule weights both for amylose and amylopectin, shorter chains, a decreased proportion of amorphous phase, and an increased amount of double helices [35,61]. In the case of yam starch, the decreased solubility and swelling power were also evident [35]. Microwave heating is a relatively novel application and the generated direct and indirect effects on foodstuffs are strongly influenced by moisture content, since the microwaves can affect water molecules only. In the case of cereal carbohydrates, the use of microwave heating has been evaluated, and a treatment like 900 W for 2 min makes the wheat bran spread and generate a 0.3 mm layer with a slightly reduced water absorption capacity and dough stability when added into a 30% biscuit dough, though the time to dough formation was reduced. Peak viscosity was also improved compared to untreated bran, but not significantly [59]. The 5, 10, and 20 min long microwave treatments diminished the relative crystallinity of starch by 10.47, 6.42, and 2.91% [62]. Microwave heating has also been combined with HMT for canna (*Canna edulis* Ker) starch, which increased the resistant starch content of starch from 27.7% to 55.5% and the amylose content from 12.5% to 18.5% [32]. Boiling and frying also can influence the carbohydrate content by decreasing the total carbohydrate content, while cooking increased the reducing sugar content by 9%, and frying diminished it by 10% [39].

As is known, the physiological properties of starch are also influenced by high temperature, for example, baking leads to an increased resistant starch content, but the ratio of slowly digestible starch (SDS) to rapidly digestible starch (RDS) can also be affected by these modifications, and a higher SDS/RDS ratio seems to generate more beneficial physiological effects. The higher resistant starch content is also beneficial both for its physiological and technological effects, and, being classified as dietary fiber, this could influence the digestibility. Raw potatoes contain large amounts of resistant starch, which is significantly reduced during cooking and steaming, but higher amounts of RS can be measured after baking compared to other heat treatments due to the formation of amylose–lipid complexes [39]. Microwave treatment also has an effect on resistant starch content. As a result of the treatment, a significant part of the starch is hydrolyzed, but resistant starch is also formed [4,39]. After boiling, steaming, and cooking under pressure, the total carbohydrate content of raw potatoes changed from 20% to 18.1%, 18.5%, and 16%,

respectively, while microwave treatment increased it to 25.3% due to leaching and changes in water content [63]. However, Singh et al. reported a larger reduction of up to 40% in the case of potato starch after conventional cooking. Interestingly, the decrease in carbohydrate content has a positive effect on the glycemic index of raw materials, while the structural changes produced by cooking, steaming, and baking might positively influence the availability of starch to enzymes, so the glycemic index remains high in these processed foods. These methods also have a reducing effect on the proportion of amylose [39]. Annealing combined with drying caused a significant increase in SDS and a decrease in RDS, as well as a slight reduction of the resistant starch content. Similarly, the amount of SDS in corn increased from 2.08% to 9.98%, compared to native corn starch, while the amount of resistant starch decreased from 5.44% to 3.94%. Opposite effects were found in the case of potato starch: the amount of resistant starch increased significantly, from 5.68% to 10.7%. The different features presented above could be also be caused by the structural differences of various plant-derived starch structures. The amount of RDS was reduced by 44% for both corn and potato starches. Based on these results, Chi et al. found that combined treatments could generate more significant effects on carbohydrates than just applying individual treatments alone [38]. HMT increased the resistant starch content of maize, lentils, and peas by 7.7, 10.4, and 11.2%, respectively, compared to the values of untreated raw materials, which was further increased by the use of annealing. In other studies, a significant increase in the resistant starch content for waxy corn, rice, and potato starch was reported by the use of HMT, while starches from other raw materials showed opposing trends [32]. The amount of SDS in sweet potato starch increased threefold compared to native starch as a result of HMT treatment [29]. As a result of cooking, the digestibility and glycemic index of such starches were modified. Cooking in boiling water can alter the gelatinization of starch granules, and will increase the efficiency of digestive enzymes [39].

Heat treatments affect not only the starch but also dietary fibers, such as arabinoxylans and β -glucans, and the effect is more significant when heat treatment is performed under high pressure. Steiner et al. applied hydrothermal treatment to solubilize these components and split long chains. For this, brewer's spent grain was treated hydrothermally at 160 to 240 °C, 150 bar, for 2, 5, and 10 min. The applied treatment did not produce any changes to cellulose, as was seen for a higher temperature like 300–330 °C, but it significantly affected the length of the chains in the case of the arabinoxylans and glucans. The average molecular weight of untreated β -glucans was 248 kDa, which decreased to 179, 29, and 16 kDa after 2 min of treatment, while the β -glucan content was decomposed totally above 200 °C. Similar changes were found for arabinoxylan, but at higher (180–220 °C) temperatures. Hemicellulose was also affected by this hydrothermal treatment, 90% of which was decomposed to poly- and oligosaccharides. Additionally, a slight pH decrease was observed in the case of β -glucans, while for arabinoxylans, the pH decreased to 4.3, inducing the formation of organic acids such as formic acid and levulinic acid [64]. Dry and wet heat treatments also affected the dietary fiber content of whole grain flours, so the amount of arabinoxylan fell, but the soluble dietary fiber content increased [34].

3.3. High Pressure and Its Combination with Heat Treatment

The use of high pressure generated a novel processing technology for the food industry, and it is based on high hydrostatic pressure (HHP) or high-pressure steam. In the case of HHP application, a canned or vacuum packaged product is placed in water under high, 10–1200 MPa, pressure which induces molecular changes in the product. Starch is partially gelatinized, and its enzymatic availability, together with digestibility, fall [32]. In such process, starch is partially dehydrated, followed by irreversible crystal structure decomposition and granule disintegration. Starch with high amylopectin content is more sensitive to such a treatment compared to starch rich in amylose [62]. On the other hand, type A starch with its compact structure is more sensitive than type B, which is mostly due to its looser structure, and as such, the technological process can induce structural changes. Duration, temperature, starch properties, and moisture content are the main properties

influenced by the treatment [62,65]. Colussi et al. applied HPP alone and combined with HMT to potato starch, and they found that HMT alone decreased starch viscosity, while the combination of processes had an opposing effect. Their explanation for this phenomenon invoked the pressure-induced release and higher water absorption capacity of starch. The combined application of processes also increased breakdown viscosity, and therefore increased the stability of starch [57]. Others have found that HHP decreased the swelling power and viscosity [66]. While HMT promotes the formation of bonds between amylose and amylopectin, and increased pasting temperature, HPP has a reverse effect by limiting the swelling power and decreasing viscosity [57,67]. HHP increased the temperature of thermal transition, indicating that crystals with lower melting points are more sensitive, and decreased the relative crystallization, therefore, less energy was needed for gelatinization [57]. Liu et al. confirmed these findings on sorghum starch too. High pressure also influenced the formation of resistant starch as the highest generated amount was observed between 100 and 600 MPa, and a tenfold increase was observed for both wheat and quinoa, but starches with low amylose content would produce less resistant starch. Such an effect strongly depends on the duration of treatment, especially at lower pressures [32,40].

The second type of high-pressure treatment, also called steam explosion, consists of cycles of alternating action and inaction that exert an explosion-like effect on the substances. Interestingly, a threefold increase was observed for both the amount of water-extractable arabinoxylan and the reduced sugar as a consequence of applying steam explosion on fine milled wheat bran besides augmenting the efficiency of enzymatic hydrolysis [37].

Autoclaving, which combines high temperature and pressure, is a widely used processing method, especially for sterilization, but could also modify the technological and nutritional properties of the autoclaved foodstuff too. Structural changes in carbohydrates were induced by the application of combined high temperature and pressure treatments in chickpeas, and the amount of degradable sugars decreased, while the content of dietary fiber increased [68]. Autoclaving also has a significant effect on the structure of starch, since during the technological process, it begins to gelatinize, then rapidly matures, with the amylose chains being rearranged to form tight double helices with hydrogen bonds. As a result of this process, type 3 resistant starch is produced. This process is achieved through repeated cycles of autoclaving at 120–145 °C for 5 to 30 s and resting that, when performed for several cycles, will induce multiple retrogradation in the starch [32].

3.4. Extrusion

Extrusion is a complex technological process, in which raw material with a high moisture content is subjected to high pressures, temperatures, and shear forces. The process and the resulting special porous structure of the final product are based on the structural transformation of starch, but fibers also play an important role in determining the properties of extruded products [1,43]. During the process, the steam released by the sudden pressure change leads to a sudden increase in the porosity and size of the raw material, while high temperature causes starch gelatinization, the loss of crystal structure, and the formation of new crosslinks between starch and proteins [41]. The extrusion of corn starch in the 50–85 °C temperature range has a particularly beneficial effect on the swelling power and water solubility of starch. The swelling power is slightly improved by 1–2%, while the solubility is significantly increased by up to 15% as a result of extrusion, and the product shows significantly improved thermodynamic stability, while the gelatinization temperature could be increased from 66 to 91 °C. These phenomena can be explained by the high degree of gelatinization during extrusion and the subsequent change-induced structural rearrangement [41]. Liu et al. studied the effect of extrusion on the short- and long-term aging of rice starch using low temperature and transport speed but a longer extruder tube than is typical. During short-term retrogradation, the amylose shows rearrangement and recrystallization, while the long-term retrogradation caused the same result for amylopectin. Extrusion leads to a higher rate of degradation and damage of

amylopectin than of amylose, because of its shorter chain length. Therefore, it can be used for long-term storage of products high in or exclusively containing amylose-derived starches [69].

During extrusion, raw materials are also subjected to strong shear forces, which also affect the properties of starch. Gelatinized starch shows shear thinning behavior, and continuous shear stress usually decreases the viscosity of both native and modified starches [70]. However, shear force can result in shear thickening actions in the case of different kinds of starch gels. Fang et al. experienced this shear thickening behavior in the case of waxy potato and waxy corn starch in a 10% dispersion at a 20 s^{-1} shear rate, but no such events were detected in the case of waxy rice starch gel. Similar effects could be observed in the case of gelatinized potato specific amylopectin, suggesting that the shear forces might induce intermolecular double helices, which were responsible for this outcome [71].

During the extrusion of corn flour, Bailoni et al. observed an increase in the amount of resistant starch from 0.7% to 5.1%, while no change was experienced for oats and rye. Examining mango starch, the extrusion increased the initial resistant starch content to 9.7%, while in combination with acid hydrolysis for corn starch, the amount of resistant starch increased from 11% to 20% [32,42].

Fibers, and especially the water-insoluble fraction, do affect negatively the extrusion and the quality parameters of a product, as they interact with starch and break down the structure formed by the starch. They also cause inhomogeneity in the structure because of their large size and reduce the amount of water available in the system, which prevents the starch from gelatinizing and also deteriorates its structural function [1,43]. To eliminate this problem, several technologies and the parameters of extrusion have been analyzed. When the different rates of material transport, moisture content, and temperature were evaluated based on the effect of fiber components in the extruded products, the rate of transport was found to be the most critical. The water-binding capacity of fibers decreased to 254–293% from the 361.9% value of the non-extruded wheat bran, but the proportion of soluble fibers increased by more than twofold from 2.3%, which contributes ultimately to the improvement of sensory and physiological characteristics of extruded wheat products [1,43]. Because of such effects during the process, extrusion can also be used as a preparing operation before other treatments, for example, to damage the structure and cell walls of plant cells from raw materials, which provides better access for further enzymatic treatments. The extrusion of soybean okara and other soybean by-products allowed 95% of cellulose to be hydrolyzed, while other acidic or alkaline treatments resulted in only 69% to 93% yields of hydrolysis [72].

3.5. Atmospheric and Cold Plasma

The use of cold or nonthermal plasma shows promising outcomes in enzyme inactivation, microbiological preservation, and starch modification. Cold plasma is a result of the atmospheric dielectric discharge, which causes the ionized gas to contain metastable atoms and molecules, such as $\text{O}\bullet$ - and $\text{OH}\bullet$, with a nearly zero net electrical charge [73]. Zhou et al. have found that atmospheric plasma treatment leads to lower gelatinization temperature and diminished relative crystallinity of normal and waxy corn starches [74]. Thirumdas et al. evaluated the cold plasma-generated effects on rice starch, and observed an elevated amylose content, while the gel hydration properties and syneresis study showed the intensification of amylose leaching, and other studies indicated the increase in pasting and final viscosities, together with the reduction of retrogradation tendency. Contrary to the former observations, Okyere et al. found the final viscosity values to drop after the treatment of waxy potato, corn, and rice starches, indicating that the effect of cold plasma treatment is largely dependent on the origin of the starch [44,75,76]. Han et al. found that the depolymerization of amylopectin and amylose, together with the cleavage of the side chains, had occurred, which caused the low weight fractions to increase from 0% to 53.4% in corn starch. In contrast, the amount of the high weight fraction increased due to the crosslinking of the smaller fractions in potato starch. In rice starch, the effect

was influenced by the strength of plasma. The amorphous part of starch is more sensitive to the treatment because of its looser texture, and the B type of starch showed larger deformations than type A [62]. The plasma types could generate differentiated effects, like helium plasma inducing visible damage to starch particles, while nitrogen plasma had no such effect. The viscosity of plasma-treated corn and tapioca starch increased [77]. Okyere et al. observed that cold plasma treatment of rice, corn, and potato waxy starches improved the resistant starch content of corn and potato, but in the case of rice, a previous CO₂ gas treatment was required to generate similar outcomes. The growing content of resistant starch in wheat flour, and in normal corn starch, was attributed to cold plasma treatments [44–46]. Having seen the multiple starch-related effects, the cold or nonthermal plasma technology emerges as a promising tool to modify flour functionality [78] and nutritional values [79], though the putative modifications of dietary fibers with such a technological process remain largely unknown.

3.6. Radiation

The evaluation of different irradiation processes on the carbohydrate properties is a novel field of food-related research, while their effects on food safety and quality are relatively well known.

Gamma radiation uses radiation from high-energy radioactive isotopes, such as ⁶⁰Co and ¹³⁷Ce, which generate free radicals, and promote structural changes like breaking crosslinks or forming new chemical bonds. Polesi et al. applied 2 kGy irradiation to the starch of two rice varieties. One of the varieties showed a decrease in the amount of short chains, and an increase in longer (with more than 24 degrees of polymerization) chains was evident, while the other rice variety-specific starch showed a totally reversed result. Radiation also affects the relative crystallinity and degradation of amorphous crystalline parts, being influenced by radiation intensity. Below 7 kGy, the amorphous, and from 9 kGy, the crystalline parts, are more sensitive to gamma radiation [62,80]. When corn starches with different amylose–amylopectin ratios were radiated with 1, 5, 10, 25, and 50 kGy, the amylose-like fraction in waxy corn starch was increased at 10 kGy, while higher doses, up to 50 kGy, caused a reduction of amylose content. Samples with low amylose content lose their pasting ability at high doses of irradiation, so the waxy corn starch looks more affected by the treatment with respect to its pasting properties, gelatinization temperatures, and relative crystallinity, indicating that amylopectin shows increased sensitivity towards gamma irradiation [47]. Similar changes (decrease in apparent amylose content, gelatinization consistency, swelling power, viscosity) in wheat and potato starches were also reported, and the potato starch was found to be more sensitive to shear-dependent changes [48]. The ionizing radiation-induced changes are quite similar for other kinds of starches (e.g., tapioca, elephant foot yam, or bean) [49].

Microwave radiation is a non-ionizing radiation, which can increase temperature and cause fast changes in the affected material. Its effect of increasing the gelatinization temperature and decreasing the solubility and crystallinity were reported both for normal corn and wheat starch, but no influence was found on waxy corn starch, meaning that the previously mentioned effects are greatly dependent on amylopectin [81]. Shen et al. found similar, but greater, changes in the double helical structure and the crystallinity of potato starch induced upon microwave treatment as compared to modifications related to conventional heating. Corn flours treated with 400 W microwave radiation showed a higher level of V-type crystalline structure, indicating the formation of amylose–lipid complexes. Shorter (0.5 and 1 min) treatments resulted in a higher peak viscosity compared to the untreated corn starch, but longer (3 and 4 min) treatments resulted in lower values, showing an increase with the duration of microwave treatment in shear stability [82,83].

Another kind of radiation applied in the food industry is the UV radiation, which has been used to control insects or spices, but can induce chemical changes too. It is a well-documented fact that UV radiation can modify starches by depolymerizing them. This kind of radiation breaks the bonds at 1–6 positions, thus shortening starch chains, and

debranching the amylopectin. Amylopectin requires a higher energy level of UV radiation to make it break. This method successfully altered the physicochemical properties of starch in the way that the smaller molecular weight and lower crystallinity of starch were obtained [84]. Another study mentioned that UV radiation caused free radicals that induced crosslinking and depolymerization, and moreover, the formation of starch-derived dextrans was also facilitated [85]. Bajer et al. [86] evaluated the effect of UV radiation on starch from normal and waxy corn, wheat, and potato, and found that the chemical structure was not affected, suggesting a relatively substantial photostability, while starches lost the absorbed water and decreased the crystallinity property. Potato starch showed a lower level of photostability. The UV-B radiation degraded amylose, while UV-C decreased both amylose and amylopectin in cassava starch right after a pre-treatment with lactic acid and followed by UV irradiation [87], and the obtained flour showed higher baking expansion [88]. Exposure of durum wheat bran to UV radiation for 48 h showed a 25% decrease in the ferulic acid content of bran, and a 44% decrease in dehydrodiferulic acid content, which binds to dietary fibers, just like arabinoxylan. UV radiation also reduced the solubility of fibers by forming new crosslinks between the arabinoxylans. The extensibility of bran was reduced by 54%, but the strength of the stress required to break it was increased by 30% when exposed to UV radiation [67].

4. Conclusions

The growing knowledge on the physical and chemical properties of carbohydrates continuously brings newer and newer information about this staple nutrient and the changing demands of consumers. Therefore, the need for the application of new technological processes in the food industry for both the development of new products and the improvement of nutritional, technological, and sensory properties of foodstuffs is an obvious priority. Physical methods (size reduction, heat treatment, high pressure and its combination with heat treatment, extrusion, atmospheric and cold plasma, radiation) are favored in several situations as they are easy to apply, toxicologically safer, more accepted than chemical methods, relatively inexpensive, and there are several nutritional aims that can be reached through their application. Despite all the progress seen in this field, several explanations are still missing, especially when it comes to the mechanisms of action and their effects on rheological and nutritional properties of the newly developed foodstuff.

The presented physical food processing methods can modify the structure, quantity, and digestibility of amylose/amylopectin, and could inflict changes upon the quantity and quality of dietary fiber. Furthermore, the abovementioned modifications could alter the ratios of macronutrients, most likely on the side of carbohydrate components, including the non-starch polysaccharides. It is also evident that through physical interventions, the resistant starch and dietary fiber proportions could be significantly increased, considering that such food components have beneficial effects on the human digestive and acquired immune systems. Through the synthesis of short-chain fatty acids, resistant starch helps maintain colon function, regulates colonocyte gene expression, cell cycle, and apoptosis. Increased SCFA production lowers colonic pH and stimulates bile acid secretion, and inhibits the conversion of primary and secondary bile acids, which is beneficial because secondary bile acids are cytotoxic to colon cells. Therefore, the food processing-related physical methods can directly affect the physicochemical properties of foods, while through the resistant starch and dietary fiber content, they can positively influence the blood sugar level, the insulin response, prevent colorectal cancer, etc. [17,89,90]. Future efforts should be directed to the comparative analysis of foodstuff-specific macro- and micronutrients in addition to dietary fibers and phytonutrient profiles in the context of food processing technologies, food safety, bioavailability, and the maintenance of the health of consumers.

Author Contributions: R.N. and P.S. made the conception and contributed to writing, J.C. reviewed and edited the chemical parts, E.M. reviewed and revised the manuscript and edited the nutritional parts, P.S. and E.M. finalized the manuscript. All authors have read and agreed to the published version of the manuscript.

Funding: This research received no external funding.

Institutional Review Board Statement: Not applicable.

Informed Consent Statement: Not applicable.

Data Availability Statement: Data sharing not applicable.

Conflicts of Interest: The authors declare no conflict of interest.

References

1. Aktas-Akyldiz, E.; Masatcioglu, M.T.; Köksel, H. Effect of extrusion treatment on enzymatic hydrolysis of wheat bran. *J. Cereal Sci.* **2020**, *93*, 102941. [CrossRef]
2. Arslan, M.; Rakha, A.; Xiaobo, Z.; Mahmood, M.A. Complimenting gluten free bakery products with dietary fiber: Opportunities and constraints. *Trends Food Sci. Technol.* **2018**, *83*, 194–202. [CrossRef]
3. Coda, R.; Katinka, K.; Rizello, C.G. Bran bioprocessing for enhanced functional properties. *Curr. Opin. Food Sci.* **2015**, *1*, 50–55. [CrossRef]
4. Tian, S.; Sun, Y. Influencing factor of resistant starch formation and application in cereal products: A review. *Int. J. Biol. Macromol.* **2018**, *149*, 424–431. [CrossRef]
5. Kaur, B.; Ariffin, F.; Bhat, R.; Karim, A.A. Progress in starch modification in the last decade. *Food Hydrocoll.* **2012**, *26*, 398–404. [CrossRef]
6. Chen, X.; Luo, J.; Fu, L.; Cai, D.; Lu, X.; Liang, Z.; Zhua, J.; Lia, L. Structural, physicochemical, and digestibility properties of starch-soybean peptide complex subjected to heat moisture treatment. *Food Chem.* **2019**, *297*, 124957. [CrossRef]
7. Al-Laham, S.H.; Peppelenbosch, M.P.; Roelofsen, H.; Vonk, R.J.; Venema, K. Biological effects of propionic acid in humans, metabolism potential applications and underlying mechanism. *Biochim. Biophys. Acta* **2010**, *1801*, 1175–1183. [CrossRef]
8. Tungland, B.C.; Meyer, D. Nondigestible oligo- and polysaccharides (dietary fiber): Their physiology and role in human health and Food. *Compr. Rev. Food Saf. Food Saf.* **2002**, *3*, 90–109. [CrossRef]
9. Bhise, S.; Kaur, A. Synergetic effect of polyols and fibres on baking, sensory and textural quality of bread with improved shelf life. *Int. J. Curr. Microbiol. Appl. Sci.* **2017**, *6*, 1–12. [CrossRef]
10. Chu, J.; Zhao, H.; Lu, Z.; Lu, F.; Bie, X.; Zhang, C. Improved physicochemical and functional properties of dietary fiber from millet bran fermented by *Bacillus natto*. *Food Chem.* **2019**, *294*, 79–86. [CrossRef]
11. Marco, C.; Rosell, C.M. Breading performance of protein enriched, gluten-free breads. *Eur. Food Res. Technol.* **2008**, *227*, 1205–1213. [CrossRef]
12. Zheng, Y.; Li, Y. Physicochemical and functional properties of coconut [*Cocos nucifera* L] cake dietary fibres: Effects of cellulase hydrolysis, acid treatment and particle size distribution. *Food Chem.* **2018**, *257*, 135–142. [CrossRef] [PubMed]
13. Peerjait, P.; Chiwchan, N.; Dehavastin, S. Effects of pretreatment methods on health-related functional properties of high dietary fibre powder from lime residues. *Food Chem.* **2012**, *132*, 1891–1898. [CrossRef]
14. Botham, R.L.; Ryden, P.; Robertson, J.A.; Ring, S.G. Structural features of polysaccharides and their influence on fermentation behavior. In *Functional Properties of Nondigestible Carbohydrates*; Guillon, F., Ed.; INRA: Nantes, France, 1998; pp. 46–49.
15. Slavin, J. Fiber and prebiotics: Mechanisms and health benefits. *Nutrients* **2013**, *5*, 1417–1435. [CrossRef] [PubMed]
16. Rowland, I.R.; Rumney, C.J.; Coutts, J.T.; Lievense, L.C. Effect of *Bifidobacterium longum* and inulin on gut bacterial metabolism and carcinogen-induced aberrant crypt foci in rats. *Carcinogenesis* **1998**, *19*, 281–285. [CrossRef]
17. Louis, P.; Hold, G.L.; Flint, H.J. The gut microbiota, bacterial metabolites and colorectal cancer. *Nat. Rev. Microbiol.* **2014**, *12*, 661–672. [CrossRef]
18. Brownlee, I.A. The physiological roles of dietary fibre. *Food Hydrocoll.* **2011**, *25*, 238–250. [CrossRef]
19. Makare, N.; Scott, M.; Quatromoni, P.; Jacques, P.; Parekh, N. Trends in dietary carbohydrate consumption from 1991 to 2008 in the Framingham Heart Study Offspring Cohort. *Br. J. Nutr.* **2014**, *111*, 2010–2023. [CrossRef]
20. El Khoury, D.; Balfour-Ducharme, S.; Joye, I.J. A review on the gluten-free diet: Technological and nutritional challenges. *Nutrients* **2018**, *10*, 1410. [CrossRef]
21. Bonilla, J.C.; Erturk, M.Y.; Kokini, J.L. Understanding the role of gluten subunits [LMW, HMW glutenins and gliadin] in the networking behavior of a weak soft wheat dough and a strong semolina wheat flour dough and the relationship with linear and non-linear rheology. *Food Hydrocoll.* **2020**, *108*, 106002. [CrossRef]
22. Kalichevsky, M.T.; Jaroszkievicz, E.M.; Blanshard, J.M.V. Glass transition of gluten 1: Gluten and gluten–sugar mixtures. *Int. J. Biol. Macromol.* **1992**, *14*, 257–266. [CrossRef]
23. Wang, P.; Zhengyu, J.; Xu, X. Physicochemical alterations of wheat gluten proteins upon dough formation and frozen storage. A review from gluten, glutenin and gliadin perspectives. *Trends Food Sci. Technol.* **2015**, *46*, 189–198. [CrossRef]
24. Csapó, J.; Csapóné, K.Z. *Élelmiszer-Kémia; Mezőgazda Kiadó: Budapest, Hungary*, 2003; p. 468.
25. Ojogbo, E.; Ogunsona, E.O.; Mekkonen, T.H. Chemical and physical modifications of starch for renewable polymeric materials. *Mater. Today Sustain.* **2020**, *7–8*, 100028. [CrossRef]
26. Ratnayake, W.S.; Jackson, D.S. Chapter 5 Starch Gelatinization. *Adv. Food Nutr. Res.* **2008**, *55*, 221–268.
27. Zheng, X.; Li, L.; Wang, X. Molecular characterization of arabinoxylans from hull-less barley milling fractions. *Molecules* **2011**, *16*, 2743–2753. [CrossRef]

28. Farooq, Z.; Boye, J.I. Novel food and industrial applications of pulse flours and fractions. In *Pulse Foods: Processing, Quality and Nutraceutical Applications*; Academic Press: London, UK, 2011; pp. 283–323.
29. Prückler, M.; Siebenhandl-Ehn, S.; Apprich, S.; Höltinger, S.; Haas, C.; Schmid, E.; Kneifel, W. Wheat bran-based biorefinery. 1: Composition of wheat bran and strategies of functionalization. *LWT* **2013**, *56*, 211–221. [CrossRef]
30. Van Craeyveld, V.; Holopainen, U.; Selinheimo, E.; Poutanen, K.; Delcour, J.A.; Courtin, C.M. Extensive dry ball milling of wheat and rye bran leads to in situ production of arabinoxylan oligosaccharides through nanoscale fragmentation. *J. Agric. Food Chem.* **2009**, *57*, 8467–8473. [CrossRef] [PubMed]
31. Noort, M.W.J.; van Haaster, D.; Hemery, Y.; Schols, H.A.; Hamer, R.J. The effect of particle size of wheat bran fractions on bread quality—Evidence for fibre-protein interactions. *J. Cereal Sci.* **2010**, *52*, 59–64. [CrossRef]
32. Chen, J.S.; Fei, M.J.; Shi, C.L.; Tian, C.J.; Sun, C.L.; Zhang, H.; Ma, Z.; Dong, H.X. Effect of particle size and addition level of wheat bran on quality of dry white Chinese noodles. *J. Cereal Sci.* **2011**, *53*, 217–224. [CrossRef]
33. Zhang, D.; Moore, W. Wheat bran particle size effects on bread baking performance and quality. *J. Sci. Food Agric.* **1999**, *79*, 805–809. [CrossRef]
34. Coda, R.; Kärki, I.; Nordlund, E.; Heiniö, R.-J.; Poutanen, K.; Katina, K. Influence of particle size on bioprocess induced changes on technological functionality of wheat bran. *Food Microbiol.* **2014**, *37*, 69–77. [CrossRef]
35. Bucsellera, B.; Takács, Á.; Reding, W.; Schwendener, U.; Kálmán, F.; Tömösközi, S. Rheological and stability aspects of dry and hydrothermally heat treated aleurone-rich wheat milling fraction. *Food Chem.* **2017**, *220*, 9–17. [CrossRef] [PubMed]
36. Yan, H.; Zhengbiao, G.U. Morphology of modified starches prepared by different methods. *Food Res. Int.* **2010**, *43*, 767–772. [CrossRef]
37. Chi, C.; Li, X.; Lu, P.; Miao, S.; Zhang, Y.; Chen, L. Dry heating and annealing treatment synergistically modulate starch structure and digestibility. *Int. J. Biol. Macromol.* **2019**, *137*, 554–561. [CrossRef]
38. Marston, K.; Khouryieh, H.; Aramouni, F. Effect of heat treatment of sorghum flour on the functional properties of gluten-free bread and cake. *LWT* **2016**, *65*, 637–644. [CrossRef]
39. Padalino, L.; Caliandro, R.; Chita, G.; Conte, A.; Del Nobile, M.A. Study of drying process on starch structural properties and their effect on semolina pasta sensory quality. *Carbohydr. Polym.* **2016**, *153*, 229–235. [CrossRef] [PubMed]
40. Liu, X.-X.; Liu, H.-M.; Fan, L.-Y.; Qin, G.-Y.; Wang, X.-D. Effect of various drying pretreatments on the structural and functional properties of starch isolated from Chinese yam [*Dioscorea opposita* Thumb.]. *Int. J. Biol. Macromol.* **2019**, *153*, 1299–1309. [CrossRef] [PubMed]
41. Colussi, R.; Kringel, D.; Kaur, L.; Zavareze, E.R.; Dias, A.R.G.; Singh, J. Dual modification of potato starch: Effects of heat-moisture and high pressure treatments on starch structure and functionalities. *Food Chem.* **2020**, *318*, 126475. [CrossRef] [PubMed]
42. Cahyana, Y.; Wijaya, E.; Halimah, T.S.; Marta, H.; Suryadi, E.; Kurniati, D. The effect of different thermal modifications on slowly digestible starch and physicochemical properties of green banana flour [*Musa acuminata* colla]. *Food Chem.* **2019**, *274*, 274–280. [CrossRef]
43. Huang, T.-T.; Zhou, D.-N.; Jin, Z.-Y.; Xu, X.-M.; Chen, H.-Q. Effect of debranching and heat-moisture treatments on structural characteristics and digestibility of sweet potato starch. *Food Chem.* **2015**, *187*, 218–224. [CrossRef]
44. Hung, V.P.; Binh, T.V.; Nhi, Y.H.P.; Phi, L.T.N. Effect of heat-moisture treatment of unpolished red rice on its starch properties and in vitro and in vivo digestibility. *Int. J. Biol. Macromol.* **2020**, *154*, 1–8. [CrossRef] [PubMed]
45. Zara, M.; Collins, S.A.R.; Elliston, A.; Wilson, D.R.; Käsper, A.; Waldron, K.W. Characterization of cell wall components of wheat bran following hydrothermal pretreatment and fractionation. *Biofuels* **2015**, *8*, 23.
46. Nandeesh, K.; Jyotsana, R.; Rao, G.V. Effect of differently treated wheat bran on rheology, microstructure and quality characteristics of soft dough biscuits. *J. Food Process. Preserv.* **2011**, *35*, 179–200. [CrossRef]
47. Nyström, L.; Lampi, M.-A.; Rita, H.; Aura, A.-M.; Oksman-Caldentey, K.-M.; Piironen, V. Effects of processing on availability of total plant sterols, steryl ferulates and steryl glycosides from wheat and rye bran. *J. Agric. Food Chem.* **2007**, *55*, 9059–9065. [CrossRef]
48. Aktas-Akyıldız, E.; Matilla, O.; Sozer, N.; Poutanen, K.; Köksel, H.; Nordlund, E. Effect of steam explosion on enzymatic hydrolysis and baking quality of wheat bran. *J. Cereal Sci.* **2017**, *78*, 25–32. [CrossRef]
49. Wang, S.; Liu, C.; Wang, S. Drying methods used in starch isolation change properties of C-type chestnut [*Castanea mollissima*] starches. *LWT* **2016**, *73*, 663–669. [CrossRef]
50. Han, Z.; Shi, R.; Sun, D.-W. Effects of novel physical processing techniques on the multi-structures of starch. *Trends Food Sci. Technol.* **2020**, *97*, 126–135. [CrossRef]
51. Dupuis, J.H.; Liu, Q.; Yada, R.Y. Methodologies for increasing the resistant starch content of food starches: A review. *Compr. Rev. Food Sci. Food Saf.* **2014**, *13*, 1219–1234. [CrossRef]
52. Singh, A.; Raigond, P.; Lal, M.K.; Singh, B.; Thakur, N.; Changan, S.S.; Kumar, D.; Dutt, S. Effect of cooking methods on glycemic index and in vitro bioaccessibility of potato [*Solanum tuberosum* L.] carbohydrates. *LWT* **2020**, *127*, 109363. [CrossRef]
53. Bembem, K.; Sadana, B. Effect of cooking methods on the nutritional composition and antioxidant activity of potato tubers. *Int. J. Food Sci. Nutr.* **2013**, *2*, 26–30.
54. Steiner, J.; Franke, K.; Kießling, M.; Fischer, S.; Töpfl, S.; Heinz, V.; Becker, T. Influence of hydrothermal treatment on the structural modification of spent grain specific carbohydrates and the formation of degradation products using model compounds. *Carbohydr. Polym.* **2018**, *184*, 315–322. [CrossRef]

55. Pei-Ling, L.; Xiao-Song, H.; Qun, S. Effect of high hydrostatic pressure on starches: A review. *Starke* **2010**, *62*, 615–628. [CrossRef]
56. Zavareze, R.E.; Pinto, Z.V.; Klein, B.; El Halal, M.L.S.; Elias, C.M.; Prentice-Hernández, C.; Dias, G.R.A. Development of oxidised and heat–moisture treated potato starch film. *Food Chem.* **2012**, *132*, 344–350. [CrossRef]
57. Liu, H.; Fan, H.; Cao, R.; Blanchard, C.; Wang, M. Physicochemical properties and in vitro digestibility of sorghum starch altered by high hydrostatic pressure. *Int. J. Biol. Macromol.* **2016**, *92*, 753–760. [CrossRef]
58. Sun, B.; Rahman, M.M.; Tar'an, B.; Yu, P. Determine effect of pressure heating on carbohydrate related molecular structures in association with carbohydrate metabolic profiles of cool-climate chickpeas using global spectroscopy. *Spectrochim. Acta A* **2018**, *201*, 8–18. [CrossRef]
59. Santala, O.; Kiran, A.; Sozer, N.; Poutanen, K.; Nordlund, E. Enzymatic modification and particle size reduction of wheat bran improves the mechanical properties and structure of bran-enriched expanded extrudates. *J. Cereal Sci.* **2014**, *60*, 448–456. [CrossRef]
60. Yan, X.; Wu, Z.-Z.; Li, Y.-L.; Yin, F.; Ren, K.-X.; Tao, H. The combined effects of extrusion and heat-moisture treatment on the physicochemical properties and digestibility of corn starch. *Int. J. Biol. Macromol.* **2019**, *134*, 1109–1112. [CrossRef]
61. Liu, Y.; Chen, J.; Wu, J.; Luo, S.; Chen, R.; Liu, C.; Gilbert, R.G. Modification of retrogradation property of rice starch by improved extrusion cooking technology. *Carbohydr. Polym.* **2019**, *213*, 192–198. [CrossRef]
62. Yousefi, A.R.; Razavi, S.M.A. Steady shear flow behavior and thixotropy of wheat starch gel: Impact of chemical modification, concentration and saliva addition. *J. Food Process Eng.* **2016**, *39*, 31–43. [CrossRef]
63. Fang, F.; Martinez, M.M.; Campanella, O.H.; Hamaker, B.R. Long-term low shear-induced highly viscous waxy potato starch gel formed through intermolecular double helices. *Carbohydr. Polym.* **2020**, *232*, 115815. [CrossRef]
64. Bailoni, L.; Mantovani, R.; Pagnin, G.; Schiavon, S. Effects of physical treatments on the resistant starch content and in vitro organic matter digestibility of different cereals in horses. *Livest. Sci.* **2006**, *100*, 14–17. [CrossRef]
65. Al-Loman, A.; Ju, L.-K. Enzyme-based processing of soybean carbohydrate: Recent developments and future prospects. *Enzyme Microb. Technol.* **2017**, *106*, 35–47. [CrossRef]
66. Misra, N.N.; Yadav, B.; Roopesh, M.S.; Jo, C. Cold plasma for effective fungal and mycotoxin control in foods: Mechanisms, inactivation effects, and applications. *Compr. Rev. Food Sci. Food Saf.* **2019**, *18*, 106–120. [CrossRef]
67. Zhou, Y.; Yan, Y.; Shi, M.; Liu, Y. Effect of an atmospheric pressure plasma jet on the structure and physicochemical properties of waxy and normal maize starch. *Polymers* **2019**, *11*, 8. [CrossRef]
68. Thirumdas, R.; Deshmuk, R.R.; Annapure, U.S. Effect of low temperature plasma on the functional properties of basmati rice flour. *J. Food Sci. Technol.* **2016**, *53*, 2742–2751. [CrossRef]
69. Thirumdas, R.; Trimukhe, A.; Deshmuk, R.R.; Annapure, U.S. Functional and rheological properties of cold plasma treated rice starch. *Carbohydr. Polym.* **2017**, *157*, 1723–1731. [CrossRef]
70. Okyere, A.Y.; Bertoft, E.; Annor, G.A. Modification of cereal and tuber waxy starches with radio frequency cold plasma and its effects on waxy starch properties. *Carbohydr. Polym.* **2019**, *223*, 115075. [CrossRef]
71. Banura, S.; Thirumdas, R.; Kaur, A.; Deshmuk, R.R.; Annapure, U.S. Modification of starch using low pressure radio frequency air plasma. *LWT* **2017**, *89*, 719–724. [CrossRef]
72. Held, S.; Tyl, C.E.; Annor, G.A. Effect of radio frequency cold plasma treatment on intermediate wheatgrass [*Thinopyrum intermedium*] flour and dough properties in comparison to hard and soft wheat [*Triticum aestivum* L.]. *J. Food Qual.* **2019**, *2019*, 1085172. [CrossRef]
73. Nguyễn, L.T.; Trinh, S.K. Structural, functional properties and in vitro digestibility of maize starch under heat-moisture and atmospheric cold plasma treatments. *Vietnam J. Sci. Technol.* **2018**, *56*, 751–760. [CrossRef]
74. Scholtz, V.; Sera, B.; Khun, J.; Sery, M. Effects of nonthermal plasma on wheat grains and products. *J. Food Qual.* **2019**, *1*, 1–10. [CrossRef]
75. Bahrami, N.; Bayliss, D.; Chope, G.; Penson, S.; Pehinec, T.; Fisk, I.D. Cold plasma: A new technology to modify wheat flour functionality. *Food Chem.* **2016**, *202*, 247–253. [CrossRef] [PubMed]
76. Polesi, L.F.; Sarmiento, S.B.S.; de Moraes, J.; Franco, C.M.L.; Carniatti-Brazaca, G.S. Physicochemical and structural characteristics of rice starch modified by irradiation. *Food Chem.* **2016**, *191*, 59–66. [CrossRef] [PubMed]
77. Chung, K.-H.; Othman, Z.; Lee, J.-S. Gamma irradiation of corn starches with different amylose-to-amylopectin ratio. *J. Food Sci Technol.* **2015**, *52*, 6218–6229. [CrossRef]
78. Atrous, H.; Benbettaieb, N.; Chouaibi, M.; Attia, H.; Ghorbel, D. Changes in wheat and potato starches induced by gamma irradiation: A comparative macro and microscopic study. *Int. J. Food Prop.* **2015**, *20*, 1532–1546. [CrossRef]
79. Braşoveanu, M.; Nemptanu, M.-R. Aspects on starches modified by ionizing radiation processing. In *Applications of Modified Starches*; Huicochea, E.F., Villalobos, R.R., Eds.; IntechOpen: London, UK, 2018. [CrossRef]
80. Lewandowicz, G.; Jankowski, T.; Fornal, J. Effect of microwave radiation on physico-chemical properties and structure of cereal starches. *Carbohydr. Polym.* **2000**, *42*, 193–199. [CrossRef]
81. Shen, H.; Fan, D.; Huang, L.; Gao, Y.; Lian, H.; Zhao, J.; Zhang, H. Effects of microwaves on molecular arrangements in potato starch. *RSC Adv.* **2017**, *7*, 14348–14353. [CrossRef]
82. Román, L.; Martínez, M.M.; Rosell, C.M.; Gómez, M. Effect of microwave treatment on physicochemical properties of maize flour. *Food Bioprocess Technol.* **2015**, *8*, 1330–1335. [CrossRef]

83. Kurdziel, M.; Labanowska, M.; Pietrzyk, S.; Sobolewska-Zielinska, J.; Michalec, M. Changes in the physicochemical properties of barley and oat starches upon the use of environmentally friendly oxidation methods. *Carbohydr. Polym.* **2019**, *210*, 339–349. [CrossRef]
84. Nawaz, H.; Waheed, R.; Nawaz, M.; Shahwar, D. Physical and chemical modifications in starch structure and reactivity. In *Chemical Properties of Starch*; Emeje, M., Ed.; IntechOpen Ltd.: London, UK, 2020. [CrossRef]
85. Bajer, D.; Kaczmarek, H.; Bajer, K. The structure and properties of different types of starch exposed to UV radiation: A comparative study. *Carbohydr. Polym.* **2013**, *98*, 477–482. [CrossRef]
86. Vatanasuchart, N.; Naivikul, O.; Charoenrein, S.; Siroth, K. Molecular properties of cassava starch modified with different UV irradiations to enhance baking expansion. *Carbohydr. Polym.* **2005**, *61*, 80–87. [CrossRef]
87. Franco, C.M.L.; Ogawa, C.; Rabachini, T.; Rocha, T.S.; Cereda, M.P.; Jane, J.-L. Effect of lactic acid and UV irradiation on the cassava and corn starches. *Braz. Arch. Biol. Technol.* **2010**, *53*, 443–454. [CrossRef]
88. Peyron, S.; Abecassis, J.; Autran, J.-C.; Rouau, X. Influence of UV exposure on phenolic acid content, mechanical properties of bran, and milling behavior of durum wheat [*Triticum Durum* Desf.]. *Cereal Chem.* **2002**, *79*, 726–731. [CrossRef]
89. Reynolds, A.N.; Akerman, A.P.; Mann, J. Dietary fibre and whole grains in diabetes management: Systematic review and meta-analyses. *PLoS Med.* **2020**, *17*, e1003053. [CrossRef]
90. Ocvirk, S.; Wilson, A.S.; Appolonia, C.N.; Thomas, T.K.; O'Keefe, S.J.D. Fiber, fat, and colorectal cancer: New insight into modifiable dietary risk factors. *Curr. Gastroenterol. Rep.* **2019**, *21*, 62. [CrossRef]

Review

Magnetic Fields in Food Processing Perspectives, Applications and Action Models

Hubert Luzdemio Arteaga Miñano ¹, Ana Carolina de Sousa Silva ², Sergio Souto ²
and Ernane José Xavier Costa ^{2,*}

¹ Department of Engineering and Agroindustrial Management, Faculty of Agricultural Sciences, Campus Colpa Huacariz, National Autonomous University of Chota, Chota 06121, Peru; hlarteagam@unach.edu.pe

² Department of Basic Science, Faculty of Animal Science and Food Engineering, Campus Fernando Costa, University of São Paulo, Pirassununga 13635-900, Brazil; anacss@usp.br (A.C.d.S.S.); Ssouto@usp.br (S.S.)

* Correspondence: ernane@usp.br

Received: 11 June 2020; Accepted: 7 July 2020; Published: 10 July 2020

Abstract: Magnetic fields (MF) are increasingly being applied in food processing to preserve food quality. They can be static (SMF), oscillating (OMF) or pulsed (PMF) depending on the type of equipment. The food characteristics can be influenced by several configurations of the applied magnetic field as its flux density, frequency, polarity and exposure time. Several mechanisms have been proposed to explain the effects of magnetic fields on foods. Some of them propose interactions at the subatomic particle level that show quantum behavior, such as the radical pair and cyclotron resonance mechanisms. Other proposals are at the level of DNA, compounds, subcellular organelles and cells. The interactions between food and magnetic fields are addressed in a general way in this work, highlighting the applications and action models involved and their effects on the physicochemical, enzymatic and microbiological characteristics of food.

Keywords: electromagnetic fields; physicochemical characteristic; enzyme activity; microorganism inactivation; magnetic fields mechanisms

1. Introduction

Emerging technologies, alone or combined, are focused on improving food processing. Among them are magnetic fields (MFs), which have been applied to the enzymes, microorganisms and quality of foods [1–4]. However, conflicting results on their performance have been reported [5,6] and it has been suggested that MFs can act through the window effect [7] and through the underlying effects of field gradients on specific biological goals [8]. Compared with other techniques, the main advantage of the magnetic field is the way it interacts with the food that encompasses both thermodynamic aspects and quantum effects. The way the interaction occurs is not yet clear, so understanding the models of action of MFs on processing foods has become a challenge. This communication is focused on describing the applications of MFs in food processing, emphasizing the magnetic variables involved such as the magnetic flux density, frequency and exposure time, among others and moreover, the suggested action models that are behind those effects

Understanding them could lead to improvements in transformation and conservation processes in the food industry.

2. Procedural Principles and Technical Aspects of Magnetic fields

MFs are generated by electric currents direct or alternating (AC/DC) in conductors or by permanent magnets. According to their behavior over time, they may be static magnetic field (SMF), oscillating (OMF) or pulsed (PMF). The spatial distribution of an MF may be homogenous if the field gradient is zero over the space where samples are exposed or heterogeneous in other cases [9].

Considering the magnetic flux density, SMFs are classified as super weak (100 nT to 0.5 mT), weak (<1 mT), moderate (1 mT to 1 T), strong (1 to 5 T) and ultra-strong (>5 T) [10]. With regard to EMFs and PMFs, the factors considered are the magnetic flux density, frequency, waveform, exposure time and polarity [7]. In the function of frequency, they are considered as extremely low frequency (0 to 300 Hz), intermediate frequency (300 Hz to 1 MHz), radio frequency (1 MHz to 500 MHz), microwave frequency (500 MHz to 10 GHz) and high frequency (>10 GHz) [1].

The interaction of an MF with a biological system such as food depends on physical quantities and system characteristics such as resistivity, electrical conductivity, thickness and magnetic susceptibility [9] and this dependence can be modeled according to Equations (1) and (2). The main components of foods and cells can be modeled as a charged system in motion. So, the Lorentz force (FL) can act on them (Equation (3)) if the applied MF is strong enough. In fact, the main force acting on such magnetic components of cells is the electric force (FE) under an SMF because $FL \ll FE$ [8]; however FL in intracellular components (diamagnetic and paramagnetic) can have an important role that needs to be investigated. In addition, for a component with volume V and magnetic susceptibility χ , the magnetic force (FGM) arising from a time-variant magnetic field interacting with a magnetic dipole in a certain medium is presented in Equations (4) and (5), respectively. The magnetic force FGM may be responsible for activating certain mechanisms in the cell's compounds that modify its structure and functionality [8].

$$\vec{B} = \mu_0(\vec{H}) \quad (1)$$

$$\vec{M} = \chi_m \vec{H} \quad (2)$$

$$\vec{F}_L = q \vec{v} \times \vec{B} \quad (3)$$

$$\vec{F}_{GM} = \vec{p}_m \frac{d\vec{B}}{dl} \quad (4)$$

$$\vec{F}_{GM} = \frac{\Delta\chi_v}{\mu_0} \nabla \left(\frac{\vec{B}^2}{2} \right) \rightarrow f_{GMz} = \frac{(\chi_{v1} - \chi_{v2})}{\mu_0} B_z \frac{dB_z}{dz}, \quad (5)$$

where \vec{H} = magnetic field intensity (A/m), \vec{B} = magnetic flux density (T), \vec{M} = magnetization (A/m), μ_0 = magnetic permeability of the vacuum (H/m), χ_m = mass magnetic susceptibility (m^3/kg), χ_v = volumetric magnetic susceptibility (dimensionless), \vec{p}_m = magnetic dipole moment of charged particle, l = direction parallel to the magnetic dipole moment of a charged particle (m), q = charged particle, \vec{v} = velocity of charged particle (m/s).

3. Magnetic Field and Its Interaction with the Physicochemical Properties of Foods

The physicochemical characteristics of food are related to its compounds, which include mainly water, proteins, carbohydrates, fiber, lipids and minerals. However, the investigations carried out so far on the application of MFs to foods have been described as a black box, except in water, where there is information on MF effects. Table 1 summarizes the MF effects.

Table 1. Overview of oscillatory (OMF), static (SMF) and pulsed (PMF) magnetic fields effect on physicochemical characteristics of selected food products.

Product	Characteristics	Equipment	Experimental Conditions	Main Results	Ref.
Cantaloupe melon cut	Firmness, Soluble solids, Respiration rate, Electrolyte leakage, Titratable acidity	OMF	B: 2 mT f:- t:0-25 min	At 15 min, maintain the quality until 4 days at 5 °C.	[5]
Cheese	Yield and sensory characteristics	SMF	B: 0.365 T t: 0-60 min	Increased and better acceptability	[10]
Strawberry	Yield of fruits	OMF	B: 0.096–0.384 T f: 50 Hz B: 117.3, 192.9 and 228.9 mT	Increased at 0.096T after decreased	[4]
Honey	Rheological and physicochemical characteristics	SMF	T: 15, 28 °C t: 2 h	Improve flowability and maintaining its physicochemical quality	[7]
Ground beef	pH, Color, Myoglobin, lipid oxidation	PMF	B: 10 mT f:1 Hz t: 0–12 days	At 1 Hz for 2 h preserved	[6]
Apple	Content of fructose and glucose	PMF	B: 50–150 μ T f: 10–100 Hz t: 5 min/Week	Increase by 8% fructose and 25% glucose	[11]

Each compound of the food is formed from atoms and molecules. When an MF is applied to it, depending on its isotropy and magnetic susceptibility χ , if $\chi < 0$ it is diamagnetic otherwise it is paramagnetic, it has different behavior. Thus, carbon atoms exhibit isotropic susceptibility but organic molecules present in food have anisotropic susceptibility [1]. Therefore, the properties of the molecules and compounds of food should be determined, which will help to understand the effects of an MF on the physicochemical characteristics of foods. With regard to this property, Maki and Hirota [2] succeeded in completely separating sorbitol and sucrose in compressed oxygen gas by applying a gradient MF, which was possibly due to the 8.2% difference in magnetic susceptibility between them.

In cherry tomatoes, the average weight and content of lycopene and total soluble solids increased with MF and were greater within a PMF than with a SMF [3]. Also, Eşitken and Turan [4] reported that MF stimulation of strawberries was able to increase the plant metabolism and the number of ions in the leaves that were corroborated by work of Jia et al. [5] that reported that an OMF significantly prolonged the shelf life of cantaloupes by slowing respiration. Lins et al. [6] reported that PMF prevented possible changes in the oxidative state of the iron atom of the harem group, decreasing the rate of oxidation of Fe^{2+} to Fe^{3+} and hence allowing the ground beef to keep its color for a longer time.

In honey, the application of an MF decreased the pH and increased the soluble solids by breaking up macromolecules like pollen, which facilitated the release of ascorbic acid and sugars [7]. On the other hand, Otero et al. [8] reviewed the effects of MFs on the freezing of biological products, reaching the conclusion that many doubts remain about the effectiveness of low-intensity MFs (<1 mT) on the crystallization of water and suggested that the range of strength and frequency should be increased. Indeed, Zhao et al. [9] reported that strong magnetic fields may harm cell properties and should not be used to preserve biological samples and fresh food. However, a weak magnetic field (<0.5 mT) is not effective either but when the MF strength exceeds 1 mT, its application may play a significant role in food freezing and preservation at the low cost of implementation.

An Overview of the effects of magnetic fields on the physicochemical characteristics of foods is summarized in Table 1.

3.1. Effects of Magnetic Fields on Food Enzymes

Enzymes are proteins that have a specific activity in food, which can be beneficial or harmful to the quality of the food. Therefore, choosing the action levels of an MF will depend on whether we want to stimulate or inactivate the enzymes. MFs can change the structure of enzymes, affecting the related biochemical processes. This fact was reported by Jia et al. [12], who showed changes in four secondary conformations of α -amylase when it was subjected to an SMF. Likewise, in peroxidase under a PMF, conformational changes were evaluated by UV and confirmed by fluorescence spectra [13]. Also,

it is suggested by Buchachenko [14] that biochemical reactions are controlled by the angular moment and energy, with the first being more strict as its spin state selectivity is identical in reactants and products and when is an atomic forbidden state it can be overcome by synchronized spin with an MF. In general, biochemical reactions that involve more than one unpaired electron will be affected by an MF [15]. Mizuki et al. [16] mention that to increase the enzymatic activity it is necessary to synchronize the relative motion between enzymes and substrate molecules. They did it by immobilizing enzymes using magnetic particles to control the movement of the enzymes through the frequency used in the MF. At a frequency of 5 Hz, an MF can increase the activity of α -amylase [17].

The main results of the effects of MFs on the enzymes of interest in the food industry that can be used to improve the action models are summarized in the Table 2.

Table 2. Overview of oscillatory (OMF), static (SMF) and pulsed (PMF) magnetic fields effect on enzymes of foods.

Food/Substrate	Enzyme	Equipment	Experimental Conditions	Main Results	Ref.
Starch	α -amylase activity	OMF	B: 12 mT f: 1–30 Hz t: 30 min	Increased being higher at 5 Hz	[17]
Glycine max L. Merr. Roots	Catalase activity	SMF	B: 2.9–4.6. mT t: 2.2–33s	Increased	[15]
Fruits and vegetables	PPO activity	PMF	B: 2.5–4.5 T Pulses: 5–40 H: 12 mT	Decreased by 93.10%	[13]
p-nitrophenyl palmitate	Lipase activity	OMF	f: 1–30 Hz t: 30 min	Increased	[16]
Methoxyphenol and hydrogen peroxide	Peroxidase activity	PMF	B: 2–4T Pulses: 5–40	Decreased by 67.67%	[13]

3.2. Effects of Magnetic Fields on Microorganisms of Foods

The main objective of the application of MFs to microorganisms is to reduce the content of species that are pathogenic or that deteriorate foods and to stimulate the growth of beneficial strains to produce fermented foods. For the inactivation of microorganisms in sealed foods, Barbosa-Cánovas et al. [18] suggest the use of PMF conditions ranging from 5 to 50 T, 1 to 100 pulses, 5 to 500 Hz, 0 to 50 °C and 25 to 100 μ s of exposure time, reduced the microorganism growth by at least 2 log(CFU) (Colony Formation Unit). Liu et al. [19] argue that an MF acts on the passivation of cells, which inhibits their growth and reproduction. Low-frequency MFs have a great impact on cells and tissues and low frequency; high-intensity PMFs destroy microbial cell membranes and organelles. Thus, Ji et al. [20] showed damage to the cell membrane of *E. coli* after the application of an SMF. Membrane channels of *E. coli* is affected by SMF as reported by Strašák et al. [21] they concluded that an SMF has a bactericidal effect since it forms free radicals that attack cell membrane. Wu et al. [22] state that changes in expression and stability of intracellular proteins can be another way by which *Listeria* strains may be inactivated when subjected to a PMF. Besides, Bayraktar [23] reported that an OMF changes the activity of enzymes in *Saccharomyces cerevisiae*, limiting its growth and even causing the death of some individuals. However, after being subjected to MFs, survivors have higher activity, which is also related to potassium, calcium and magnesium levels. When an SMF was applied to *Saccharomyces cerevisiae* ethanol production was [24], suggesting that the ethanol-glucose conversion mechanisms were probably modified.

On the other hand, Masakazu et al. [25] reported that in fermentation it is important to consider the paramagnetic behavior of oxygen molecules and the diamagnetic behavior of carbon dioxide under an MF, which limited the mass transfer. In *Lactococcus lactis*, the application of an MF led to a deviation of the metabolic pathway in order to intensify or to inhibit nisin production [26].

The differentiated results of MFs on microorganisms have led to the hypothesis that they act under the window effect, which implies that specific parameters can be tuned for each microorganism [27–29]. Thus, in *Staphylococcus aureus*, a PMF of 1.5 mT and 300 Hz is suggested [30]. Moreover, the growth phase, shape and type of cell, eukaryotic or prokaryotic, should be considered [31].

Table 3 presents an overview of the effects of an MF on microorganisms of interest in the food industry applied to both food and nutritive broth.

Table 3. Overview of oscillatory (OMF), static (SMF) and pulsed (PMF) magnetic fields effect on microorganisms of foods.

Food/Medium	Microorganism	Equipment	Experimental Conditions	Main Results	Ref.
Cheese whey permeate	<i>Lactococcus lactis</i> growth. Nisina production	SMF	B: 5–20 mT v: 0.85–1.5 m/s (recycling) t: 4–12 h	Increased at 5 mT, 1.5 m/s and 4h	[26]
TY broth	<i>Escherichia coli</i> growth.	OMF	B:2.7–10 mT f:50 Hz t: 0–12 min	Decreased	[21]
Luria-Bertani medium	<i>Escherichia coli</i> growth.	SMF	B: 45–3500 mT (homogeneous) t: 0–60 min v: 120 strokes/min	At 450 mT decreased exponentially with the time exposure and temperature.	[20]
Nutrient broth	<i>Escherichia coli</i> growth	PMF	B: 0–4.5T f: 50Hz t pulse: 1–6ms Pulses: 0–40	Decreased by 18%	[29]
Phosphate buffer McIlvaine buffer Peptonized water	<i>Escherichia coli</i> <i>Saccharomyces cerevisiae</i> growth	PMF	B: 18T f: 10–15kHz t pulse: 20–40us Pulses: 0–50 t: 52 min Glass vial	Not inactivation for both	[28])
Nutrient	<i>Escherichia coli</i> <i>Staphylococcus aureus</i> <i>Saccharomyces cerevisiae</i> <i>Bacillus subtilis</i> growth	PMF	B: 1.29–9.48T Pulses:5–35 Static tube B: 2.11–3.79T Pulses:20	Results varied in either them	[27]
Liquid medium (Peptone-Glucose)	<i>Saccharomyces cerevisiae</i> growth	SMF	B: 5–14T (inhomogeneous dB/dx: 94 T/m) Angle: 15° T: 30 °C v: 120 strokes/min	Decreased after 16 h of incubation	[25]
Growth medium	<i>Saccharomyces cerevisiae</i> growth	SMF	B:220 mT t: 24 h	Increased	[24]
Grape must	<i>Saccharomyces cerevisiae</i> growth	OMF	B: 5 mT f: 160 Hz t: 30 min B:10 mT	Decreased	[23]
Malt extract broth	<i>Saccharomyces cerevisiae</i> growth	OMF	f: 50 Hz t: 24 min	Decreased	[31]
Nutrient broth	<i>Bacillus subtilis</i> growth	PMF	B: 3–3.3 T Pulses:5–30	Decreased	[32]
Lysogeny broth	<i>Listeria grayi</i> growth	PMF	B: 1–3.5 T Pulses: 10–35	Better inactivation to 2.5 T with 25 pulses	[22]
Columbia	<i>Staphylococcus aureus</i> growth	PMF	B: 0.5–2.5 mT f: 2–500 Hz t: 90 min B: 0.2–1 mT	Decreased	[30]
Liquid Charles	<i>Aspergillus Niger</i> growth	OMF	f: 50 Hz t: 4–8 h	Increased	[33]

4. Main Action Models of Magnetic Fields on Foods

The effect of MFs on food, since it is complex biological systems, follows a hierarchy from the atomic and molecular level to the system level, with the last level depending on the interaction of the first two levels [34]. Several action models of the effects MFs on biological systems have been proposed [35–37]. However, experimental evidence to confirm them is lacking, especially in foods, where there are few reports on this topic. The main action models proposed will describe in the next sections.

4.1. Radical Pair (RP)

This action model is related to radicals, where an MF can induce spin singlet-triplet transitions in each of them, changing its reactivity [34]. Therefore, MF can change a series of reactions that occur

within foods. Because radical pair (RP) recombination and diamagnetic anisotropy act only on elements with a magnetic dipole, RP effects are expected to be non-deterministic [37]. RP recombination implies the influence of four kinds of interactions: hyperfine interaction, inter-radical exchange interaction, electronic Zeeman interaction and the resonance effect [38]. Each interaction presents its own restrictions imposed by the participating elements and by the lifetime of radicals. In this sense, Hore [39] warns that the effect of reproducible radical pairs on biomolecular systems should not be taken to imply a similar effect at the cellular or whole-organism level. Albuquerque et al. [37] put some restrictions on the RP mechanism related to the growth of cells in an SMF, which seems to occur only in a weak SMF.

Associated with this action model is the production of free radicals (FRs) by an SMF in cells, increasing their concentration, which provokes oxidative stress and, as a result, damages the ion channels, leading to changes in cell morphology and the expression of different genes and proteins [40].

4.2. Ion Cyclotron Resonance (ICR)—Ion Paramagnetic Resonance (IPR) and Ion Interference (II)

Ion cyclotron resonance (ICR) is an action model in which ions should circulate in a plane perpendicular to an external MF (SMF or OMF) with Larmor frequencies and respective harmonics [41]. Due to the fact that ions like Ca^{2+} , Na^{+} and Mg^{2+} are implicated in biochemical reactions. So, any biological response is then expected to depend on the ratio of the frequency of the OMF to the flux density of the SMF, both at weak values [42]. However, Bingi [35] doubt the effectiveness of the action model, arguing that the coincidence in the case of calcium with a resonance frequency does not allow extrapolation to other ions. On the other hand, the IPR is an action model derived from ICR with the difference that it considers the cyclotron and subharmonic frequencies. However, quantic coherence and decoupled temperature in specific reactions are required for both mechanisms [42].

The II action model is normally applied in rotating ion-protein complexes, where an SMF induces an inhomogeneous density pattern that begins to rotate with the cyclotron frequency. The addition of an OMF results in the cessation of rotation and finally in the release of the bound ion, a process that may elicit a biological response [42] for example, in calcium-binding protein that can bind to and regulate a multitude of different protein targets, thereby affecting many different cellular functions [41].

4.3. Stochastic Resonance (SR)

This action model suggests that noise tuning can be incorporated in a system to maximize the signal-to-noise ratio, in order to take into account underlying effects in mono and bistable systems [35]. There are no reports of the application of this action model in foods but there are some studies related to enzymes in biological systems related to medicine.

4.4. Membrane Channels

Rosen [43] indicated that a moderate-intensity SMF can influence the properties of membrane channels (MCs) by changing calcium ion flux deforming or embedding ion channels, thereby altering their activation kinetics. A similar effect was reported for sodium channels, although to a lesser degree. The distinct sensitivity of ion channels to MFs may also be governed by the geometry of the ion pore and/or the presence of a voltage sensor, as in voltage-gated ion channels [44].

4.5. DNA Interaction

MFs can interact with DNA directly (breaking its structure), for example, when a PMF of 3 T with 30 pulses is applied to *Bacillus subtilis* [32] and indirectly (free radicals), when reacts with nucleic acids, causing damage to DNA. Also decreases in carbohydrate metabolism and energy metabolism through the formation of different types of expressed up-regulated and down-regulated proteins were identified by proteomics, which explains the death of cells [45].

4.6. Changes in Water Properties

Biological systems are mainly composed of water, which can change its properties and structure when interacting with an MF. This interaction should increase the chemical activity or hydration of proteins and other cellular structures [46]. Rai [47] considered the size of the ions and mentioned that small cations like Na^+ are fully hydrated in dense, reactive and weakly bound water, while large cations like K^+ are individually hydrated in water that is less dense and viscous. In relation to this, an MF could affect this behavior of the cells in six ways: (a) by inducing cytoplasmic ionic partitioning, (b) by changing cytoplasmic organization, (c) through changes in cellular proteins, (d) by alteration of the enzymatic activity, (e) by changing the behavior of the active transport and (f) by altering the formation of biopolymers. These events are closely related to the physiology of food fresh; however, no clear direction is indicated to find results that allow the conservation of fresh food.

4.7. Protein Structure and Functionality

Brizhik [34] reported that an MF influenced system redox named solitons, which are electrons that are self-trapped in alpha-helical polypeptides due to the moderately strong electron–lattice interaction, resulting in non-thermal resonant effects that affect the metabolism of the organism in general. Bingi [35] proposed ion–protein dissociation, where an ion can enter a protein cavity containing a ligand but an MF disturbs this equilibrium redistribution in the ion cloud, causing different biological responses. Moreover, the structural changes [13,14] modify biological functionality.

The main action models proposed are summarized and illustrate in Figures 1–3.

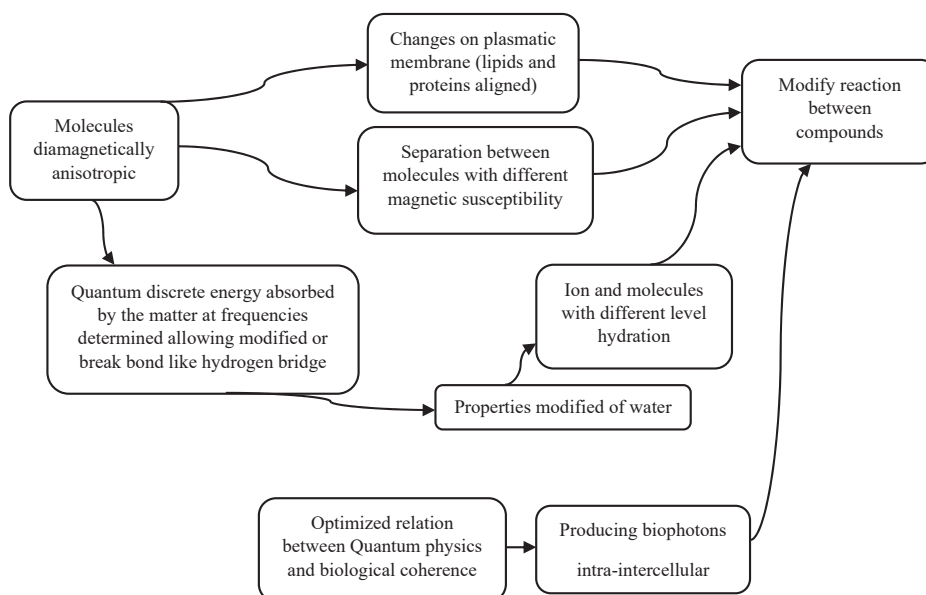


Figure 1. Action models of magnetic fields on physicochemical characteristics of foods.

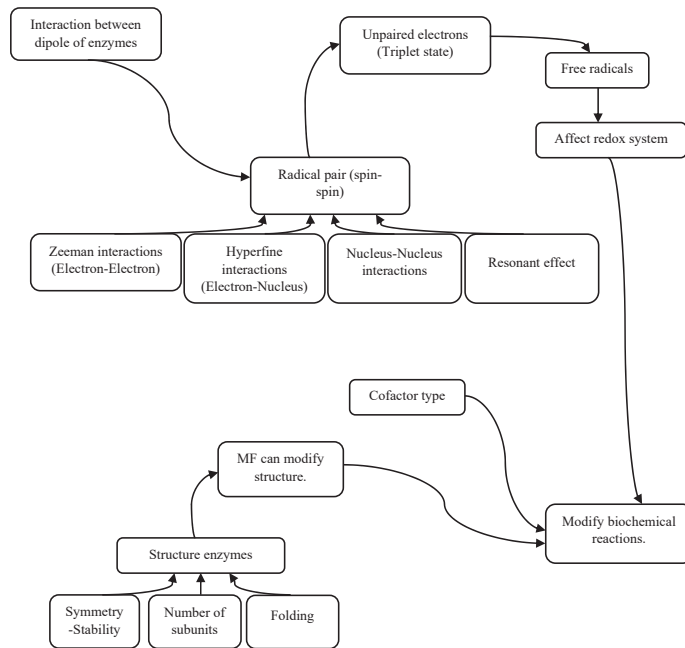


Figure 2. Action models of magnetic fields on enzymes of foods.

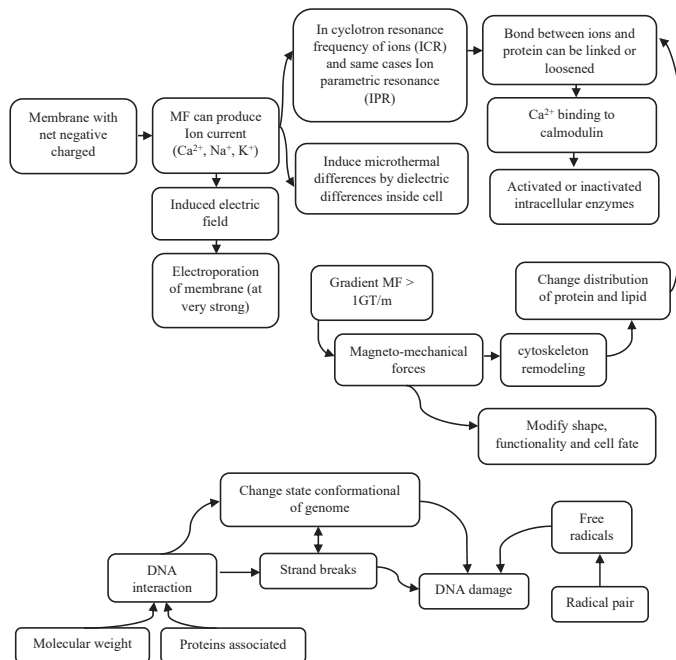


Figure 3. Action models of magnetic fields (MF) on microorganisms of foods.

5. Conclusions and Perspectives

MFs applied in different frameworks lead to promising results in the transformation and preservation of some foods with respect to their physicochemical, enzymatic and microbiological characteristics. As the food industry includes various food types, further studies are required to elucidate the levels and factors to be tuned to obtain specific results and also to understand the underlying action models. Until now, the action models that have been related to the biological systems like foods are the radical pair mechanism, ion cyclotron resonance, the formation of free radicals and structural changes of proteins and DNA.

To understand the effects of MFs on foods it is necessary to determine the magnetic and electric properties of food components and to conduct research both at the quantum level and at compound and system level, which today can be supported by various instrumental techniques and assisted by disciplines such as spintronic, bioinformatics and proteomics, among others. All these techniques will be useful to test different hypotheses and models regarding the action of the magnetic field in food.

Since the action of the magnetic field on food is non-invasive, such technology becomes very interesting in terms of food processes and improve food quality attributes by acting in its different aspects from the physical-chemical to microbiological level.

Author Contributions: H.L.A.M.: Methodology, Investigation; E.J.X.C.: Conceptualization, Supervision, Writing—Original draft preparation, Methodology, Funding acquisition; S.S.: Visualization, Investigation, Writing—Review & Editing; A.C.d.S.S.: Formal analysis, Investigation Validation, Writing—Review & Editing. All authors have read and agreed to the published version of the manuscript.

Funding: This research was funded by FONDECYT-CONCYTEC (grant contract number 271-2015-FONDECYT), the São Paulo Research Foundation (FAPESP, Brazil) grant number 2018/05871-3, CNPq proc. Num. 305295/2018-7.

Conflicts of Interest: The authors declare no conflict of interest.

References

1. Grigelmo-Miguel, N.; Soliva-Fortuny, R.; Barbosa-Cánovas, G.; Martín-Belloso, O. Use of Oscillating Magnetic Fields in Food Preservation. In *Nonthermal Processing Technologies for Food*, 1st ed.; Zhang, H.Q., Barbosa-Cánovas, G.V., Balasubramaniam, V.M., Dunne, C.P., Farkas, D.F., Yuan, J.T.C., Eds.; Wiley-Blackwell: Ames, IA, USA, 2011; p. 675.
2. Maki, S.; Hirota, N. Magnetic separation technique on binary mixtures of sorbitol and sucrose. *J. Food Eng.* **2014**, *120*, 31–36. [CrossRef]
3. Gupta, M.K.; Anand, A.; Paul, V.; Dahuja, A.; Singh, A.K. Reactive oxygen species mediated improvement in vigour of static and pulsed magneto-primed cherry tomato seeds. *Indian J. Plant Physiol.* **2015**, *20*, 197–204. [CrossRef]
4. Eşitken, A.; Turan, M. Alternating magnetic field effects on yield and plant nutrient element composition of strawberry (*Fragaria x ananassa* cv. camarosa). *Acta Agric. Scand. Sect. B-Soil Plant Sci.* **2004**, *54*, 135–139. [CrossRef]
5. Jia, J.; Wang, X.; Lv, J.; Gao, S.; Wang, G. Alternating Magnetic Field Prior to Cutting Reduces Wound Responses and Maintains Fruit Quality of Cut cucumis melo L. cv Hetao. *Open Biotechnol. J.* **2015**, *9*, 230–235. [CrossRef]
6. Goldschmidt Lins, P.; Aparecida Silva, A.; Marina Piccoli Pugine, S.; Ivan Cespedes Arce, A.; José Xavier Costa, E.; De Pires Melo, M. Effect of Exposure to Pulsed Magnetic Field on Microbiological Quality, Color and Oxidative Stability of Fresh Ground Beef. *J. Food Process Eng.* **2016**. [CrossRef]
7. Sakdatorn, V.; Thavarungkul, N.; Srisukhumbowornchai, N.; Intipunya, P. Improvement of rheological and physicochemical properties of longan honey by non-thermal magnetic technique. *Int. J. Food Sci. Technol.* **2018**, *53*, 1717–1725. [CrossRef]
8. Otero, L.; Rodríguez, A.C.; Pérez-Mateos, M.; Sanz, P.D. Effects of Magnetic Fields on Freezing: Application to Biological Products. *Compr. Rev. Food Sci. Food Saf.* **2016**, *15*, 646–667. [CrossRef]
9. Zhao, H.; Zhang, F.; Hu, H.; Liu, S.; Han, J. Experimental study on freezing of liquids under static magnetic field. *Chin. J. Chem. Eng.* **2017**, *25*, 1288–1293. [CrossRef]

10. Ali Hayder, I.; Al-HilphyAsaad, R.S.; Al-Darwash, A.K. The effect of magnetic field treatment on the characteristics and yield of Iraqi local white cheese. *IOSR J. Agric. Vet. Sci.* **2015**, *8*, 63–69. [CrossRef]
11. Zaguła, G.; Puchalski, C. Changes in Glucose And Fructose in Apples Exposed To Constant And Slowly Changing Magnetic Fields. *Zywnosc Nauka Technol. Jakosc/Food Sci. Qual.* **2013**. [CrossRef]
12. Jia, S.; Liu, Y.; Wu, S.; Wang, Z. Effect of static magnetic field on α -amylase activity and enzymatic reaction. *Trans. Tianjin Univ.* **2009**, *15*, 272–275. [CrossRef]
13. Ma, H.; Huang, L.; Zhu, C. The effect of pulsed magnetic field on horseradish peroxidase. *J. Food Process Eng.* **2011**, *34*, 1609–1622. [CrossRef]
14. Buchachenko, A. Why magnetic and electromagnetic effects in biology are irreproducible and contradictory? *Bioelectromagnetics* **2016**, *37*, 1–13. [CrossRef] [PubMed]
15. Çelik, Ö.; Büyüksulu, N.; Atak, Ç.; Rzakoulieva, A. Effects of magnetic field on activity of superoxide dismutase and catalase in Glycine max (L.) Merr. roots. *Polish J. Environ. Stud.* **2009**, *18*, 175–182.
16. Mizuki, T.; Sawai, M.; Nagaoka, Y.; Morimoto, H.; Maekawa, T. Activity of Lipase and Chitinase Immobilized on Superparamagnetic Particles in a Rotational Magnetic Field. *PLoS ONE* **2013**, *8*, e66528. [CrossRef] [PubMed]
17. Mizuki, T.; Watanabe, N.; Nagaoka, Y.; Fukushima, T.; Morimoto, H.; Usami, R.; Maekawa, T. Activity of an enzyme immobilized on superparamagnetic particles in a rotational magnetic field. *Biochem. Biophys. Res. Commun.* **2010**, *393*, 779–782. [CrossRef] [PubMed]
18. Barbosa-Canovas, G.V.; Schaffner, D.W.; Pierson, M.D.; Zhang, Q.H. Oscillating Magnetic Fields. *J. Food Sci.* **2000**, *65*, 86–89. [CrossRef]
19. Liu, Z.; Gao, X.; Zhao, J.; Xiang, Y. The Sterilization Effect of Solenoid Magnetic Field Direction on Heterotrophic Bacteria in Circulating Cooling Water. *Procedia Eng.* **2017**, *174*, 1296–1302. [CrossRef]
20. Ji, W.; Huang, H.; Deng, A.; Pan, C. Effects of static magnetic fields on Escherichia coli. *Micron* **2009**, *40*, 894–898. [CrossRef]
21. Strašák, L.; Vetterl, V.; Šmarda, J. Effects of low-frequency magnetic fields on bacteria Escherichia coli. *Bioelectrochemistry* **2002**, *55*, 161–164. [CrossRef]
22. Wu, P.; Qu, W.; Abdualrahman, M.A.Y.; Guo, Y.; Xu, K.; Ma, H. Study on inactivation mechanisms of *Listeria grayi* affected by pulse magnetic field via morphological structure, Ca^{2+} transmembrane transport and proteomic analysis. *Int. J. Food Sci. Technol.* **2017**, *52*, 2049–2057. [CrossRef]
23. Bayraktar, V.N. Magnetic field effect on yeast *saccharomyces cerevisiae* activity at grape must fermentation. *Biotechnol. Acta* **2013**, *6*, 125–137. [CrossRef]
24. da Motta, M.A.; Muniz, J.B.F.; Schuler, A.; da Motta, M. Static Magnetic Fields Enhancement of *Saccharomyces cerevisiae* Ethanolic Fermentation. *Biotechnol. Prog.* **2008**, *20*, 393–396. [CrossRef]
25. Iwasaka, M.; Ikehata, M.; Miyakoshi, J.; Ueno, S. Strong static magnetic field effects on yeast proliferation and distribution. *Bioelectrochemistry* **2004**, *65*, 59–68. [CrossRef] [PubMed]
26. Alvarez, D.C.; Pérez, V.H.; Justo, O.R.; Alegre, R.M. Effect of the extremely low frequency magnetic field on nisin production by *Lactococcus lactis* subsp. *lactis* using cheese whey permeate. *Process Biochem.* **2006**, *41*, 1967–1973. [CrossRef]
27. Haile, M.; Pan, Z.; Gao, M.; Luo, L. Efficacy in Microbial Sterilization of Pulsed Magnetic Field Treatment. *Int. J. Food Eng.* **2008**, *4*. [CrossRef]
28. Harte, F.; Martin, M.F.S.; Lacerda, A.H.; Lelieveld, H.L.M.; Swanson, B.G.; Barbosa-Cánovas, G.V. Potential use of 18 tesla static and pulsed magnetic fields on *escherichia coli* and *saccharomyces cerevisiae*. *J. Food Process. Preserv.* **2001**, *25*, 223–235. [CrossRef]
29. He, R.; Ma, H.; Wang, H. Inactivation of *E. coli* by high-intensity pulsed electromagnetic field with a change in the intracellular Ca^{2+} concentration. *J. Electromagn. Waves Appl.* **2014**, *28*, 459–469. [CrossRef]
30. Ahmed, I.; Istivan, T.; Cosic, I.; Pirogova, E. Evaluation of the effects of Extremely Low Frequency (ELF) Pulsed Electromagnetic Fields (PEMF) on survival of the bacterium *Staphylococcus aureus*. *EPJ Nonlinear Biomed. Phys.* **2013**, *1*, 5. [CrossRef]
31. Novák, J.; Strašák, L.; Fojt, L.; Slaninová, I.; Vetterl, V. Effects of low-frequency magnetic fields on the viability of yeast *Saccharomyces cerevisiae*. *Bioelectrochemistry* **2007**, *70*, 115–121. [CrossRef]
32. Qian, J.; Zhou, C.; Ma, H.; Li, S.; Yagoub, A.E.A.; Abdualrahman, M.A.Y. Biological Effect and Inactivation Mechanism of *Bacillus subtilis* Exposed to Pulsed Magnetic Field: Morphology, Membrane Permeability and Intracellular Contents. *Food Biophys.* **2016**, *11*, 429–435. [CrossRef]

33. Gao, M.; Zhang, J.; Feng, H. Extremely low frequency magnetic field effects on metabolite of *Aspergillus niger*. *Bioelectromagnetics* **2011**, *32*, 73–78. [CrossRef] [PubMed]
34. Brizhik, L. Biological effects of pulsating magnetic fields: Role of solitons. *arXiv* **2014**, arXiv:1411.6576.
35. Bingi, V.N.; Savin A, V. Effects of weak magnetic fields on biological systems: Physical aspects. *Physics-Usppekhi* **2003**, *46*, 259–291. [CrossRef]
36. Mousavian-Roshanzamir, S.; Makhdoumi-Kakhki, A. The Inhibitory Effects of Static Magnetic Field on *Escherichia coli* from two Different Sources at Short Exposure Time. *Rep. Biochem. Mol. Biol.* **2017**, *5*, 112–116. [PubMed]
37. Albuquerque, W.W.C.; Costa, R.M.P.B.; de Salazar e Fernandes, T.; Porto, A.L.F. Evidences of the static magnetic field influence on cellular systems. *Prog. Biophys. Mol. Biol.* **2016**, *121*, 16–28. [CrossRef]
38. Steiner, U.E.; Ulrich, T. Magnetic field effects in chemical kinetics and related phenomena. *Chem. Rev.* **1989**, *89*, 51–147. [CrossRef]
39. Hore, P.J. Are biochemical reactions affected by weak magnetic fields? *Proc.Natl. Acad. Sci. USA* **2012**, *109*, 1357–1358. [CrossRef]
40. Ghodbane, S.; Lahbib, A.; Sakly, M.; Abdelmelek, H. Bioeffects of Static Magnetic Fields: Oxidative Stress, Genotoxic Effects, and Cancer Studies. *Biomed Res. Int.* **2013**, *2013*, 1–12. [CrossRef]
41. Pothakamury, U.R.; Barbosa-Canovas, G.V.; Swanson, B.G. Magnetic-field inactivation of microorganisms and generation of biological changes. *Food Technol.* **1993**, *47*, 85–93.
42. Pazar, A.; Schimek, C.; Galland, P. Magnetoreception in microorganisms and fungi. *Open Life Sci.* **2007**, *2*, 597–659. [CrossRef]
43. Rosen, A.D. Studies on the Effect of Static Magnetic Fields on Biological Systems. *Piers Online* **2010**, *6*, 133–136. [CrossRef]
44. Tolosa, M.F.; Bouzat, C.; Cravero, W.R. Effects of static magnetic fields on nicotinic cholinergic receptor function. *Bioelectromagnetics* **2011**, *32*, 434–442. [CrossRef]
45. Qian, J.; Zhou, C.; Ma, H.; Li, S.; Yagoub, A.E.A.; Abdualrahman, M.A.Y. Proteomics Analyses and Morphological Structure of *Bacillus subtilis* Inactivated by Pulsed Magnetic Field. *Food Biophys.* **2016**, *11*, 436–445. [CrossRef]
46. Torgomyan, H.; Trchounian, A. Bactericidal effects of low-intensity extremely high frequency electromagnetic field: An overview with phenomenon, mechanisms, targets and consequences. *Crit. Rev. Microbiol.* **2013**, *39*, 102–111. [CrossRef] [PubMed]
47. Ratter, J. The Brazilian Cerrado Vegetation and Threats to its Biodiversity. *Ann. Bot.* **1997**, *80*, 223–230. [CrossRef]



© 2020 by the authors. Licensee MDPI, Basel, Switzerland. This article is an open access article distributed under the terms and conditions of the Creative Commons Attribution (CC BY) license (<http://creativecommons.org/licenses/by/4.0/>).

Article

Heterotrophic Plate Count for Bottled Water Safety Management

Anna Rygala *, Joanna Berlowska and Dorota Kregiel *

Department of Environmental Biotechnology, Lodz University of Technology, Wolczanska 171/173, 90-924 Lodz, Poland; joanna.berlowska@p.lodz.pl

* Correspondence: anna.rygala@p.lodz.pl (A.R.); dorota.kregiel@p.lodz.pl (D.K.)

Received: 27 May 2020; Accepted: 23 June 2020; Published: 24 June 2020

Abstract: Heterotrophic bacteria are able to form biofilms in water processing systems, adhering to pipe materials and colonizing surfaces. The aim of our research was to identify the critical points in the process of bottled water production at which controls can be applied to prevent, reduce, or eliminate water safety hazards. Microbiological monitoring was conducted using the plate count method and luminometry. To identify the bacterial isolates, we used polyphasic identification based on biochemical tests and molecular analysis using ribosomal RNA. The heterotrophic plate counts were higher in the water filtration station, ultrafiltration (UV) disinfection station, and holding tank. At these points of the industrial process, the water is stagnant or there is poor flow. Molecular analysis identified the bacterial isolates as belonging to *Acinetobacter*, *Agrobacterium*, *Aeromonas*, *Brevundimonas*, *Citrobacter*, *Enterobacter*, *Klebsiella*, *Pantoea*, and *Rhizobium* genera. Bacterial isolates showed various levels of biofilm formation, and the best adhesion properties were exhibited by the *Aeromonas hydrophila* and *Citrobacter freundii* strains.

Keywords: bottled water; technology; biofilm; heterotrophic plate count; bacteria

1. Introduction

The quality of drinking water is a worldwide concern and has a great impact on human health. In Europe, consumer demand for mineral water is increasing, including for bottled waters containing varying amounts of minerals, such as magnesium, calcium, potassium, or sodium. Estimated per capita, the consumption of bottled water in the European Union increased from 43 L in 2003 to 119 L in 2018 [1]. Mineral waters are recommended for patients with immune-system deficiencies and kidney disorders, as well as for those with urinary and heart diseases. It is therefore important to make sure the water is safe to drink, otherwise bacteria in the water may harm consumers. Moreover, bottled water is often shared between persons, and as a consequence microorganisms including opportunistic or true pathogens may be transferred by this route [2,3].

Bottled waters may be derived from natural spring water or from processed water. Spring water may be bottled directly, without any processing, or it may be subjected to a number of processes to modify its physical, chemical, biological, and microbiological properties. The type of treatment procedure depends on the origin and quality of the raw source [4]. Often, particulate matter is congregated with coagulants, then the water is mixed with clarifiers. Larger particles of sediment and smaller particles that are left after clarification are directed to the filtration system. Finally, various disinfection methods (ultrafiltration, UV) may be used [2].

Water quality does not depend solely on the raw water. It is also affected by the formation of biofilms in installation systems. Dissolved organic compounds in drinking water are responsible for the growth of heterotrophic bacteria, which colonize installation materials. Heterotrophs are microorganisms that require organic carbon for proliferation. This term includes bacteria and fungi capable of growing in a water environment. They are therefore counted among the normal, saprophytic water microorganisms.

However, under certain circumstances pathogenic or opportunistic microorganisms can also appear from diverse sources. The main source of heterotrophs is raw water. Microbial cells can also enter water networks during the repair or replacement of sections of the installation, as well as during failures that lower pressure. As a consequence, biofilms may harbor and support the proliferation of pathogenic cells, thereby contributing to the spread of waterborne diseases [3,5].

Heterotrophic plate count (HPC) is a parameter that quantifies the formation of biofilm in water systems. It has been widely adopted as a standard and simple technique for microbiological testing and safety management of drinking water [6]. The HPC method has a long history in drinking water microbiology. At the end of the nineteenth century, HPC was used as an indicator of the proper functioning of water treatment systems (filtration, disinfection), and as an indirect indicator of water safety. In the twentieth century, the use of HPC as a safety indicator declined due to the application of fecal indicators, namely coliforms and enterococci. Nevertheless, HPC measurements and limits are still included in the water regulations and guidelines of many countries [4].

Bottled water is a specific environment for the multiplication of microorganisms. It may contain natural or added carbon dioxide, which restricts microbial growth. However, no long-acting disinfectants are present. Moreover, the final product is often exposed to elevated (room) temperatures, for a few days or weeks before consumption. The type of packaging used, such as plastic bottles, can also affect the development of spoilage microorganisms [7]. Therefore, the levels of HPC recovered from bottled water in the distribution period can be significantly higher than those found in water from industrial systems before or shortly after bottling [4,8].

Given the importance of ensuring the safety of drinking water and identifying potential microbial contaminants, this study was carried out to assess the microbiological quality of bottled water and of the industrial distribution system. To our knowledge, there have been only a few previous studies on the bacteriological quality of both the installation lines and the final bottled water [9,10]. In particular, we analyzed the critical points that influence the microbial quality of processed water. Since the bacteriological quality of drinking water is highly dependent on the bacterial species present, the dominant heterotrophic bacteria were identified along with their capacity for biofilm formation.

2. Materials and Methods

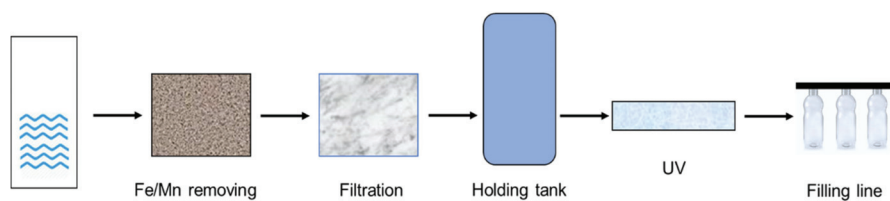
2.1. Water Analysis

In total, 30 samples of spring bottled water (volume 500–1500 mL) were subjected to HPC analysis: 10 samples of still mineral water, 10 samples of lightly carbonated water (<1500 mg/L CO₂) and 10 samples of carbonated water (>1500 mg/L CO₂). All the samples had been packaged in polyethylene terephthalate (PET) bottles and sourced from a single Polish manufacturer during two summer months. All cleaning and sanitization procedures in the plant were conducted according to detailed procedures and an internal CIP (Cleaning In Place) program.

All the bottled waters were stored at 20–25 °C for at least two weeks after bottling. At the same time as the bottled water was being produced, 23 samples of processed water were also collected. The processed water was taken from six different collection stages: (i) raw water; (ii) water after Fe/Mn removal; (iii) water after microfiltration; (iv) water from a holding tank; (v) water after UV disinfection; (vi) water before filling (bottling) (Table 1, Figure 1). In this technological process, carbonization was performed just before filling.

Table 1. Processed water samples used in the research.

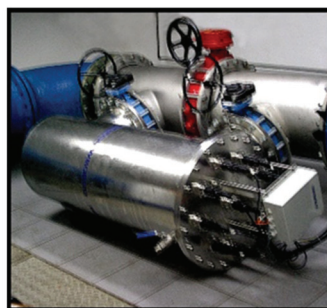
Collection Stage	No of Samples
Raw water	3
Clarification (Fe/Mn removal)	3
Filtration	3
Holding tank	5
UV station	5
Filling	4



(a)



(b)



(c)

Figure 1. Bottled water processing: (a) general scheme; (b) holding tank; (c) UV station.

For HPC analysis, the samples were agitated by vortexing, filtered (0.45 μm -pore-size filter, Merck KGaA, Darmstadt, Germany), plated on R2 Agar medium (Merck KGaA, Darmstadt, Germany), and incubated for 2 or 3 days at two different temperatures, 37 °C and 22 °C, respectively. All the tested samples were also analyzed for sanitary indicators (coliforms/*Escherichia coli*, enterococci, *Pseudomonas aeruginosa*) [11]. The agar media and incubation conditions for the inoculated plates are shown in Table 2.

Table 2. Agar media and incubation conditions.

Detection	Agar Medium	Temperature [°C]	Time [Day]
HPC	R2 Agar, TSA Agar	22, 37	3, 2
Coliforms/ <i>E. coli</i>	Chromocult Coliform Agar	37	2
Enterococci	Slanetz-Bartley Agar	37	2
<i>P. aeruginosa</i>	Cetrimide Agar	37	2
<i>Pseudomonas/Aeromonas</i> sp.	GSP Agar	25	1

2.2. HPC Isolation and Identification

Characteristic slimy colonies were picked up from the agar plates, restreaked to ensure purity, and cultivated on TSA slants (Merck KGaA, Darmstadt, Germany) at 22 °C. The following biochemical methods were used to identify the bacteria: Gram staining, the aminopeptidase test

(Bactident® Aminopeptidase, Merck KGaA, Darmstadt, Germany), the oxidase test (Bactident® Oxidase, Merck KGaA, Darmstadt, Germany), and the catalase test (Bactident® Catalase, Merck KGaA, Darmstadt, Germany). The growth and morphology of the bacteria were also analyzed on agar plates and under a microscope. Identification of isolates was confirmed using the PCR technique described previously [12]. The 16S rRNA gene sequences were compared with those obtained from the NCBI database, using the program BLASTN 2.2.27 + (<https://blast.ncbi.nlm.nih.gov/Blast.cgi>). The nucleotide sequences were deposited in the GenBank with accession numbers.

2.3. Assessment of Bacterial Adhesion

Bacterial adherence was evaluated under laboratory conditions. Experiments were conducted using white glass as the reference hydrophilic material (Star Frost 76 × 26 mm, Knittel Glass, Germany). Sterile glass carriers were placed in sterile 25 mL Erlenmeyer flasks with 20 mL of 50-fold diluted buffered peptone water (Merck KGaA, Darmstadt, Germany). The amount of bacterial inoculum (0.1 mL) was standardized densitometrically (1°McF). The samples were incubated at 22 °C with agitation on a laboratory shaker (135 rpm) for 6 days. Cell adhesion to the carriers was evaluated using luminometric sampling pens (Merck KGaA, Darmstadt, Germany). The measurements were expressed in RLU/cm² using a HY-LiTE2 luminometer (Merck KGaA, Darmstadt, Germany) [13,14].

2.4. Statistical Methods

The results were calculated as the means and standard deviations in the data from three independent tests. Analysis of variance (ANOVA) was used to examine the differences between group means representing the adhesion results (OriginLab Corporation, Northampton, USA). The results were compared to those for the control samples (without inoculation). Values with letters show statistically significant differences: a, $p \geq 0.05$; b, $0.005 < p < 0.05$; c, $p < 0.005$.

3. Results and Discussion

3.1. Bacteriological Analysis of Processed Water and Bottled Water

The results of bacteriological analysis of the processed water are presented in Figure 2. Sand filtration was found to have a negative effect on the HPC, with the number of detected bacteria increasing by up to 100-fold. In addition, more HPC bacteria were detected in the holding tank and UV station. At these points in the technological process, the water is stagnant or the flow is very poor. This suggests that that water processing may promote growth of the detected HPC. The WHO reports that elevated HPC levels are particularly likely to occur in the various parts of distribution systems where the water is stagnant [15]. A similar tendency has been observed by Wang et al. [16], who found that the filtration processes in advanced drinking water treatment systems promote the development of HPC bacteria considerably. Hydrodynamics impacts the interactions between free microbial cells and regulates biofilm formation in drinking water systems. It can either promote biofilm formation (in the case of water stagnation or weak flow) or induce bacteria to escape from the biofilm matrix (in the case of rapid velocity and turbulence) [17,18].

The HPC results indicate that the numbers of bacterial colonies in all the tested types of bottled water exceeded 100 CFU/100 mL after incubation at both 22 °C and 37 °C (Figure 3). The HPC determined at 22 °C was between 450 and 266 CFU/100 mL, for still water and carbonated water, respectively. Therefore, carbonation contributed to a slight reduction in the number of microorganisms determined by the plate count method at 22 °C. Smaller differences were noted at 37 °C.

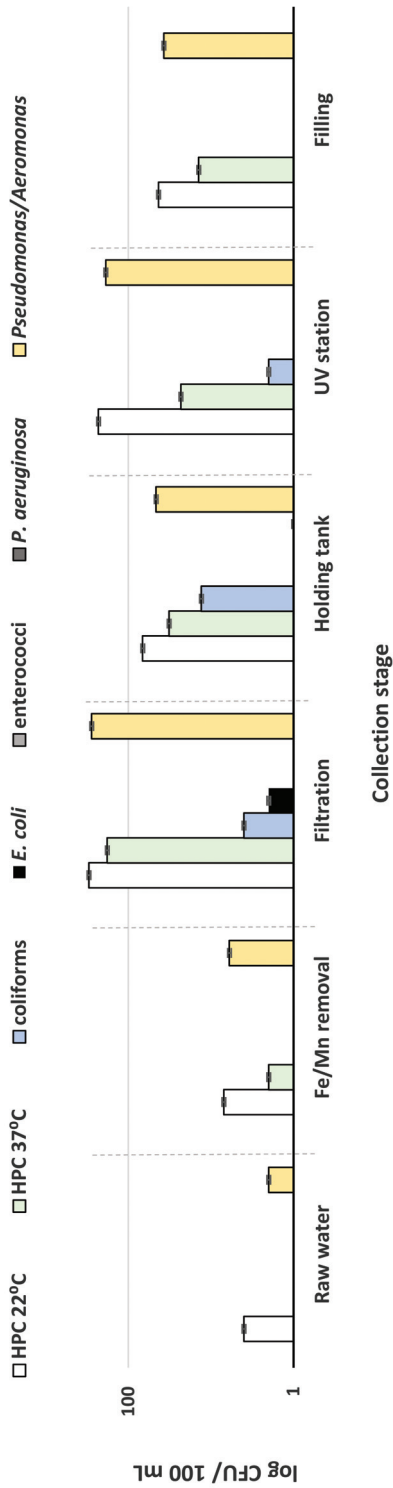


Figure 2. Bacteriological analysis of processed water.

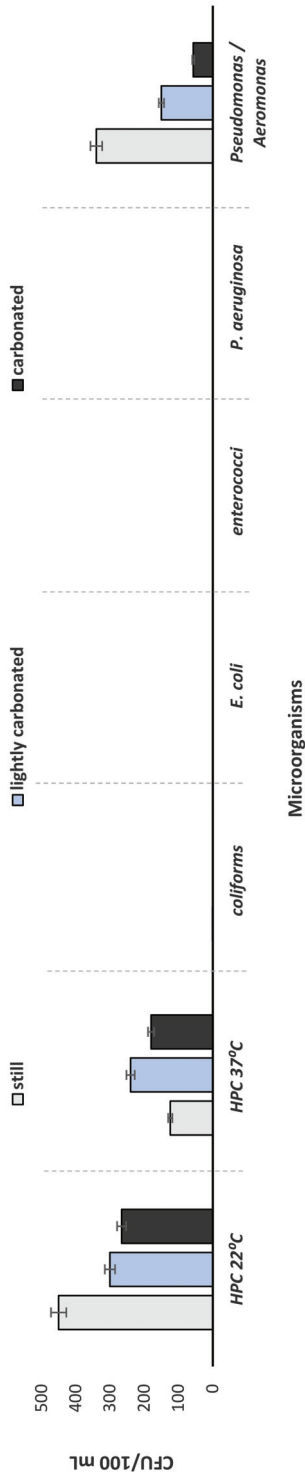


Figure 3. Bacteriological analysis of bottled water.

At 22 °C, the HPC results are described as being of little sanitary value, but are a good indication of the efficiency of water treatment. However, some HPC increases at 22 °C may be attributed to the aerobic bacteria *Aeromonas* sp. or *Pseudomonas* sp., often associated with opportunistic infections. It was confirmed by the results on GSP agar. At 37 °C, the HPC results are formed mainly by indicator organisms, namely facultative anaerobes (coliforms) and other Enterobacteriaceae [4].

The utility of carbon dioxide in extending the shelf-lives of some food products has been well established [19]. Increased CO₂ levels are beneficial for reducing microbial growth directly, although facultative anaerobes such as coliform bacteria favor growth in an atmosphere high in CO₂ and proliferate due to the reduction in levels of competing aerobic microorganisms. Our study therefore confirms that CO₂ treatment may contribute to bacterial destruction, and was most effective against aerobic bacteria growing at 22 °C [20].

The typical microbiota found in the process and bottled water were Gram-negative rods belonging to *Pseudomonas/Aeromonas* genera. On TSA agar, the bacterial colonies varied from small (2 mm) and regular to large (6 mm) with irregular structures and edges. On the GSP agar, the bacteria were able to grow as regular red (*Pseudomonas* sp.) or yellow (*Aeromonas* sp.) colonies (Figure 4a). In total, 20 different bacterial isolates were obtained from the samples. The bacterial morphotypes were diverse, from small circular colonies to larger (4–5 mm) irregular colonies. Some of the colonies had a characteristic slimy appearance (Figure 4b).

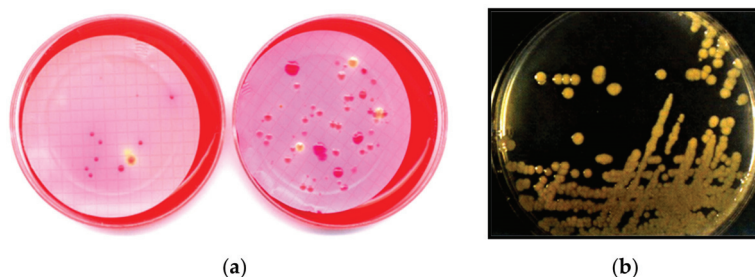


Figure 4. Growth of bacteria on: (a) GSP agar; (b) TSA agar.

The bacterial isolates were identified as Gram-negative bacteria. Ten bacterial monocultures forming characteristic slimy colonies were selected for molecular identification. The nucleotide sequences of the isolates were deposited in the GenBank (presented with accession numbers in Table 3).

Table 3. Bacterial strains isolated from the processed water system.

Isolate	Cell Shape	Gram	Oxidase	GenBank Number
<i>A. johnsonii</i>	¹ R	² N	N	KT751294
<i>A. hydrophila</i>	R	N	³ P	KC756842
<i>A. tumefaciens</i>	R	N	P	KJ719245
<i>B. vesicularis</i>	R	N	P	KT751295
<i>C. freundii</i>	R	N	N	KJ995856
<i>E. aerogenes</i>	R	N	N	KJ995857
<i>E. soli</i>	R	N	N	KJ995858
<i>K. oxytoca</i>	R	N	N	KJ995859
<i>P. agglomerans</i>	R	N	N	KJ995860
<i>R. giardinii</i>	R	N	P	KT751297

¹ R—rods; ² N—negative; ³ P—positive.

The bacterial isolates were identified as *Acinetobacter johnsonii*, *Aeromonas hydrophila*, *Agrobacterium tumefaciens*, *Brevundimonas vesicularis*, *Citrobacter freundii*, *Enterobacter aerogenes*, *E. soli*, *Klebsiella oxytoca*, *Pantoea agglomerans*, and *Rhizobium giardinii*. Some of isolates were

typical microbiota commonly found in water systems. Vaz-Moreira et al. [21] confirmed the presence in drinking water systems of the following Gram-negative rods: *Blastomonas*, *Brevundimonas*, *Sphingomonas*, *Acinetobacter*, *Aeromonas*, *Enterobacter*, and *Pseudomonas*. The following strains from the Enterobacteriaceae family were also detected: *Citrobacter*, *Enterobacter*, *Klebsiella*, and *Pantoea*. Some of these are opportunistic pathogens responsible for numerous infections [22]. These bacteria were detected in process/bottled water, although *E. coli* (a standard fecal contamination indicator) was not. Non-enteric Gram-negative rods were also detected in the processed water and bottled water. *Agrobacterium* and *Brevundimonas* originate in plants and soil [23,24]. *A. hydrophila* frequently colonizes water installation surfaces, ventilation systems, as well as medical equipment [13]. These bacteria can cause opportunistic infections (endocarditis, bacteremia, meningitis, respiratory and urinary tract infections) which are often difficult to treat. Despite their various taxonomies and biochemical characteristics, the bacterial isolates were able to form slimy colonies on the agar plates. It seems that this ability may facilitate aggregation and adhesion, and therefore stimulate biofilm formation in water installation systems.

3.2. Adhesion Abilities

Bacterial adhesion to the glass carriers was assessed in minimal medium. According to the literature, biofilm formation may be stimulated in water environments poor in organic carbon sources [25]. Adhesion ability is usually correlated strongly with the ability to form biofilm. Of course, initial adhesion does not ensure the ability of the tested drinking water-isolated bacteria to form mature biofilms, but it may make it much easier. Other important events, including phenotypic and genetic switching during biofilm development, the production of extracellular polymeric substances, and water stagnation, as well as the kind of abiotic surface, also play a significant role in biofilm formation and differentiation [26].

The physicochemical properties of the surface are an important factor in the adhesion of bacteria to inert surfaces. The degree of hydrophobicity, in particular, is correlated with biofilm formation. More hydrophilic surfaces usually reduce the growth of biofilms. In our study, we chose a glass surface for adhesion tests. Due to its high hydrophilicity, glass is similar to stainless steel, another inert surface commonly used in the food industry. However, it is worth noting that all surfaces are modified rapidly by immersion in water and adsorption of conditioning films, which change the properties of these materials [27].

In our study, the adhesion samples on glass were incubated with agitation on a laboratory shaker. The assumption was made that if bacteria have the ability to form biofilm on hydrophilic surfaces in water with regular flow, then under industrial conditions, where water may be stagnant, the formation of biofilms will be even more likely.

Figure 5 shows the results of cell adhesion expressed in Relative Light Units per cm^2 (RLU/ cm^2). For each of the tested bacterial strains, various levels of cell adhesion can be observed. The RLU values are the highest for *A. hydrophila* and *C. freundii* at 138–142 RLU/ cm^2 . For the other strains, the RLU results are significantly lower, from 28 to 102 RLU/ cm^2 . In this monitored technological process, CO_2 saturation occurred in the final stage before the filling of processed water, so it did not affect biofilm formation in the installation pipes. Therefore, the influence of carbon dioxide on biofilm formation was not studied in this research.

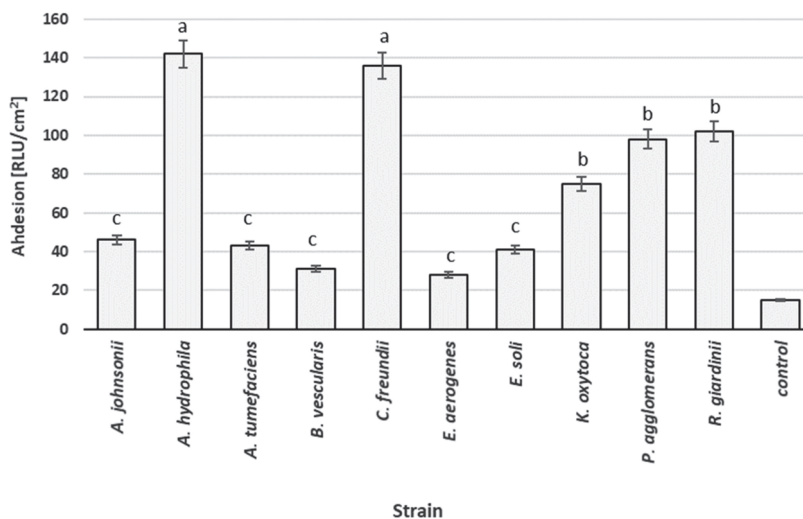


Figure 5. Adhesion of bacterial isolates to a glass surface after 6 days of incubation.

4. Conclusions

Biofilm formation by heterotrophic bacteria in various water distribution systems can lead to the contamination of drinking water and the transmission of various opportunistic pathogens. The WHO recommends the use of molecular techniques to identify specific heterotrophs of potential concern for human health [28]. The best strategy for water industries is to monitor HPC levels regularly. Most producers conduct regular scheduled reviews, and also test in case of failures. Such monitoring has a formal structure based on the international standard ISO 9000. In this study, HPC testing was used to identify the critical points in the production of bottled drinking water responsible for biofilm formation and contamination of the final products. Microbiological monitoring was conducted using the plate count method and luminometry. The identification methodology used in this study can be used for differential identification of microbiota in specific water environments. More research is needed to explore the potential role of the HPC method in reducing or preventing the colonization of water systems and products by harmful microorganisms.

Author Contributions: Conceptualization, A.R. and D.K.; methodology, A.R.; writing—original draft preparation, A.R.; writing—review and editing, D.K.; visualization, J.B. All authors have read and agreed to the published version of the manuscript.

Funding: This research received no external funding.

Acknowledgments: We would like to thank Anna Otlewska for help with molecular analysis, and John Speller for editorial assistance.

Conflicts of Interest: The authors declare no conflict of interest.

References

1. Natural Waters: The Natural Choice for Hydration. Available online: <https://www.efbw.org> (accessed on 8 May 2020).
2. Rosenberg, F.A. The microbiology of bottled water. *Clin. Microbiol. Newsl.* **2003**, *25*, 41–44. [CrossRef]
3. Farhadkhani, M.; Nikaeen, M.; Akbari Adergani, B.; Hatamzadeh, M.; Nabavi, B.F.; Hassanzadeh, A. Assessment of drinking water quality from bottled water coolers. *Iran J. Public Health.* **2014**, *43*, 674–681. [PubMed]
4. Heterotrophic Plate Count Measurement in Drinking Water Safety Management. Available online: https://www.who.int/water_sanitation_health/dwq/WSH02.10.pdf (accessed on 8 May 2020).

5. Douterelo, I.; Boxall, J.B.; Deines, P.; Sekar, R.; Fish, K.E.; Biggs, C.A. Methodological approaches for studying the microbial ecology of drinking water distribution systems. *Water Res.* **2014**, *48*, 134–156. [CrossRef] [PubMed]
6. Diduch, M.; Polkowska, Ż.; Namieśnik, J. The role of heterotrophic plate count bacteria in bottled water quality assessment. *Food Control* **2016**, *61*, 188–195. [CrossRef]
7. Kregiel, D.; Otlewska, A.; Antolak, H. Attachment of *Asaia bogorensis* originating in fruit-flavored water to packaging materials. *Biomed. Res. Int.* **2014**, *2014*, 514190. [CrossRef]
8. Kregiel, D.; Antolak, H. Growth of *Asaia* spp. in flavored mineral water—evaluation of the volumetric “bottle effect”. *Int. J. Food Process. Technol.* **2016**, *3*, 62–65. [CrossRef]
9. Zamberlan da Silva, M.E.; Santana, R.G.; Guilhermetti, M.; Filho, I.C.; Endo, E.H.; Ueda-Nakamura, T.; Nakamura, C.V.; Filho, B.P.D. Comparison of the bacteriological quality of tap water and bottled mineral water. *Int. J. Hyg. Environ. Health* **2008**, *211*, 504–509. [CrossRef]
10. Fujioka, T.; Ueyama, T.; Mingliang, F.; Leddy, M. Online assessment of sand filter performance for bacterial removal in a full-scale drinking water treatment plant. *Chemosphere* **2019**, *229*, 509–514. [CrossRef]
11. Directive 2009/54/EC of the European Parliament and of the Council on the Exploitation and Marketing of Natural Mineral Waters. Available online: <https://eur-lex.europa.eu/legal-content/EN/ALL/?uri=CELEX%3A32009L0054> (accessed on 8 May 2020).
12. Kregiel, D.; Rygała, A.; Libudzisz, Z.; Walczak, P.; Oltuszek-Walczak, E. *Asaia lannensis* the spoilage acetic acid bacteria isolated from strawberry-flavored bottled water in Poland. *Food Control* **2012**, *26*, 147–150. [CrossRef]
13. Kregiel, D. Adhesion of *Aeromonas hydrophila* to modified glass surfaces with organosilanes. *Food Technol. Biotechnol.* **2013**, *51*, 345–351.
14. Kregiel, D.; Niedzielska, K. Effect of plasma processing and organosilane modifications of polyethylene on *Aeromonas hydrophila* biofilm formation. *BioMed Res. Int.* **2014**, *2014*, 23251. [CrossRef]
15. Heterotrophic Plate Counts and Drinking-Water Safety. The Significance of HPCs for Water Quality and Human Health. Available online: http://www.who.int/water_sanitation_health/dwq/HPCFull.pdf (accessed on 15 May 2020).
16. Wang, F.; Li, W.; Zhang, J.; Qi, W.; Zhou, Y.; Xiang, Y.; Shi, N. Characterization of suspended bacteria from processing units in an advanced drinking water treatment plant of China. *Environ. Sci. Pollut. Res.* **2017**, *24*, 12176–12184. [CrossRef] [PubMed]
17. Chen, X.; Wang, Y.; Li, W.; Zhang, J.; Qi, W.; Lu, Y.; Ding, Z. Coupling changes of disinfectant and bacteria induced by the water stagnation and disinfection strategy. *Chemosphere* **2020**, *242*, 125190. [CrossRef] [PubMed]
18. Zlatanović, L.; van der Hoek, J.P.; Vreeburg, J.H.G. An experimental study on the influence of water stagnation and temperature change on water quality in a full-scale domestic drinking water system. *Water Res.* **2017**, *123*, 761–772. [CrossRef] [PubMed]
19. Izumi, H.; Inoue, A. Viability of sublethally injured coliform bacteria on fresh-cut cabbage stored in high CO₂ atmospheres following rinsing with electrolyzed water. *Int. J. Food Microbiol.* **2018**, *266*, 207–212. [CrossRef] [PubMed]
20. Debs-Louka, E.; Louka, N.; Abraham, G.; Chabot, V.; Allaf, K. Effect of compressed carbon dioxide on microbial cell viability. *Appl. Environ. Microbiol.* **1999**, *65*, 626–631. [CrossRef] [PubMed]
21. Vaz-Moreira, I.; Nunes, O.C.; Manaia, C.M. Ubiquitous and persistent Proteobacteria and other Gram-negative bacteria in drinking water. *Sci. Total Environ.* **2017**, *586*, 1141–1149. [CrossRef]
22. Guentzel, M.N. *Escherichia*, *Klebsiella*, *Enterobacter*, *Serratia*, *Citrobacter*, and *Proteus*. In *Source Medical Microbiology*, 4th ed.; Baron, S., Ed.; University of Texas Medical Branch at Galveston: Galveston, TX, USA, 1996.
23. Krenek, P.; Samajova, O.; Luptovciak, I.; Doslakova, A.; Komis, G.; Samaj, J. Transient plant transformation mediated by *Agrobacterium tumefaciens*: Principles, methods and applications. *Biotechnol. Adv.* **2015**, *33*, 1024–1042. [CrossRef]
24. Padikasan, I.A.; Chinnannan, K.; Kumar, S.; Subramaniyan, G. Agricultural Biotechnology: Engineering Plants for Improved Productivity and Quality. In *Omics Technologies and Bio-Engineering*; Barh, D., Azevedo, V., Eds.; Academic Press: London, UK, 2018; Volume 2, pp. 87–104.

25. Myszka, K.; Czaczyk, K. Effect of starvation stress on morphological changes and production of adhesive exopolysaccharide (EPS) by *Proteus vulgaris*. *Acta Sci. Pol. Technol. Aliment.* **2011**, *10*, 305–312.
26. Simões, L.C.; Simões, M.; Vieira, M.J. Adhesion and biofilm formation on polystyrene by drinking water-isolated bacteria. *Antonie Leeuwenhoek* **2010**, *98*, 317–329. [CrossRef]
27. Kregiel, D. Attachment of *Asaia lannensis* to materials commonly used in beverage industry. *Food Control* **2013**, *32*, 537–542. [CrossRef]
28. Priority Pathogens List for R&D of New Antibiotics. Available online: <http://www.who.int/mediacentre/news/releases/2017/bacteria-antibiotics-needed/en/> (accessed on 5 May 2020).



© 2020 by the authors. Licensee MDPI, Basel, Switzerland. This article is an open access article distributed under the terms and conditions of the Creative Commons Attribution (CC BY) license (<http://creativecommons.org/licenses/by/4.0/>).

MDPI AG
Grosspeteranlage 5
4052 Basel
Switzerland
Tel.: +41 61 683 77 34

Processes Editorial Office
E-mail: processes@mdpi.com
www.mdpi.com/journal/processes



Disclaimer/Publisher's Note: The statements, opinions and data contained in all publications are solely those of the individual author(s) and contributor(s) and not of MDPI and/or the editor(s). MDPI and/or the editor(s) disclaim responsibility for any injury to people or property resulting from any ideas, methods, instructions or products referred to in the content.



Academic Open
Access Publishing

mdpi.com

ISBN 978-3-0365-7779-1